ULB FACULTÉ DES SCIENCES
UNIVERSITÉ LIBRE DE BRUXELLES

LIÈGE université

Marine benthic hypoxia and its consequences for sediment-water exchanges and early diagenesis

Thesis submitted by Audrey PLANTE

Under Joint Supervision

in fulfilment of the requirements of the PhD Degree in Sciences (“Docteur en Sciences”)

Academic year 2019-2020

SUPERVISORS:

Professors Lei CHOU & Pierre REGNIER
(Université libre de Bruxelles)

Professor Nathalie FAGEL
(Université de Liège)

Thesis jury:

Marilaure GRÉGOIRE (Université de Liège, Chair)
Sandra ARNDT (Université libre de Bruxelless, Secretary)
Martine LEERMAKERS (Vrije Universiteit Brussel)
Christophe RABOUILLE (Laboratoire des Sciences du Climat et de l'Environnement)
Arthur CAPET (Université de Liège)

fnrs
LA LIBERTÉ DE CHERCHER

Abstract

The northwestern (NW) continental shelf of the Black Sea undergoes seasonal hypoxia. The benthic environment, the exchanges at the water-sediment interface and the diagenetic reactions are influenced by this phenomenon. In the framework of the BENTHOX project, two field cruises were conducted on the shelf in spring 2016 and in summer 2017.

The first part of this investigation concerned the study of the impact of low oxygen levels in bottom waters on the diagenetic reactions. The microprofilings of geochemical parameters and the flux measurements showed both spatial and temporal variabilities in the benthic compartment of the NW continental shelf for the two seasons studied. The areas closest to the coasts exhibited the most important fluxes of oxygen consumption and of sulfate. These regions were strongly influenced by riverine inputs inducing a higher productivity and in turn resulting in an increase in the fluxes of organic matter deposited on the seabed.

The diagenetic reactions were impacted by seasonal deoxygenation in bottom waters. The oxic respiration was less important in the summer as reflected by the shallower penetration depth of dissolved oxygen. Since 1995, the diffusive oxygen uptake (DOU) reported during hypoxic period indicated that the concentration of dissolved oxygen played an important role in the benthic exchange fluxes. Furthermore, a shallower reduction of sulphate and of Mn- and Fe-oxides observed in the sediments evidenced the impact of low oxygen levels on the diagenetic cascade. As a consequence, the benthic mineralization of organic matter was affected. During summer 2017, the oxic mineralization of organic carbon was less important and the contribution of the reducing species to oxygen consumption increased. The anaerobic mineralization of organic matter became thus the dominant process during the period of deoxygenation.

The second part concerned the study of the sulfur and iron cycling in the shelf sediments during the low oxygen event of summer 2017. The sediments from the station close to the mouth of the Danube and that near the Dnieper exhibited a signature of detrital material different from that of the upper crust. The inputs of organic matter, in particular transported by the rivers, could influence the signal. The sediments of the NW shelf investigated were however of marine origin.

Following the sulfate reduction already observed and mentioned above, the hydrogen sulfides produced were rapidly consumed as suggested by the low concentrations of acid volatile

sulfide (AVS) and of the dissolved sulfide. The presence of pyrite in the upper layers of the sediments close to the water-sediment interface was plausible because the formation of pyrite in the water column had been reported due to the higher resistance of pyrite to oxidation compared to AVS (Wijsman et al. 2001). A non steady-state deposition was observed as suggested by Wijsman et al. (1999). It was characterized by an abrupt drop in the pyrite content caused possibly by fluctuations in salinity, dissolved O_2 concentrations and organic matter fluxes.

The non-reactive iron constituted the principal fraction of the total iron present in the sediments. Its contribution fell in the range reported for the marine sediments of the continental margins. A spatial variation of the concentration of highly reactive iron was nevertheless observed. Near the Dnieper mouth, the contents of reactive iron were lower and could be attributed to the less important fluvial inputs, to the sorption and/or precipitation processes or yet to the reallocation of the reactive iron of the shelf deposits towards the sediments in deep and euxinic waters.

The last part of this thesis concerned the biogeochemistry of metals (Fe, Mn, Zn, Cu, Ni, Hg, Co and Cd) during the early diagenesis and the assessment of enrichment and pollution of these metals in the sediments of the shelf. The results showed that trace metals are probably linked to iron and manganese oxides as well as to sulphides. Ni and Zn could be involved in adsorption onto and co-precipitation with Fe- and Mn-oxides. Cu seemed to be associated preferentially to sulphides but no clear correlation was found. The enrichment and pollution of these metals in the shelf sediments showed spatial variability. The Danube delta area was enriched in Ni, Cu and Zn while the Odessa region was enriched in Co and Cd. The pollution of shelf sediments ranged from “unpolluted” to “very highly polluted”. Since the late 20^{th} century, the heavy metal contents in shelf sediments remained stable in the Odessa region but increased in the Danube delta area.

Résumé

Le plateau continental du Nord-Ouest de la Mer Noire subit une hypoxie saisonnière. L'environnement benthique, l'échange à l'interface eau-sédiment et les réactions diagénétiques sont influencés par ce phénomène. Dans le cadre du projet BENTHOX, deux campagnes de prélèvement ont été menées sur le plateau au printemps 2016 et à l'été 2017 dans le but de comprendre ces changements.

La première partie de cette recherche concerne l'impact des faibles concentrations en oxygène dans les eaux de fond sur les réactions diagénétiques. Les micro-profils de paramètres géochimiques et les mesures de flux ont montré des variabilités spatiales et temporelles dans le compartiment benthique pour les deux saisons étudiées. Les zones les plus proches des côtes ont présenté les flux les plus importants de consommation d'oxygène et de sulfate. Ces régions ont été fortement influencées par les apports fluviaux induisant une productivité plus élevée et entraînant à son tour une augmentation des flux de matière organique déposée sur le fond marin.

Les réactions diagénétiques sont affectées par la désoxygénation saisonnière des eaux de fond. La respiration oxique etait moins importante en été comme en témoigne la profondeur de pénétration moins profonde de l'oxygène. Depuis 1995, l'absorption d'oxygène dissous (DOU) rapportée pendant la période limitée en oxygène a indiqué que la concentration d'oxygène dissous jouait un rôle important dans les flux d'échanges benthiques. De plus, une diminution de la profondeur à laquelle la réduction des sulfates et la réduction des oxydes métalliques témoigne de l'impact d'une faible concentration en oxygène sur la cascade diagénétique. En conséquence, la minéralisation benthique de la matière organique a été affectée. Au cours de l'été 2017, la minéralisation oxique du carbone a été moins importante et la contribution des espèces réductrices à la consommation d'oxygène a augmenté. La respiration anaérobie de la matière organique est ainsi devenue le processus dominant pendant la période d'hypoxie.

La deuxième partie portait sur l'étude du cycle du soufre et du fer dans les sédiments du plateau lors de l'événement de faible teneur en oxygène de l'été 2017. Les sédiments de la station proche de l'embouchure du Danube et de celle du Dniepr présentaient une signature de matière détritique différente de celle de la croûte supérieure. Les apports de matière

organique, notamment transportés par les rivières, pourraient influencer le signal. Les sédiments du plateau nord-ouest étudiés étaient cependant d'origine marine.

Suite à la réduction du sulfate déjà observée et mentionnée ci-dessus, les sulfures d'hydrogène produits ont été rapidement consommés comme le suggèrent les faibles concentrations en sulfure acide volatil (AVS) et en sulfure dissous. La présence de pyrite dans les couches supérieures des sédiments près de l'interface eau-sédiment était plausible car la formation de pyrite dans la colonne d'eau avait été signalée en raison de la résistance plus élevée de la pyrite à l'oxydation par rapport à l'AVS (Wijsman et al., 2001). Un dépôt à l'état non stationnaire a été observé comme le suggèrent Wijsman et al. (1999). Elle a été caractérisée par une chute brutale de la teneur en pyrite causée peut-être par des fluctuations de salinité, des concentrations d'O_2 dissous et des flux de matière organique

Le fer non réactif constituait la fraction principale du fer total présent dans les sédiments. Sa contribution est tombée dans la gamme signalée pour les sédiments marins des marges continentales. Une variation spatiale de la concentration en fer hautement réactif a néanmoins été observée. Près de l'embouchure du Dniepr, les teneurs en fer réactif étaient plus faibles et pouvaient être attribuées aux apports fluviaux moins importants, aux processus de sorption et / ou de précipitation ou encore à la réallocation du fer réactif des dépôts du plateau vers les sédiments en profondeur et eaux euxiniques.

La dernière partie de cette thèse concerne la biogéochimie des métaux (Fe, Mn, Zn, Cu, Ni, Hg, Co et Cd) lors de la diagenèse précoce et l'évaluation de l'enrichissement et de la pollution de ces métaux dans les sédiments du plateau. Les résultats ont montré que les métaux traces sont probablement liés aux oxydes de fer et de manganèse ainsi qu'aux sulfures. Ni et Zn pourraient être impliqués dans l'adsorption et la coprécipitation avec les oxydes de Fe et de Mn. Le Cu semble être associé préférentiellement aux sulfures mais aucune corrélation claire n'a été trouvée. L'enrichissement et la pollution de ces métaux dans les sédiments du plateau ont montré une variabilité spatiale. La zone du delta du Danube a été enrichie en Ni, Cu et Zn tandis que la région d'Odessa s'est enrichie en Co et Cd. La pollution des sédiments du plateau allait de « non polluée » à « très fortement polluée ». Depuis la fin du 20e siècle, la teneur en métaux lourds des sédiments du plateau est restée stable dans la région d'Odessa mais a augmenté dans la région du delta du Danube.

Acknowledgements

My first step in the oceanography world started with a cruise in the Atlantic Ocean where I met Prof. Lei Chou. During this mission, we ran into a violent storm off Brest and it was at that moment that I decided that I would want to follow this oceanographic way. Why? Because when I saw how Prof. Lei Chou was working and was motivated, she gave me all the necessary encouragement to start my career in this field. When she offered a PhD scholarship funded by the FNRS, I said to myself that this topic is done for me and that I wanted to work with this wonderful woman. During our collaboration, Lei provided me with motivation to stay enthusiastic and passionate by the biogeochemistry. I am honoured to work and share with her during this last 5 years as collaborator and as a friend. I appreciated our parties in the lab, our tours to the Christmas market, all the time spent together during conferences in Paris, Vienna and Kiel, and cruises in the Atlantic Ocean, the Black sea and the Baltic sea. These are unforgettable memories.

I would like to express my thanks to my co-supervisor Prof. Nathalie Fagel with whom I discovered the world of geology. We spent a lot of pleasant times together to open the cores, cut and analyse them. Our teamwork allowed me to learn new methods of analysis. Our discussions have been stimulating and interesting, leading me to a new approach and way to think. Thanks to this ULB-Uliège joint PhD, I learnt how to organize my work between two different places and during these years she guided me and supported me while leaving me a great deal of autonomy.

I thank all the thesis committee members who guided me through all these years. They brought me their knowledge and helped me to develop more and more my ideas. Thanks to Prof. Sandra Arndt and Prof. Pierre Regnier for their constructive feedbacks with which I improved my research.

I would like to thank the team from Mast group: Marilaure Grégoire and Arthur Capet. They helped me in my research and supported me at each step of the way. Marilaure established a pleasant atmosphere in the teamwork and helped me to participate in conferences, workshop and summer school. I liked the interesting discussions with Arthur which allowed me to have a different approach to my research.

All my gratitude goes to Nathalie Roevros. She was present for me at each moment and helped me in all circumstances. I learnt from her scientific knowledge but especially from her

personality. Today, I am proud to spend these years with her as a colleague and as a friend. She was as my second mama.

I would like to thank the ULB-Uliège team where I have been supported and helped by many people. Thanks to my office-mates: Xuefeng Li (alias Daniel) and Hailong Zhang, Master students: Olaya, Sarah, Alice and Naman for their help in my research. Many thanks to the lab members: Julien Schneider for his support and his help for the construction of our sampling material, Michel Verbank, Vincent Carbonnel, Nicolas De Ville, Dragana Petrovic, Ludovic Schmidt. I dedicate a special thanks to Stephen Louis who was there for me as my friend. I liked our scientific discussions and enjoyed sharing with him Belgium beers and watching football matches. Thanks to SaÏda El Amri for her assistance and her nice discussions around the ionic chromatography.

I would like to thank the captains and crew members of R/V Belgica and R/V Mare Nigrum for their work and assistance during our missions.

Throughout these five years, I collaborated with many teams to analyze my samples and I would like to thank them: Florian Deman, Debany Fonseca Batista, Arnout from the VUB team; Kevin Wilkinson, Marc Aymot, Magid, Justine and Karim from Montreal University; Gilles Le Point and Nicolas Gatuso from the Uliège Oceanology lab.

I am grateful to all my dear friends from Brest. We all came from IUEM and today we are all around the world, but our links stay the same and I am proud to have friends like you all: Emi, Nono, Aurélie, Julian, Laura et Adeline.

Je veux remercier toute ma famille qui m'a supporté tout au long de ces années même si elle ne comprenait pas toujours ce que je faisais. Je veux dire un énorme merci à mes parents qui m'ont suivi et m'ont aidé pendant cette aventure. Aujourd'hui, je suis fière d'être là où je suis parce que tout ça, c'est grâce à eux.

A huge thank to my boyfriend, Ali, with all my heart. He is the person who has supported me from the beginning to the end in the good and less good moments.

Table of Contents

List of Figures

Chapter 3

Chapter 4

Chapter 5

Chapter 6

Appendix

List of Tables

Appendix

Chapter 1

Introduction

Ukrainian coast during the Emblas-II cruise in the Black Sea (credit photo: Andrey Zotov)

1.1. Oxygen distribution in marine environment

Dioxygen (O_2) is essential for sustaining the life of ecosystems and takes part in the major processes regulating the biogeochemical cycles of carbon (C) and associated elements (e.g., N, P, S). In marine systems, O_2 concentrations are controlled by several physical and biological processes taking place in the water column and in the sediments (Glud, 2008). Atmosphere, photosynthesis in the photic layer and the vertical and horizontal transport are contributors of oxygen inputs to the system. Conversely, oxygen is consumed by the respiration processes in the water column and in the sediments during the mineralization of organic matter and by oxidation of the reduced compounds. The vertical and horizontal transport as well as air-sea exchanges could strengthen the oxygen removal as shown in Figure 1.1 (Testa & Kemp, 2011). The balance between the input and removal varies in time and in space.

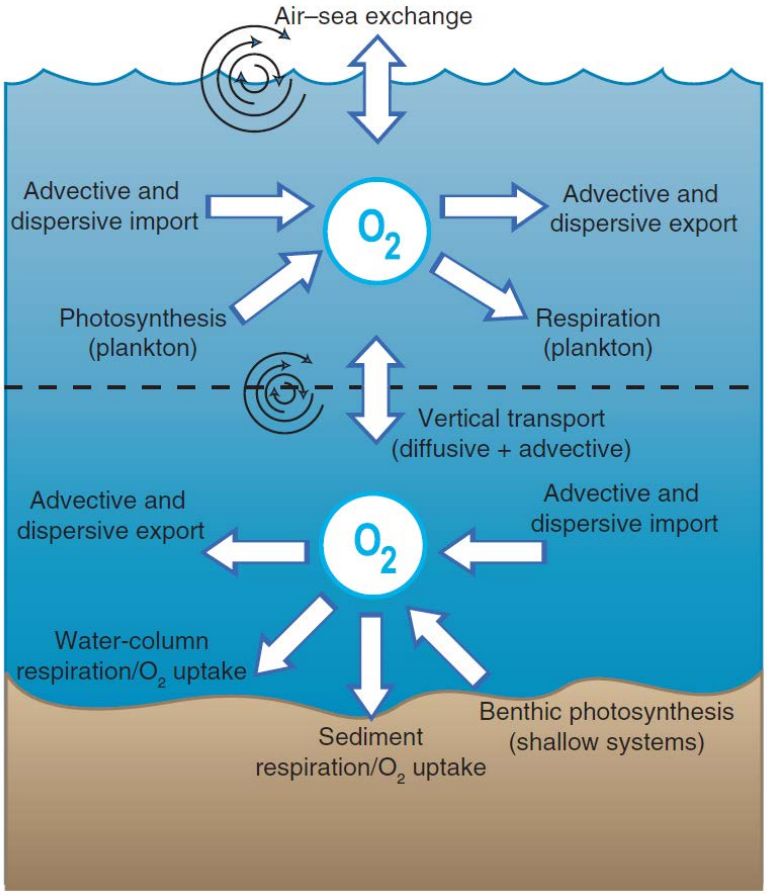

Figure 1.1. Biological and physical processes that regulate O2 concentrations in coastal waters (from Testa & Kemp, 2011).

During the Phanerozoic (from 542 million years ago to today), the oxygen level has experienced fluctuations which brought about oceanic hypoxia and marine biological crisis (Falkowski et al., 2011). In the Middle Devonian to Early Carboniferous (385 – 360 million years ago), anoxia of shallow continental seas coincided with an extended biotic crisis at a global scale. Another widespread anoxia both in shallow and deep waters was concurrent with a massive Permian-Triassic extinction event of marine animals 252 million years ago (Erwin, 2006). The extent of ocean circulation and ventilation are influenced by the continental configuration and by climate (Zhang et al., 2001). Indeed, Ocean Anoxic Events appeared when both the atmospheric carbon dioxide and the temperature were high. Furthermore, long-term events associated with other triggers such as the large-scale tectonic processes like volcanisms or outgassing of methane from sediments generated a massive extinction. For more recent times, the size of oxygen-depleted zones would contract or expand during a cold or a warm period respectively, showing that the expansion of anoxic zones was sensitive to climate change (Galbraith et al., 2004).

The latitudinal O_2 distribution is not uniform, however, and depends on primary productivity, physical mixing and solubility. In high latitudes, waters are well oxygenated because of the higher solubility in colder waters (Figure 1.2A). Conversely, oxygen depleted areas are often developed in deep basins, fjords and near continental margins with oxygen minimum layers (Rabalais et al., 2002; Falkowski et al., 2011). Mid-water layers between 200 and 1000 m in the eastern Pacific Ocean, the south-eastern Atlantic Ocean and the northern Indian Ocean exhibit the largest deficiency in oxygen and are referred to as the oxygen minimum zones (OMZs) (Stramma et al., 2008). Within these systems, an upwelling would bring cold deep waters rich in nutrients to the photic layer simulating primary production and organic matter produced would sink to deeper layers and be respired (Helly & Levin, 2004). Moreover, shallow, coastal and estuarine zones are nowadays impacted by the increasing occurrence of hypoxia and anoxia (Figure 1.2B) due to anthropogenic activities (Rabalais et al., 2002).

A

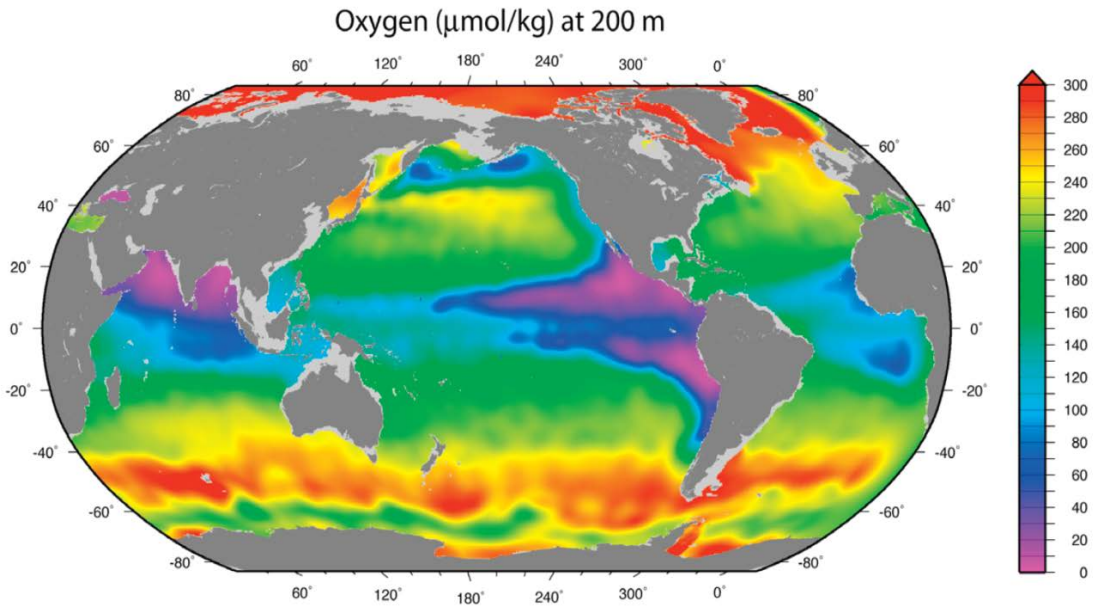

B

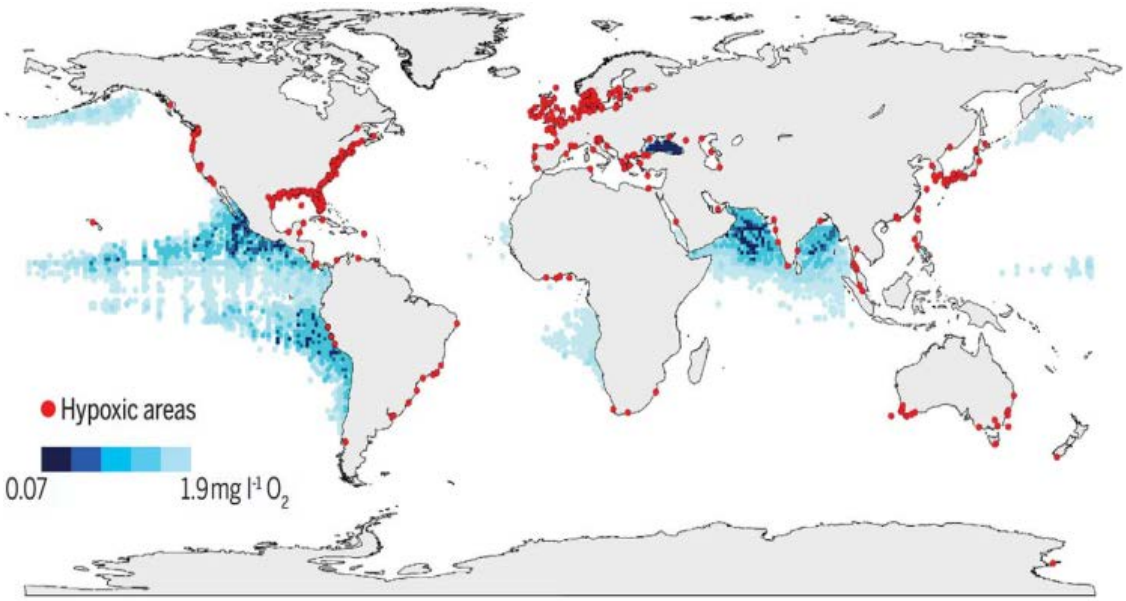

Figure 1.2. (A) Mean global ocean oxygen concentrations at 200 meters below the surface using data from the World Ocean Circulation Experiment Global Hydrographic Climatology (modified by Falkowski et al., 2011). (B) Global map with coastal sites where anthropogenic nutrient inputs caused O_2 declines; red dots indicate hypoxic areas (O_2 < 2 mg L^{-1}) and blue shaded regions denote the ocean oxygen-minimum zones at 300 m of depth (modified by Breitburg et al., 2018).

1.2. Coastal hypoxia

1.2.1 Global carbon cycle and hypoxia development

The atmosphere, hydrosphere, geosphere and biosphere constitute the different reservoirs of our planet and are interconnected with each other. Chemical elements are subjected to biological, physical and chemical transformations exhibiting cyclic nature. Biogeochemical cycle of carbon is an important component of the Earth system and plays a major role in regulating the Earth's climate (Berner, 1981). Two-time scales are involved in the carbon cycle: the short-term cycle (days to thousands of years) and the long-term cycle (millions of years). During the short-term cycle, the carbon exchange between the atmosphere, the biosphere and the hydrosphere is fast. Photosynthesis (Eq. 1.1) participates in the fast cycle of carbon, which converts the light energy into chemical energy and synthesizes organic matter from carbon dioxide and water with the release of oxygen. The organic matter can be degraded by the process of respiration (Eq. 1.2) consuming oxygen and releasing CO_2 back to the atmosphere.

$$CO_2 + H_2O \rightarrow CH_2O + O_2 \qquad \text{(Eq. 1.1)}$$

$$CH_2O + O_2 \rightarrow CO_2 + H_2O \qquad \text{(Eq. 1.2)}$$

The atmospheric CO_2 and O_2 contents evolved over geological times, taking part in the long-term cycle. During the Archean, more than 2.5 billion years ago, the atmosphere was 100 to 1000 times richer in CO_2 compared to the present-day level and O_2 concentrations were in trace quantities (Figure 1.3). The rise of oxygen in Earth's atmosphere begin 2.7 billion years ago or earlier after the cyanobacteria came into existence, producing oxygen via photosynthesis and altering the atmospheric composition (Brocks et al., 1999). During the early history of the Earth, the reducing atmosphere contained no free oxygen, which evolved into an oxidizing state after the massive oxygenation due to photosynthesis, named as the 'Great Oxidation Event' (Holland, 2002). This transition represents the evolution of photosynthesis and demonstrates the importance of this process in the global biogeochemical cycles.

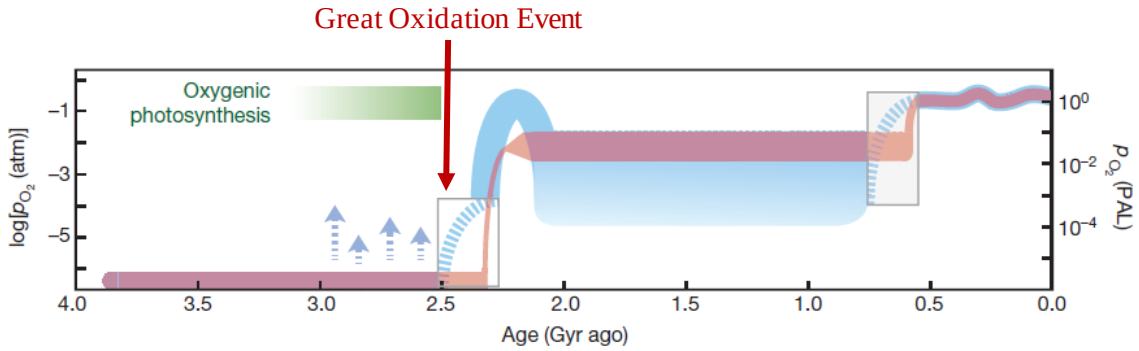

Figure 1.3. Evolution of atmospheric oxygen partial pressure (modified after Lyons et al., 2014).

After the Great Oxidation Event, O_2 levels fluctuate in the atmosphere, reflecting an imbalance between the photosynthesis and the respiration (Figure 1.3). A net production of organic matter and oxygen indicates that the photosynthesis has a greater weight than respiration. If all the organic matter produced during photosynthesis is consumed by respiration, the atmosphere will not be enriched in oxygen. When plants or phytoplankton die, these organisms are decomposed by micro-organisms engendering a releasing of CO_2. This process is called (re)mineralization and takes place in the oceans as well as in marine sediments and terrestrial soils. Not all the organic carbon produced by photosynthesis is mineralized and a small fraction is buried on the floor (Burdige, 2007). For the short-term carbon cycle, this fraction is negligible while for the long-term cycle, this fraction becomes important because it induces atmospheric CO_2 and O_2 variations (Burdige, 2007).

The biosphere reservoir plays a role in the storage of the carbon but at shorter time scales compared to the seafloor because carbon undergoes erosion by the rivers and can be transported to the oceans. In contrast, the seafloor is involved in both the short- and the long-term global carbon cycle and carbon is preserved in the seabed over geological time scales (Middelburg & Meysman, 2007). Escaping from mineralization after deposition, the organic carbon gets buried in the sediments. With time deeper in the sedimentary column, organic carbon could undergo transformations and become kerogen or fossil fuels. Yet, organic carbon in marine sediments can become re-oxidized if it is exposed to groundwaters or after several million years to the air due to the tectonic movements. Thus, the balance between the

burial and the re-oxidation of marine organic carbon leads to variations of O_2 and CO_2 concentrations in the atmosphere (Berner, 1989).

Carbon burial on the seafloor, a crucial component of the carbon cycle on longer time scales, creates a leak in the short-term cycle. Oxygen concentration fluctuates in the short term in the oceans and particularly in the shelf areas, influencing the degradation of the organic matter. When the concentrations of dissolved oxygen are low, less than 63 µM (2 mg L^{-1}), a hypoxia is considered to be developed. Coastal oxygen depletion is a global event as shown in Figure 1.2B and many shelf seas like the Gulf of Mexico, the Baltic Sea and the Black Sea are affected by hypoxia. Semi-enclosed seas, fjords and enclosed basins present a limited renewal of bottom waters and long residence times that promote oxygen limitations. The shallow waters in the shelf regions and coastal zones are also sensitive to this natural phenomenon and thus coastal environments are prone to hypoxia. On top of this natural cause, the ongoing increase of coastal hypoxia has also been induced by anthropogenic activities (Figure 1.4) (Kemp et al., 2005; Diaz & Rosenberg, 2008). Consequently, deoxygenation is the environmental response to a series of natural and anthropogenic causes.

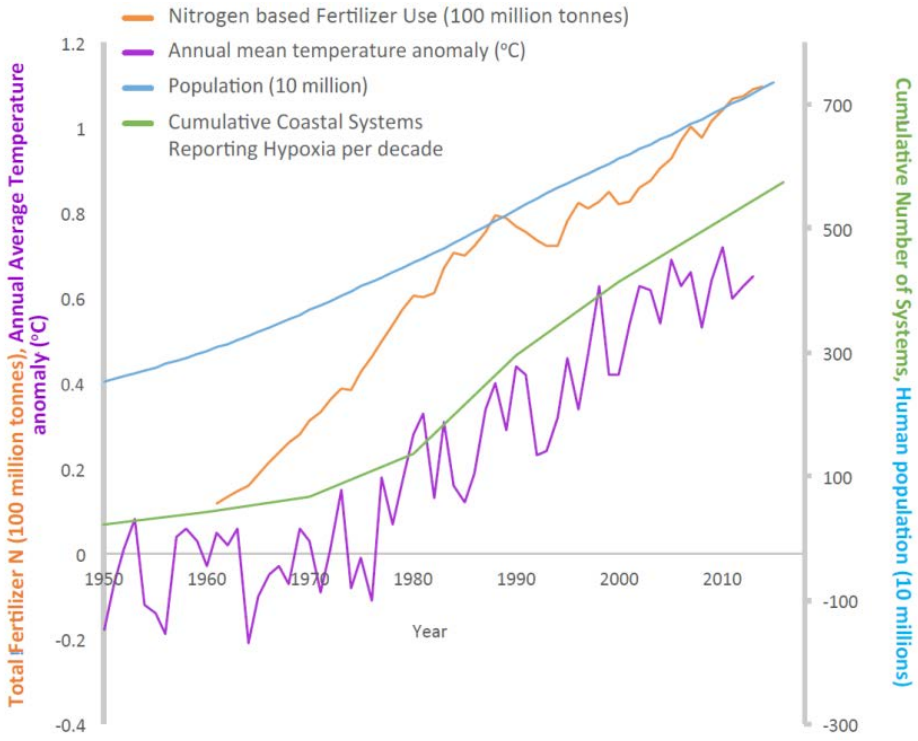

Figure 1.4. Evolution of the cumulative number of coastal hypoxic systems associated with eutrophication since 1950, as well as the use of nitrogen fertilizer, annual mean temperature anomaly and population growth (from Isensee et al., 2016).

The occurrence of hypoxia is associated with eutrophication resulting from excessive nutrient inputs (Figure 1.4). Following the massive inputs from rivers, phytoplankton blooms develop. After the collapse of the bloom, algae sink to the bottom providing a rich food source for bacteria which consume dissolved oxygen in the bottom waters to decompose this organic matter (Figure 1.5). Moreover, the stratification of the water column, especially during summer, accentuates the development of hypoxia. These phenomena take place on different time scales, which could be annual, periodic or an isolated event (Diaz & Rosenberg, 2008).

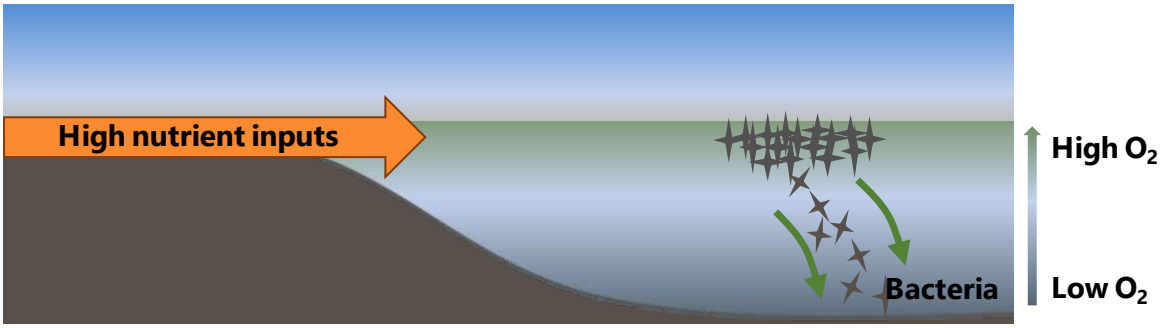

Figure 1.5. Simplified scheme of hypoxia development in a shallow system.

1.2.2 Early diagenesis

The upper layer of the seafloor occupies an important place in the mineralization of organic matter. The process named 'early diagenesis', as defined by Berner (1980), refers to '*changes occurring during burial to a few hundred meters where elevated temperatures are not encountered and where uplift above sea level (or lake level) does not occur, so that the pore spaces of the sediment are continually filled with waters*'. Early diagenesis takes place in different types of sedimentary environments. In the present study, the focus is placed on the diagenetic processes in the coastal sediments. Coastal ocean is defined as the continuity of the continental shelf with a water depth from 0 to 200 m (Convention on the Continental Shelf, 1958). Coastal zones, including estuaries, constitute the interface between the land and the ocean and receive important inputs from the land by rivers. In these regions, high fluxes of organic matter to the sediments are often observed, contributing to a high intensity of early diagenesis. Due to the substantial loading from rivers and the chemical fluxes across the sediment-water interface, coastal areas are fertilized and constitute a carbon sink (Chen & Borges, 2009; Cai, 2011). In addition, the residence time of organic matter in the water

column is shorter compared to the open ocean, leading to a high export of organic carbon produced in the photic zone (between 15 and 50%) to the sediments in the coastal zone (Canfield et al., 1993a; Wollast, 1998). With these characteristics of coastal sediments, organic matter is mineralized from the first millimetres (Glud, 2008). Organic carbon has an oxidation state of 0 and will be oxidized according to the diagenetic sequence (Burdige, 2006). Oxygen is the most favourable electron acceptor in terms of Gibbs free energy yield for the mineralization of organic matter. Once the oxygen is consumed, other electron acceptors are used such as nitrate (NO_3^-), manganese oxides (MnO_2), iron oxyhydroxides (FeOOH) and sulphate (SO_4^{2-}). In reality, this succession of reactions is more complex, and the different zones are overlapped (Canfield et al., 1993a). The origin and reactivity of organic matter can influence the reaction rate and the transport processes.

1.2.2.1. Early diagenesis: aerobic pathways

Oxygen is the first oxidant to be used in the oxic mineralization of organic carbon because it provides the maximum of energy to organisms. Within the first mm, O_2 is consumed either by oxic mineralization or by re-oxidation of reduced compounds liberated by anaerobic pathways of diagenesis. Therefore, oxygen is a good tracer to estimate the organic matter mineralization if all reduced species are re-oxidized by oxygen in the sediments (Glud, 2008). In deep-sea sediments, organic carbon inputs are generally low which makes aerobic respiration the main pathway in the mineralization of organic matter (Burdige, 2011). In contrast, shallower sediments, receiving higher inputs, are prone to anaerobic pathway.

In coastal sediments, oxygen penetration depth (OPD) is only a few millimetres. The determination of OPD needs technical measurements with high resolution. The use of a microelectrode allows the detection of the presence of a thin layer over the sediment, called Diffusive Boundary Layer (DBL), through which the transfer of dissolved material is achieved via molecular diffusion. The thickness of the DBL, rarely exceeding 1 mm, depends on the rugosity of the sediment and the water stirring at the sediment-water interface.

1.2.2.2. Early diagenesis: anaerobic pathways

Below the oxic layer, the processes of anaerobic mineralization take place. The first step is realized by the nitrate reduction which may lead to denitrification with production of CO_2 and N_2 or to the dissimilatory nitrate reduction to ammonium (DNRA) also known as nitrate ammonification. In addition, organic nitrogen, introduced to sediments by allochthonous or autochthonous mechanisms, may be remineralized bringing more ammonium (NH_4^+) within

the sediments. Once nitrates are consumed, manganese oxides reduction is followed by dissimilatory iron reduction releasing Mn^{2+} and Fe^{2+}. When all these oxidants become depleted, sulphate reduction takes place and generates sulphides creating a sulphidic zone (Froelich et al., 1979). Thus, the anaerobic mineralization of organic carbon releases dissolved reduced species such as NH_4^+, Mn^{2+} and Fe^{2+} which will be transformed in the sediments or released to the water column. In the sediments, ammonium can be oxidized in two ways, either aerobically by bacteria and archaea (Wüchter et al., 2006) or anaerobically by anammox process (Strous & Jetten, 2004). Dissolved iron and manganese can be oxidized by microbes using oxygen or nitrate as electron acceptors, reproducing the oxidized form of these metals. There exists thus a continuous cycle of each element trapped between oxidized and reduced forms at different depths called a redox shuttle (Scholz et al., 2014).

In coastal sediments, organic carbon inputs are high and prone to the anaerobic pathways in the mineralization processes. The high carbon loading and also the high production of reduced compounds create a more important oxygen demand than oxygen supply (Stoetaert et al., 1996). In unbioturbated sediments, sulphate reduction (Eq. 1.3) is the dominant pathway because of the abundance of sulphates in the seawater compared to other oxidants (Jorgensen, 1977). This process leads to an accumulation of a large pool of metal sulphides in sediments and/or free sulphides in porewaters (Figure 1.6) (Jorgensen, 1982).

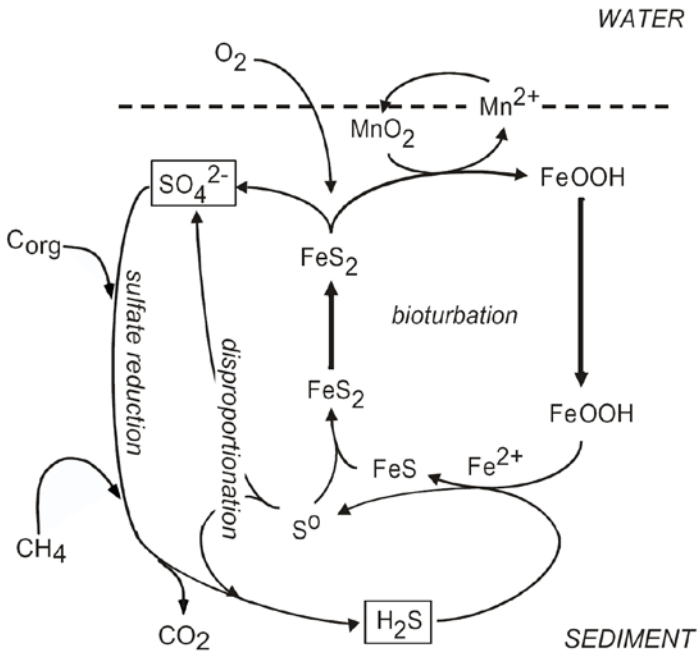

Figure 1.6. Sulphur and iron cycle in bioturbated marine sediments (from Jorgensen & Nelson, 2004).

$$2\,CH_2O + SO_4^{2-} + 2\,H^+ \rightleftarrows 2\,CO_2 + H_2S + 2\,H_2O \qquad \text{(Eq. 1.3)}$$

$$\frac{1}{2}\,H_2S + O_2 \rightleftarrows \frac{1}{2}\,SO_4^{2-} + H^+ \qquad \text{(Eq. 1.4)}$$

When the sulphate reduction occurs, free sulphides are produced and move up through the sediments until they are oxidized (Eq. 1.4). Temperature, pH and ionic strength affect the rate of oxidation of hydrogen sulphide which can be rapid (Millero et al., 1987).

The fraction of free sulphides which are re-oxidized is smaller than the production of free sulphides by the sulphate reduction leading to an imbalance between these two reactions (Eq. 1.3 and Eq. 1.4). This disproportion tends to reduce the consumption of oxygen for the re-oxidation of sulphides. The sedimentary sulphur cycle presents the same leak as the short-term carbon cycle allowing the burial of reduced sulphur, which is closely linked to the iron cycle. Free sulphides in the porewaters react with iron (hydr)oxides and precipitate instantaneously as mackinawite (FeS) (Eq. 1.5) (Rickard, 2006). The mackinawite is a metastable iron mineral and will be converted into the more stable pyrite (FeS_2), which will get buried (Rickard & Luther, 2007). The pyrite pool in the seabed represents 10-25% of reduced sulphides produced by sulphate reduction (Bottrell & Newton, 2006). The iron sulphides produced in the anoxic zone may be transported to the surface of the sediments and be re-oxidized (Eq. 1.6) due to the bioturbation. The efficiency of re-oxidation of reduced forms of sulphur depends on bioturbation stimulating the contact between reduced and oxidized compounds.

$$3\,H_2S + 2\,FeOOH \rightleftarrows S^0 + 2\,FeS + 4\,H_2O \qquad \text{(Eq. 1.5)}$$

$$FeS + \frac{9}{4}\,O_2 + \frac{3}{2}\,H_2O \rightleftarrows FeOOH + SO_4^{2-} + 2\,H^+ \qquad \text{(Eq. 1.6)}$$

Carbon and sulphur cycles are also coupled to other biogeochemical cycles such as nitrogen, iron and manganese through the degradation of organic matter. The seafloor plays thus an important role in the biogeochemical cycling of elements.

1.2.2.3. Effect of low oxygen concentration in bottom waters on diagenetic pathways

Organic matter is mineralized following the sequence of redox reactions regulated by oxygen. The fluctuation of oxygen concentrations impacts the metabolism of microorganisms involved in the diagenetic reactions and also the secondary redox reactions taking place in the sediments or the porewaters (Glud, 2008; Conley et al., 2009; Kemp et al., 2009). Oxic respiration is directly affected by the depletion of oxygen in the bottom waters, and thus would be inhibited with a reduction of the gradient of oxygen concentration at the sediment-water interface and a shallower oxygen penetration depth. Regarding the nitrification-denitrification, these reactions are limited by the availability of oxygen (see section 1.2.3).

Organic carbon loading, bioturbation and also bottom water oxygen levels influence the formation of iron and manganese oxides (Thamdrup et al., 1994). Oxygen depletion causes a reduction of the thickness of the oxic zone in the sediments and hence dissolved compounds, such as Fe^{2+} and Mn^{2+}, are diffused from the porewater to the water column. This upward diffusion contributes to an increase in the pool of dissolved Fe and Mn in the bottom waters, rendering them more depleted in the hypoxic sediments (Konovalov et al., 2007). Owing to the shallower oxygen penetration depth, re-oxidation of reduced species becomes less efficient, reducing the precipitation of Fe and Mn oxides, recycling efficiency and thus the contribution of oxides to organic matter mineralization. Fe and Mn cycles are linked to the S-cycle differently. Aller (1988) showed that the reduction of Mn oxides could be coupled to the oxidation of reduced sulphur compounds. However, Suess (1979) attested that precipitation of manganese sulphide is unexpected and typical of anoxic marine waters under particular conditions. Regarding the iron, its interaction with reduced sulphur involves the formation of iron sulphides which are important in the biogeochemical processes (Berner, 1984). The presence of authigenic form of iron sulphide, the pyrite, caused by the presence of sulphate and organic matter, without who the reduction of sulphate to sulphide is not possible, helps to determine the anaerobic, sulfidic diagenesis (Berner, 1980).

Under hypoxic and anoxic conditions, sulphate reduction is the most important pathway in the decomposition of the organic matter in laminated sediments (unbioturbated) whereas iron reduction occupies a more important place in bioturbated sediments (Thamdrup et al., 1996). When oxygen levels become low, the dissolved reduced sulphur species are less oxidized inducing a larger fraction of buried sulphur as well as a greater fraction of diffused sulphide to the water column (Jorgensen, 1982). Several locations, with higher rate of releasing of

sulphide to water column and burying of sulphur, have been reported such as the Cariaco basin and the Black Sea (Lyons et al., 2003).

Sulphur oxidation is mediated by large bacteria (Luther III et al., 2011), e.g., *Beggiatoaceae*, when the sediment is mostly overlain by oxygen-poor waters. *Beggiatoaceae* are mainly localized at the interface between oxygen and sulphide in order to use oxygen as electron acceptor (Schulz & Jorgensen, 2001). Two steps are involved in the oxidation. During the first one, bacteria oxidize sulphides to produce elemental sulphur which is stored intracellularly (Eq. 1.6).

$$2\ HS^- + O_2 \rightarrow 2\ S^0 + 2\ OH^- \qquad \text{(Eq. 1.6)}$$

Other kind of *beggiatoaceae* are also found in the sediments, more precisely below the oxic zone, which are able to stock nitrate in their internal vacuoles and use it to oxidize sulphur (Eq. 1.7) in the anoxic zone of the sediment.

$$4\ HS^- + NO_3^-{}_{intracell} + 6\ H^+ \rightarrow 4\ S^0{}_{intracell} + NH_4^+ + 3\ H_2O \qquad \text{(Eq. 1.7)}$$

For both kinds of *beggiatoaceae*, the second step consists of oxidizing elemental sulphur to sulphate (Eq. 1.8).

$$2\ S^0 + 2\ H_2O + 3\ O_2 \rightarrow 2\ SO_4^{2-} + 4\ H^+ \qquad \text{(Eq. 1.8)}$$

Usually, these giant bacteria are present in abundance and cover the sediments to form microbial mats, leading to a reduced efflux of sulphide to the water column. These microbial mats contribute also to the formation of authigenic apatite in anoxic and hypoxic sediment (Schulz & Schulz, 2005).

1.2.3 Effect of hypoxia on nutrient exchanges at the sediment-water interface

Oxygen concentrations in the bottom waters has a direct impact on the sediment-water exchanges. At the sediment-water interface, the gradient of oxygen is lower at low oxygen concentrations than at elevated levels. Oxygen takes part in nutrient cycling, especially in key processes of the nitrogen cycle such as nitrification and denitrification. The reaction of nitrification requires oxygen and thus low oxygen concentrations would lead to an inhibition

of this process, limiting the denitrification. The contribution of denitrification is more or less constant in oxic or hypoxic systems, but the individual species involved are dependant of oxygen levels. When oxygen in the bottom waters decreases, ammonium flux increases on the account of the decreased re-oxidation of ammonium produced by the remineralization of organic matter. This may be due to the less efficient nitrification related to hypoxia, as well as to the higher mineralization rate and DNRA (McCarthy et al., 2008). Previous studies have reported increased ammonium effluxes under hypoxic conditions, e.g., Chesapeake Bay (Kemp et al., 2005) and Danish coastal systems (Conley et al., 2007). Nitrate influxes are impacted by both oxygen and nitrate concentrations in the bottom waters. Mostly, sediments are a source of NO_3^- under oxic conditions. Under hypoxic conditions, sediments can play two roles in the exchange of NO_3^- across the sediment-water interface. If the NO_3^- levels are important in the water column, sediments will behave as a sink whereas if nitrates are low and quickly consumed, sediments will behave as a source. In hypoxic systems with low NO_3^- concentrations, the denitrification rate lessens because the nitrification is limited and the denitrification cannot take place. Thus, the coupling of nitrification and denitrification is limited; nitrification requires oxygen and the low oxygen concentrations inhibit this reaction as a consequence the denitrification.

Phosphorus is a crucial element for the phytoplanktonic growth. Organisms use this nutrient during photosynthesis which will be incorporated into organic matter. Phosphorus may be regenerated during the decomposition of organic matter in the water column. In shallow systems, such as lakes, estuaries and continental shelves, the regeneration occurs preferentially in the sediment due to the shallow depth (Sundby et al., 1992). The seabed receives different forms of phosphorus which can be labile or refractory, organic or inorganic. Some of these species escape from the mineralization and are buried in the sediments. The regenerated forms, the least inert, are decomposed or dissolved in porewater. Decomposed species are reprecipitated in the sediments as authigenic phase or adsorbed onto metal oxides (Slomp et al., 1996). Under oxic conditions, phosphorus is mainly adsorbed on the insoluble oxides and hydroxides of Fe and Mn. In contrast, under hypoxic and anoxic conditions, dissolved inorganic phosphorus is released in porewaters due to the reductive dissolution of metal oxides, resulting in an upward diffusion or an accumulation of this nutrient in porewaters (Jilbert et al., 2011). When the dissolved phosphorus reaches the water column and is mixed into surface waters, the biological production can be stimulated and hence increase marine deoxygenation. Conley (2009) pointed out that the expansion of

hypoxia areas in the Baltic Sea reduced the burial and absorption of phosphorus in the sediments providing available phosphorus in the water column for the primary production.

1.2.4 Impact of hypoxia on the macrofaunal communities

Marine ecosystems are sensitive to oxygen depletion. The behaviour, physiology and ecology of invertebrate communities suffer from hypoxia. Below the conventional threshold of hypoxia, fixed at ~ 63 µM O_2, organisms are affected differently. This threshold varies according to the taxa and life stage but below this given concentration, most organisms are impacted (Steckbauer et al., 2011). The diversity and the density of these communities and also their activities such as bioturbation and bioirrigation are affected (Diaz & Rosenberg, 1995). In the seasonal hypoxic or anoxic systems, when the shift from normal levels of oxygen (normoxia) to hypoxia occurs, the species abundance declines rapidly due to migration of the largest mobile species to areas where the oxygen levels are higher. Conversely, the mortality of sedentary species increases (Levin et al., 2009). Hypoxia has major consequences on the bioirrigation and bioturbation. Indeed, activity of organisms is restrained which influences the burrow depth as well as the particle mixing, modifying the flow dynamics at the sediment-water interface. Furthermore, the emission of hydrogen sulphide from sediments affects the organisms and leads to a higher mortality of these organisms. After the period of oxygen depletion, the species recolonize the environment with mainly juvenile organisms and larger species arrive later.

1.3. Paleoenvironment study: multiproxies approach

Eutrophication, one of the adverse environmental impacts of human activities, began thousands of years ago with an increase in intensity and frequency during the 20th Century (Jackson et al., 2001). Analysis of proxies in the sediments provides information on environmental changes, in particular, a glimpse of natural conditions of the past. To reconstruct the history of bottom hypoxia, a variety of biological, sedimentary, mineralogical or geochemical proxies can be applied to the sedimentary records.

1.3.1 Faunal indicators

Microfossils have been used for many years as indicators of environmental conditions in the past (Murray, 2001; Sen Gupta, 1999). Many dominant macrofaunal and meiofaunal groups,

such as polychaeta and nematodes, are almost never preserved in the sediment. However, small benthic organisms, such as foraminifera and ostracods, are preserved and used to trace the response of benthic communities to environmental changes (Alve, 2003; Fernandes Martins et al., 2010; Zaïbi et al., 2012). The main advantage of the use of microfossils is that it is possible to find them even in small samples and everywhere, but they are light and can be laterally transported. Foraminifera and ostracods are usually present in layers deposited under oxic conditions. However, during an extended anoxic period, microfossils would be absent in the sediments unless allochthonous microfossils were transported laterally. If there are re-oxygenation events during the anoxic phase, microfossils will be representative for the most oxygenated phases. Thus, an alternation between oxic and hypoxic conditions leads to a complex mixture of fauna (Alve, 2003) .

Foraminifera are present in all marine environments and are abundant on seafloor off major rivers and other productive areas (Arnold & Parker, 1999). Being sensitive to hypoxia or other environmental conditions and more tolerant than metazoans of oxygen depletion, they are used for paleo-reconstruction of bottom water hypoxia. Some of the foraminifera are also resistant to severe hypoxia and short-term anoxia. They disappear if the anoxia lasts too long bringing about the production of the hydrogen sulphide gas by sulphate reduction (Schmiedl et al., 2003; Alve, 1990). In hypoxic environments, the richness of species is low, and few hypoxia-tolerant species such as *Rotaliida* dominate. The decrease in species richness and the dominance by a single species may be an indicator of oxygen depletion in the bottom waters. The variation in the abundance of foraminifera is linked to organic matter flux to the seafloor if the sedimentation rate remains constant. The species *Ammonia* is known to be resistant to severe hypoxia and dominant in brackish, polyhaline estuarine and coastal environments. For examples, Thomas et al., (2000) showed the increase of *Ammonia* species and a decrease of the diversity between 1960 and 1990 in Long Island Sound, attributed to seasonal anoxia and eutrophication. Variations of *Ammonia* were observed in Chesapeake Bay also in the late 20th century, which was linked to the fertilizer use, nutrient loadings and oxygen depletion in the bottom waters (Karlsen et al., 2000). Thus, foraminifera respond to environmental parameters in coastal environments such as quantity, quality and regularity of food inputs, salinity, currents, wave activities and oxygen concentrations.

1.3.2 Sulphur and sulphides

Berner (1984) used concentrations of native sulphur and sulphides as proxy of bottom water oxygenation. In the absence of oxygen, organic matter is degraded by other electron acceptors such as nitrate, metals oxides and sulphates (Froelich et al., 1979). Sulphate reduction is an important process in the diagenesis of the organic matter, which produces hydrogen sulphides. Once this gas is generated, it reacts with reactive iron minerals or is oxidized chemically or biologically. The presence of oxygen determines the importance of the re-oxidation of the hydrogen sulphide. Thus, oxygen limitation in hypoxic or anoxic bottom waters promotes the formation of iron or other metal sulphide minerals. The correlation between organic carbon and reduced sulphur contents in the sediments has been used as proxy of bottom water oxygenation. Studies conducted in the Chesapeake Bay show that eutrophication and thus hypoxia contribute to the formation of pyrite (Cooper & Brush, 1991). The texture of minerals gives also information on the bottom water oxygenation (Wilkin et al., 1996). The formation of pyrite framboids requires limited amount of oxygen. The size of the pyrite framboids is small (< 5 μm) if they were formed close to the oxic-anoxic interface in the water column while their size becomes bigger if they were formed close the oxic-anoxic boundary in the sediments (Brunner et al., 2006).

The ratio of acid volatile sulphide (AVS: FeS) to chromium reducible sulphur (CRS: FeS_2) can also provide indications on the bottom water conditions. The conversion from AVS to CRS requires oxidant and time (Jorgensen & Kasten, 2006). Zimmerman and Canuel (2000, 2002) have used the AVS:CRS ratio to identify anoxic events in the Chesapeake Bay. However, in order for this ratio to be used, the sedimentation rate has to remain constant so that the indications found will not be biased.

To identify hypoxic episodes in ancient and modern sediments, the degree of pyritization (DOP) (Eq. 1.9) or the degree of sulphidization (DOS) (Eq. 1.10) have been used by Raiswell et al. (1988) and by Wijsman et al. (2001) according to the following equations:

$$DOP = \frac{Fe_{pyr}}{Fe_{pyr} + Fe_H} \qquad \text{(Eq. 1.9)}$$

$$DOS = \frac{Fe_{pyr} + Fe_{AVS}}{Fe_{pyr} + Fe_H} \qquad \text{(Eq. 1.10)}$$

where Fe_{pyr} is the iron contained in the pyrite, Fe_H is the reactive iron that has not yet reacted with sulphide, Fe_{AVS} is the iron associated with the AVS fraction. A good correspondence between the degree of pyritization and eutrophication was highlighted in a study on the Chesapeake Bay (Cooper & Brush, 1993).

1.3.3 Trace elements

Under hypoxic or anoxic conditions, sediments are enriched in trace elements which can be used as indicator of bottom water oxygenation (Tribovillard et al., 2006; Calvert & Pedersen, 2007). Comparison of the element/Al ratio of sediments with that of a reference material such as crustal material allows the assessment of the enrichment of trace elements in sediments. In non-hydrothermal environments, excess of trace element is attributed to organic matter inputs associated to biogenic phase (Ba, Cd, Ni, Zn, Cu) or to diagenetic enrichment (Re, Mo, V, U). Trace metals such as Ba, Cd and Zn are used as proxy of eutrophication and Re, Mo, V and U as proxy of hypoxia (Calvert & Pedersen, 2007; Tribovillard et al., 2006). The latter ones exhibit higher concentrations in deoxygenated environments due to the fact that their reduced forms are less soluble than their oxidized forms. Re, V and U are reduced under less reducing conditions compared to Mo which requires sulphidic conditions. Thus, the distinction between suboxic/anoxic and euxinic environments can be made thanks to the different behaviour of trace elements.

1.3.4 Sedimentary geochemistry

Hypoxic areas are prone to high accumulation of total organic carbon (TOC) in modern sediments. TOC increase can be translated into a short-time decomposition, a rise of primary productivity, an increase of allochthonous organic matter loading or an intensification of oxygen depletion or all of the above. Previous studies (e.g., Pinturier-Geiss et al., 2002) have related the increase of TOC to eutrophication and oxygen depletion. For instance, in the Baltic Sea the authors attributed the elevated amount of TOC to primary production and eutrophication, and in the Chesapeake Bay to oxygen depletion via DOP and AVS:CRS ratio (Struck et al., 2000; Andrén, 1999; Cooper & Brush, 1993).

1.4. The Black Sea

1.4.1 General description: origins, morphology and inputs

The Black Sea is one of the largest and deepest semi-enclosed basins, located between south-eastern Europe and Asia Minor. Its area covers 423 000 km² and its maximum depth is 2258 m (Kosarev & Kostianoy, 2007). The riparian countries of the Black Sea are Bulgaria and Romania to the west, Ukraine and Russia to the north, Georgia to the east and the Turkey to the south (Figure 1.7).

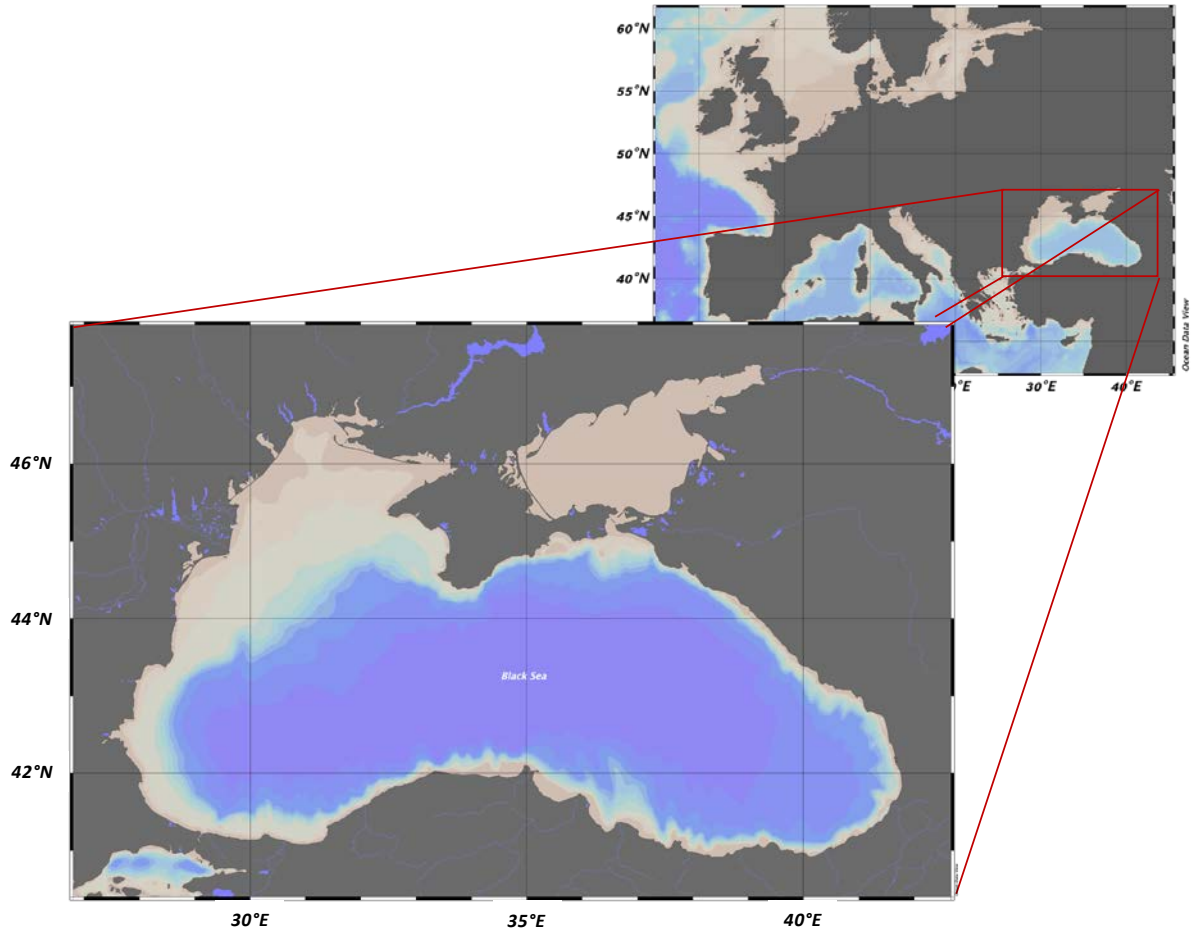

Figure 1.7. Map of the Black Sea (Ocean Data View).

Several hypotheses on the origins of the Black Sea were formulated over time. The first ages estimated by the different authors varied significantly, from Precambrian to Inferior-Quaternary. The Black Sea basin is considered as a vestige of Tethys Ocean. Geological data confirmed the oceanic nature of the basin, considered as an old oceanic basin dated

Precambrian, Paleozoique (Dewey et al., 1973) and Inferior-Mezoique (Gorur, 1988). In the 1970s, Hsü (1977) and Letouzey (1977) emitted the hypothesis that the opening of the Black Sea was due to the extension of back-arc basins. Indeed, two basins with different directions were highlighted and unified during the post-rift phases. The opening of the West basin is estimated to be Upper Barremian (Gorur, 1988) whereas that of the East basin, more recent, is dated Mid, Upper Paleocene (Robinson et al., 1995). The regions around these two basins were also impacted by the closing of the Tethys Ocean.

The Black Sea is composed of four types of seafloor morphology: the continental shelf, the continental slope, the basin apron and the abyssal plain. The shelf, characterized by a flat topography, covers ca. 25 % of the total area and is well-developed in the northwest. The platform is large, reaching a maximum of 190 km west of the Crimea. In front of the Romanian coast, it extends over 140 km at the mouth of the Danube river. For the other part, the shelf is narrow or non-existent in the south close to the Sakarya Canyon. The limit of the depth is marked by the isobath of 100 m (Ozsoy & Unluata, 1997). The continental slope covers ca. 27 % of the total area and two kinds of slopes can be distinguished (Ross, 1974, in Panin & Jipa, 2002). The first one is abrupt, around 2.5 %, and is located in front of Caucasus, Turkish regions and in the south of Crimea. The second one is less abrupt and can be found close to the West of Crimea and the South-east of Azov Sea. The limit of depth is the isobath of 1000 m. The basin apron represents ca. 31 % of the basin and is located at the basis of the continental slope. The apron has a slope varying from 0.1 % to 2.5 % and is located between 1000 m and 2000 m depth. Its width varies depending on the terrigenous inputs, with a maximum situated close to the Danube and Dnieper rivers. Finally, the abyssal basin represents more than 60 % of the total area and is characterized by a slope inferior to 0.1 % and a depth superior to 2000 m.

The waters of the Black Sea are nearly isolated from the global ocean. The Black Sea constitutes the main receptacle of the inputs from Central Europe and Eastern Europe. The sea is connected to the Azov Sea through the Kerch Strait to the northeast. To the southwest, the Black Sea is connected with the open ocean only by the Marmara Sea through the Bosporus Strait (Figure 1.7, Figure 1.8). The Turkish Straits system between the Black Sea and the Mediterranean Sea extends over 300 km with 31 km for the Bosporus Strait (width between 0.7 and 3.5 km and depth between 30 m and 110 m), 210 km for the Marmara Sea and 62 km for the Dardanelles Strait (Ivanov & Belokopytov, 2013; Kerey et al., 2004). The water exchange is limited but operates in both directions. Calculated fluxes for the water

output via Bosporus and Dardanelles Straits are positive (Figure 1.8). Indeed, ca. 600 km^3 yr^{-1} of water leave whereas ca. 300 km^3 yr^{-1} enter the basin (Ozsoy et al., 1995). The saltiest water (17.5 – 18.5 psu) is found in the surface flowing from the Black Sea to the Mediterranean Sea while the more saline deep waters of the Mediterranean Sea (35 psu) enter the Black Sea. Due to the absence of vertical mixing, the Black Sea is strongly stratified with an increase of salinity with depth to 22.33 psu (Murray et al., 1991). This permanent stratification of the water column leads to a depletion of oxygen in the bottom waters resulting in widespread hydrogen sulphide.

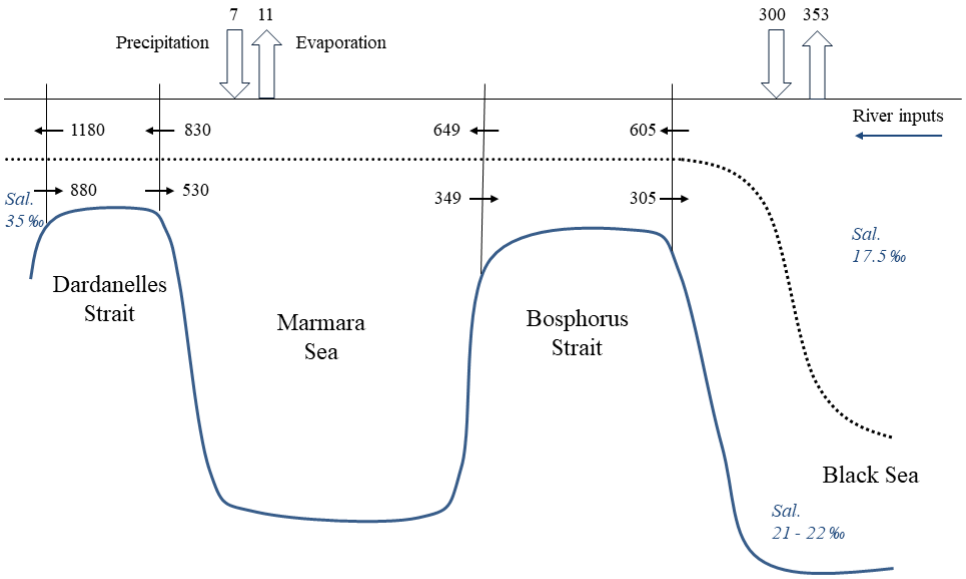

Figure 1.8. Water exchanges (km^3 yr^{-1}) of the Black Sea with the Mediterranean Sea as well as at the air-sea interface (from Ünlüata et al., 1990; Özsoy et al., 1995).

1.4.2 Evolution of the Black Sea during the Quaternary: the early stages of anoxia

During the Pleistocene, the Earth underwent climatic oscillations involving changes of climatic conditions (cold – warm period). The causes of these changes are linked in majority to variations of orbital parameters of the Earth and to changes of CO_2 concentrations in the atmosphere (Ehlers et al., 2011). Over cold periods, ice caps were developed and could be extended over the continent and the sea. They acted as a barrier to the river flow and also played a role in the sea level change, leading to modifications in the inputs in the basins, isolated or connected to the open ocean.

Several hypotheses were emitted about the last rise of water level during the Holocene. The first one, called the classical theory, evokes a gradual increase in water levels, mainly supported by Russian literature (Ross et al., 1970; Deuser, 1974). The authors stated that water levels of the Black Sea and Mediterranean Sea increased at the same time during the last deglaciation until the connexion was established through the Bosporus Strait. Salty waters of the Mediterranean Sea entered via a bottom current into the Black Sea, leading to a stratification of the water column and hence to anoxia in the bottom waters. The catastrophic theory (Ryan et al., 1997) hypothesized that the rise of sea level was faster after the last glacial maximum (14,000 years ago), inducing a flow to the Marmara and Mediterranean Seas. After the Younger Dryas, a new decrease of water level of 150 m occurred because of strong evaporation and low fluvial inputs until 7150 years ago (the supposed date of reconnexion). In the Mediterranean, the water level continued to increase to reach the threshold of the Bosporus Strait, suggesting the last rise of seawater level in the Black Sea. The third theory (Aksu et al., 2002) proposed an increase of water level in the Black Sea following the ice melting after the Younger Dryas. About 9500 years ago, the connexion by the Bosporus Strait was re-established by an outflux of freshwater from the Black sea and the influx of salty waters was stopped by the strong current from the Black Sea. During the period 7200 – 7000 years ago, mitigation of the current from Black Sea facilitated the influx current to enter the Black Sea establishing a two-way circulation regime at the Bosporus Strait. However, recently Yanko-Homback (2014) used different groups of organisms to study the evolution of salinity with time in the Black Sea and demonstrated that the marine level rise took place progressive.

1.4.3 Sedimentary deposits across the Black Sea basin

Sediments of the deep Black Sea basin are divided into three units over the Late Quaternary. The two first units - Unit I and II - represent the last marine stage deposited during the Holocene. Unit III refers to the last lacustrine stage. Unit I shows an alternation between white and black laminae. White laminae are characterized of coccolith-rich layers and testify a phytoplanktonic bloom during the summer-autumn. The black layer corresponds to deposits of terrigenous materials from fluvial discharges. Unit II is a sapropel-rich layer characterized by thin laminae of dark olive green to dark brown color. The organic matter found in this unit is of marine origin. Based on the studies of varves and ^{14}C data, Jones and Gagnon (1994) synthetized the previous results and indicated that the base of Unit I was dated 2720 ± 160

years BP and the base of Unit II was dated 7540 years BP corresponding to an anoxic regime in the deep basin. However, Soulet (2011) revised the calendar age of the last reconnection of the Black Sea lake to the global ocean, which was estimated to be at 8995 ± 145 cal years BP. Unit III was deposited during the oldest Pleistocene-Holocene and was characterized by laminated organic carbon poor clays. The dark laminae were formed by high concentrations of unstable iron-mono-sulphides.

The NW shelf extends over a width of 140 km at the mouth of Danube with maximum depths ranging between 100 m and 170 m. Sedimentary processes on the shelf are linked to river inputs, leading to a spatial variation of deposits on the continental plateau. In front of the Danube, two deposit zones are observed; the internal shelf is characterized by fine sediments that are brought to the south of the prodelta by the littoral current whereas the external shelf, also called the starving shelf, is a non-accessible zone for the river loading with a biogenic origin of sediments. To the North, the area is weakly influenced by the inputs of the Dnieper and Dniester because the spits protect the sea from the inputs. Suspended sediments are deposited close to the river mouths and form a black muddy deposit of high organic matter content. Regarding the lithology, Unit I consists of mud rich in Modiolus which can be found between 50 m and 125 m depth. Unit II is composed of mud rich in Mytilus in majority and are covered again by Modiolus Unit. The last layer, Unit III, is named Dreissena mud, rich in freshwater to brackish water bivalves (Soulet et al., 2011).

1.4.4 Modern anoxia in the deep basin

After the intrusion of the salty waters of the Mediterranean Sea in the Black Sea, the water column can be divided in two parts creating a permanent double stratification in the deep basin. This stratification impedes the vertical mixing of oxygen, contributing to the development of anoxia. Due to the currents forming two main gyres in the central basin, three water masses can be distinguished (Capet et al., 2016b). At the surface, the water in contact with the atmosphere is oxygenated, less salty due to the river inflow, and warm but subjected to atmospheric temperature variations. On top of the permanent halocline, an oxygenated dense water mass called Cold Intermediate Layer (CIL), is formed by winter cooling and mixing (Staneva & Stanev, 2002). The deepest layer, consisting of Mediterranean water, is cooled upon contact with the CIL and a limited amount of oxygen is transferred from CIL to the bottom waters, which is too small to renew the oxygen in the deepest layer. Due to the absence of vertical mixing, the deep layer is depleted in oxygen leading to enrichment of

hydrogen sulphide. Thus, the central basin of the Black Sea is the largest euxinic basin in the world with an estimated flux of H_2S from the sediments to the water column comprising between 3.0 and 5.0 10^{12} g S yr^{-1}. This hydrogen sulphide would remain in the water column for 90-150 years which is comparable to the time necessary to exchange water between the oxic and the anoxic layers (Volkov & Neretin, 2008).

1.4.5 Evolution of the Danube Delta during Holocene

The Danube Delta was formed during the Upper Pleistocene and Holocene (Panin & Jipa, 2002; Figure 1.9). The interactions between the river and the sear during the last 12,000 years led to the current shape of the delta. Geomorphologic, textural, geochemical and mineralogical data as well as ^{14}C dating allowed the identification of the different stages of formation of the delta.

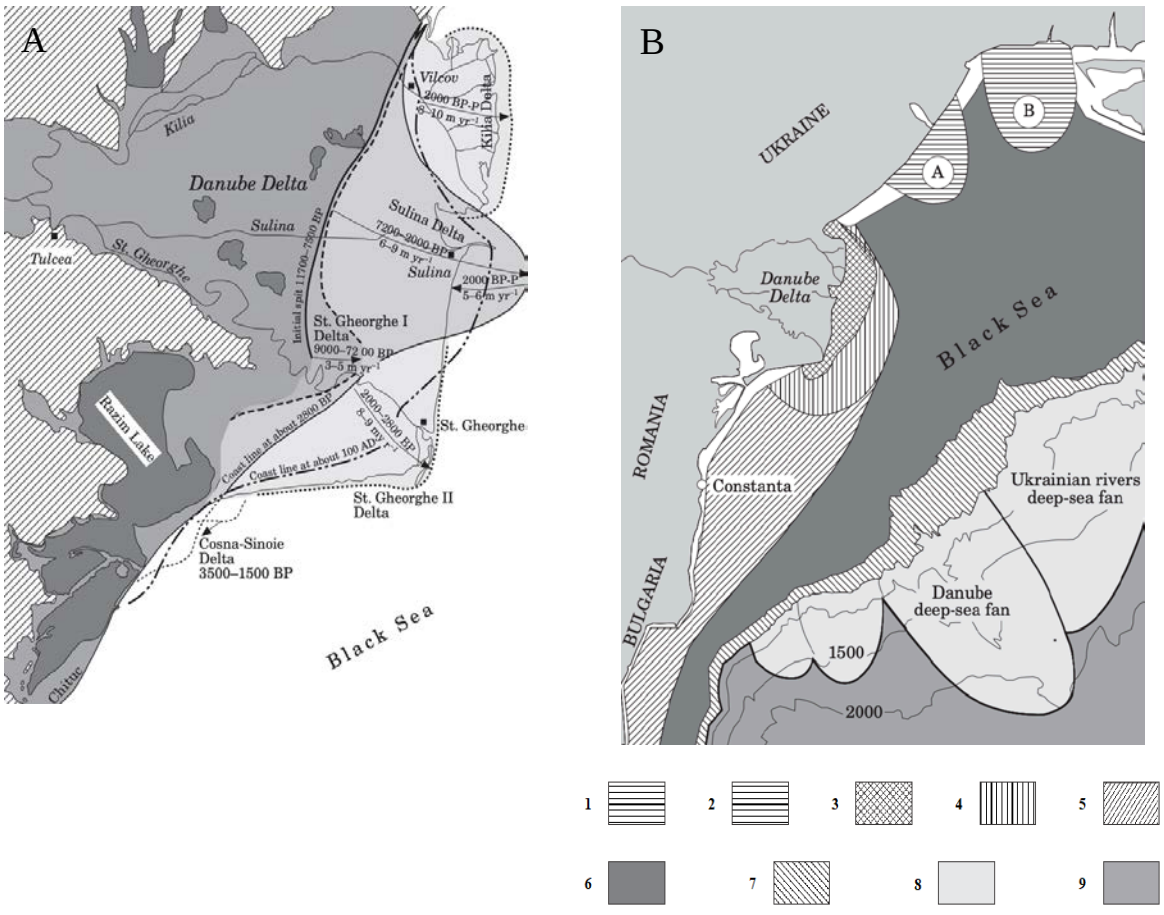

Figure 1.9. A) Evolution of the Danube Delta during the Holocene and B) Main sedimentary environments in the NW Black Sea. From Panin & Jipa (2002).
1-2, zones under the influence of Ukrainian rivers (A: Dniester, B: Dnieper); 3, Danube delta front area; 4, Danube prodelta area; 5-6, western Black Sea continental shelf area (5: area under the influence of the Danube originated sediment drift, 6: sediment-starved area); 7, shelf break and the uppermost continental slope zone; 8, deep-sea fan area; 9, deep sea floor area.

An alternation between active propagation and strong erosion was revealed, building the delta by step. At the beginning of the Holocene, the Danube flowed into a Gulf, named Gulf of the Danube, which had been closed with time by a spit on an axis orienting north-south. In the south of the spit, the first branch of the Danube (Paleo-St. Gheorghe) could flow into the sea forming the first delta: St. Gheorghe I delta. From 9000 years BP to 7200 years BP, the first delta progressed by ca. 8 km seaward. Over the next 5000 years, the depocenter migrated to the north and crossed the Sulina Delta by ca. 30-35 km. The last phase of the formation concerned the development of the Chilia and St. Gheorghe II Delta by extension offshore of ca. 16-18 km. At the same time, the Sulina Delta underwent a strong period of erosion leading to a regression of the coastline by 10-12 km. Nowadays, the Danube Delta is composed of three deposit systems: the deltaic plain, the delta front and the prodelta.

1.4.6 Current loading in the watersheds of the Danube and Ukrainian rivers

The Black Sea receives freshwater from several rivers. The discharge of the Danube, the Dnieper, the Dniester and the Southern Bug into the Black Sea represents ca. 70 % of freshwater inputs, ca. 75 % of which coming from the Danube (Panin & Jipa, 2002). The second longest river in Europe (more than 2800 km) after the Volga, the Danube is originated in Germany, in particular from the Black Forest Mountains. The Danube river passes through 15 countries and spans over 817,000 km^2. Before the construction of the dam, the annual average of the particulate flux from the Danube watershed was estimated to be 67.5 10^6 t yr^{-1} with ca. 10 % of sandy alluvial deposits (Panin & Jipa, 2002). The solid discharge is provided by three tributaries, Chilia (66 %), Sulina (14.5 %) and Sfântul Gheorghe (19.3 %). Following the construction of the first dam (Iron Gate I) during the 1970s, the sedimentary fluxes decreased to 30 10^6 t yr^{-1}, representing a reduction of ca. 30 – 40 % of the initial flux. Due to the construction of the second dam (Iron Gate II) in 1983, the Black Sea received only 50 % of the initial flux with 25-35 10^6 t yr^{-1}. Today, the sandy deposits represent only 4-6 10^6 t yr^{-1} and the major part of the sediments flowing into the Black Sea are silts (0.063 – 0.250 mm) (Panin & Jipa, 2002).

Ukrainian rivers discharge into lagoons that are separated from the sea by spits, reducing the sedimentary inputs into the Black Sea. The development of reservoirs in the Ukrainian region and the increasing use of water for irrigation, led to a reduced water discharge (Table 1.1).

Table 1.1. Fluvial water and sediment discharge into the Black Sea (Panin & Jipa, 2002).

Rivers	Length km	Drainage basin area km^2	Water discharge $km^3\ yr^{-1}$	Sediment discharge $Mt\ yr^{-1}$
NW Black Sea		1 455 800	255.7	56.85
Danube	2 860	817 000	190.7	51.70
Dniester	1 360	72 100	9.8	2.50
Dnieper	2 285	503 000	52.6	2.12
Southern Bug	806	63 700	2.6	0.53
Sea of Azov		500 400	42.9	14.80
Caucasian coast rivers			41.0	29.00
Anatolian coast rivers			29.7	51.00
Bulgarian coast rivers			3.0	0.50
Total			**372.3**	**152.15**

In 2015, a new assessment of nutrient loadings was made and showed that the Danube was the main river bringing high contents of nutrients (Table 1.2). The contribution of total nitrogen and total phosphorus represented 45 % and 30 %, respectively of the riverine inputs to the NW shelf. The Odessa region received 2050 tons per year of total nitrogen and 597 tons per year of total phosphorus from the Dniester and Dnieper rivers representing a low contribution of nutrient loading to the NW shelf (Ukrayinskyy et al., 2017).

Table 1.2. Riverine nitrogen and phosphorus loads to the NW shelf of the Black Sea assessed in 2015 (from Ukrayinskyy et al., 2017).

	Danube (Ukrainian part - 2015)	Odessa region (2015)	NW shelf (2015)
Nitrate ($t\ yr^{-1}$)	89 180	1 706	199 100
Nitrite ($t\ yr^{-1}$)	5 817	26	3 020
Ammonia ($t\ yr^{-1}$)	1 448	318	1 2680
Total Nitrogen ($t\ yr^{-1}$)	**96 445**	**2 050**	**214 800**
Total Phosphorus ($t\ yr^{-1}$)	**6 748**	**597**	**22 370**

1.4.7 Modern eutrophication of the NW shelf

Coastal eutrophication is caused by an excess delivery of nutrients by rivers due to human activities stimulating primary production (Gray et al., 2002). The increasing density of the phytoplankton communities triggers the benthic activities in the shallow areas, inducing the

development of hypoxia when the mixing of the water column is insufficient (Jackson et al., 2001). The NW shelf of the Black Sea constitutes a dramatic example of how the ecosystems can be destroyed by excess nutrient excess and also how they can recover (Capet et al., 2013; Langmead et al., 2009). Before the 1960s, the shelf was a highly productive system sheltering bottom-living brown algae and offshore red algae – *Phyllaphora* which got along with beds of bivalves, such as mussels. Algal production would oxygenate the bottom waters whereas the mussels filtered the seawater to maintain a good condition of light to allow the photosynthesis. Between the 1960s and the 1980s, the agricultural and industrial activities developed and the use of fertilizers contributed to the increased concentrations of nutrients discharged in rivers such as the Danube. Indeed, previous studies have shown that total inorganic nitrogen and the phosphorus fluxes increased between 1960s and 1990s (Almazov, 1961; Cociasu et al., 1996) contrary to the dissolved silicate which decreased during the same period due to the construction of the dam. All these inputs from the rivers to the Black Sea induced hypoxia on the shelf between 1973 and 2000 (Figure 1.10).

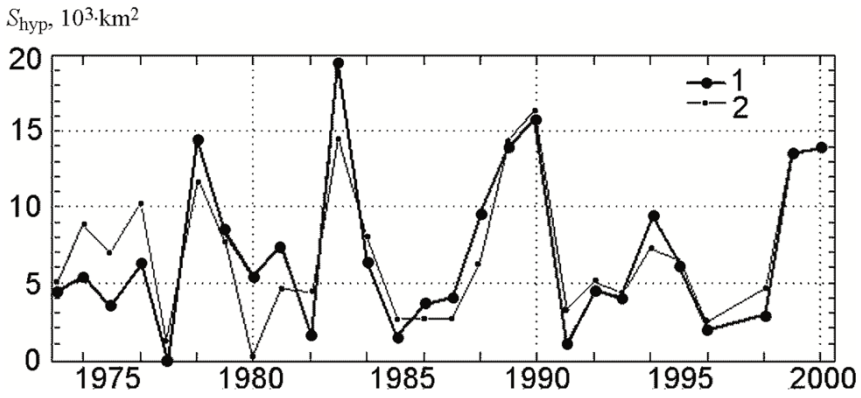

Figure 1.10. Interannual variabilities of surface areas of hypoxic zones (in 10^3 km^2) on the NW shelf of the Black Sea between 1973 and 2000. Large dots refer to observational data and small dots denote modeled data. From Ukrainskii & Popov (2009).

At the end of the communist regimes in Eastern Europe, the shelf ecosystems began to recover. The farmers could not afford to buy fertilizers and support the modernisation; thus, the agricultural activities became less intense leading to a decrease in nutrient runoff. Friedrich et al. (2002) highlighted that nitrogen and phosphorus loadings decreased between 1992 and 1997 whereas dissolved silicate remained stable during this period. The recovery has been gradual especially in the re-establishment of benthic communities. From 2008 onwards, the annual water discharge to the NW shelf fluctuated with peaks observed during

2010 and 2013 (Figure 1.11, Ukrayinskyy et al., 2017). The inputs of total nitrogen and total phosphorus follow the same trend as that of the annual water flux. Since 2013, the annual water discharge has decreased suggesting a new recovery of the oxic conditions of the NW shelf of the Black Sea.

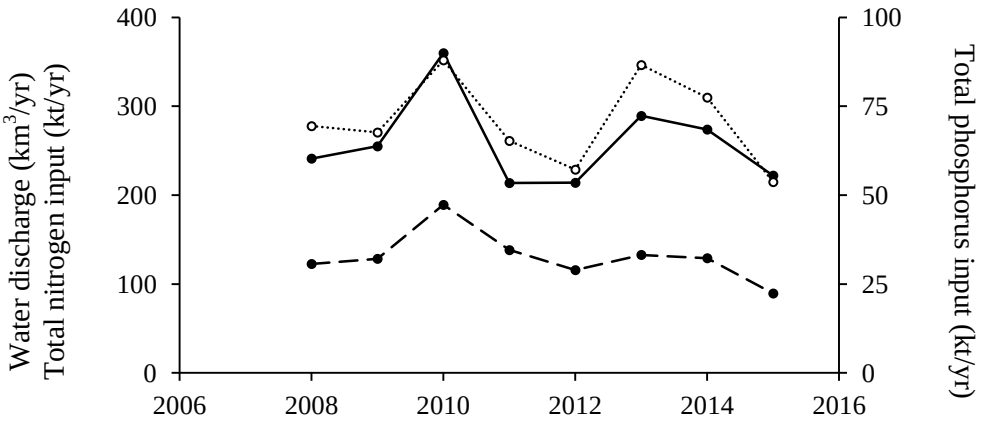

Figure 1.11. Temporal evolution of the annual water discharge (black line), total nitrogen (dotted line) and total phosphorus (dashed line) inputs to the NW shelf.

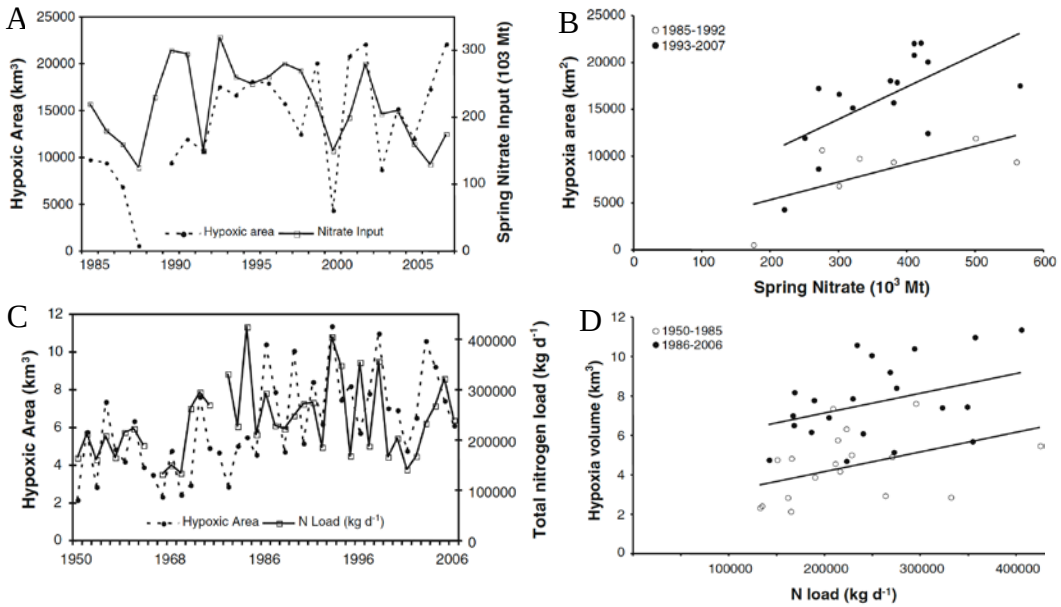

Figure 1.12. Temporal evolution of hypoxic area and nitrogen inputs in the northern Gulf of Mexico (A and B) and in the Chesapeake Bay (C and D). From Conley et al. (2009).

Other systems affected by bottom water hypoxia, such as the Chesapeake Bay and the Gulf of Mexico, were subjected over the years to variations in nutrient inputs and thus to a fluctuation of the hypoxic zone area (Figure 1.13). For example, in 1993 flooding was recorded in the

Mississippi river leading to an important increase of the hypoxic area in the Gulf of Mexico due to a higher sedimentary oxygen demand. Since 1993, the hypoxia has spread over 15 000 km^2 and has been linked to a smaller river flow. Furthermore, nitrogen inputs in the Gulf was studied and showed a correlation with the oxygen concentrations; an increase in the nitrogen loading would cause the spreading of the hypoxic zone. The same relationship was found in the Chesapeake Bay and other systems (Conley et al., 2009).

Furthermore, metallic components can affect the quality of waters and sediments and pose a threat of toxicity for ecosystems at certain levels of concentration. Heavy metals can be brought by various sources such as atmospheric depositions or river inputs.

Table 1.3. Heavy metal concentrations in the surface waters and in sediments of the NW shelf of the Black Sea in the past and in 2016 (From Denga et al., 2017). MAC-EQS: Maximum Allowed Concentrations – Environmental Quality Standards.

	Shelf		**MAC-EQS**	**Sediments**	
			Directive 2013/39/EU		
	Past ($\mu g\ L^{-1}$)	2016 ($\mu g\ L^{-1}$)	$\mu g\ L^{-1}$	Past ($\mu g\ g^{-1}$)	2016 ($\mu g\ g^{-1}$)
Hg	0.041	0.03	0.07	$0.05 \rightarrow 0.28$	$0 \rightarrow 0.409$
Zn	22.83	3.56		$30 \rightarrow 170$	$5.49 \rightarrow 180$
Ni	1.96	5.25	34		$0 \rightarrow 63.4$
Cu	21.63	0.32		$13 \rightarrow 85$	$0 \rightarrow 68.6$
Pb	3.56	0.20	14	$5.2 \rightarrow 46.2$	$4.39 \rightarrow 28.8$
Cd	0.56	0.00	1.5	$0.12 \rightarrow 0.49$	$0 \rightarrow 0.63$

During a survey in 2016, trace metals (Hg, Cd, Cu, Pb and Zn) were investigated in the surface waters and in sediments of the shelf (Table 1.3). The results were compared to the MAC-EQS of the Directive 2013/39/EU of European legislation and revealed no toxicity of these waters for most of these metals despite an increase over the years of Ni concentrations. In sediments, the range of concentrations increased in 2016 except for Cu and Pb but no standards were defined in the European legislation for sediments. In the same study, the Danube, Dniester, Dnieper areas and the Odessa Bay were qualified as polluted sediment areas due to the influence of the sewage discharges (Denga et al., 2017).

1.4.8 Benthic-pelagic coupling

On the NW shelf of the Black Sea, the nitrogen load in the surface waters is mostly related to the pelagic primary production while the degradation of organic matter in the benthic compartment is attributed to the early diagenesis. These two processes are responsible for maintaining the depletion of oxygen in the water column due to the difference between production and degradation cycles of organic matter. Indeed, the primary production occurs seasonally while the recovery of the sediment compartment via benthic diagenesis of organic matter is estimated to be 9.3 yrs after an important eutrophication event. The water column biogeochemistry is also affected by the benthic release of ammonium which consumes oxygen during its pelagic oxidation during the stratified period. Thus, the benthic respiration plays an essential role in the regulation of oxygen concentrations in the sediments and the water column (Capet et al., 2013).

In their modeling study of the Black Sea, Capet et al. (2016a) have shown that variation in environmental parameters could lead to modifications of diagenetic reactions and in turn to benthic-pelagic fluxes. On the shelf, the average annual carbon input to the sediment was estimated to represent 27 % of the net primary production, amounting to 404 Gmol C yr^{-1} (13 mmol C m^{-2} d^{-1}) and 90% of the depositional flux of organic matter was remineralized in the sediments. The authors have identified three regions on the shelf going from the coast to offshore which exhibit different mineralization rates of organic matter over the year with varying contribution of oxic vs. anoxic processes (Table 1.4). The benthic fluxes decreased with increasing distance from the coast. However, in all regions, the organic matter mineralization rates were lower in winter compared to summer-fall, presumably due to the low oxygen uptake in sediments as revealed by the low efflux of phosphate and inorganic nitrogen.

The authors showed also an important seasonality. For the region located near the coast, the organic carbon mineralization rate reached it maximum in October due to a progressive accumulation of fresh organic matter and the increase of bottom water temperature. For the most remote regions, this maximum occurred rather in May-June. These higher mineralization rates induced a rise of oxygen consumption and a larger ammonium release from sediments to the water column. Near the coast, the ammonium flux was estimated to be 10 times more important than in the other two regions. From summer to fall, this region was subjected to oxygen depletion in the bottom waters and led to an intensification of anoxic

processes of the organic matter degradation inducing a larger release of reduced species to the water column where they will be re-oxidized.

Table 1.4. Organic matter mineralization rate in mmol C m^{-2} d^{-1} and the contributions of oxic and anoxic mineralization in % on the shelf of the Black Sea (from Capet et al., 2016a).

Region	**Organic carbon mineralization rate** (mmol C m^{-2} d^{-1})	**Oxic mineralization** (%)	**Anoxic mineralization** (%)	**Denitirification** (%)
Coastal	25	18.3	76.0	5.7
Central shelf	9.8	41.8	51.9	6.3
Deepest part of the shelf	4.3	68.8	26.1	5.1

1.4.9 Importance of carbon loading in the mineralization pathways and in the cycling of iron and sulphur

The inputs and quality of organic matter occupy an important place in the mineralization pathways. Soetaert et al. (1996b) highlighted the dominance of oxic mineralization and denitrification in the deep-sea systems receiving low organic carbon content. However, the abundance of fresh organic matter, containing small particles, should accelerate the biologic activity and thus the processes of organic matter degradation in the sediments. In some systems with high organic carbon fluxes, the suboxic and anoxic pathways of mineralization become dominant in sediments (Canfield et al., 1993b).

A steady-state budget for iron and sulphur was established by Wijsman et al. (2002), which took into account the carbon loading (Figure 1.13). The authors revealed that according to the intensity of organic carbon flux, the mineralization pathways are impacted. With a low carbon mineralization rate, the iron dominated the situation while with a high carbon mineralization rate, sulphur species becomes dominant compared to iron species. In the Fe-dominated situation, no free hydrogen sulphide is observed in the porewaters. The S-dominated situation leads to an increase of iron monosulphide and pyrite contents in the

sediments, trapping the reduced iron. Thus, the sulfate reducers receive more carbon to mineralize due to the less available iron.

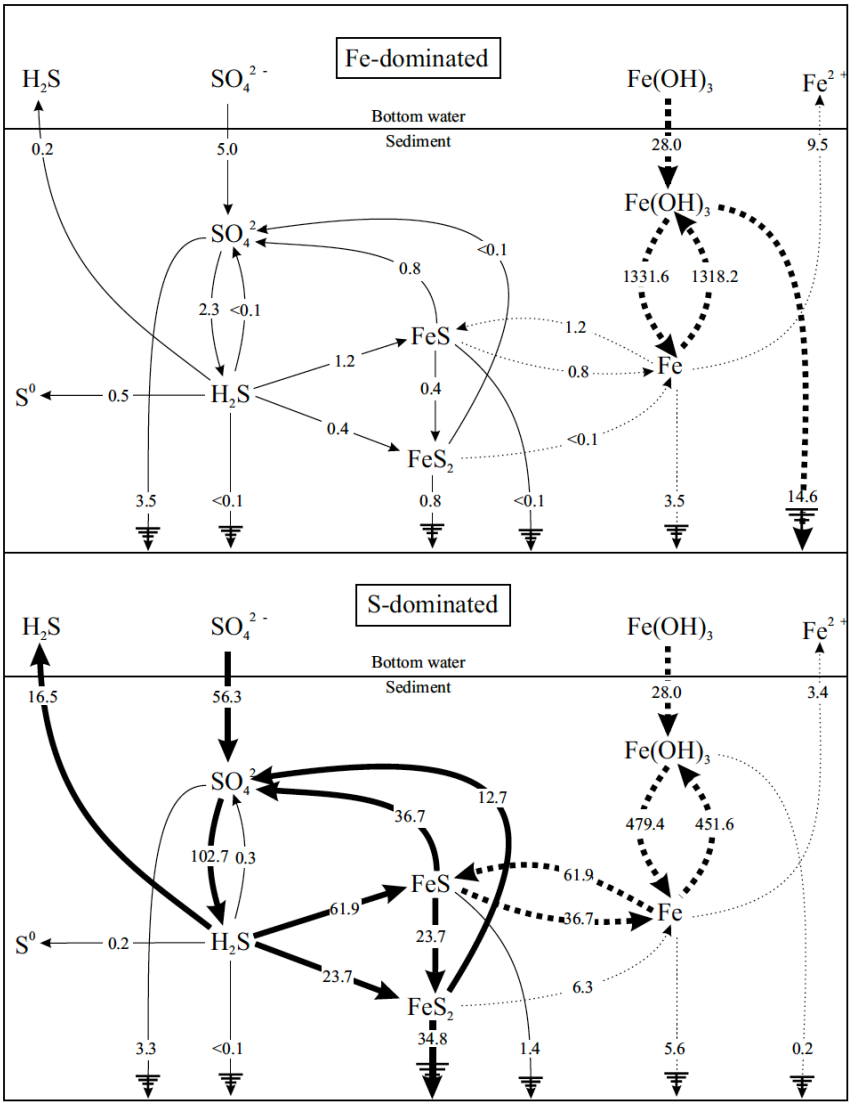

Figure 1.14. Schematic representation of iron (dashed arrows) and sulphur cycling (solid arrows). Fe-dominated situation is represented in the upper panel corresponding to a carbon flux of 0.24 mmol C cm^{-2} yr^{-1} and S-dominated situation in the lower panel with a carbon flux of 0.25 mmol C cm^{-2} yr^{-1}. The fluxes are in nmol $cm^{-2}d^{-1}$. From Wijsman et al. (2002).

1.5. Research objectives

The present research has been carried out in the framework of the BENTHOX project, aiming to better understand the causes of marine benthic hypoxia and to evaluate its impacts on the benthic ecosystem and biogeochemical cycling. In this context, the principal objectives of this thesis are to study the biogeochemical changes taking place in the sediments and to

assess the exchange fluxes across the sediment-water interface in response to marine benthic deoxygenation. The following key research questions are addressed and tackled:

- What are the dynamics of oxygen and organic matter degradation in coastal sediments?
    - How does the sedimentary oxygen consumption respond to seasonal oxygen depletion in the bottom water?
    - What is the impact of seasonal bottom water hypoxia on:
        - Diagenetic pathways
        - Sediment-water exchanges
    - How is the mineralization of organic matter affected by oxygen depletion?
    - Are there spatial and temporal variabilities of organic matter degradation in the sediments of the NW shelf of the Black Sea?
- How does benthic hypoxia affect the sulphur and iron cycling in the sediments?
    - What is the distribution of iron and sulphur species?
    - What is the speciation of reactive iron and sulphur in the shelf sediments?
    - Are the sediments subjected to a Fe-dominated and/or an S-dominated regime?
- What is the biogeochemistry and the distribution of trace metals in the sediments of the NW shelf?
    - What is the link between diagenetic reactions and trace elements in sediments?
    - What is the impact of heavy metals on the quality of the shelf sediments?

1.6. Thesis outline

Chapter 1 gives an overview of the coastal hypoxia development, early diagenesis and different proxies used for paleoenvironment studies on hypoxia. An introduction is presented of the Black Sea, its evolution and the NW shelf of the Black Sea which is the field investigation site of this thesis.

Material and methods used in this research are described in **Chapter 2**. Two sampling campaigns were conducted in spring 2016 and summer 2017 in the NW shelf area of the Black Sea. Field sampling (water column, sediments and porewaters) and sample treatment are described. The analytical aspects area also provided for the determination of the various parameters, contributing to the hypoxia study.

Chapter 3 investigates the effects of hypoxia on biogeochemical cycling of major and minor elements (carbon, nutrients, iron, manganese and sulphur) during field biogeochemical

investigations on the NW shelf of the Black Sea conducted in spring 2016 and summer 2017. The sites were shallow and muddy (~20 m water depth) with an oxygenated water column. In summer 2017, a hypoxic sediment-water interface was revealed by microprofiling. These measurements combined with porewater and sediment analyses demonstrated the impact of low oxygen concentration in the bottom waters on the dissolved oxygen uptake, benthic fluxes and mineralization of organic carbon.

Study of iron and sulphur cycling in surface sediments of the NW shelf of the Black Sea during a seasonal hypoxia is presented in **Chapter 4**. A combination of porewater analyses with the determination of speciation of the solid phase provided insight on the diagenesis of iron and sulphur during bottom hypoxia and the spatial distribution of these elements on the shelf.

Chapter 5 examines the biogeochemistry of trace elements in the sediments on the NW shelf of the Black Sea. The distribution of trace metals in the sediments on the shelf was determined. Data analyses of porewaters, solid phases and sediment-water exchanges allowed the identification of the link between trace elements and diagenesis of organic matter, influencing the mobility of trace metals. Depending on the location, the data suggested that the sediments were enriched in certain heavy metals leading to different levels of pollution.

General conclusions obtained in this study with more clarity on hypoxia development on the NW shelf of the Black Sea are summarized in **Chapter 6**. The consequences of the seasonal hypoxia on the diagenetic pathways and sediment-water exchanges are highlighted. The role of iron and sulphur in early diagenesis are discussed especially during a hypoxic event and the biogeochemistry of trace metals is illustrated. Trace metal enrichment has shown that human activities are still playing a role in the pollution assessment in the sediments of the shelf of the Black Sea. Finally suggestions for future research are proposed.

Appendix A is attached which relates to a paleoproxy study carried out in collaboration with the Master's students from the Université de Liège. Sedimentological and paleontological proxies were tested in order to understand and reconstruct the history of hypoxia during the Holocene.

References

Aller, R. C., & Rude, P. D. (1988). Complete oxidation of solid-phase sulphides by manganese and bacteria in anoxic marine sediments. Geochim. Cosmochim. Acta., 52, 751–765.

Aksu, A. E., Hiscott, R. N., Mudie, P. J., Rochon, A., Kaminski, M., Abrajano, T., & Yasar, D. (2002). Persistent Holocene outflow from the Black Sea to the Eastern Mediterranean contradicts Noah's Flood hypothesis. GSA Today, 12, 4-10.

Almazov, N. M. (1961). Stok ratverennykh soley I biogennykh veschetv kotorye vynoseatsya rekami USSR v Chernoe More. Naukovi Zapiski Odes. Biol. St. Kiev, 99-107.

Altabet, M. A., & Francois, R. (1994). Sedimentary isotopic ratio as a recorder for surface ocean nitrate utilization. Global Biogeochem. Cy., 8, 103–116.

Alve, E. (1990). Variations in estuarine foraminiferal biofacies with diminishing oxygen conditions in Drammensfjord, SE Norway. In C. Hemleben, M. A. Kaminski, W. Kuhnt, & D. B. Scott (Eds.), Paleoecology, Biostratigraphy, Paleoceanography and Taxonomy of Agglutinated Foraminifera (Vol. 327). Dordrecht: Springer.

Alve, E. (2003). A common opportunistic foraminiferal species as an indicator of rapidly changing conditions in a range of environments. Estuarine coastal and shelf science, 57, 501-514.

Andrén, E. (1999). Changes in the composition of the marine diatom flora ´ during the past century indicate increased eutrophication of the Oder estuary, southwestern Baltic Sea. Estuarine, Coastal and Shelf Science, 48, 665-676.

Arnold, A. J., & Parker, W. C. (1999). Biogeography of Planktonic Foraminifera. In Modern Foraminifera (pp. 103-122). Dordrecht: Springer.

Berner, R. (1980). Early Diagenesis: A theoretical approach. Princeton University Press.

Berner, R. A. (1980). Early diagenesis: a theorical approach. Princeton University Press, Princeton.

Berner, R. A. (1981). A new geochemical classification of sedimentary environments. J. Sediment. Petrol, 51, 359-365.

Berner, R. A. (1984). Sedimentary pyrite formation: An update. Geochim. Cosmochim. Acta, 48, 605-615.

Berner, R. A. (1989). Biogeochemical cycles of carbon and sulfur and their effect on atmospheric oxygen over phanerozoic time. Paleogeography, Paleoclimatology, Paleoecol., 75, 97-122.

Bottrell, S. H., & Newton, R. J. (2006). Reconstruction of changes in global sulfur cycling from marine sulfate isotopes. Earth Sci. Rev., 75, 59-83.

Brandes, J. A., & Devol, A. H. (2002). A global marine-fixed nitrogen isotopic budget: Implications for Holocene nitrogen cycling. Global Biogeochem. Cy., 14, 1120.

Brandes, J. A., Devol, A. H., Yoshinari, T., Jayakumar, A., & Naqvi, S. W. (1998). Isotopic composition of nitrate in the central Arabian Sea and eastern tropical North Pacific: A tracer for mixing and nitrogen cycles. Limnol. Oceanogr., 43, 1680–1689.

Bratton, J. R., Colman, S. M., & Seal, R. R. (2003). Eutrophication and carbon sources in Chesapeake Bay over the last 2700 yr: human impacts in context. Geochim. Cosmochim. Ac., 67, 3385–3402.

Breitburg, D., Levin, L. A., Oschlies, A., Grégoire, M., Chavez, F. P., Conley, D. J., . . . Rose, K. (2018). Declining oxygen in the global ocean and coastal waters. Science, 359(46).

Brocks, J. J., Logan, G. A., Buick, R., & Summons, R. E. (1999). Archean molecular fossils and the early rise of eukaryotes. Science, 285, 1033-1036.

Brunner, C. A., Beall, J. M., Bentley, S. J., & Furukawa, Y. (2006). Hypoxia hotspots in the Mississippi Bight. J. Foramin. Res., 36, 95–107.

Burdige, D. J. (2006). Geochemistry of Marine Sediments. New Jersey: Princeton University Press.

Burdige, D. J. (2007). Preservation of organic matter in marine sediments: controls, mechanisms, and an imbalance in sediment organic carbon budgets? Chem. Rev., 107, 467-485.

Burdige, D. J. (2011). Estuarine and coastal sediments - Coupled biogeochemical cycling. In D. J. Burdige, Treatrise on estuarine and coastal science (Vol. 5, pp. 279-308). Academic Press.

Cai, W.-J. (2011). Estuarine and coastal ocean carbon paradox: CO2 sinks or sites of terrestrial carbon incineration? Annual Review of Marine Science, 3, 123-145.

Calvert, S. E., & Pedersen, T. F. (2007). Elemental proxies for paleoclimatic and palaeoceanographic variability in marine sediments: interpretation and application. In C. Hillaire-Marcel, & A. De Vernal (Eds.), Proxies in Late Cenozoic Paleoceanography (pp. 567-644). Amsterdam, Boston, Heidelberg, London, New York, Oxford, Paris, San Diego, San Francisco, Singapore, Sydney, Tokyo: Elsevier.

Canfield, D. E., Jorgensen, B. B., Fossing, H., Glud, R., Gundersen, J., Ramsing, N., . . . Hall, P. (1993a). Pathways of organic carbon oxidation in three continental margin sediments. Marine Geology, 113, 27-40.

Canfield, D. E., Thamdrup, B., & Hansen, J. W. (1993b). The anaerobic degradation of organic matter in Danish coastal sediments: Iron reduction, manganese reduction, and sulfate reduction. *Geochimica et Cosmochimica Acta, 57,* 3867-3883.

Capet, A., Beckers, J.-M., & Gregoire, M. (2013). Drivers, mechanisms and long-term variability of seasonal hypoxia on the Black Sea northwestern shelf – is there any recovery after eutrophication? Biogeosciences, 10, 3943–3962.

Capet, A., Meysman F. J.R., Akoumianaki I., Soetaert K., Grégoire M., (2016a). Integrating sediment biogeochemistry into 3D oceanic models: A study of benthic-pelagic coupling in the Black Sea. Ocean Modelling, 101, 83-100.

Capet, A., Stanev, E. V., Beckers, J.-M., Murray, J. W., & Grégoire, M. (2016b). Decline of the Black Sea oxygen inventory. Biogeosciences, 13, 1287-1297.

Chen, C.-T. A., & Borgès, A. V. (2009). Reconciling opposing views on carbon cycling in the coastal ocean: Continental shelves as sinks and near-shore ecosystems as sources of atmospheric CO2. Deep Sea Research Part II: Tropical studies in oceanography, 8, 578-590.

Cociasu, A., Dorogan, L., Humborg, C., & Popa, L. (1996). Long-term ecological changes in the Romanian coastal waters of the Black Sea. Marine Pollution Bulletin, 32, 32-38.

Commission, n. L. (1958). Convention on the Continental Shelf. United Nations. Geneva: Treaty Series.

Conley, D. J., Bjorck, S., Bonsdorff, E., Carstensen, J., Destouni, G., Gustafsson, B. G., . . . Rosenberg, R. (2009). Hypoxia-related processes in the Baltic Sea. Environ. Sci. Technol, 43, 3412–3420.

Conley, D. J., Carstensen, J., Ærtebjerg, G., Christensen, P. B., Dalsgaard, T., Hansen, J. L., & Josefson, A. B. (2007). Long-term changes and impacts of hypoxia in Danish coastal waters. Ecol. Appl., 17, 165-184.

Cooper, S. R., & Brush, G. S. (1991). Long-Term History of Chesapeake Bay Anoxia. Science, 254, 992-996.

Cooper, S. R., & Brush, G. S. (1993). A 2500-year history of anoxia and eutrophication in Chesapeake Bay. Estuaries, 16, 617-626.

Denga, Y., Orlova, I., Komorin, V., Oleynik, Y., Korshenko, A., Hushchyna, K., . . . Zhugailo. (2017). National Pilot Monitoring Studies & Joint Open Sea Surveys in Georgia, Russian Federation and Ukraine, 2016.

Deuser, W. G. (1974). Evolution of anoxic conditions in Black Sea during Holocene. In E. T. Degens, & D. A. Ross, The Black Sea-Geology, chemistry and biology (pp. 133-136). Tulsa: AAPG Memoir 20.

Dewey, J. F., Pittman, W. C., Ryan, W. B., & Bonnin, J. (1973). Plate tectonics and the evolution of the Alpine System. Geol. Soc. Am. Bull., 84, 3137-3180.

Diaz, R. J., & Rosenberg, R. (1995). MArine benthic hypoxia: a review of its ecological effects and the behavioural responses of benthic macrofauna. Oceanogr. and Mar. Biol., 33, 245-303.

Diaz, R. J., & Rosenberg, R. (2008). Spreading dead zone and consequences for marine ecosystems. Science, 321, 926-929.

Ehlers, J., Gibbard, P. L., & Hughes, P. D. (2011). Quaternary glaciations: extent and chronology: a closer look. Amsterdam: Elsevier.

Erwin, D. H. (2006). Extinction: How Life on Earth Nearly Ended 250 Million Years Ago. Princeton: Princeton Univ. Press.

Falkowski, P. G., Algeo, T., Codispoti, L., Deutsch, C., Emerson, S., Hales, B., . . . Pilcher, C. B. (2011). Past, Present, and Future. Eos, 92, 409-410.

Fernandes Martins, M. J., Namiotko, T., Cabral, M. C., Fatela, F., & Boavida, M. J. (2010). Contribution to the knowledge of the freshwater Ostracoda fauna in continental Portugal, with an updated cheklist of Recent and Quaternary species. J. Limnol., 69, 160-173.

Friedrich, J., Dinkel, C., Friedl, G., Pimenov, N., wijsman, J., Gomoiu, M.-T., . . . Wehrli, B. (2002). Benthic nutrient cycling and diagenetic pathways in the North-western Black Sea. Estuarine, Coastal and Shelf Science, 54, 369-383.

Froelich, P. N., Klinkhammer, G. P., Bender, M. L., Luedtke, N. A., Heath, G. R., Cullen, D., . . . Hartman, B. (1979). Early oxidation of organic matter in pelagic sediments of the eastern equatorial Atlantic: suboxic diagenesis. Geochim. Cosmochom., 43, 1075-1090.

Galbraith, E. D., Kienast, M., Pedersen, T. F., & Calvert, S. E. (2004). Glacial-interglacial modulation of the marine nitrogen cycle by high-latitude O2 supply to the global thermocline. Paleoceanography, 19, PA4007.

Glud, R. N. (2008). Oxygen dynamics of marine sediments. Mar. Biol., 4, 243-289.

Gorur, N. (1988). Timing of opening of the Black Sea. Tectonophys., 147, 247-262.

Gray, J. S., Wu, R. S., & Or, Y. Y. (2002). Effects of hypoxia and organic enrichment on the coastal marine environment. Mar. Ecol. Prog. Ser., 238, 249-279.

Helly, J., & Levin, L. (2004). Global distribution of naturally occurring marine hypoxia on continental margins. Deep See Res.I, 51, 1159-1168.

Holland, H. D. (2002). Volcanic gases, black smokers, and the great oxidation event. Geochim. Cosmochim. Acta., 66, 3811-3826.

Hsü, K. J., Nacev, I. K., & Vuchev, V. T. (1977). Geologic evolution of Bulgaria in the light of plate tectonics. Tectonophys., 40, 245-256.

Isensee, K. (2016). The Ocean is Losing its Breath. In Ocean and Climate Scientific Notes, ed. 2 (pp. 20-32).

Ivanov, V. A., & Belokopytov, V. N. (2013). Oceanography of the Black Sea. Sevastopol: National Academy of Science of Ukraine, Marine Hydrophysical Institute.

Jackson, J. B., Kirby, M. X., Berger, W. H., Bjorndal, K. A., Botsford, L. W., Bourque, B. J., . . . Steneck. (2001). Historical Overfishing and the Recent Collapse of Coastal Ecosystems. Science, 293, 629– 637.

Jilbert, T., Slomp, C. P., Gustafsson, B. G., & Boer, W. (2011). Beyond the Fe-P-redox connection: preferential regeneration of phosphorus from organic matter as a key control on Baltic Sea nutrient cycles. Biogeosciences, 8, 1699 - 1722.

Jones, G. A., & Gagnon, A. R. (1994). Radiocarbon chronology of Black Sea sediments. Deep-Sea Research l, 41, 531-557.

Jorgensen, B. B. (1977). Sulphur cycle of a coastal marine sediment (Limfjorden, Denmark). Limnol. Oceanogr., 22, 814-832.

Jorgensen, B. B. (1982). Mineralization of organic matter in the seabed – the role of sulphate reduction. Nature, 296, 643-645.

Jorgensen, B. B., & Kasten, S. (2006). Sulfur Cycling and Methane Oxidation. In H. D. Schulz, & M. Zabel (Eds.), Marine Geochemistry. Berlin: Springer.

Jorgensen, B. B., & Nelson, D. C. (2004). Sulfide oxidation in marine sediments: geochemistry meets microbiology. In J. P. Amend, K. J. Edwards, & T. W. Lyons (Eds.), Sulfur biogeochemistry-past and present (pp. 283-284). The Geochemical Society of America.

Karlsen, A. W., Cronin, T. M., & Ishman, S. E. (2000). Historical trends in Chesapeake Bay dissolved oxygen based on benthic foraminifera from sediment cores. Estuaries, 23, 488–508.

Kemp, W. M., Boynton, W. R., Adolf, J. E., Boesch, D. F., Boicourt, W. C., Brush, G., . . . St. (2005). Eutrophication of Chesapeake Bay: historical trends and ecological interactions. Marine Ecology Progress Series, 303, 1-29.

Kemp, W. M., Testa, J. M., Conley, D. J., Gilbert, D., & Hagy, J. D. (2009). Temporal responses of coastal hypoxia to nutrient loading and physical controls. Biogeosciences, 6, 2985-3008.

Kerey, I. E., Meric, E., Tunoglu, C., Kelling, G., Brenner, R. L., & Dogan, A. U. (2004). Black Sea-Marmara Sea Quaternary connections: new data from the Bosporus, Istanbul, Turkey. Paleogeography, paleolim., paleoecol., 204, 277-295.

Konovalov, S. K., Luther, G. W., & Yucel, M. (2007). Porewater redox species and processes in the Black Sea sediments. Chem. Geol., 245, 254–274.

Kosarev, A. N., & Kostianoy, A. G. (2007). Introduction. In A. N. Kosarev, The Black Sea Environment (Vol. 5, pp. 1-10). Berlin: Springer Berlin Heidelberg.

Langmead, O., McQuatters-Gollop, A., Mee, L. D., Friedrich, J., Gilbert, A. J., Gomoiu, M.-T., . . . Todorova, V. (2009). Recovery or decline of the northwestern Black Sea: A societal choice revealed by socio-ecological modelling. Ecological Modelling, 220, 2927-2939.

Letouzey, J., Biju-Duval, B., Dorkel, A., Gonnard, R., Kristchev, K., Montadert, L., & Sungurlu, O. (1977). The Black Sea-a marginal basin. In Structural history of the Mediterranean basins (pp. 363- 376). Paris: Editions Technip.

Levin, L. A., Ekau, W., Gooday, A. J., Jorissen, F., Middelburg, J. J., Naqvi, W., . . . Zhang, J. (2009). Effects of natural and human-induced hypoxia on coastal benthos. Biogeosciences, 6, 3563–3654.

Luther III, G. W., Findlay, A. J., MacDonald, D. J., Owings, S. M., Hanson, T. E., Beinart, R. A., & Girguis, P. R. (2011). Thermodynamics and kinetics of sulfide oxidation by oxygen: a look at inorganically controlled reactions and biologically mediated processes in the environment. Front. Microbiol., 2, 1-9.

Lyons, T. W., Reinhard, C. T., & Planavsky, N. J. (2014). The rise of oxygen in Earth's early ocean and atmosphere. Nature, 506, 307–315.

Lyons, T. W., Werne, J. P., Hallander, D. J., & Murray, R. W. (2003). Contrasting sulfur geochemistry and Fe/Al and Mo/Al ratios across the last oxic-to-anoxic transition in the Cariaco Basin, Venezuela. Chem. Geol., 195, 131-157.

McCarthy, J. J., Yilmaz, A., Coban-Yildiz, Y., & Nevins, J. L. (2007). Nitrogen cycling in the offshore waters of the Black Sea. Estuar. Coast. Shelf Sci., 74, 493-514.

McCarthy, M. J., McNeal, K. S., Morse, J. W., & Gardner, W. S. (2008). Bottom-water hypoxia effects on sediment-water interface nitrogen transformations in a seasonally hypoxic, shallow bay (Corpus christi bay, TX, USA). Estuar. Coasts, 31, 521–531.

McClelland, J. W., & Valiela, I. (1998). Linking nitrogen in estuarine producers to land-derived sources. Limnol. Oceanogr., 43, 577– 585.

Middelburg, J. J., & Meysman, F. J. (2007). Burial at sea. Science, 316, 1294-1295.

Millero, F. J., Hubinger, S., Fernandez, M., & Garnett, S. (1987). Oxidation of H2S in seawater as a function of temperature, pH, and ionic strength. Envir. Sci. Technol., 21, 439-443.

Murray, J. W. (2001). The niche of benthic foraminifera, critical threshold and proxies. Marine Micropaleontology, 1-7.

Murray, J. W., Top, Z., & Ozsoy, E. (1991). Hydrographic properties and ventilation of the Black Sea. Deep-Sea Res., 38, S663-S689.

Ozsoy, E., & Unluata, U. (1997). Oceanography of the Black Sea: a review of some recent results. Earth-Science Reviews, 42, 231-272.

Özsoy, E., Latif, M. A., Tugrul, S., & Ünlüata, Ü. (1995). Exchanges with the Mediterranean, fluxes, and boundary mixing processes in the Black Sea. Bulletin de l'Institut océanographique, 15, 1-25.

Ozsoy, E., Latif, M. A., Tugrul, S., & Ünlüata, U. (1995). Exchanges with the Mediterranean, fluxes, and boundary mixing processes in the Black sea. In F. Briand (Ed.), Mediterranean Tributary Seas (pp. 1-25). Monaco: Bull. Inst. Oceanogr. Monaco.

Panin, N., & Jipa, D. (2002). Danube River Sediment Input and its Interaction with the North-western Black Sea. Estuarine, Coastal and Shelf Science, 54, 551–562.

Pinturier-Geiss, L., Méjanelle, L., Dale, B., & Karlsen, D. A. (2002). Lipids as indicators of eutrophication in marine coastal sediments. J. Microbiol. Meth., 48, 239-257.

Rabalais, N. N., Turner, E. R., & Wiseman, Jr., W. J. (2002). Gulf of Mexico hypoxia, aka ''The dead zone.''. Ann. Rev. Ecol. Syst., 33, 235-263.

Raiswell, R., Buckley, F., Berner, R. A., & Anderson, T. F. (1988). Degree of pyritization of iron as a paleoenvironmental indicator of bottom-water oxygenation. Journal of Sedimentary Research, 58, 812-819.

Rickard, D. (2006). The solubility of FeS. Geochim. Cosmochim. Acta., 70, 5779-5789.

Rickard, D., & Luther, G. W. (2007). Chemistry of iron sulphide. Chem. Rev., 107, 514-562.

Robinson, A., Spadini, G., Cloetingh, S., & Rudat, J. (1995). Stratigraphic evolution of the Black Sea: interferences from basin modelling. Marine and Petroleum Geology, 12, 821-835.

Ross, D. A., Degens, E. T., & MacIlvaine, J. (1970). Black sea: recent sedimentary history. Science, 170, 163-165.

Ross, D. A., Uchupi, E., Prada, K. E., & MacIlvaine, J. C. (1974). Bathymetry and microtopography of Black Sea. In The Black Seageology, chemistry and biology (pp. 1-10). Tulsa: AAPG Memoir 20.

Ryan, W. B., Pitman, W. C., Major, C. O., Shimkus, K., Moskalenko, V., Jones, G. A., . . . Yuce, H. (1997). An abrupt drowning of the Black Sea shelf. Marine Geology, 138, 119-126.

Schmiedl, G., Mitschele, A., Beck, S., Emeis, K.-C., Hemleben, C., Schulz, H., . . . Weldeab, S. (2003). Benthic foraminiferal record of ecosystem variability inthe eastern Mediterranean Sea during times of sapropel S5and S6 deposition. Palaeogeography, Palaeoclimatology, Palaeoecology, 190, 139-164.

Scholz, F., Severmann, S., McManus, J., Noffke, A., Lomnitz, U., & Hensen, C. (2014). On the isotope composition of reactive iron in marine sediments: Redox shuttle versus early diagenesis. Chemical Geology, 389, 48-59.

Schulz, H. N., & Jorgensen, B. B. (2001). Big Bacteria. Annu. Rev. Microbiol., 55, 105-137.

Schulz, H. N., & Schulz, H. D. (2005). Large sulfur bacteria and the formation of phosphorite. Science, 307, 416-418.

Sen Gupta, B. K. (Ed.). (1999). Modern Foraminifera. Dordrecht: Kluwer.

Slomp, C. P., Epping, E. H., Helder, W., & Van Raaphorst, W. (1996). A key role for iron-bound phosphorus in authigenic apatite formation in North Atlantic continental platform sediments. J. Mar. Res., 54, 1179–1205.

Soulet, G., Ménot, G., Lericolais, G., & Bard, E. (2011). A revised calendar age for the last reconnection of the Black Sea to the global ocean. Quaternary Sci. Rev., 30, 1019-1026.

Staneva, J., & Stanev, E. (2002). Water mass formation in the Black Sea during 1991–1995. J. Marine Syst., 32, 199-218.

Steckbauer, A., Duarte, C. M., Carstensen, J., Vaquer-Sunyer, R., & Conley, D. J. (2011). Ecosystem impacts of hypoxia: Thresholds of hypoxia and pathways to recovery. Environ. Res. Lett., 6, 025003.

Stoetaert, K., Herman, P. M., & Middelburg, J. J. (1996). A model of early diagenetic processes from the shelf to abyssal depths. Geochim. Cosmochim. Acta., 60, 1019-1040.

Stramma, L., Johnson, G. C., Sprintall, J., & Mohrholz, V. (2008). Expanding oxygen-minimum zones in the tropical oceans. Science, 320, 655-658.

Strous, M., & Jetten, M. S. (2004). Anaerobic oxidation of methane and ammonium. Annu. Rev. Microbiol., 58, 99-117.

Struck, U., Emeis, K.-C., Voss, M., Christiansen, C., & Kunzendorf, H. (2000). Records of southern and central Baltic Sea eutrophication in δ 15N of sedimentary organic matter. Mar. Geol., 164, 157-171.

Suess, E. (1979). Mineral phases formed in anoxic sediments by microbial decomposition of organic matter. Geochim. Cosmochim. Acta, 43, 339–352.

Sundby, B., Gobeil, C., Silverberg, N., & Mucci, A. (1992). The phosphorus cycle in coastal marine sediments. Limnol. Oceanogr., 37, 1129-1145.

Testa, J. M., & Kemp, W. M. (2011). Oxygen—dynamics and biogeochemical consequences. In J. M. Testa, W. M. Kemp, E. Wolansky, & D. S. McLusky (Eds.), Treatise on Estuarine and Coastal Science (Vol. 5, pp. 163-199). Waltham: Academic Press.

Thamdrup, B., Canfield, D. E., Ferdelman, T. G., Glud, R. N., & Gundersen, J. K. (1996). A biogeochemical survey of the anoxic basin Golfo Dulce, Costa Rica. Rev. Biol. Trop., 3, 19–33.

Thamdrup, B., Fossing, H., & Jorgensen, B. B. (1994). Manganese, iron, and sulfur cycling in a coastal marine sediment, Aarhus Bay, Denmark. Geochim. Cosmochim. Acta, 58, 5115-5129.

Thomas, E., Gapotchenko, T., Varekamp, J. C., Mecray, E. L., & Buchholtz ten Brink, M. R. (2000). Benthic Foraminifera and Environmental Changes in Long Island Sound. Journal of Coastal Research, 16, 641-655.

Tribovillard, N., Algeo, T. J., Lyons, T., & Riboulleau, A. (2006). Trace metals as paleoredox and paleoproductivity proxies: An update. Chemical Geology, 232, 12-32.

Ünlüata, Ü., Oğuz, T., Latif, M. A., & Özsoy, E. (1990). On the physical oceanography of the Turkish straits (NATO /ASI Series Kluwer ed.). Dordrecht : Pratt, L.J.

Ukrainskii V.V. & Popov Y.I. 2009. Climatic and hydrophysical conditions of the development of hypoxia in waters of the northwest shelf of the Black Sea. *Physical Oceanography* 19 (3), 140–150.

Ukrayinskyy, V., Komorin, V., Kovalyshyna, S., Hushchyna, K., Korshenko, A., Mikaelyan, A., . . . Zhugailo, S. (2017). *National Pilot Monitoring Studies & Joints Open Sea Surveys in Georgia, Russian Federation and Ukraine, 2016.*

Voss, M., Larsen, B., Leivuori, M., & Vallius, H. (2000). Stable isotope signals of eutrophication in Baltic Sea sediments. J. Marine Syst., 25, 287-298.

Wijsman, J. W., Middelburg, J. J., Herman, P. M., Böttcher, M. E., & Heip, C. H. (2001). Sulfur and iron speciation in surface sediment along the northwestern margin of the Black Sea. Marine Chemistry, 74, 261-278.

Wijsman, J. W., Herman, P. M., Middelburg, J. J., & Soetaert, K. (2002). A model for early diagenetic processes in sediments of the continental shelf of the Black Sea. *Estuarine, Coastal and Shelf Science, 54*, 403-421.

Wilkin, R. T., Barnes, H. L., & Brantley, S. L. (1996). The size distribution of framboidal pyrite in modern sediments: An indicator of redox conditions. Geochim. Cosmochim. Ac., 60, 3897–3912.

Wollast, R. (1998). Evaluation and comparison of the global carbon cycleinthe coastal zone and in the open ocean. In R. Wollast, K. H. Brink, & A. R. Robinson (Eds.), The Sea: Ideas and Observations on Progress in the Study of the Seas. (Vol. 10, pp. 213-252). Hoboken: John Wiley & sons.

Wüchter, C., Abbas, B., Coolen, M. J., Herfort, L., van Bleijswijk, J., Timmers, P., . . . Damsté, J. S. (2006). Archeal nitrification in the oceans. P. Natl. Acad. Sci. USA, 103, 12317-12322.

Yanko-Hombach, V., Mudie, P. J., Kadurin, S., & Larchenkov, E. (2014). Holocene marine transgression in the Black Sea: New evidence from the northwestern Black Sea shelf. Quaternary International, 345, 100–118.

Zaïbi, C., Carbonel, P., Kamoun, F., Fontugne, M., Azri, C., Jedoui, Y., & Montacer, M. (2012). Evolution of the sebkha Dreîaa (South-Eastern Tunisia, Gulf of Gabes) during the Late Holocene: response of ostracod assemblages. Revue de Micropaléontologie, 55, 83-97.

Zhang, R., Follows, M. J., Grotzinger, J. P., & Marshall, J. (2001). Could the Late Permian deep ocean have been anoxic? Paleoceanography, 16, 317-329.

Zillén, L., Conley, D. J., Andrén, T., Andrén, E., & Björck, S. (2008). Past occurrences of hypoxia in the Baltic Sea and the role of climate variability,environmental change and human impact. 81Earth-Science Reviews, 91, 77–92.

Zimmerman, A. R., & Canuel, E. A. (2000). A geochemical record of eutrophication and anoxia in Chesapeake Bay sediments: anthropogenic influence on organic matter composition. Marine Chemistry, 69, 117-137.

Zimmerman, A. R., & Canuel, E. A. (2002). Sediment geochemical records of eutrophication in the mesohaline Chesapeake Bay. Limnol. Oceanogr., 47, 1084-1093.

Chapter 2

Material and methods

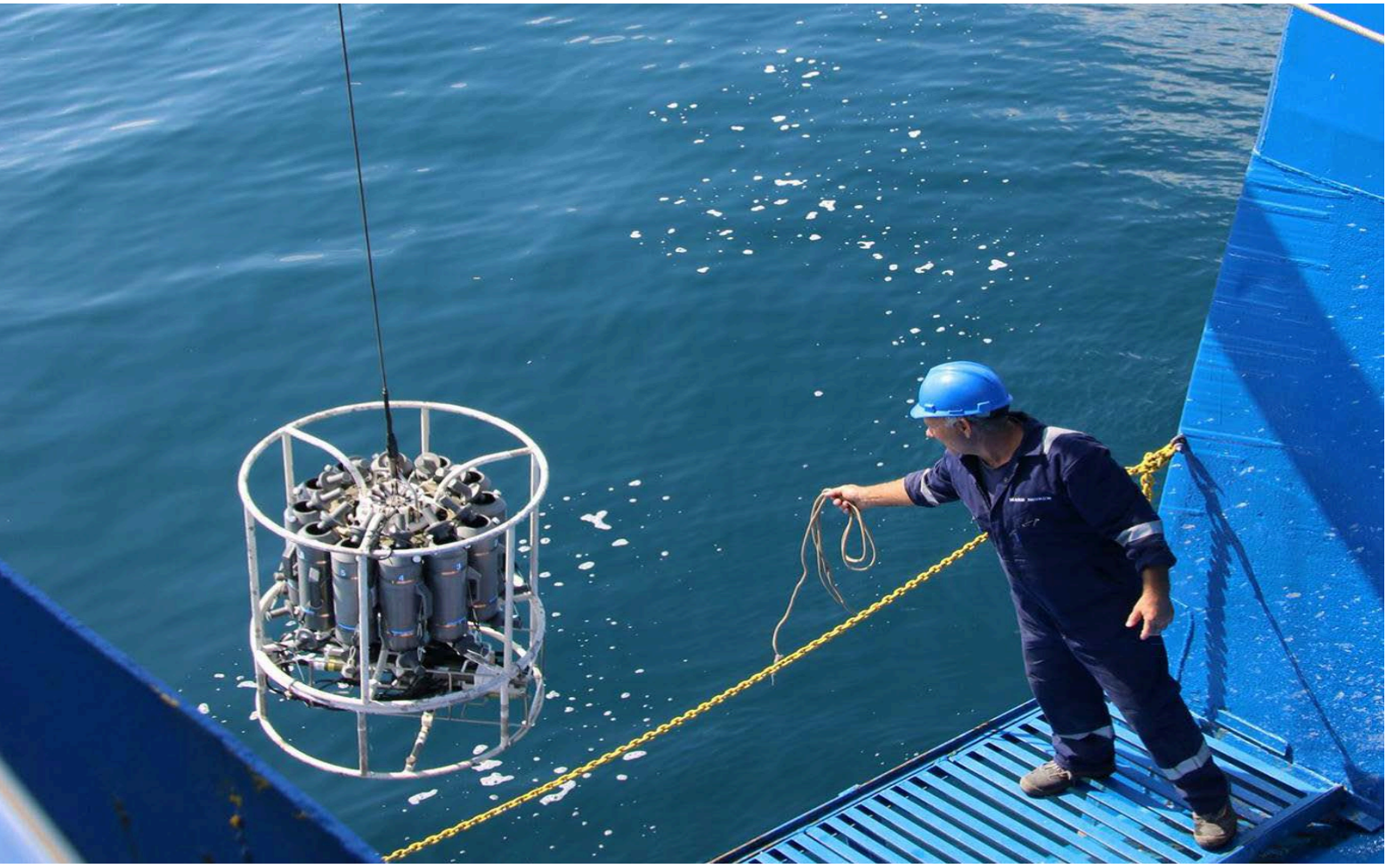

Water column sampling on the Ukrainian shelf in 2017 (Photo credit: Oskana Savenko).

2.1 Sampling

2.1.1 Location

The Emblas II project, aiming to improve the environmental monitoring in the Black Sea and organized several cruises aboard the R/V *Mare Nigrum* and provided the Benthox project with two berths in May 2016 and August 2017. The area investigated concerned the NW shelf which was subject to seasonal and summer hypoxia (Figure 2.1). The stations visited and water depths are summarized in Table 2.1 in addition to operations performed. In spring 2016, two sites (Stations 6 and 7) were sampled in the delta front of the Danube river, Station 12 was in the Dnieper region and Station 15 was in the Odessa Bay. During summer 2017, samples were taken at Station 1A' corresponding to the same position as Station 7 sampled in 2016 and the second site (Station 1) was on the central shelf in the Dnieper region.

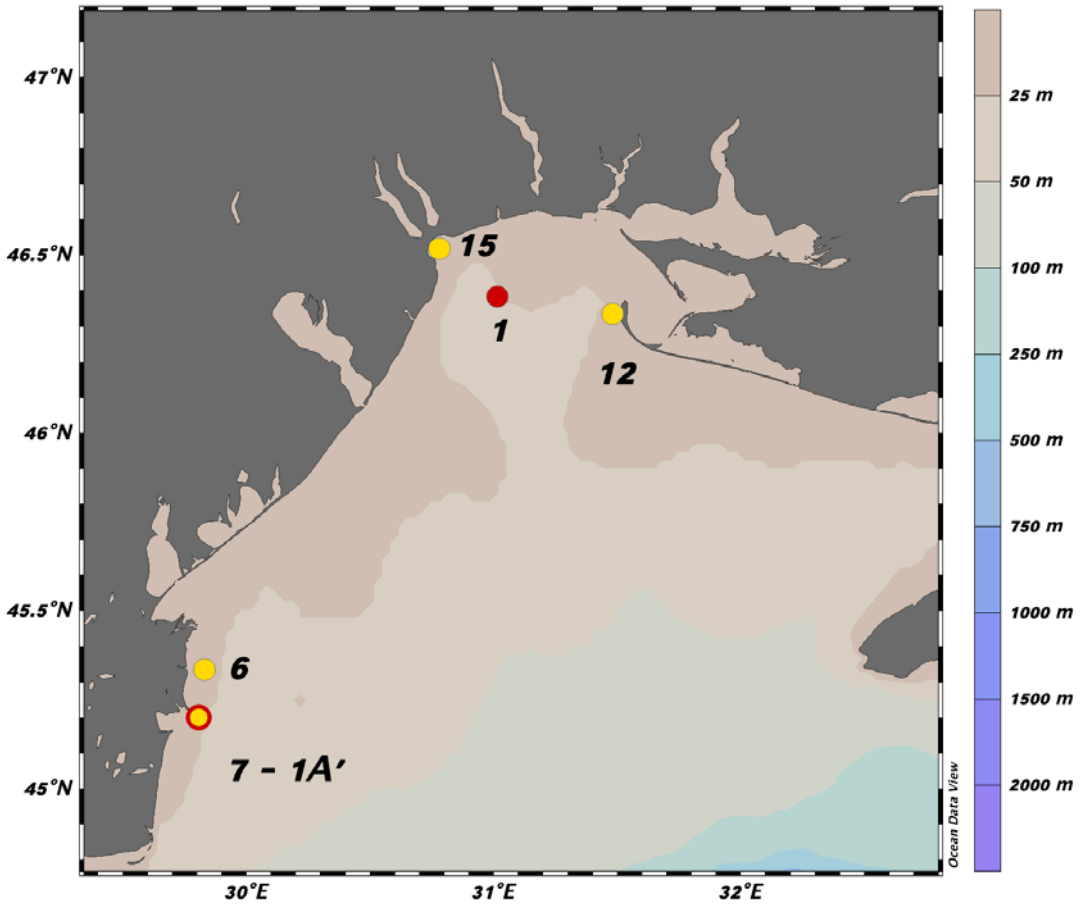

Figure 2.1. Map of the Black Sea and map focused on the NW shelf showing sampling stations (yellow dot: sampled in 2016, red dot: sampled in 2017, yellow dot with red circle: sampled in 2016 and 2017).

Table 2.1. Sampling stations in the NW shelf of the Black Sea. BW: bottom water, MC: multicore, GC: gravity core.

Station	Location	Sampling year	Depth (m)	Sampling
6	Danube delta	2016	21	BW, MC, GC
7	Danube delta	2016	18.6	BW, MC, GC
12	Split	2016	14.4	BW, MC
15	Odessa Bay	2016	17.1	BW, MC, GC
1A’	Danube delta	2017	20	BW, MC
1	Central shelf	2017	20.7	BW, MC

2.1.2 Sediment sampling

Multicore

Three sediment cores (∅ 10 cm) were sampled with a Mark II-400 multicorer at Stations 6, 7, 12, 15, 1A’ and 1 (Figure 2.2). The water depth varied from 14.4 m to 21 m. After recovery, one core was reserved for microprofilings of geochemical parameters as O_2, H_2S and pH using micro-sensors. The extraction of the pore waters was performed on a second core. The last core was dedicated to the analysis of the solid phase and was sliced at 1-4 cm intervals with a plastic ring and a plate.

Gravity core

During spring 2016, three gravity cores (Ø 10 cm, length 5 m) were collected at Statons 6, 7 and 15 at the same positions as for the coring with the multicorer (Figure 2.3, left top panel). The length of the cores varied from 197 cm to 215 cm. The cores were sliced on board 1 m intervals and stored at 4°C when arriving at the laboratory. The cores were opened in two parts along the length (Figure 2.3, bottom panel). The first half-core was sliced at 1-5 cm intervals with a plastic plate. Each layer was subdivided in four parts. The first one was dedicated to foraminifera determination, the second for the reactive iron analysis, the third for the determination of sediment mineralogy, and the last one for the analysis of organic carbon and carbonates contents as well as for dating by ^{210}Pb and ^{14}C. The second half-cores were used to subsample for the XRF core scanning, X-Ray radiography (Scopix) and magnetic susceptibility measurements.

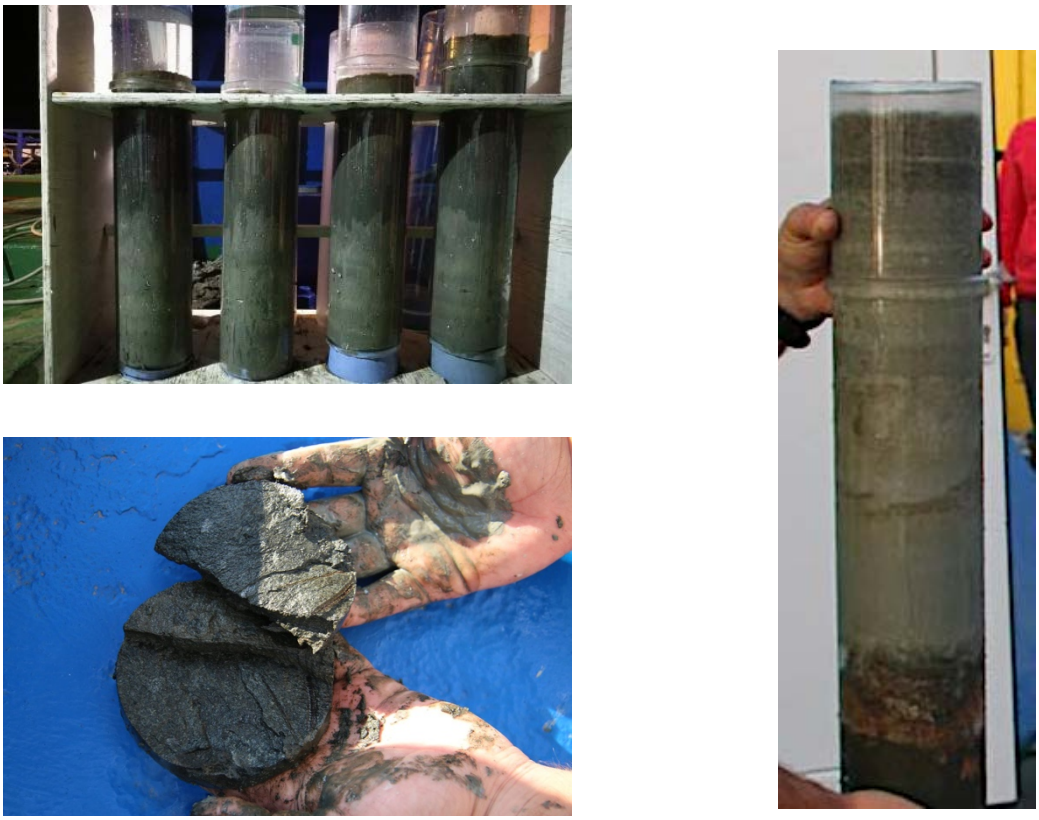

Figure 2.2. Pictures of the cores taken by multicorer and placed on the rack (left top panel), section of the sediments (left bottom panel) and entire core (right panel). Photo credit: Oksana Savenko.

Figure 2.3. Pictures of the gravity corer (top panel, photo credit: Peter Oswald), and opened gravity cores (bottom panel).

2.1.3 Water sampling

Water column

The temperature, salinity and oxygen concentrations were recorded with a CTD system equipped with *Niskin* bottles for water column sampling (Figure 2.4). Samples for dissolved oxygen were also collected and analysed on board with the Winkler method by the Ukrainian colleagues. For BENTHOX, bottom water samples were taken and filtered (Nucleopore 0.4 μm) for nutrient analyses (NO_3^-, NO_2^-, NH_4^+, PO_4^{3-}, Si). Filtered water samples for inorganic nitrogen and phosphate determinations were stored frozen and those for the dissolved silicate measurements were acidified and kept at 4 °C.

Figure 2.4. Picture of the CTD rosette equipped with *Niskin* bottles.

Porewaters extraction

The core tube used to extract porewaters from the sediments was predrilled with holes at every 2 cm and covered with electrical tape during sampling with the multicorer. Once the core was on board, it was placed in a glove bag under continuous flashing with N_2 gas in order to avoid oxidation of reduced species and the porewaters were extracted using the *Rhizon* technique (Figure 2.5). This method consists of the introduction of a Rhizon (*Rhizonsphere*, The Netherlands) in the sediments through the predrilled holes and to connect

them to a syringe to apply vacuum. The Rhizon (5 cm or 10 cm long) is composed of a hydrophilic porous polymer with a pore size of 0.15 µm in average and a wire to support the polymer allowing the insertion of the Rhzion into the sediments. A syringe or a vacuum tube is linked to the polymer *via* a PVC tube. New Rhizon samplers were used for each extraction in this study, but they could be rinsed with water for reuse. Once the volume extracted was sufficient in the syringe, samples were distributed in sample tubes for the determination of alkalinity, dissolved Fe^{2+}, Mn^{2+} and Si, chloride and sulphates and stored at 4 °C. Samples were also taken for the analysis of hydrogen sulphides (fixed as ZnS) and stored in the dark at room temperature. For nutrients, samples for the analyses of NO_3^-, NO_2^-, NH_4^+, PO_4^{3-} were kept frozen and those for dissolved Si measurements were acidified and stored at 4°C.

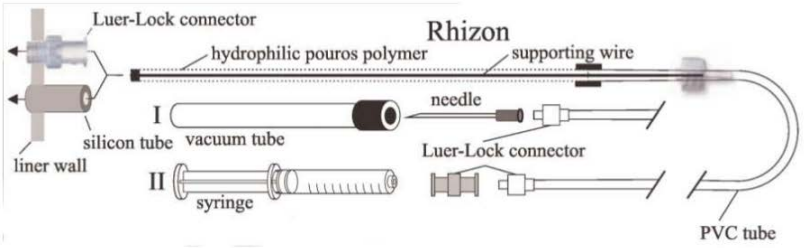

Figure 2.5. Schematic diagram of Rhizon and its periphery (top panel) and picture of the setup for porewater extractions using Rhizons (bottom panel).

2.2 Analytical methods

2.2.1 Microprofiling

The study of benthic mineralization of organic matter in marine sediments, especially in coastal sediments, is on sub-millimetric scale. Glud (2008) indicated that the diffusive boundary layer might be less than 1 mm for coastal sediments. Thus, the use of a microelectrode is required for the study of benthic dynamics. O_2, H_2S and pH depth microprofilings were performed on fresh cores using 100 um or 200 µm sensors (*Unisense*, A/S, Denmark), a multimeter amplifier and a motorized manipulator (Figure 2.6). Each profile was measured under a continuous flux of N_2 in the headspace of the core. The electrodes were inserted 2 by 2 by the micromanipulator at intervals between 250 µm and 500 µm into the sediments. The oxygen content is important because it provides a good indication on the mineralization of organic matter. The H_2S and pH measurements give precious information on the diagenesis (Jourabchi et al., 2005).

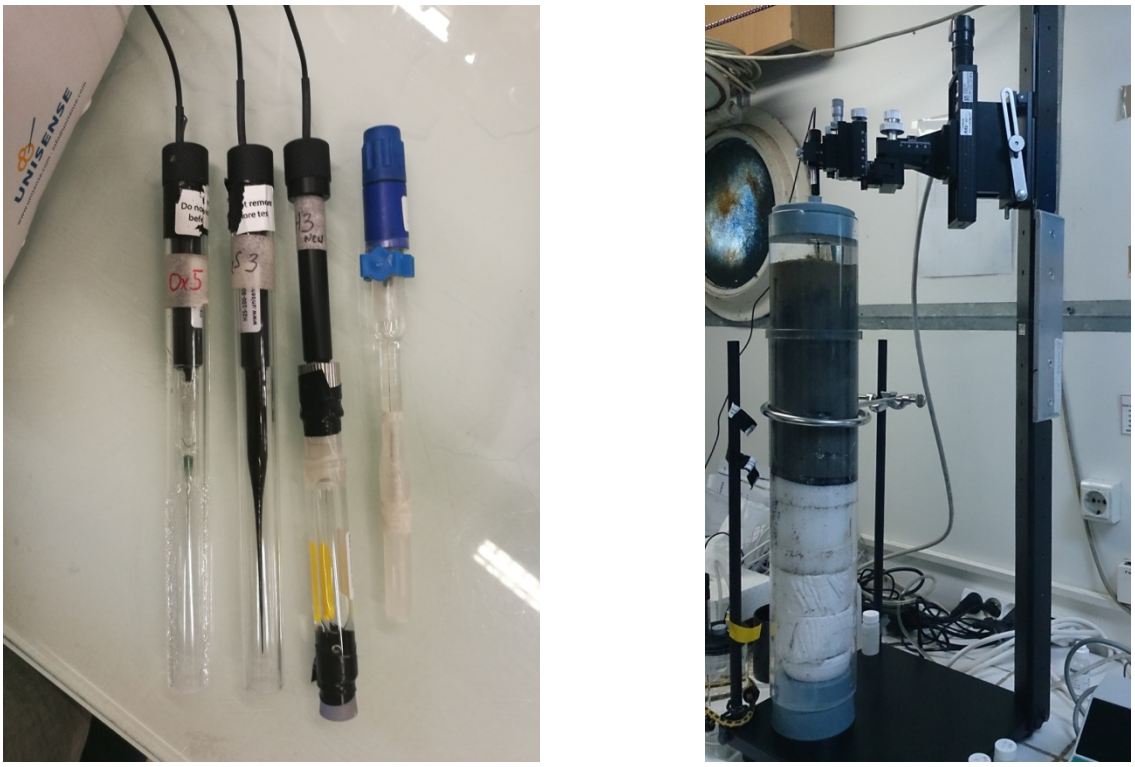

Figure 2.6. Pictures of microsensors of O_2, H_2S, pH and the reference electrode (left panel) and of setup for microprofiling (right panel).

Oxygen microsensor

The 100 µm microelectrode of oxygen is a Clark type electrode composed of gold cathode, silver guard cathode and a silver reference anode in a KCl 0.5 M solution. The silicon membrane allows the diffusion of the oxygen to the cathode. The polarization of the cathode at -0.8 V leads to the reduction of the oxygen which generates a current measured with a microsensor multimeter. The oxygen microelectrode has a fast response time and allows the measurement of low concentrations. It also has an insignificant stirring sensitivity and gives a linear response. For dissolved oxygen, a 2-point calibration was made using air-saturated water (100 % saturation). A solution of sodium ascorbate 0.1 M was used to determine the 0 % saturation. Note that the measurements of oxygen cannot be too deep in the sediment as it may be disturbed by the presence of H_2S.

Sulphide microsensor

The H_2S-100 sensor is composed of a Pt anode, a Pt guard anode and a Pt cathode. The gaseous sulphide enters the basic electrolyte by the silicon rubber membrane. The anode is polarized at +0.085 V. The H_2S is converted into HS^- which is immediately oxidized to elemental sulphur via iron-cyanide redox mediator. This signal is generated by re-oxidation of ferrocyanide at the anode. The schematic diagram of the reaction is shown in Figure 2.7 (Jeroschewski et al., 1996).

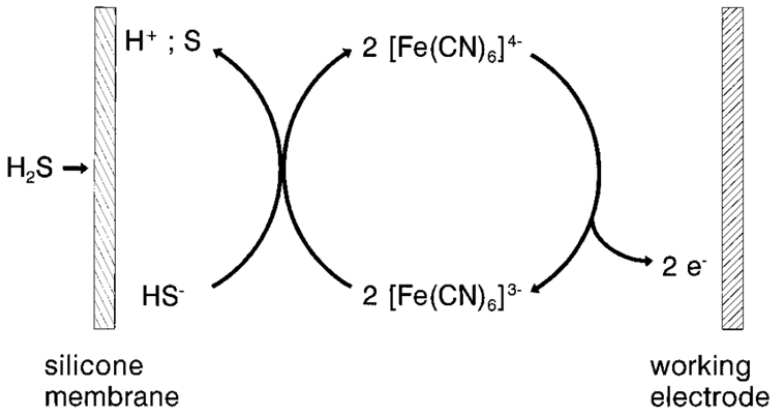

Figure 2.7. Conversion of H_2S in elemental sulphur with a ferricyanide.

The electrode displays an excellent response time and a minimal stirring sensitivity. This kind of electrode is reliable and allows fast measurements at high spatial resolution. The sulphide electrode was calibrated using a set of Na_2S solutions of different concentrations prepared

each day. Moreover, the sensor is painted in black as electrochemistry is light-sensitive. Some chemicals such as carbon monoxide and methyl captan may interfere with the electrochemistry of the electrode.

2.2.2 Nutrient Analyses

Dissolved nitrate and nitrite (NOx)

Dissolved NOx were determined by colorimetry with a *SKALAR* Autoanalyzer system following the method of Grasshoff et al. (1983). Dissolved nitrates are quantitatively reduced in nitrites by passing through a cadmium-copper column. In that case, the autoanalyzer measures the sum of nitrate and nitrite concentrations. To determine only nitrates, the samples are analysed without passing through the Cd-Cu column (NO_2^- only) and the nitrates are determined by difference between both measurements. NO_2^- is diazotized with the sulphanilamide ($C_6H_8N_2O_2S$) as shown in Figure 2.8.

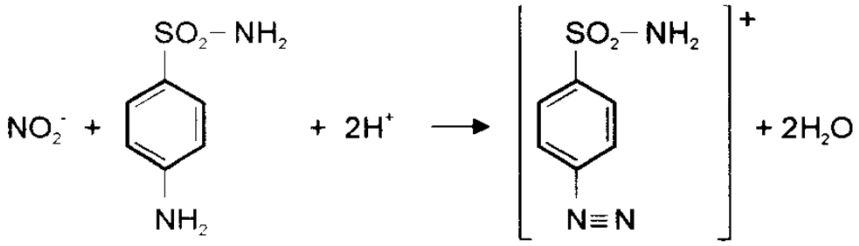

Figure 2.8. Reaction between the nitrites and the sulphanilamide.

The diazonium compound reacts with the N-1-naphtylendiamine dihydrochloride ($C_{12}H_{16}Cl_2N_2$) to produce an azo dye shown in Figure 2.9.

The colour of the dye is measured colorimetrically at 520 nm wavelength. The signal measured by the spectrophotometer is recorded with a chart recorder as peaks. The peak heights are proportional to the nitrite concentration. A standard calibration curve is established as shown as an example in Figure 2.10. Precision was < 2 %.

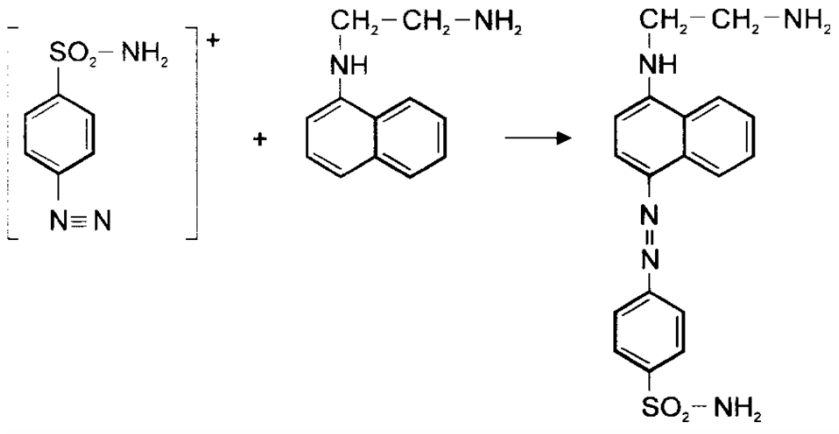

Figure 2.9. Reaction between the diazonium compound and the N-1-naphtylendiamine dihydrochloride.

Dissolved Phosphate

Phosphate concentration was determined by spectrophotometry using the method of Grasshoff et al. (1983). Orthophosphate ions are susceptible to react with ammonium molybdate ($(NH_4)_6Mo_7O_{24}\cdot 4H_20$) and the potassium antimony tartrate in acid environment to form a yellow complex, the ammonium phosphomolybdate. A blue colour is obtained by reduction of this complex using ascorbic acid as reducing agent. The absorbance is measured at 880 nm wavelength with a cell of 1 cm for porewaters and of 10 cm for water column samples. The absorbance is proportional to the PO_4^{3-} concentrations and follows the Beer-Lambert's law. No salt effect was observed. An example of the calibration curve is given in Figure 2.10. Precision was < 2 %.

Dissolved Silicate

The colorimetric method was used to determine the dissolved silicon according to the molybdate/ascorbic acid method (Grasshoff et al., 1983). The dissolved silicon in seawater present in the form of orthosilicic acid reacts in an acid environment with molybdate ions to form a heteropolyacid: the silicomolybdic acid. The yellow complex is reduced by the ascorbic acid to form a blue complex. The interference with the phospho- and arsenio-molybdate is avoided by the addition of oxalic acid before the addition of ascorbic acid. The absorbance is measured at 810 nm. The salinity should to be adapted to the salinity of the samples because of a possible effect of salt. The calibration curve is presented in Figure 2.10. Precision was < 2 %.

Ammonia – OPA

Ammoniacal nitrogen exists in two forms in solution, the ammonia and the ammonium. The proportion depends on the pH, the temperature and the salinity. In the marine and estuarine waters, NH_4^+ is the predominant species, delivered from both animal excretions and bacterial degradation of the organic matter. Once the samples are thawed, NH_4^+ can be measured by fluorometry following the method of Holmes (1999). The principle is that the ammonium reacts with the Ortho-phthalaldehyde (OPA) in the presence of a sulphur reducer in a slightly basic environment (sodium sulphite and borate buffer). The background fluorescence was measured in a borate buffer. No salt effect was observed for this method and the settings of the fluorometer are presented in Table 2.2. Precision was < 9 %.

Table 2.2. Conditions of the fluorometer for the ammonium analyses.

Parameter	
Excitation wavelength	360 nm
Emission wavelength	460 nm
Excitation band	10 nm
Emission band	10 nm
Sensitivity	Low
Response	0.02 s

Ammonium – Classical method

Ammonium concentration was also determined using the method of Grasshoff (Grasshoff et al., 1983). In moderately alkaline solution, dissolved NH_3 reacts with hypochlorite (HClO) to give monochloramine. This will occur in the presence of phenol and in an oxidizing medium (excess of HClO) leading to the formation of indophenol blue. At 20 °C, this reaction, catalysed by the nitroprusside ($Na(Fe(CN)_5NO).2H_2O$), will take around 6 hours to be complete. In seawater at a pH > 9.6, the precipitation of calcium and manganese is avoided by Figure 2.10. Precision was < 1 %.

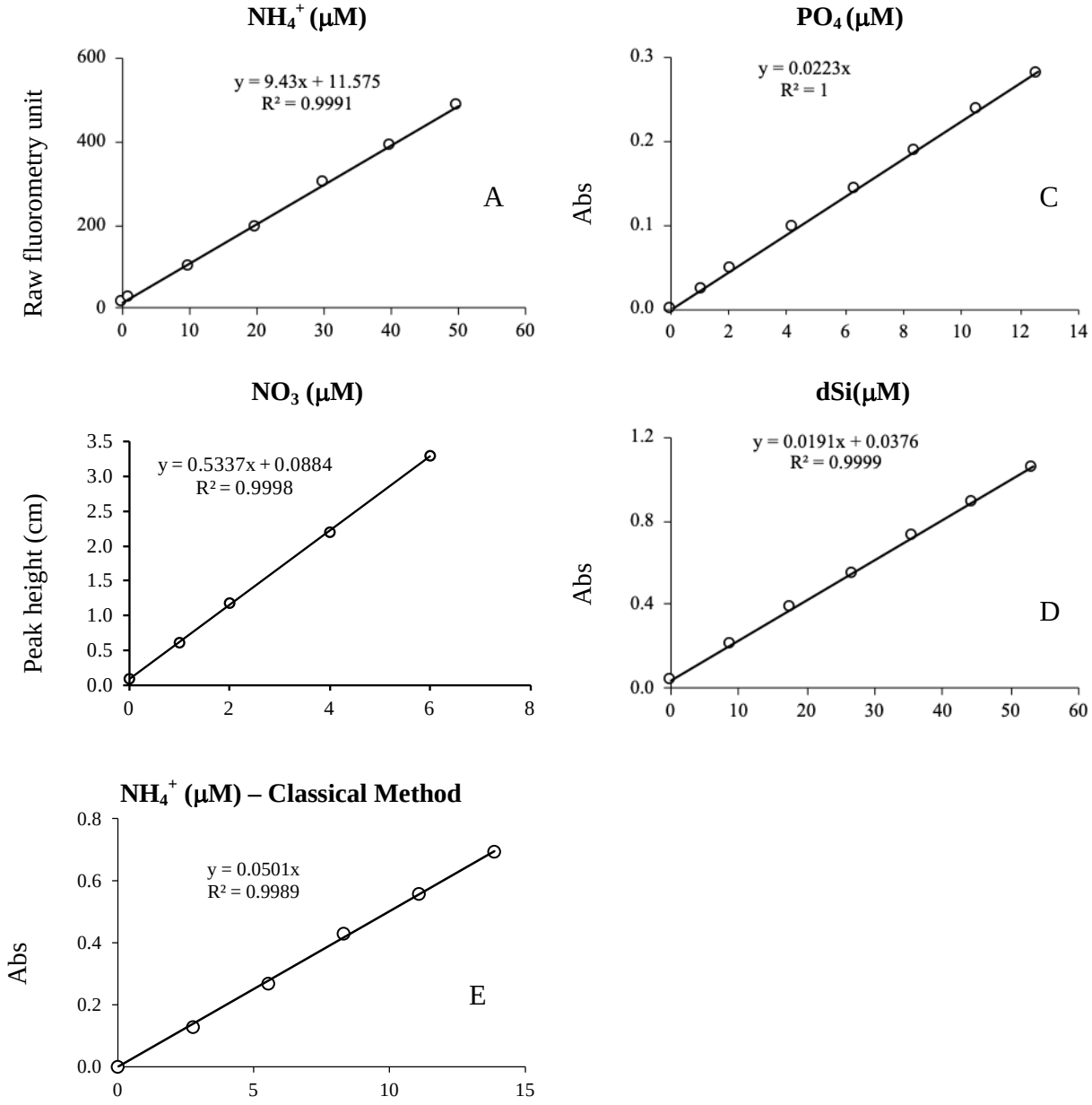

Figure 2.10. Examples of calibration curves of (A) ammonium – OPA method, (B) nitrate, (C) phosphate, (D) silicon and (E) ammonium – Classical method.

2.2.3 Dissolved Inorganic Carbon system

Total Alkalinity

The content in moles of hydrogen ions required to neutralise the weak bases in one kilogramme of seawater defines the total alkalinity (TA). In marine chemistry, it represents weak basis with a pKa ≥ 4.5 (Dickson, 1981).

$$TA = [HCO_3^-] + 2[CO_3^{2-}] + [B(OH)_4^-] - [H^+] + [OH^-] + 2[PO_4^{3-}] + [HPO_4^{2-}] - [H_3PO_4] + [SiO(OH)_3^-] + [HS^-] \quad \text{(Eq. 2.1)}$$

where hydroxide, phosphate, silicate and other bases represent a weak contribution (usually < 1 mol kg^{-1}). TA is sometimes considered as a conservative variable in the seawater and is influenced by changes of temperature, pressure and even if the speciation of element varies. TA was analysed by spectroscopic method (Sarazin et al., 1999). The reagent is composed of methanoïc acid, bromophenol-blue and an ionic strength buffer. The reagent converts the dissolved basic species, HCOOH, into $HCOO^-$ (Eq. 2.2, Eq. 2.3).

$$HCOOH + HCO_3^- \rightarrow HCOO^- + CO_2 + H_2O \quad \text{(Eq. 2.2)}$$

$$2HCOOH + CO_3^{2-} \rightarrow 2HCOO^- + CO_2 + H_2O \quad \text{(Eq. 2.3)}$$

Other dissolved alkaline species are neutralized at the same time because their dissociation constants are smaller than the first dissociation constant of CO_2. The method measures not only alkalinity related to carbonates but also the total alkalinity. The colour change of the dye (yellow to blue) depends on the amount of neutralized protons and can be quantified by UV-visible spectroscopy. This method presents a salt effect and several calibration curves need to be performed regarding the salinities of the samples. An example is given in Figure 2.11. Precision was <1 %.

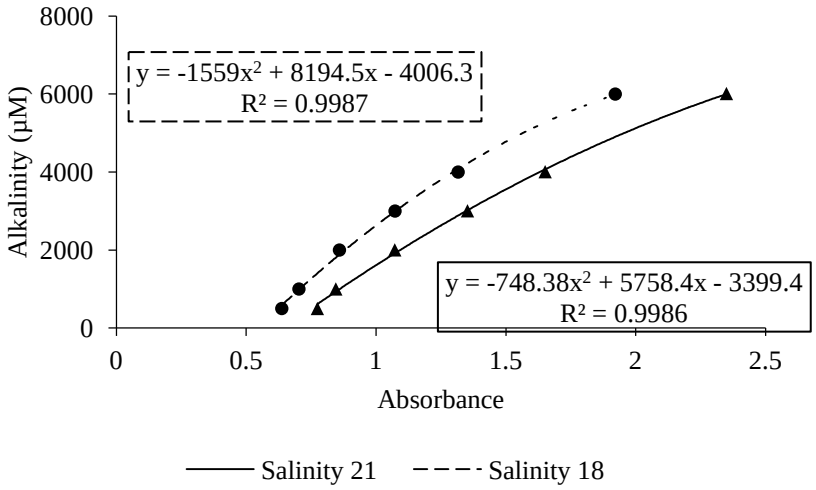

Figure 2.11. Calibration curves carried out in solutions of different salinities (dashed curve: salinity = 21, solid curve: salinity = 18).

2.2.4 Sulphide

The sulphide concentrations were determined colorimetrically using the method of Cline et al. (1969). The hydrogen sulphide reacts, as shown in Figure 2.12, with two molecules of N,N-dimethyl-p-phenylenediamine in the presence of the oxidant iron (III) chloride. This reaction produces methylene blue which is measured at 670 nm. This method does not present a salt effect over salinities from 0 to 40.

Reagent concentrations, cell sizes and calibration curves were adapted according to the concentrations of sulphide in the samples. Precision was < 2 %.

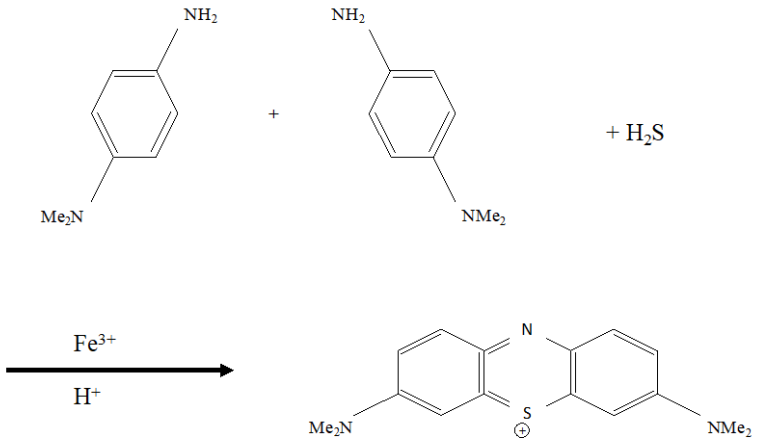

Figure 2.12. Reaction between H_2S and the reagents of the Cline's method.

2.2.5 Dissolved Fe & Mn

The measurements of dissolved iron and manganese were performed by Inductively Coupled Plasma – Atomic Emission Spectrometry (ICP-AES). All the samples were diluted. Calibration curves were realized with standards prepared in acidified Milli-Q water (Figure 2.13). External calibrations were performed at the beginning and the middle of the run to detect an eventual drift of the signal. Precision was < 2 %.

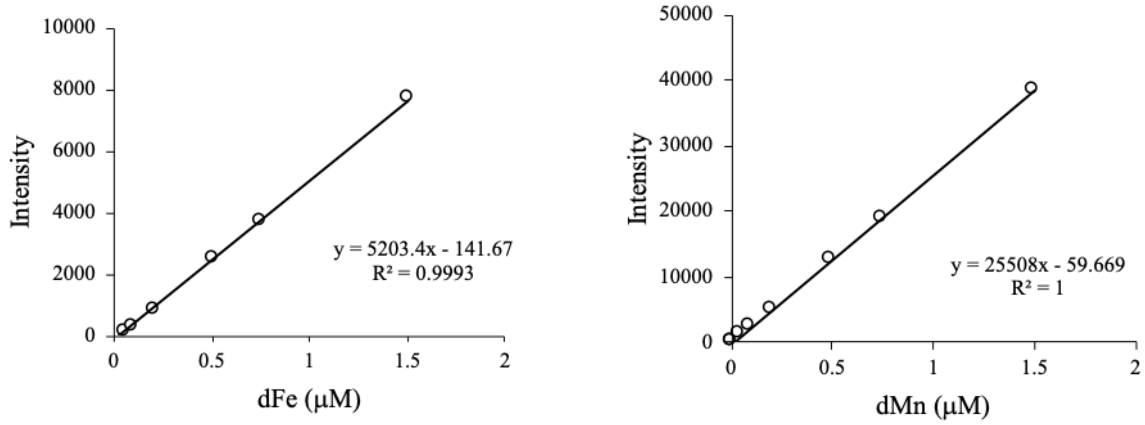

Figure 2.13. Calibration curve of dFe and dMn in µM obtained by ICP-AES.

2.2.6 Chloride and Sulphate

Porewater samples were analysed by ion chromatography for chloride and sulphate after dilution of 250 times. The analyses were carried out at the Laboratoire de Glaciologie at the University libre de Bruxelles with the agreement of J-L. Tison and the help of S. El Amri. The ionic chromatography separates ions in a liquid sample, as a function of their affinity for the mobile or the stationary phase. The mobile phase is composed of an ionic eluent and the stationary phase of a chromatography column. After the conductivity of the eluent has been neutralized by a suppressor, ions are detected using a conductivity detector at the exit of the column. The system used is a Dionex-ICS5000. The two eluents used are MSA (49mM, 0.36 ml/min) for cation separation and KOH (15-40mM, 0.01ml/min) for anion separation on a capillary system. The latter has the advantage of using less eluent (0.01 ml/min instead of 0.36 ml/min for analytical systems). This method has been tested on blank ice samples and on RBIS10 ice core. The system has a standard deviation of 2 ppb for SO_4^{2-} and 8 ppb for Cl^-. Examples of calibration are shown in Figure 2.14.

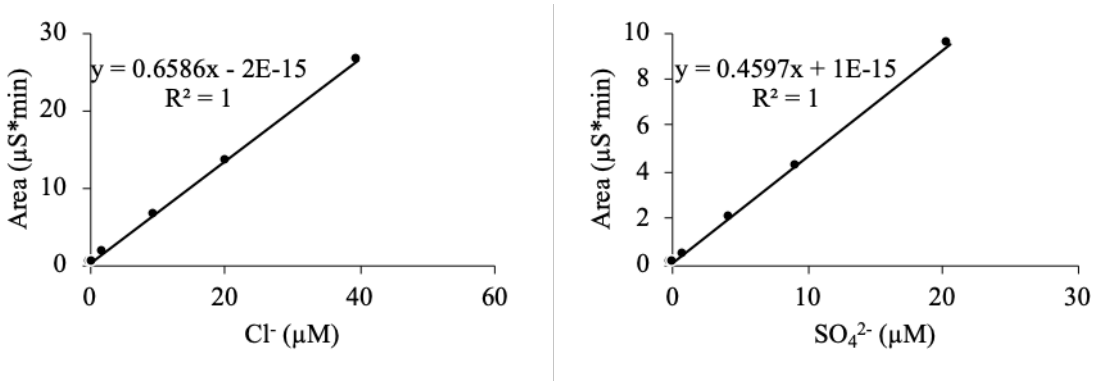

Figure 2.14. Calibration curves of Cl^- and SO_4^{2-} in µM obtained by ionic chromatography.

2.2.7 Diffusive fluxes and benthic mineralization rate calculations

Diffusive fluxes of dissolved species were calculated based on the porewater profiles using the Fick's first law:

$$J = -\frac{\varphi}{\theta^2} D_0(S,T) \frac{\partial C}{\partial x} \qquad \text{(Eq. 2.4)}$$

where J (mmol m^{-2} d^{-1}) is the flux of the dissolved species at the sediment-water interface, φ the porosity of the sediments, θ^2 the correction factor for sediment tortuosity ($\theta^2 = 1 - 2\ln(\varphi)$ (Boudreau, 1996), $D_0(S,T)$ (m^2 d^{-1}) the molecular diffusion coefficient for measured salinity and temperature which is calculated using the R package CRAN:marelac (Soetaert et al., 2010a), C (mmol m^{-3}) the concentration of dissolved species in the porewater and x (m) the sediment depth. The concentration gradient ($\partial C/\partial x$) is obtained by linear regression based on the concentration profile right below the sediment-water interface. The depths selected for the calculation of the concentration gradient depend on the shape of the profile and on the dissolved species in question, the details of which are given in §3.2.5 of Chapter 3.

The flux of dissolved oxygen uptake (DOU, in mmol m^{-2} d^{-1}) can be calculated from the dissolved oxygen profile obtained from microprofiling using O_2 microsensors. Near the sediment-water interface the flux of oxygen consumed by the oxidation of reduced species (NH_4^+, Mn^{2+}, Fe^{2+}), $JO_{2\ Red.Sp.}$ (mmol m^{-2} d^{-1}), can be evaluated from the fluxes of these dissolved species taking into account the stoichiometry of the redox reactions. Knowing DOU and $JO_{2\ Red.Sp.}$, the organic carbon mineralization rates can be estimated. The stoichiometry of mineralization reaction of organic matter (C/N/P = 106/16/1 for organic matter, Redfield, 1958) and the reaction for sulphate reduction (Eq. 2.5 and Eq. 2.6) are used to determine the

oxic and anoxic mineralization rate of organic carbon (mmol C m^{-2} d^{-1}). The ammonium diffusing upward is presumably re-oxidized in the oxic layer.

$$(CH_2O)_{106}(NH_3)_{16}(H_3PO_4)_1 + 138\ O_2 \rightarrow 106\ CO_2 + 16\ HNO_3 + H_3PO_4 + 122\ H_2O \quad \text{(Eq. 2.5)}$$

$$(CH_2O)_{106}(NH_3)_{16}(H_3PO_4)_1 + 53\ SO_4^{2-} \rightarrow 53\ S^{2-} + 106\ CO_2 + 16\ NH_3 + 106\ H_2O + H_3PO_4 \quad \text{(Eq. 2.6)}$$

The calculations of oxic and anoxic mineralization rates of organic carbon are also detailed in §3.2.5 of Chapter 3.

2.2.8 Solid phase characterization

Grain size

The grain size is one of the most fundamental physical properties of sediments. This parameter is used to study the surface processes linked to the dynamic conditions of transport and deposition of sediments. Grain size determination was performed on the gravity cores and on the Van Veen samples by laser diffraction using a *Malvern Mastersizer 2000* particle sizer. Wet sediment was dried at 105 °C during 2 to 3 days. Dried samples were sieved at 2 mm. An aliquot was suspended in demineralized water and mixed 5 to 10 min. A statistical analysis with mean size (%), clay content (%), silt content (%) and sand content (%) is performed for each determination.

Bulk parameters

Water contents, dry densities and porosities were determined on the gravity core and the multicore samples. Porosity (ϕ) is an important parameter to calculate the time of transport of chemical species in the sediments. Porosity represents the relative amount of pore space in a given volume (Schulz & Zabel, 2006). To obtain porosity profiles at each level of sediment cores a fraction of wet sediments is weighted with an analytical balance and placed in an oven at 105 °C. After one week of drying, the sample is weighted. The weight difference represents the evaporation of the pore waters (Eq. 2.7). W_c is the fraction of water contained in the pore spaces that evaporates (Eq. 2.8).

$$V_w = (m_w - m_s) / \rho_{water} \quad \text{(Eq. 2.7)}$$

$$W_c = \frac{(m_w - m_s)}{m_w} \times 100 \qquad \text{(Eq. 2.8)}$$

where V_w is the volume of water in the sediments, m_w the mass of the wet sediments and m_s the mass of the dry sediments.

The density of the shelf sediments of the NW Black Sea is estimated to be 2.6 g cm^{-3}. With the volume of water (V_w) and the volume of the sediment (V_{sed}), the porosity can be calculated according to Eq. 2.10.

$$V_{sed} = \frac{m_s}{2.6} \qquad \text{(Eq. 2.9)}$$

$$\phi = \frac{V_w}{V_w + V_{sed}} \qquad \text{(Eq. 2.10)}$$

LOI: organic carbon and carbonate contents

The Loss of Ignition (LOI) is a common method (Dean, 1974) widely used to determine the organic carbon and carbonate contents in sediments. The technique consists of a sequential heating of samples in a furnace and estimates the weight loss of organic material and calcium carbonate. The first step consists of weighing the samples, dried at 105 °C beforehand, and heating at 550 °C during 4 h. The samples are weighed after cooling in a desiccator at room temperature. The weight difference corresponds to the amount of organic carbon lost after combustion of the organic carbon.

$$CH_2O + O_2 \rightarrow CO_2 + H_2O \qquad \text{(Eq. 2.11)}$$

$$LOI_{550} = \frac{m_{105} - m_{550}}{m_{105}} \times 100 \qquad \text{(Eq. 2.12)}$$

where LOI_{550} is the LOI at 550 °C expressed as a percentage, m_{105} is the dry weight of the sample dried at 105 °C, m_{550} is the dry weight of the sample after degradation of the organic matter (OM) at 550 °C (both in g).

$$\% OM = LOI_{550} \qquad \text{(Eq. 2.13)}$$

The second step is to remove the carbon dioxide from the carbonates.

$$LOI_{950} = \frac{m_{550} - m_{950}}{m_{105}} \times 100 \qquad \text{(Eq. 2.14)}$$

where LOI_{950} is the LOI at 950 °C, m_{550} is the dry weight after heating at 550 °C, m_{950} is the dry weight after calcination at 950 °C and m_{105} is the initial dry weight at 105 °C (all in g).

The weight loss represents the amount of CO_2 released from the calcination reaction.

$$CaCO_3 \rightarrow CaO + CO_2 \qquad \text{(Eq. 2.15)}$$

To determine the carbonate content, LOI_{950} has to be multiplied by 2.27 with a weight of 44 g mol^{-1} for CO_2 and 100 g mol^{-1} for carbonates.

$$\% CaCO_3 = LOI_{950} \times \frac{M_{CaCO_3}}{M_{CO_2}} \qquad \text{(Eq. 2.16)}$$

Figure 2.15. Pictures of crucibles containing sediments after LOI (Photo credit: Nathalie Roevros).

2.2.9 ICP: Major, minor and trace elements of the sediments

The concentrations of particulate elements were determined after total digestion using ICP-MS Nexion 300X (Département de Chimie at the Université de Montréal with K. Wilkinson) and ICP-AES (Service de Biogéochimie et Modélisation du Système Terre at the Université libre de Bruxelles). The multicore samples of Stations 6 and 7 were analysed by ICP-MS and the other stations by ICP-AES.

Total digestion

For all stations, the sediments underwent tri-acid closed-vessels microwave total digestion (HCl-HF-HNO_3) following to the procedure indicated below:

50 mg of dry sediments are weighted and placed in Teflon bombs (PARR company instrument). 0.5 mL of 40 % HF, 0.5 ml of 65 % HNO_3 and 1.5 mL of 30 % HCl are added in the bombs. Once all acids added, the vessels (series of 5) are closed and placed in a microwave following the home-made programme below:

- P1 (Power 1300 W) during 3 min and pause during 12 min

- P1 (Power 1300 W) during 3 min and pause during 12 min

- P1 (Power 1300 W) during 3 min and pause during 12 min

- P2 (Power 2300 W) during 3 min and pause during 12 min

- P2 (Power 2300 W) during 3 min and pause during 12 min

- P2 (Power 2300 W) during 3 min and pause during 60 min before opening

Following the opening, 0.3 g of boric acid are added in each vessel. The recipients are closed and placed in ultrasonic bath during 5-10 min. Once this step is finished, the digested solution is transferred in a plastic volumetric flask of 25 mL and stored in fridge until analysis.

Blanks were taken with every series to determine the reproducibility (RSD < 9 %). Between each series of digestion, the material is washed with acid and is place in M.Q. water bath for the night.

The digested solutions in the flask correspond to a dilution of 40 times. For Stations 6 and 7, the samples were diluted 200 times or more prior to ICP-MS analysis (Precision < 2 %) which was far more sensitive than optical ICP. Precision was < 2 % for major elements and < 5 % for minor elements. Regarding the other stations, the second dilutions were adapted according to the element measured. For Stations 6 and 7, Al, Mn, Co, Ni, Cu, Zn, Cd and Fe were analysed at the University of Montreal and for Stations 12, 15, 1A' and 1, Al, Mn, Fe, Co, Cd, Ni, Zn, Cu were determined at the ULB. The precision and the accuracy were assessed by analysing the Certified Reference Materials (CRM) BCR-277 (Table 2.3).

Table 2.3. Certified or indicative values, measured concentration (mg kg^{-1}) and recovery (%) of the BCR-277 analyzed by ICP-MS and ICP-AES.

BCR - 277	Certified/indicative value (mg/kg)	Measured value (mg/kg)		Recovery (%)	
		ICP-MS	ICP-AES	ICP-MS	ICP-AES
Al	49000 ± 1000	45668 ± 312	50218 ± 1742	93	102
Mn	1580 ± 10	1520 ± 19	1335 ± 76	96	85
Co	17.9 ± 0.5	17.4 ± 0.2	16.0 ± 2.1	99	90
Ni	43.4 ± 1.6	76.7± 1.0	58.0	177	134
Cu	101.7 ± 1.6	103.2 ± 1.0	103.3 ± 5.7	101	102
Zn	547 ± 12	539 ± 4	475 ± 16	99	87
Cd	11.9 ± 0.4	11.62± 0.4	15.1	98	126
Fe	46100 ± 1500	43623 ± 595	50034 ± 2614	95	106

External calibrations were made at the beginning and the middle of the run to detect an eventual drift. All the results were corrected by a correction factor determined with the recovery of BCR-277 measurements. For example, the measured concentrations of Al on samples with ICP-AES were corrected by a factor of 1.02.

Total Hg was also determined at the University of Montreal using a Direct Mercury Analyzer (DMA 80, Milestone Inc., Pittsburgh, PA). The samples were placed in a small bowl and were combusted at 750 °C. The vapors of mercury were retained on a gold trap for analysis by cold vapor atomic absorption spectrometry. Certified reference materials (Tort-2: Lobster Hepatopancreas, Dorm-2: Fish protein, Institute for Environmental Chemistry, National Research Council of Canada, Ottawa, Canada, and SO-2: sediment, Canadian Centre for Mineral and Energy Technology) were used to standardize the instrument. Tort-2 recovery averaged 284.3 ± _14.4 ng g^{-1} (n = 2) corresponding to 105 ± 5 % of the certified value. SO-2 recovery averaged 85.5 ± 1.3 ng g^{-1} (n = 8) corresponding to 104 ± 2 % of the certified value.

2.2.10 Organic carbon and total nitrogen

The content of total organic carbon (TOC) and nitrogen (TN) were analysed on samples from the multicorer, the gravity corer and the Van Veen grab. An aliquot from each dried sample was selected and placed in a tube of 15 mL. The sample was acidified with 1 N HCl to remove the carbonates during 24 h. After the acidification step, the sample was rinsed with water and dried in an oven at 45 °C during 48h. Then, the sediment was ground into powder. Finally, the sample was precisely weighted in an aluminium cup and analysed with a Vario microcube CNS elemental analyser coupled with an IRMS Isoprime 100 isotope ratio mass spectrometer. The analyses were performed at the laboratoire d'Océanologie Biologique of the Université de Liège with the help of G. Lepoint.

2.2.11 Iron speciation

The speciation of iron was determined on freeze-dried sediment samples using the procedure described by Claff et al. (2010) suitable for sulphide-rich sediments. The sequential extraction includes four steps summarized in Table 2.4. The first step extracts the HCl extractable iron (Fe_H) representing labile ferrous (FeS, $FeCO_3$) and ferric iron minerals (ferrihydrite, akaganéite, lepidocrocite). The second step consists of isolating the iron linked to the organic matter (Fe_{org}) with a solution of Na-pyrophosphate. The third one extracts the iron in crystalline oxide minerals such as goethite and hematite (Fe_{ox}). The last step concerns the extraction of the iron in pyrite with concentrated HNO_3. Reactive iron (Fe_{HR}) is represented by the sum of all the extracted phases ($Fe_{HR} = Fe_H + Fe_{org} + Fe_{ox} + Fe_{pyr}$).

Table 2.4. Sequential extraction of Fe species in the sediments.

Step	Extractant – duration	Term
1	1 M HCl - 4h	Fe(II), Fe(III), FeH=Fe(II) + Fe(III)
2	0.1 M Na-pyrophosphate, pH 10.4 - 16h	Fe_{org}
3	0.35 M acetic acid/ 0.2 M Na_3-citrate with 50 g L^{-1} sodium dithionite, pH 4.8 - 4h	Fe_{ox}
4	Concentrated HNO_3 - 2h	Fe_{pyr}

For the analytical method, the Fe(III) were reduced to Fe(II) by 0.4 M hydroxylamine hydrochloride in all extracts. The total Fe was measured as Fe(II) by colorimetry using the

1,10-phenanthroline method (APHA, 2005). In the extract of the first step, the Fe(III) was determined by difference between the total Fe(II+III) and Fe(II). (Precision < 5 %).

2.2.12 Sulphur speciation

Determination of sulphur speciation was also performed on freeze-dried sediment samples using the diffusion method (Burton et al., 2008). This extraction technique is composed of two steps.

Step 1:

The sample is placed in a 100-mL glass Schott bottle, with a septum cap coated with Teflon, containing a 15-mL small polypropylene tube filled with 7 mL of a 5% ZnAc solution (Figure 2.16). Once the system purged with N_2, a needle and a syringe are used to introduce 1 ml of ascorbic acid to reduce the Fe(III) to Fe(II), then 5 mL of 10 N HCl in the glass bottle (Eq. 2.17). The system is mixed on a shaker at 100 rpm during 24 h and by diffusion the H_2S produced is precipitated in the ZnAc solution trap as ZnS (Eq. 2.18). After 24h, the trap tube is changed with a new one containing fresh ZnAc solution.

$$FeS_{(s)} + 2HCl \rightarrow H_2S_{(g)} + FeCl_{2_{(aq)}} \qquad \text{(Eq. 2.17)}$$

$$H_2S + Zn^{2+} \rightarrow ZnS + 2H^+ \qquad \text{(Eq. 2.18)}$$

Step 2:

The system is purged again with N_2. 5 mL of $CrCl_2$ are added using a syringe and a needle into the system. After 48 h of mixing on the shaker at 100 rpm, the solution of ZnAc would trap all the H_2S produced (Eq. 2.19).

$$FeS_{2_{(l)}} + 4CrCl_2 + 4HCl \rightarrow 2H_2S + Fe^{2+} + 4CrCl_3 \qquad \text{(Eq. 2.19)}$$

Following the extractions of sulphur, all the trap solutions were analyzed using the method proposed by Cline et al. (1969) described in §2.2.5 of this chapter. Precision is < 10 % for each step of the extraction.

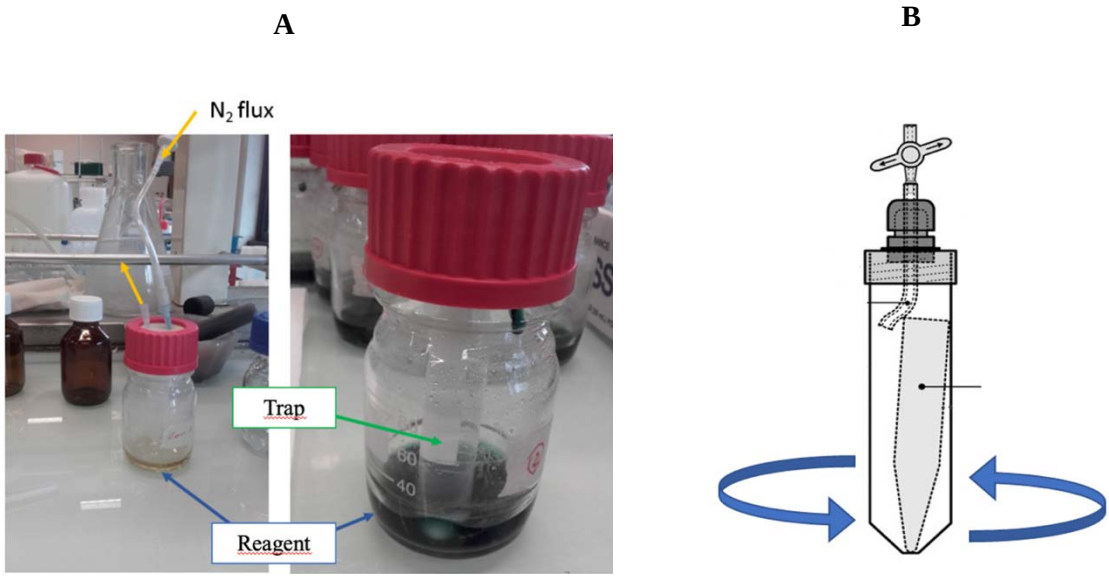

Figure 2.16. Photos of the setup for the extraction of sulphur using the diffusion method. (A) The apparatus used in this study and (B) the orginal design of Burton et al. (2008).

References

APHA. (2005). Standard Methods for the Examination of Water and Wastewater, 21st ed. American Public Health Association – American Water Works Association – Water Environment Federation.

Burton, E. D., Sullivan, L. A., Bush, R. T., Johnston, S. G., & Keene, A. F. (2008). A simple and inexpensive chromium-reducible sulfur method for acid-sulfate soils. Applied Geochemistry, 23, 2759–2766.

Claff, S. R., Sullivan, L. A., Burton, E. D., & Bush, R. T. (2010). A sequential extraction procedure for acid sulfate soils: Partitioning of iron. Geoderma, 155, 224–230.

Cline, J. D. (1969). Spectrophotometric determination of hydrogen sulfide in natural waters. Limnol. Oceanogr., 14, 454-458.

Dean, W. E. (1974). Determination of carbonate and organic matter in calcareous sediments and sedimentary rocks by loss of ignition: comparison with other methods. J. of Sedimentary Petrology, 44, 242-248.

Dickson, A. G. (1981). An exact definition of total alkalinity and a procedure for the esti- mation of alkalinity and total inorganic carbon from titration data. Deep Sea Research, 28, 609–623.

Glud, R. N. (2008). Oxygen dynamics of marine sediments. Mar. Biol., 4, 243-289.

Grasshoff, K., Ehrhardt, M., & Kremling, K. (1983). Methods of Seawater Analysis. Weinheim: Verlag Chemie.

Holmes, R. M., Aminot, A., Kérouel, R., Hooker, B. A., & Peterson, B. J. (1999). A simple and precise method for measuring ammonium in marine and freshwater ecosystems. Can. J. fish. Aqua. Sci., 56, 1801-1808.

Jeroschewski, P., Steuckart, C., & Kühl, M. (1996). An Amperometric Microsensor for the Determination of H2S in Aquatic Environments. Anal. Chem., 68, 4351–4357.

Jourabchi, P., Van Cappellen, P., & Regnier, P. (2005). Quantitative interpretation of pH distributions in aquatic sediments: A reaction-transport modeling approach. Am. J. Sci., 305, 919–956.

Sarazin, G., Michard, G., & Prevot, F. (1999). A rapid and accurate spectroscopic method for alkalinity measurment in sea water samples. Water Ressources, 33, 290-294.

Schulz, H. D., & Zabel, M. (2006). Marine Geochemistry (2nd edition ed.). Springer.

Chapter 3

Impact of bottom water deoxygenation on early diagenesis and benthic fluxes on the NW shelf of the Black Sea

Picture of the departure of the R/V *Mare Nigrum* for the Black Sea in 2016.

Impact of bottom water deoxygenation on early diagenesis and benthic fluxes on the NW shelf of the Black Sea

Audrey Plante, Arthur Capet, Nathalie Roevros, Marilaure Grégoire, Nathalie Fagel and Lei Chou

Keywords : oxygen, Black Sea, early diagenesis, benthic fluxes

Submitted to *Estuarine, Coastal and Shelf Science*.

ABSTRACT

Oxygen depletion in the bottom waters of some coastal systems is a natural-recurring phenomenon known as hypoxia, observed especially in basins with limited water circulation and on continental shelves exposed to nutrient upwelling and riverine discharges. Anthropogenic activities may affect the frequency, extent and duration of hypoxia. The occurrence of seasonal hypoxia implies a seasonal biogeochemical cycling of the benthic compartment which remains poorly quantified. The northwestern (NW) shelf of the Black Sea is impacted by yearly recurrent bottom water hypoxia. Diagenetic pathways, sedimentary oxygen consumption and benthic fluxes of nutrients were investigated during spring 2016 and summer 2017. Sediment cores were collected using a multicorer and microprofiling of oxygen were performed. Porewaters were exacted under nitrogen atmosphere and analysed for nutrients, anions (chloride, sulphate, sulphide) and redox sensitive metals (iron, manganese). Our results reveal seasonality in the sedimentary oxygen consumption with low uptake rates in summer caused by oxygen limitation. Diagenetic reactions may be affected by oxygen availability which in turn will alter the benthic fluxes of nutrients and other reduced compounds. Benthic mineralization of organic matter on the NW shelf of the Black Sea exhibited spatial and temporal variations with the dominance of oxic mineralization during spring and of sulphate reduction during a bottom water deoxygenation event in summer.

3.1 Introduction

Shallow coastal ecosystems, such as estuaries and continental shelves, cover about 10 % of the total surface of the ocean and support 30 % of the primary production as well as 90 % of fisheries, which constitutes precious resources (LOICZ, 1995). Over the years, humans live more and more closely to the shoreline, causing a degradation of these coastal environments. The intensifying input of nutrients such as nitrogen and phosphorus, issued from agricultural, livestock, industrial and human waste, contributes to the coastal eutrophication. The excess nutrients lead to an increase of organic matter export from the surface water to the sediment which enhances the microbial respiration in the bottom waters and generates a greater demand of oxygen (Diaz & Rosenberg, 2008). Besides the anthropogenic impacts, natural variabilities such as the stratification of the water column may affect the oxygen concentrations of the bottom waters and contribute to deoxygenation of the coastal waters. Some semi-enclosed seas, like the Baltic Sea or the Black Sea, undergo hypoxia with dissolved O_2 < 63 µM (Diaz & Rosenberg, 2008). In the case of the Black Sea, the north-western (NW) shelf endures a seasonal hypoxia since the 1970s. Dam constructions, overfishing and eutrophication have increased the extent of hypoxia and as a consequence have altered the biogeochemical cycling of carbon and associated elements (Capet et al., 2013).

Throughout the years, nutrient inputs by the Danube river have evolved. During the 1960s, the Danube discharged annually 1.4 x 10^5 t of total inorganic nitrogen, 0.12 x 10^5 t of phosphate and 7.9 x 10^5 t of dissolved silicate into the Black Sea (Almazov, 1961). Monitoring between 1988 and 1992 revealed that the Danube river delivered 6-8 x 10^5 t yr^{-1} of total nitrogen, 0.23-0.32 x 10^5 t yr^{-1} of phosphate et 3 x 10^5 t yr^{-1} of dissolved silica (Cociasu et al., 1996). These data highlighted an increase of the nitrogen and phosphate loads and a decrease of the dissolved silica inputs, which had an impact on the biogeochemistry of the NW shelf of the Black Sea in general and on the exchange across the sediment-water interface in particular. Moreover, seasonal variability of the nutrient fluxes at the sediment-water interface of the shelf was reported between summer 1995 and spring 1997 by Friedrich et al. (2002) supporting the development of hypoxia.

The oxic and anaerobic mineralization of the organic matter deposited on the seabed takes place in the sediments and regulates the biogeochemistry of the water column. Conversely, changes of the chemical composition of the water column, in particular the oxygen concentrations, can affect the biogeochemistry of the sediments (Middelburg & Levin, 2009).

Thermodynamically, oxygen is the most favourable electron acceptor of the diagenetic sequences providing a higher energy gain to organisms involved in the mineralization of the organic matter (Froelich, et al., 1979). When the environment becomes hypoxic, the diagenetic reactions are disturbed, and the anoxic pathways become dominant.

In this work, the effects of seasonal deoxygenation in bottom waters on the diagenetic pathways have been investigated during two biogeochemical surveys on the NW shelf of the Black Sea. Oxygen consumptions are estimated from microprofilings of dissolved oxygen in the sediments collected with the multicorer and benthic fluxes are evaluated from the porewater profiles. The temporal and spatial variabilities of benthic mineralization of organic matter are discussed.

3.2 Material and methods

3.2.1 Location

During two research cruises onboard the R/V *Mare Nigrum* in the Ukrainian coastal zone (Figure 3.1), sediment samples were taken at four stations (Stations 6, 7, 12 and 15) in May 2016 and two stations (Stations 1 and 1A') in August 2017. Note that the Stations 7 and 1A' are situated next to each other. Stations 6, 7 and 1A' are located in the Danube delta front, Stations 1 and 12 are in the Dnieper region and Station 15 is in the Odessa Bay (Table 3.1).

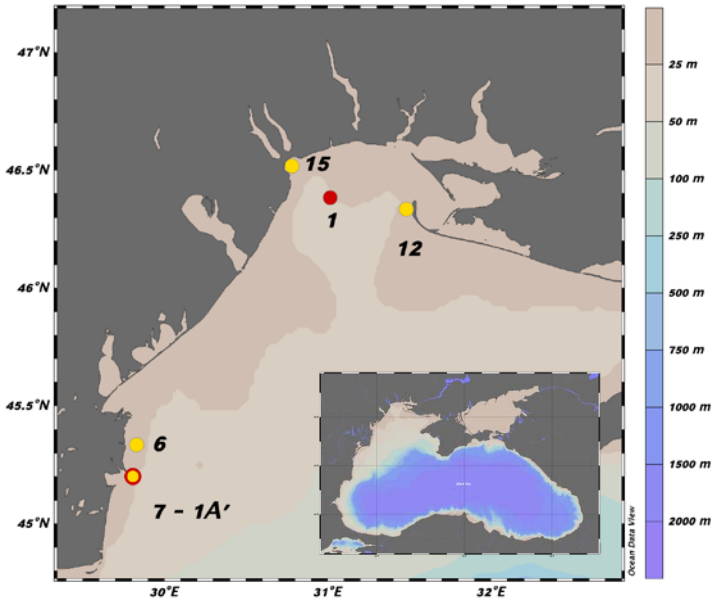

Figure 3.1. Map of the Black Sea (bottom right corner) and map of the sampling stations on the NW shelf. Yellow dot: 2016-cruise, red dot: 2017-cruise, yellow dot with red circle: 2016-2017-cruises.

Table 3.1. Positions and dates of stations sampled on the Ukrainian shelf. Water depths and O_2 concentrations in the bottom waters above the sediment-water interface measured by microprofiling are also indicated.

Station	Year sampling	Position	Water depth (m)	O_2 (μM)
6	19/05/2016	45°20.0'N, 29°50.6'E	21.0	108.9
7	19/05/2016	45° 12.0'N, 29° 48.6'E	18.6	144.6
12	21/05/2016	46° 20.0'N, 31° 29.0'E	14.4	181.6
15	21/05/2016	46° 31.6'N, 30° 47.5'E	17.1	265.2
1A'	27/08/2017	45° 12.0'N, 29° 48.6'E	19.9	7.39
1	29/08/2017	46° 26.0'N, 31° 01.0'E	22.0	58.2

3.2.2 Sampling procedure

Water-column sampling was performed at each station using a CTD rosette, mounted with temperature, salinity, pressure and oxygen sensors, and equipped with Niskin bottles. Sediment cores were retrieved using a multicorer for microprofiling of geochemical gradients and for porewater sampling. Oxygen depth profiles were recorded on fresh cores with a 100 μm oxygen microsensor, using a motorized microprofiling system equipped with a microsensor multimeter (*Unisense*, A/S., Denmark). The Rhizon technique (Seeberg-Elverfeldt et al., 2005) was performed using Rhizon samplers (pore size 0.15 μm, *Rhizosphere*, the Netherlands) under N_2 atmosphere to extract porewaters generally at 2-cm interval resolution. Porewater extraction was completed several hours (less than 4h) after core collection. Subsamples were taken for the analysis of alkalinity, sulphate, sulphide, nutrients (NO_3^-+NO_2^-, NH_4^+, PO_4^{3-} and Si) and dissolved Fe^{2+} and Mn^{2+}. All water samples were stored at 4°C, except for samples for inorganic nitrogen (nitrate+nitrite and ammonium) and phosphate analyses which were kept frozen.

3.2.3 Porewater analyses

Alkalinity was measured with a spectrophotometric method following the procedure of Sarazin et al. (1999). Sulphate concentrations were determined by ionic chromatography after 250x dilution. Dissolved sulphides were measured spectrophotometrically according to the methylene blue method (Cline, 1969). Dissolved Fe and Mn were determined by ICP-OES on acidified samples (Grasshoff et al., 1983). Ammonium was measured by fluorometry (Holmes et al., 1999). Other nutrients (NO_3^-+NO_2^-, PO_4^{3-}, Si) were analysed by colorimetric methods (Grasshoff et al., 1983).

3.2.4 Solid phase analyses

Sediments sampled by the multicorer were sliced at 1-4 cm thickness intervals for various analyses of the solid phase. Each slice was dried at 45 °C until a constant weight was reached in order to calculate the porosity (φ) from the water content assuming a density value of 2.6 g cm^{-3}, typical value for siliciclastic sediments.

$$\varphi = \frac{volume\ of\ pore\ space}{total\ sample\ volume} \qquad \text{(Eq. 3.1)}$$

The sediment grain size distribution was determined by laser diffraction using a Malvern Mastersizer 3000 (McCave et al., 1986). Total organic carbon (TOC) and total nitrogen (TN) contents (% dry weight), $\delta^{13}C$ and $\delta^{15}N$ were measured on decarbonated sample with a Vario Microcube CNS elemental analyser coupled with an IRMS isoprime 100 isotope ratio mass spectrometer.

3.2.5 Flux and mineralization rate calculations

In muddy sediments, the main transport mechanism of solute species is the molecular diffusion in the absence of re-suspension and bioturbation. The vertical fluxes of dissolved species can be calculated using Fick's first law:

$$J = -\frac{\varphi}{\theta^2} D_0(S,T) \frac{\partial C}{\partial x} \qquad \text{(Eq. 3.2)}$$

where J (mmol m^{-2} d^{-1}) is the flux of the dissolved species, φ the porosity, θ^2 the correction factor for sediment tortuosity ($\theta^2 = 1 - 2\ln(\varphi)$) (Boudreau, 1996), $D_0(S,T)$ (m^2 d^{-1}) the molecular diffusion coefficient for measured salinity and temperature, C (mmol m^{-3}) the concentration in the porewater and x (m) the sediment depth. The molecular diffusion coefficient is calculated using the R package CRAN:marelac (Soetaert et al., 2010a). The concentration gradient ($\partial C/\partial x$) is obtained by linear regression based on the concentration profile right below the sediment-water interface. The depths were chosen mainly where the concentration gradient was the strongest and the average porosity value in the first 5 cm of the sediment was used in the flux calculation. For ammonium, iron and manganese in the case of the reduced species, the gradient was calculated with the concentration of bottom waters and the first two concentrations in porewaters of the sediments or with the average concentration of the first two points. For sulphate, the gradient was calculated between 0 cm and 10 cm depth at all stations, except for Station 7 where the concentrations between 20 cm and 30 cm were taken due to the possible presence of bioturbation as inferred by the profile. For dissolved phosphate and silicate, the gradient was calculated with the concentration in the bottom waters and the first three concentrations in porewaters. For H_2S, the flux was not taken into account due to its very low concentrations and to its involvement in other reactions such as the formation of iron sulphides.

From the flux of diffusive oxygen uptake (DOU, mmol m^{-2} d^{-1}) determined by the microprofiling of oxygen in the sediments and the fluxes (mmol m^{-2} d^{-1}) of reduced dissolved species (NH_4^+, Fe^{2+}, Mn^{2+}), the impact of the diagenetic reactions on the organic carbon mineralization can be estimated. The stoichiometry of mineralization reactions of organic matter (C/N/P = 106/16/1 for organic matter, Redfield, 1958, Eq. 3.3) and the reaction for sulphate reduction (Eq. 3.4) are used to determine the oxic and anoxic mineralization rates of organic carbon, $\Gamma min_{ox} C_{org}$ and $\Gamma min_{anox} C_{org}$ respectively.

$$(CH_2O)_{106}(NH_3)_{16}(H_3PO_4)_1 + 138\ O_2 \rightarrow 106\ CO_2 + 16\ HNO_3 + H_3PO_4 + 122\ H_2O \quad \text{(Eq. 3.3)}$$

$$(CH_2O)_{106}(NH_3)_{16}(H_3PO_4)_1 + 53\ SO_4^{2-} \rightarrow 53\ S^{2-} + 106\ CO_2 + 16\ NH_3 + 106\ H_2O + H_3PO_4 \quad \text{(Eq. 3.4)}$$

Taking into account the stoichiometry of the redox reactions for the re-oxidation of the reduced species, the flux of oxygen consumption can be calculated according to the following equation:

$$JO_{2_{Red.Sp.}} = 2\,J_{NH_4^+} + \frac{1}{2}\,J_{Mn^{2+}} + \frac{1}{4}\,J_{Fe^{2+}} \quad \text{(Eq. 3.5)}$$

where $JO_{2\ Red.Sp.}$ (mmol m^{-2} d^{-1}) is the oxygen flux necessary to oxidize the reduced species diffusing to the oxic zone, and $J_{NH_4^+}$, $J_{Mn^{2+}}$ and $J_{Fe^{2+}}$ (mmol m^{-2} d^{-1}) are the diffusive fluxes across the sediment-water interface of NH_4^+, Mn^{2+} and Fe^{2+} respectively. Knowing DOU and $JO_{2\ Red.Sp.}$, the oxic mineralization rate of organic carbon, $\Gamma min_{ox}C_{org}$ (mmol C m^{-2} d^{-1}), can be determined following Eq. 3.6.

$$\Gamma min_{ox}C_{org} = (DOU - JO_{2_{Red.Sp.}}) \times \frac{106}{138} \quad \text{(Eq. 3.6)}$$

where 106/138 is the ratio corresponding to the fraction of the total amount of oxygen respired that is consumed by the mineralization of organic carbon.

The percentage of the diffusive oxygen uptake (DOU) flux associated with the re-oxidation of reduced species during the mineralization of organic carbon, % Red. Sp., can be evaluated according to Eq. 3.7:

$$\%\ Red.Sp. = \left(\frac{JO_{2_{Red.Sp.}}}{DOU}\right) \times\ 100 \quad \text{(Eq. 3.7)}$$

The anoxic mineralization rate of organic carbon, $\Gamma min_{anox}C_{org}$ (mmol C m^{-2} d^{-1}), is assessed from the flux of dissolved sulphate, $J_{SO_4^{2-}}$ (mmol m^{-2} d^{-1}), following Eq. 3.8:

$$\Gamma min_{anox}C_{org} = J_{SO_4^{2-}} \times \frac{106}{53} \quad \text{(Eq. 3.8)}$$

where the ratio of 106/53 implies that one mole of sulphate can oxidize two moles of organic carbon (Eq. 3.4).

Finally, the relative contribution of anoxic mineralization rate of organic carbon to the overall mineralization rate, % Anox/(anox + ox), can be evaluated according to Eq. 3.9:

$$\%\ Anox/(anox + ox) = \left(\frac{J_{SO_4^{2-}} \times 2}{(J_{SO_4^{2-}} \times 2) + (DOU - JO_{2_{Red.Sp.}}) \times \frac{106}{138}}\right) \times 100 \qquad \text{(Eq. 3.9)}$$

3.3 Results

3.3.1 Water column conditions

During spring 2016, Stations 6 and 7 presented stratified conditions with dissolved oxygen concentration decreasing with depth from 322 µM to 189 µM and from 340 µM to 181 µM respectively. At Stations 12 and 15, stratification of the water column began to develop and oxygen concentration fluctuated around 277 µM and 301 µM respectively (Figure 3.2).

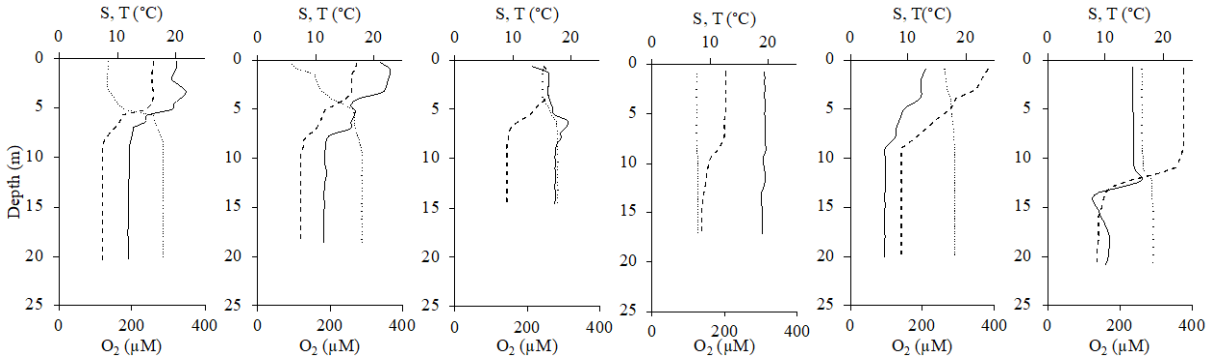

Figure 3.2. CTD profiles obtained during the two cruises. Dashed line: temperature (°C), dotted line: salinity, and black line: oxygen concentration (µM).

In contrast, salinity and temperature measurements from summer 2017 revealed a stronger thermal stratification of the water column compared to the situation in spring 2016. Dissolved oxygen concentrations at the Stations 1 and 1A' decreased with depth down to 161 µM and 95 µM respectively. Therefore, the system remained oxic at a depth 1 m above the seabed.

However, microprofilings of dissolved oxygen illustrated that the bottom waters had low oxygen contents in summer 2017 (Figure 3.3), suggesting the presence of a sharp benthic boundary layer and a strong gradient in dissolved oxygen in the last meter of the water column above the sediment-water interface.

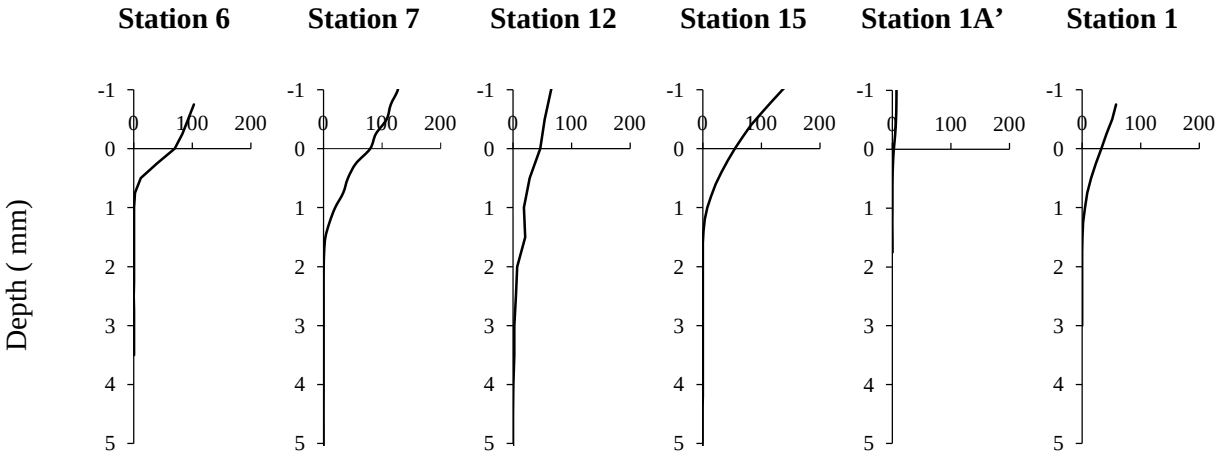

Figure 3.3. Microprofiles of oxygen (μM) for all stations sampled in spring 2016 and summer 2017.

Dissolved oxygen concentrations in the bottom waters varied over the season. At the mouth of the Danube, water close to the seafloor was more oxygenated during spring 2016 (181 μM at Station 7) than during summer 2017 (95 μM at Station 1A').

3.3.2 Sediment characteristics

Surface sediments of the NW shelf of the Black Sea were mainly composed of fine mud with a median grain size of 24 μm and a mean silt content of 85 ± 9 % (Table 3.2). Sediments at Station 12 exhibited a coarser and sandy granulometry due to its location close to the Tendra Spit. Sediment porosity was high near the water-sediment interface and decreased downcore (Figure 3.4). Compared to Stations 7 and 12, the porosities at Stations 6, 15, 1 and 1A' in the first centimetres were higher, indicating the presence of a fluffy layer, easily resuspended, with different grain size influencing the porosity.

Table 3.2. Characteristics of the surface sediments (upper 20 cm) for the various stations. $C_{org\text{-}IRMS}$ and $N_{org\text{-}IRMS}$ represent mean values.

Station	Grain size			$C_{org\text{-}IRMS}$ %	$N_{org\text{-}IRMS}$ %	$\frac{C_{org-IRMS}}{N_{org-IRMS}}$
	% Clay	% Silt	% Sand			
6	2	89	9	2.3	0.3	8.39
7	2	94	4	1.4	0.2	9.22
12	1	66	33	0.8	0.1	8.30
15	2	91	7	3.4	0.3	11.82
1A’	2	89	8	1.4	0.5	7.95
1	1	84	15	4.3	0.2	7.85
Mean ± Stdev	2 ± 0.5	85 ± 9	13 ± 11	2.3 ± 1.3	0.3 ± 0.1	8.93 ± 1.50

Moreover, the porosity in surface sediments showed a possible seasonal variability with a higher value during the summer (0.87 at Station 1A’) than in the spring (0.75 at Station 7). The NW shelf sediments exhibited high organic carbon content with higher values measured at Stations 6, 15 and 1 compared to Stations 12, 7 and 1A’, which could be attributed to the Danube and Dnieper inputs (Table 3.2).

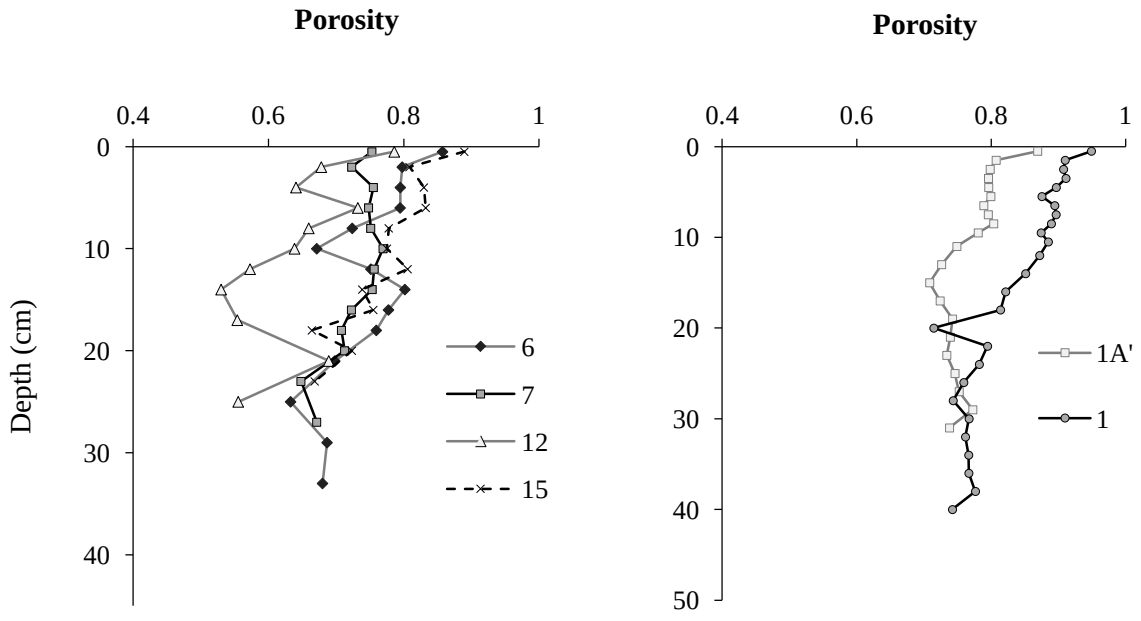

Figure 3.4. Depth profiles of porosity at the field sites during spring 2016 (left panel) and summer 2017 (right panel).

Values of $N_{org\text{-}IRMS}$ ranged between 0.1 % and 0.5 %. For all stations, the linear regression analysis showed a positive strong correlation ($R^2 = 0.842$) between $C_{org\text{-}IRMS}$ and $N_{org\text{-}IRMS}$ contents. Except for Station 15, C/N ratios varied between 7 and 10, indicative of an algal origin (Meyers, 1994). A C/N ratio < 10 suggests some microbial respiration leading to a rapid mineralization of the organic carbon. The C/N ratio slightly higher than 10 observed at Station 15 could reflect the proximity of this station to the land or a slower decomposition of organic carbon, confirming the high input of land-derived organic matter. The breakdown of land-plant material with high C/N ratios is difficult, which could restrain the aerobic activity and limit benthic oxygen consumption.

3.3.3 Oxygen microprofiling and oxygen penetration depth

All the sites investigated during spring 2016 exhibited dissolved oxygen concentrations above the hypoxic threshold in the bottom waters ($[O_2] < 63$ μM), attesting that hypoxia had not yet been developed on the shelf (Figure 3.3). In contrast, the dissolved oxygen concentrations at the sediment-water interface during summer 2017 were below this threshold, indicating the possible occurrence of hypoxia. The oxygen penetration depths (OPDs), i.e. the thickness of the oxic zone in sediments (Cai & Sayles, 1996), displayed an average value of 1.88 mm on the NW shelf of the Black Sea, typical for coastal marine sediments (Kristensen, 2000). All sediment cores retrieved in 2016 were depleted in dissolved oxygen at a depth of < 4.00 mm while in 2017 the oxygen penetration depths were shallower than 1.25 mm (Table 3.3).

Oxygen penetration depths observed on the NW shelf showed spatial variability. The OPDs were shallower at Stations 6, 7 and 15 than at Station 12 during spring 2016. Stations 6, 7 and 15 received an important organic matter inputs from the Danube and the Dnieper rivers, and the oxygen profiles highlighted the efficiency of degradation of organic matter. The deeper OPD at Station 12 (Table 3.3) could be attributed to the highest sand content (Table 3.2) in the sediments as suggested by Cai & Sayles (1996). A low hydrodynamic condition and/or the presence of bioturbation as revealed by the nonlinear gradient of oxygen concentrations could also explain the deeper OPD at this station.

In Summer 2017, a shallower OPD was observed at Station 1A' than at Station 1, which could be associated with the differences in bottom water oxygen levels and with the Danube discharge.

Table 3.3. Oxygen Penetration Depth (OPD) and Diffusive Oxygen Uptake (DOU) for the stations sampled in 2016 and 2017. Diffusive fluxes were estimated by Fick's first law. Negative values represent upward fluxes from the sediments to the overlying water and positive values are downward fluxes from the water into the sediments.

Station	**OPD**	**DOU**	**JSO_4^{2-}**	**JNH_4^+**	**JFe^{2+}**	**JMn^{2+}**	**JPO_4**	**JdSi**
	mm	mmol m^{-2} d^{-1}		μmol m^{-2} d^{-1}				
6	1.00	5.98	0.59	-303.10	-16.53	-67.95	-10.78	-35.36
7	2.00	2.38	0.87	-37.22	-161.31	-18.27	-1.59	-55.60
12	4.00	0.94	0.12	-36.45	-17.76	-7.88	-0.26	-43.87
15	2.00	4.04	1.80	-681.85	-91.45	-38.50	-32.64	-375.03
1A'	0.50	0.53	0.87	-59.36	-131.27	-17.56	-2.29	N.A.
1	1.75	2.07	1.04	-632.03	-197.65	-60.48	-41.21	N.A.
Mean	1.88	2.66	0.88	-291.67	-102.66	-35.11	-14.80	-127.47
±	±	±	±	±	±	±	±	±
Stdev	1.20	2.04	0.55	300.69	74.87	24.77	17.74	165.25

Temporal variation of dissolved oxygen concentrations in the bottom waters was observed at stations close to the mouth of the Danube. The overlying water above the sediment-water interface at Station 7 contained 144.6 μM dissolved oxygen in spring 2016, while at Station 1A' a concentration of 7.39 μM was measured with the microsensor in summer 2017 (Figure 3.3). As seasonal oxygen limitation develops in the water column close to the Danube river, the oxygen concentration decreases over summer below the hypoxic threshold affecting the OPD. The shallower OPD at Station 1A' compared to Station 7 (Table 3.3) indicated changes in diagenetic reactions in response to the bottom water deoxygenation. In the sediments, a thinner oxic zone would favor the mineralization of organic matter by oxidants other than oxygen of the diagenetic cascade.

3.3.4 Alkalinity and nutrients in porewaters

Alkalinity in the porewaters increased with sediment depth at all stations (Figure 3.5), except for Station 12 where alkalinity remained relatively constant over depth. Different shapes of the depth profile could be distinguished which appeared to be related to the sulphate profiles. Vertical distributions of alkalinity displayed that at Stations 6, 7 and 1A' the gradient was

weaker in the subsurface which became stronger at depth. In contrast, at Stations 15 and 1 the gradient was strongest at the sediment-water interface and the alkalinity values remained constant at depth below 10 cm. Alkalinity measurements exhibited spatial variation. Based on the gradients observed in spring 2016, more alkalinity seemed to be released from sediments at Stations 6, 7 and 15, close to the river mouths, than at Station 12 where the alkalinity remained relatively constant with depth. A seasonal effect has also been noted with a stronger near-surface gradient of alkalinity observed at Station 1A' during summer 2017 than that measured at Station 7, attesting the influence of low oxygen levels in the bottom waters.

The concentrations of ammonium in interstitial waters varied over space in spring 2016 (Figure 3.5). At Stations 6, 7 and 15 the concentrations increased downward, indicating that the sediment was a source of ammonium for the overlying waters with the highest flux found at Station 6 (Table 3.3). The concentrations at Station 7 were rather constant down to 15 cm and then increased with depth, suggesting some bioturbation close to the sediment-water interface. Station 12 showed no significative variations with depth. At Stations 7 and 1A' near the mouth of the Danube, different NH_4^+ concentrations were measured respectively in spring 2016 and summer 2017. Under low bottom water oxygen conditions, bioturbation seemed to occur at a shallower depth (3 cm vs. 15 cm under oxic conditions) and flux calculations indicated a higher NH_4^+ flux at Station 1A' where low oxygen concentrations were observed. Station 1 profile showed an important increase of NH_4^+ concentration first near the sediment-water interface down to a depth of 5 cm which then remained constant further down, revealing that the sediment was a source of ammonium during a deoxygenation event as well.

The profiles of phosphate were similar to those of ammonium on the shelf. Phosphate concentrations increased with depth except for Station 7 (Figure 3.5). Station 12 displayed low concentrations in the uppermost centimetres of the sediments which increased slowly from 6-cm depth downward. At Station 7, phosphate concentrations remained relatively constant through depth.

At Station 6 close to the Danube, phosphate concentration was low at the sediment-water interface, which increased first at a slower rate down to 15 cm depth and then at a higher rate reaching 264 μM at the bottom of the core. Station 15 showed the highest measured phosphate concentrations in the uppermost centimetres of the shelf sediments in spring 2016. Similar to ammonium, phosphate profiles showed a higher concentration in deeper layers in summer 2017 at Station 1A' reaching a maximal value of 97 μM at 23 cm depth, compared to spring 2016 at Station 7. Porewaters of the surface sediments were depleted in phosphates at

these two stations, which could be attributed to bioturbation resulting in the precipitation of Fe-oxides adsorbing phosphates. Phosphate profile at Station 1 was different from the others, showing that there was a subsurface maximum situated at a depth of 5 cm and the concentration remained relatively constant below 10 cm.

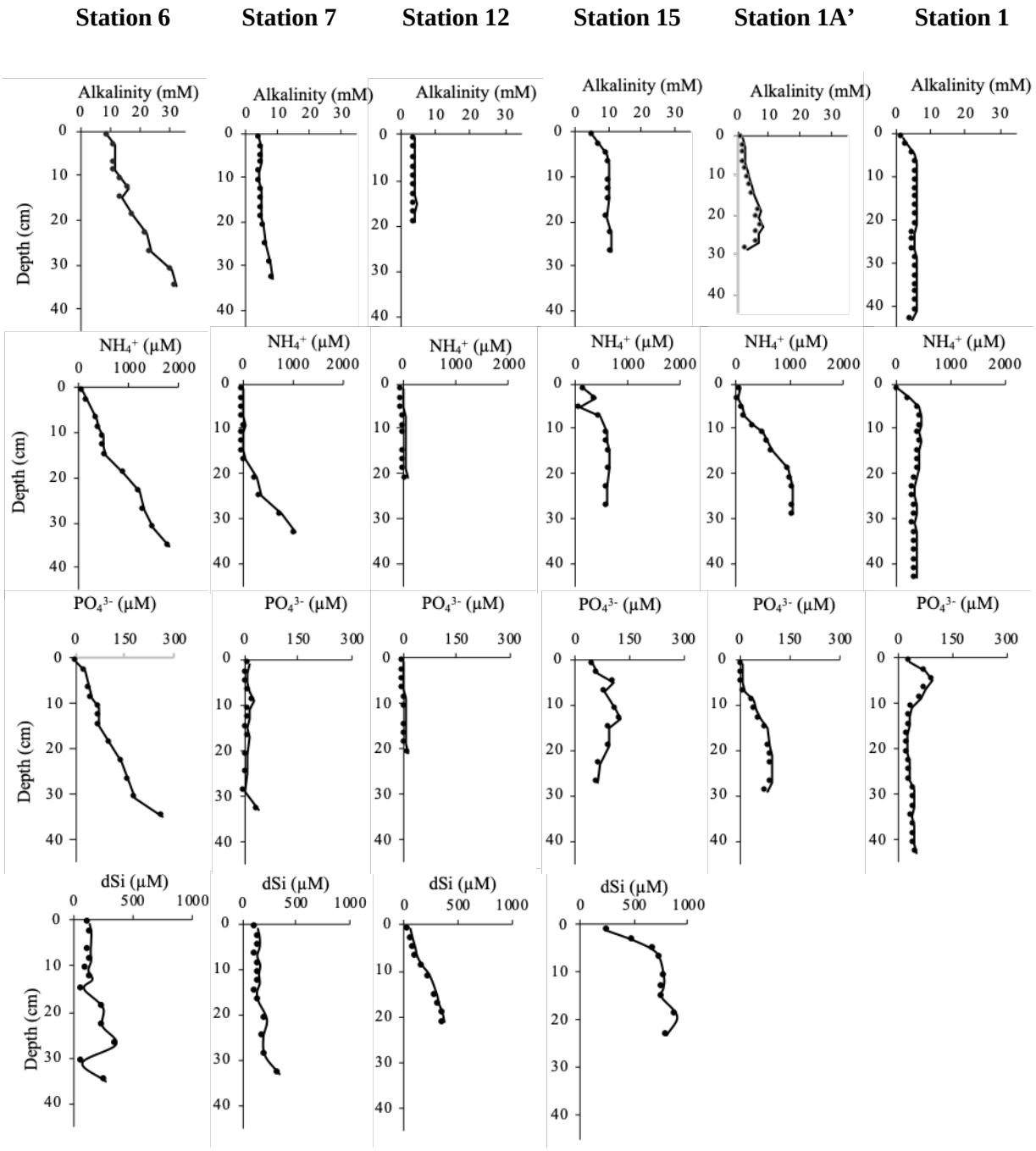

Figure 3.5. Porewater profiles of alkalinity, NH_4^+, PO_4^{3-} and dSi.

For all stations, dissolved silicate (dSi) profiles showed an increase at depth. At Stations 6 and 7, high dSi concentrations in porewaters were observed just below the sediment-water interface compared to that in the bottom waters, which remained more or less constant down to a depth of about 15 cm and then increased slowly at greater depth. At Station 15 dSi increased rapidly below the sediment-water interface with a strong gradient to a depth of 5 cm, which then increased very slowly downcore. The profile at Station 12 showed that dSi concentrations increased with depth at a relatively constant gradient. The profiles for dSi were not available for the two stations sampled in summer 2017.

3.3.5 Mn/Fe in porewaters

Manganese concentrations decreased with depth at all stations with values ranging from 11 μM to 85 μM over 2016 and 2017 (Figure 3.6). During spring 2016, the highest concentration at the surface was found at Station 6 and the lowest at Station 12. The distribution of Mn^{2+} at Station 15 exhibited a subsurface maximum of 45 μM at 3 cm depth. During summer 2017, the concentrations were lower at Station 1A' while at Station 1 a maximum of 78 μM was measured at 3 cm; for both stations, the manganese concentrations decreased with depth. The interstitial water was less enriched in Mn^{2+} at Station 1A' compared to Station 7 in spring 2016, presumably due to the lower bottom water oxygen levels leading to the precipitation of Mn sulphides.

All stations sampled in spring 2016 exhibited high contents of dissolved iron, except for Stations 6 and 12 showing depletion from the sediment-water interface down to deeper layers. The concentrations of dissolved iron decreased with depth in the top 10 cm at all stations (Figure 3.6). At the sediment-water interface, the range of concentrations varied from 18 μM at Station 6 to 236 μM at Station 7. During spring 2016, the dissolved iron concentrations showed spatial variation with the highest concentrations found at Stations 7 and 15 close to the river mouths. Although not pronounced, a seasonal effect was observed, indicating a higher concentration in the subsurface layer near the sediment-water interface at Station 7 compared to Station 1A', which would suggest that more dissolved iron was consumed during summer 2017. In deep layers, however, the dissolved iron concentrations at Station 7 became lower compared to Station 1A' implying a consumption of iron at Station 7 more important.

3.3.6 Sulphate and sulphide concentrations in porewaters

During spring 2016, a decrease of sulphate concentrations with depth was observed at Stations 6, 7 and 15, suggesting the occurrence of sulphate reduction and sulphide production at depth, while at Station 12 the concentrations remained relatively constant throughout the core (Figure 3.6). The sulphate gradient ranged from 1.6 mM m^{-1} at Station 12 (corresponding to a 2 % drop over one-meter depth interval) to 58.1 mM m^{-1} at Station 15 (72 % m^{-1}). The type of curvature was different for different stations. At Stations 6 and 7, the profiles presented a concave-up curvature. At Station 15, the shape of the sulphate profile tended to be concave-down, a typical shape for dominant sulphate reduction process (Berner, 1980).

The gradient was greater from 10 cm depth for Station 6 and from 23 cm depth for Station 7, suggesting a higher rate at depth of sulphate reduction. The depth at which sulphate reduction occurs is likely to be related to organic matter inputs, porosities and salinities (Wijsman et al., 2001). Thus, sulphate reduction on the shelf of the Black Sea exhibited spatial variability. In summer 2017, sulphate concentrations showed a decrease with depth, indicating sulphate consumption by microbial activity through sulphate reduction. The intensity of sulphate reduction was higher at Station 1A' situated in the Danube delta compared to Station 1, possibly due to a higher organic loading. At Station 1A', the decrease in sulphate concentration with depth was quasi-linear whereas the profile at Station 1 exhibited a concave-down curvature. For the delta station, the linear shape reflected the diffusive drawdown of sulphate. The profile linearity could also be induced by the decrease of porosities with depth (Jorgensen et al., 2001). The concave-down profile, as observed at Station 1, is usually attributed to a continuous reduction of sulphate by the degradation of organic matter over depth (Borowski et al., 1999). Moreover, the sulphate reduction was the strongest in the summer than in the spring.

Profiles of total sulphides at Stations 6, 7 and 15 showed an abrupt increase at the depth of close to 10 cm, revealing the production of sulphide in the anoxic sediments due to sulphate reduction. Below 10 cm, concentration of total sulphides remained relatively constant at Stations 6 and 7 while at Station 15 it increased steadily further downcore. The sulphide concentrations were much lower (< 30 µM) compared to the decline in sulphate concentration observed. During summer 2017, no significant concentrations of sulphides were measured.

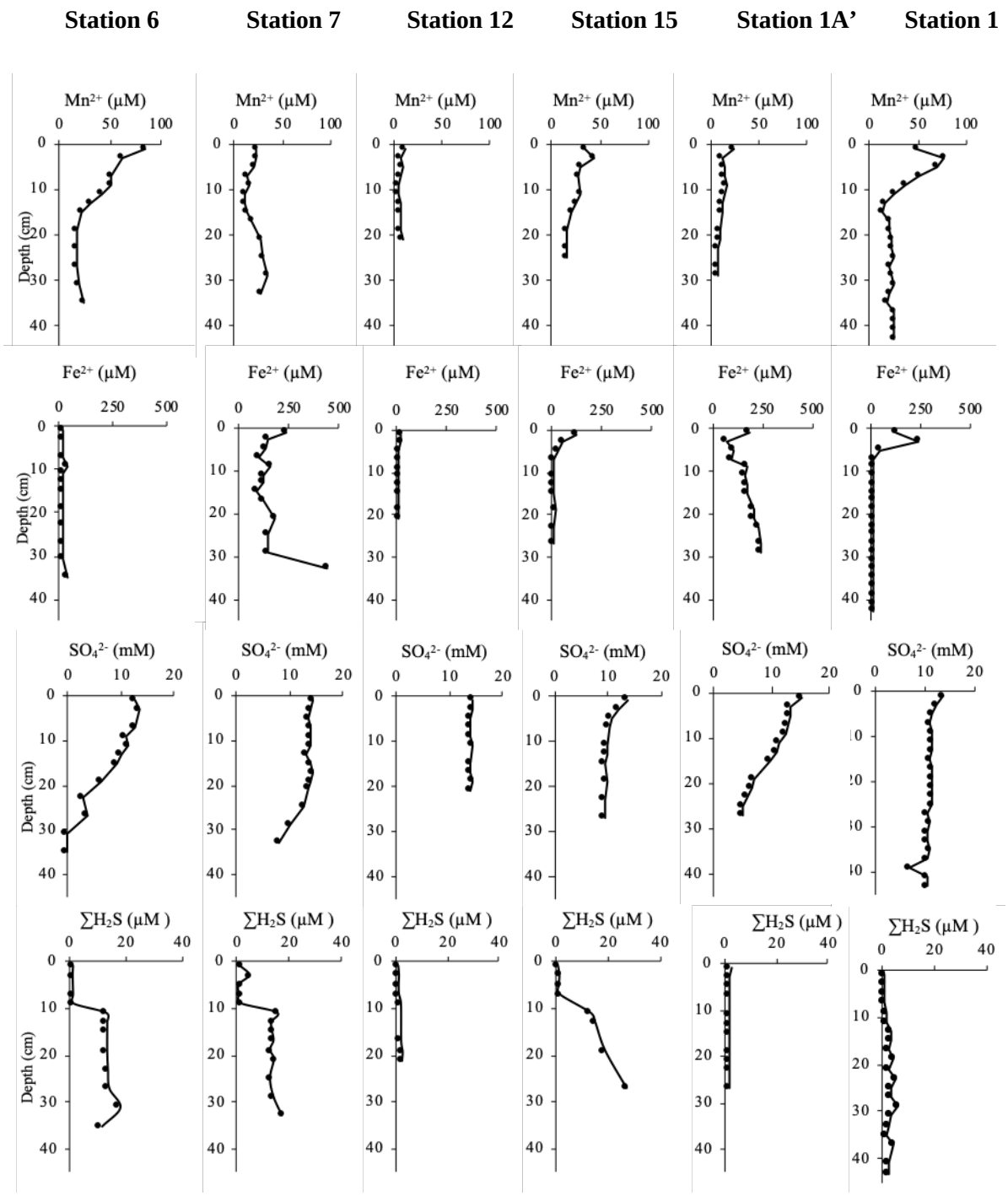

Figure 3.6. Porewater profiles of Mn^{2+}, Fe^{2+}, SO_4^{2-} and ΣH_2S.

3.3.7 Diffusive oxygen uptake and exchange fluxes across the sediment-water interface

Diffusive oxygen uptake (DOU) is the measure of the oxygen consumption by small infauna and bacteria in the sediments, and does not take into account the activity of larger organisms (Glud et al., 2003). DOU ranged from 0.53 to 5.98 mmol m^{-2} d^{-1} in 2016 and 2017, with an average value of 2.66 mmol m^{-2} d^{-1} (Table 3.3). The smallest DOU rate observed in spring 2016 at Station 12 could be explained by the sandy nature of the sediments. The variations displayed between Stations 6, 7 and 15 could be attributed to the differences in organic carbon inputs. DOU was correlated to organic carbon content ($R = 0.72$, $p = 0.02$). The calculated oxygen consumption rates at the sediment-water interface were smaller in summer 2017 than in spring 2016. In the Danube delta, a high DOU was recorded under oxic conditions (2.38 mmol m^{-2} d^{-1}) in May 2016 which was 4.9 times the lowest value observed (0.53 mmol m^{-2} d^{-1}) in August 2017, revealing the seasonal variability of the oxygen consumption.

In spring 2016, NH_4^+ fluxes at the sediment-water interface ranged from -681.85 to -36.45 μmol m^{-2} d^{-1} (Table 3.3) and stations with high organic carbon inputs would have high fluxes of ammonium. The smaller fluxes obtained at Stations 12 could be explained by the higher sand content in the sediments. Similar fluxes were found at Stations 6, 15 and 1 as in the case of their organic carbon content. A seasonal variation in ammonium flux was observed between Station 7 and Station 1A' with concentrations of -37.22 μmol $m^{-2}d^{-1}$ and -59.36 μmol m^{-2} d^{-1} respectively, indicating a higher NH_4^+ production in the sediments during summer 2017 compared to spring 2016.

Phosphate fluxes were low at Stations 7 and 12; at Stations 6 and 15 the fluxes were respectively -10.78 μmol m^{-2} d^{-1} and -32.64 μmol m^{-2} d^{-1}. A small increase in phosphate flux was observed in the Danube delta from spring 2016 to summer 2017, reaching a value of -2.29 μmol m^{-2} d^{-1} at Station 1A'. At Station 1 close to the Odessa Bay, the flux was estimated to be -41.21 μmol m^{-2} d^{-1}, the highest value observed on the shelf.

Dissolved Si fluxes were determined only during spring 2016 and showed negative values comprising between -375.03 μmol m^{-2} d^{-1} and -35.36 μmol m^{-2} d^{-1}, revealing that dSi was transferred from the sediments to the water column under oxic conditions.

Manganese fluxes were very low, ranging from -67.95 μmol m^{-2} d^{-1} to -7.88 μmol m^{-2} d^{-1}. Stations 6, 15 and 1, with the highest organic carbon contents in the sediments, presented the

highest fluxes on the shelf. Fluxes of Mn^{2+} at Stations 7 and 1A' were -18.27 μmol m^{-2} d^{-1} and -17.56 μmol m^{-2} d^{-1} respectively and Station 12 showed a flux of -7.88 μmol m^{-2} d^{-1}.

Iron fluxes ranged from -197.65 to -16.53 μmol m^{-2} d^{-1} over 2016 and 2017. During spring 2016 Station 7 displayed the most important iron flux on the shelf whereas during summer 2017 Station 1 exhibited the highest flux. Iron fluxes were the strongest under poorly oxygenated conditions at Station 1 but it was smaller at Station 1A' compared to Station 7.

Significant sulphate fluxes from the overlying water to the sediments were obtained, ranging from 0.12 to 1.80 mmol m^{-2} d^{-1}, except for Station 12 where sulphate concentrations remained relatively constant with depth. In spring 2016, highest fluxes were found at Stations 7 and 15, close to the river mouths. Comparison of Stations 7 and 1A' showed a similar flux of sulphate both in spring 2016 and in summer 2017.

3.4 Discussion

3.4.1 Oxygen dynamics and seasonality

Oxygen is the first oxidant of the diagenetic cascade and it is used by bacteria to mineralize the organic matter in the benthic layer. The aerobic respiration and the re-oxidation of reduced species released during the anaerobic diagenesis contribute to the consumption of oxygen at the sediment-water interface (Glud, 2008). Oxygen penetrations into the sediments vary from a few millimetres to centimetres. In the coastal waters of the NW shelf of the Black Sea, the oxygen penetration depths varying from 0.50 mm to 4.00 mm are typical for marine sediments (Kristensen, 2000). Spatial variation of the OPD on the shelf can be explained by changes of organic matter loading and depth of water column (Rabouille et al., 2003; Schulz & Zabel, 2006). The OPD becomes shallower with a higher organic matter input and a deeper water column (Wijsman et al., 2001). In 2016, being closer to the river mouths Stations 6 and 15 were subject to a higher organic carbon input than Stations 7 and 12 and exhibited a smaller OPD (R=-0.62). The oxygen dynamics is also influenced by the nature of the sediments. The grain size of the sediments affects the thickness of the oxic layer as reflected by the deeper OPD at Station 12. The presence of a diffusive boundary layer (DBL), dominated mostly by molecular diffusion, could produce a shallower OPD without modifying the oxygen demand of the sediments by increasing the oxygen concentration in the DBL rather than in the sediments (Jorgensen & Revsbech, 1985). The DBL measures usually 200-

300 μm in shallow sediments (Wenzhöfer & Glud, 2004). Bioirrigation is an important parameter which influences the OPD. The continuous flushing of burrows by dwelling organisms introduces dissolved oxygen deeper into the sediments leading to a deeper OPD (Rabouille et al., 2003), as reflected by the unvarying oxygen concentrations over depth at Station 12. To estimate the contribution of the faunal activity, the measurement of TOU (Total Oxygen Uptake), such as the one provided by incubation chambers, is necessary but could not be conducted in this study. The anaerobic mineralization of organic matter generates reduced substances, such as Fe^{2+} and HS^-, in the deeper sediments. These reduced chemical species diffuse from the deep sediments to the sediment-water interface and react with the available oxygen close to the interface. The diffusion of reduced chemical species engenders a reduction of the thickness of the OPD due to their possible re-oxidation (Canfield et al., 1993; Middelburg & Levin, 2009).

Table 3.4. Estimation of respiration rates (mmol m^{-2} d^{-1}) and mineralization rates (mmol C m^{-2} d^{-1}) associated to primary processes of diagenetic pathways. % Γred. sp. represents the % of O_2 necessary to oxidize the reduced species (Fe^{2+}, Mn^{2+}, NH_4^+) which diffuse upward. % Γanox/(ox+anox) is the contribution of anoxic processes, dominated by sulfate reduction, to the organic matter degradation.

Station	**6**	**7**	**12**	**15**	**1A'**	**1**
DOU	5.98	2.38	0.94	4.04	0.53	2.07
% Γred. sp.	11	5	9	35	30	65
$\Gamma min_{ox} C_{org}$	**4.10**	**1.73**	**0.66**	**2.02**	**0.28**	**0.56**
$\Gamma min_{anox} C_{org}$	**1.18**	**1.75**	**0.25**	**3.60**	**1.75**	**2.08**
% Γanox/(ox+anox)	22	50	27	64	86	79

Oxic mineralization is an important pathway of early diagenesis. The mineralization rate of organic carbon by oxygen is estimated to range from 0.66 mmol C m^{-2} d^{-1} to 4.10 mmol C m^{-2} d^{-1} on the shelf during spring and from 0.28 mmol C m^{-2} d^{-1} to 0.56 mmol C m^{-2} d^{-1} during summer (Table 3.4). Oxic mineralization has been considered to be the dominant pathway for the degradation of organic matter in the sediments when carbon inputs are low (Wijsman et al., 2002). Although this relation could not be confirmed in our study during spring (linear function: $R^2 = 0.25$), the organic carbon contents and oxic mineralization rate seemed rather to be linked following a power function (R^2=0.60).

Bottom waters of the NW shelf of the Black Sea are frequently depleted in dissolved oxygen during summer, but the hypoxia duration varies from year to year. At the beginning of the 2000s oxygen was below the hypoxic threshold during ca. 95 days while during 2008 and 2009, the hypoxic period lasted for ca. 130 days (Capet et al., 2013). Even though our data coverage in 2016 and 2017 were not sufficient to define the length of hypoxia, the O_2 microprofilings highlighted the seasonality of oxygen concentrations on the Ukrainian shelf. The oxygen concentrations in the bottom waters were higher in spring 2016 compared to summer 2017 during which the dissolved oxygen contents revealed oxygen limitation resulting in a reduction of the OPD. Despite the changes of season, bottom water temperature remained relatively constant ruling out any temperature-driven changes in dissolved oxygen content. Sediment type and biological activity are important factors controlling the oxygen dynamics.

3.4.2 Sedimentary oxygen consumption

The calculated DOU values revealed spatial variability on the shelf in 2016. These fluctuations might be induced by variations in sediment type and by the organic matter inputs. The sites close to the river mouths would have higher DOU rates. The calculated oxygen consumptions obtained in this study are in general smaller than measurements of O_2 uptake by the sediments in different shelf, coastal and estuarine areas (Table 3.5). Dauwne et al. (2001) measured 95 mmol O_2 m^{-2} d^{-1} in the Westerschelde; Devol & Christensen (1993) found an oxygen consumption rate of 18.2 mmol O_2 m^{-2} d^{-1} on the Eastern N-Pacific shelf; Archer & Devol (1992) reported an O_2 uptake of 5.7 mmol O_2 m^{-2} d^{-1} on the Washington shelf. In our study, the values are ten times smaller than those obtained during the summer of 1995 and the spring of 1997 by Friedrich et al. (2002) or by Wijsman et al. (1999). Nonetheless, Capet et al. (2016) found spatial variation in oxygen fluxes on the shelf and showed that in the deepest region the fluxes were lower than those close to the coast. The oxygen fluxes obtained in this study are comparable to those in the deepest region reported by Capet et al. (2016). Previous investigations (Cai & Sayles, 1996; Glud, 2008) revealed an inverse relationship between OPD and DOU. Figure 3.7 shows DOU as a function of OPD on the shelf, confirming the heterogeneity of the sediments and the high variability in oxygen dynamics.

Table 3.5. Oxygen consumption rates (mmol m^{-2} d^{-1}) in some hypoxic areas.

Area	DOU mmol m^{-2} d^{-1}	Reference
Westerschelde	95	Dauwe, Middelburg, & Herman, 2001
Eastern N-Pacific shelf	18.2	Devol & Christensen, 1993
Washington shelf	5.7	Archer & Devol, 1992
Crimean area	1.3 - 4.6	Lichtschlag, et al., 2015
North-western shelf	13 – 26	Friedrich, et al., 2002
North-western shelf	21	Wijsman et al., 1999
North-western shelf	2.66	This study

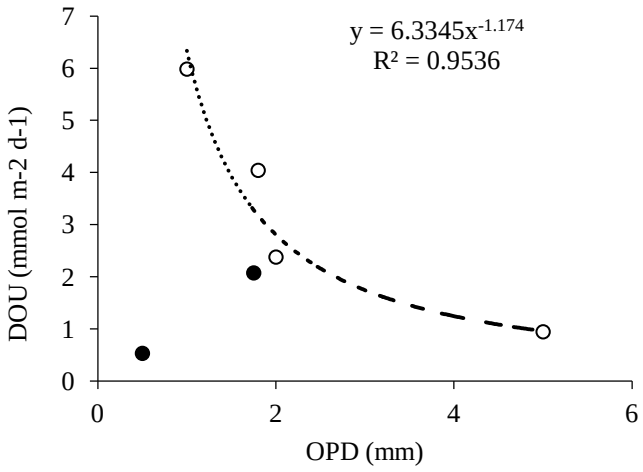

Figure 3.7. DOU as a function of OPD derived from microprofiling of oxygen. Open circles: spring 2016 stations, Solid circles: summer 2017 stations.

Moreover, the data point with low values of both DOU and OPD (Station 1A'), highlights that re-oxidation of reduced compounds could be a larger component of the O_2 consumption than organic matter degradation, indicating thus the deoxygenated character of the station. In spring 2016 re-oxidation of reduced species produced during diagenesis was not the dominant pathway of oxygen consumption on the shelf, despite a contribution of 35 % at Station 15, while in summer 2017 this process contributed more extensively to oxygen consumption, in

particular at Station 1. Re-oxidation of reduced compounds was estimated to account for 5-35 % of the oxygen consumption in spring 2016 and for 30-65 % in summer 2017 (Table 3.4). The highest contribution during summer could be attributed to higher rates of anaerobic mineralization. Temperature can be a factor altering the oxygen consumption but, in this study, the variation of temperature was too small to infer such an influence.

3.4.3 Impact of oxygen depletion on the diagenetic pathways

Over previous decades, the bottom waters of the NW shelf of the Black Sea have been subjected to recurring deoxygenation (Capet et al., 2013). Such seasonal oxygen depletion would have impacts on the biogeochemistry of the sediments, in particular the diagenetic pathways. As oxygen levels drop, the redox reactions are perturbed and adapt to environmental conditions. As observed on the NW shelf, oxic respiration is the first reaction impacted by the loss of oxygen in bottom waters. Indeed, the seasonal low level of oxygen leads to a shoaling of oxygen penetration depth and in turn to a less important DOU. Thus, oxic respiration becomes less efficient during a poorly oxygenated period such as was the case in the Chesapeake Bay (Brady et al., 2013). In this study, DOU values of 2.38 mmol m^{-2} d^{-1} and 0.53 mmol m^{-2} d^{-1} were obtained under oxic and oxygen-poor conditions respectively.

Porewater nitrate concentrations at all stations were low (data not shown), suggesting that the peak of nitrate was very narrow between oxic and anoxic layers, characteristic of nitrification. Also, the increasing NH_4^+ concentration with depth was indicative of denitrification as shown by all profiles on the shelf. However, the higher accumulation of ammonium in the upper sediments at Stations 1 and 1A' would suggest less NH_4^+ re-oxidation than what was reported for the Chesapeake Bay (Kemp et al., 1990, 2005) or for the Danish Coastal system (Conley et al., 2007). Thus, the enhanced NH_4^+ efflux observed in this study could be explained by a lower intensity of nitrification due to oxygen depletion and also by a higher contribution of anaerobic mineralization to the organic matter degradation (86 % during a poorly oxygenated event vs. 50 % under oxic conditions), or by higher levels of dissimilatory nitrate reduction to ammonium as suggested by McCarthy et al. (2008). Moreover, at low levels of oxygen, the high organic matter loading would amplify the importance of the anaerobic degradation processes in the sediments.

The contribution of manganese and iron reduction to organic matter degradation depends on the organic carbon inputs, the intensity of bioturbation and also bottom water oxygen levels (Thamdrup, 2000; Burdige, 2006). Under oxygenated conditions in spring 2016, reduced

species such as manganese and iron had a minor importance in the anaerobic mineralization, accounting for less than 11 % of oxygen consumption, except for Station 15 (Table 3.4). Under low oxygen conditions in summer 2017, the oxygen penetration depth was shallower, allowing Mn^{2+} and Fe^{2+} to diffuse from a reduced to a more oxidized layer leading to a larger contribution of re-oxidation of reduced species to oxygen consumption, representing 30 % and 65 % at Station 1A' and Station 1 respectively. Thus, a larger proportion of dissolved manganese and iron, with the highest important fluxes observed at Station 1 (Table 3.3), would escape from the sediments to the water column leading to low oxygenated sediments depleted in Mn^{2+} and Fe^{2+}. The seasonal variation observed on the shelf confirms the reduced contribution of redox-sensitive metal oxides to organic matter mineralization (5 % under oxic conditions vs. 30 % at low oxygen levels), with a lower enrichment in dissolved Mn^{2+} and Fe^{2+} at low oxygen levels.

As suggested by Slomp et al. (2013), iron could be linked to phosphates and might explain the profile of phosphate concentrations at Station 1. Dissolved Fe^{2+} diffusing upward and phosphates downward, they meet and precipitate. Phosphate concentration increased from the sediment-water interface to 5 cm, probably due to the reductive dissolution of Fe oxides which were more abundant under oxic conditions during the year. A parallel reductive dissolution of Mn oxides occurred at the same depths. The decrease of phosphate concentrations below 5 cm could reflect the precipitation of phosphates to form: (1) Ca-P, switching from organic phosphate to authigenic Ca-P, (2) vivianite ($Fe(II)_3(PO_4)_2$) and/or ludlamite ($Fe_3(PO_4)_2.4(H_2O)$) and phosphoferrite ($Fe_3(PO_4)_2.3(H_2O)$) under strongly reducing conditions as proposed by Djiktra et al. (2014). In addition, the occurrence of maximal concentrations of Mn^{2+}, Fe^{2+} and PO_4^{3-} at a similar depth, could be attributed to the Mn-Fe-P shuttle leading to the formation of Fe-P phases following the reductive dissolution of Mn oxides from a mixture of Mn-Fe-P phases (Dijkstra et al., 2014).

Regarding the dissolved silicate, the sediments acted as a source for the water column and the profiles showed spatial variation on the shelf in spring 2016 with a particularly strong gradient at the sediment-water interface of Station 15 indicating dissolution of biogenic silica by the bacterial activity, usually high in eutrophic systems (Bidle & Azam, 1999). Reschke et al. (2002) showed the presence of opal in the sediments of the NW shelf ranging from 1.8 to 4.4 % in summer 1995. Friedrich et al. (2002) measured smaller concentrations of dSi in porewaters on the shelf, with an average value of 4 μM and higher values ranging from 10.4 to 12.1 μM at the mouth of Danube river during spring 1997. The authors attributed the

presence of dSi to dissolution of diatom frustules. This process is controlled by different factors: biological with the degradation of the membrane covering the diatom frustules (Bidle & Azam, 2001), chemical including salinity (Loucaides et al., 2008) and the concentration of dSi, and physical such as temperature (Passow et al., 2011) and pressure (Loucaides et al., 2008). Usually, the dSi concentrations increase with depth in sediments to reach an asymptotic value ranging from 100 to 850 μM between 5 cm and 30 cm depth (Fanning & Pilson, 1974; Dixit et al., 2001; Archer et al., 1993; Sayles et al., 1996). In this study, the concentrations of all stations sampled in spring 2016, except for Station 15, did not reach this asymptotic value. At Station 15, the dSi concentration reached a relatively constant value, around 770 μM below 11 cm depth, which could be explained by kinetic competition between the dissolution of biogenic silica and the formation of alumino-silicate minerals (Mackenzie & Garrels, 1966; Mackenzie & Kump, 1995; McManus, et al., 1995). Reverse weathering produces clays using biogenic silica, aluminous clays and iron oxides, and thus plays an important role in the opal preservation (Mackenzie & Kump, 1995). The profiles of dSi could be interpreted similar to the profiles of phosphates due to their link to Fe oxides. The highest concentrations of dSi in porewaters might reveal desorption from Fe oxides althhough the dissolved silica would be less affected than PO_4^{3-} (Sundby et al., 1992). The dissolution-precipitation process of the Fe cycle in sediments supports the formation of clay minerals as suggested by Michalopoulos et al. (1995).

Sulphate reduction is the dominant pathway for anaerobic mineralization of organic matter in most coastal sediments due to higher inputs of organic matter to the seabed compared to offshore sediments (Jorgensen, 1982; Soetaert et al., 1996; Burdige, 2006). Lower bottom water oxygen concentrations will result in less oxidation of reduced sulphur compounds, giving rise to more reduced sulphur being buried in the sediments and to more hydrogen sulphide escaping to the water column. Moreover, the decline of bioturbation under low oxygen conditions would lead to a decrease of vertical transport of sulphate. For most sites, the sulphate concentrations in porewaters decreased downward under oxic and low oxygen conditions in bottom waters. In hypoxic environments, sulphates are consumed faster and at a shallower depth in the sediments, highlighting the higher efficiency of sulphate reduction under low oxygen conditions. In parallel, the increases of alkalinity with depth indicated active remineralization of organic matter by sulphate reducing bacteria. No significant concentrations of sulphides were observed at Stations 1 and 1A' (Figure 3.6), which might be explained by two processes. At Station 1, in the subsurface layer, sulphides could be oxidized

by Mn and Fe oxides as suggested by the increase of Mn^{2+} and Fe^{2+} concentrations (Sørensen & Jørgensen, 1987; Aller & Rude, 1987) while deeper in the sediments, sulphides could precipitate with iron and/or manganese to form metal sulphide minerals. At Station 1A', the absence of sulphides could be justified by the precipitation of FeS and MnS, leading to a decrease in alkalinity as well as Fe^{2+} and Mn^{2+} concentrations.

3.4.4 Sediment-water exchanges influenced by oxygen availability

Stations 7 and 1A' have been selected to assess the impact of oxygen fluctuations on the benthic fluxes. Measured Mn and Fe fluxes were much lower than those obtained by Friedrich et al. (2002) in the Danube delta front who reported values of 0.43 mmol m^{-2} d^{-1} for Fe^{2+} and 0.41 mmol m^{-2} d^{-1} for Mn^{2+} in summer 1995 and of 0.26 mmol m^{-2} d^{-1} for Fe^{2+} and 0.20 mmol m^{-2} d^{-1} for Mn^{2+} in spring 1997. The Fe fluxes measured in spring 2016 and in summer 2017 were negative revealing an upward diffusion. In summer 2017, Station 1 showed a higher flux during the summer probably due to a better efficiency of Fe oxide reduction. Contrary to the studies of Friedrich et al. (2002) and Lichtschlag et al. (2015), reduction of Mn and Fe oxides contribute in a non-negligible manner to the anaerobic pathways of the mineralization of organic carbon. The magnitude of sulphate fluxes revealed the importance of sulphate reduction in the mineralization of organic matter. Stations 7 and 1A', having similar organic carbon contents (1.4 %) in the sediments (Table 3.2) and bottom water salinities (18.14 ± 0.20 psu), exhibited similar sulphate fluxes. The impact of oxygen availability cannot be directly identified *via* the fluxes of sulphate, but it can be evaluated with the contribution of anoxic mineralization rate to the degradation of organic matter. Low bottom water oxygen levels would lead to a decline of oxidation of reduced sulphur compounds, allowing the reduced sulphur to be buried and/or the hydrogen sulphide to escape from the sediments to the water column.

3.4.5 Benthic mineralization of organic matter: temporal and spatial variability

Continental shelves, especially deltaic and coastal environments, exhibit the highest burial rate of organic carbon (Berner, 1982; Hedges & Keil, 1995). Continental margins host the major part of aerobic and anaerobic mineralization of organic material. The benthic mineralisation pattern shows spatial and temporal variations which can be affected by several factors. Usually, algal blooms occur during spring, inducing the deposition of fresh organic matter onto the seafloor. Sulphate reduction is promoted, and sedimentary oxygen

consumption is enhanced. The highest rates of oxic mineralization (Table 3.4) were found at Stations 6 and 15 where the highest organic carbon contents were observed in the sediments. The oxic respiration was correlated with the organic carbon contents and thus with organic carbon flux to the seafloor ($R = 0.72$, $p = 0.02$) as suggested by Wijsman et al. (2002). If the organic carbon flux increases, the suboxic and the anoxic pathways would become dominant. Previous studies (Moodley et al., 2005; Hedges & Keil, 1995; Middelburg & Levin, 2009) have shown that under hypoxic conditions, the preservation of organic matter is enhanced and thus the mineralization rate is reduced compared to oxic environments. In muddy sediments of the shelf, the dissolved oxygen concentration in the bottom waters was slightly correlated positively with the oxic respiration ($R = 0.54$, $p = 0.03$), indicating that the oxic mineralization rate of organic carbon would lose its efficiency or that the re-oxidation of reduced species would increase during a poorly oxygenated period. Other studies reported the regulation of organic matter mineralization by bottom water temperature (Thamdrup et al., 1998; Jorgensen, 1977), but in the present study the temperature fluctuations were too low to test the temperature control.

In sediments underlying the highly productive and/or oxygen-depleted coastal waters, the main mineralization pathway of organic matter would be the sulphate reduction (Schulz & Zabel, 2006). On the NW shelf of the Black Sea, sulphate reduction constitutes a substantial diagenetic pathway for organic matter degradation. In spring 2016 sulphate reduction rates (Table 3.4) ranged from 0.25 to 3.60 mmol C m^{-2} d^{-1} (22% - 64 % of the mineralization of organic matter) whereas in summer 2017 it ranged from 1.75 to 2.08 mmol C m^{-2} d^{-1} (86 % - 79 % of the mineralization of organic matter). In spring 2016, degradation of organic matter at Stations 6 and 12 was dominated by the oxic pathway and sulphate reduction had a less important impact, contributing to < 30 % of the mineralization of organic carbon. At Stations 7 and 15, sulphate reduction represented a more important contribution with rates > 30 % inducing a dominance of anoxic mineralization. Low oxygen levels in bottom waters would influence the benthic mineralization, as revealed by the higher sulphate reduction rates observed in the Danube delta at Station 1A' compared to Station 7. The contribution of sulphate reduction rose from 50 % in spring 2016 to 86 % in summer 2017, showing the dominance of this mineralization pathway on the shelf during summer.

3.5 Conclusions

Microprofilings of oxygen in surface sediments and measurements of fluxes across the sediment-water interface conducted during two cruises (spring 2016 and summer 2017) on the NW shelf of the Black Sea revealed spatial and seasonal variations in benthic mineralization. Areas with high oxygen consumption and sulphate fluxes were located close to shore, influenced by river inputs of the Danube and the Dnieper promoting higher productivity and leading to an increase of the benthic fluxes.

Diagenetic pathways were impacted by low oxygen concentrations in the bottom waters near the Danube river plume. Oxic respiration declined under low oxygen conditions yielding a shallower OPD and a lower DOU. Compared to data reported in previous studies, DOU seemed to have decreased since 1995 indicating that oxygen depletion played a role in the benthic exchanges across the sediment-water interface. In addition, low oxygen levels in bottom waters observed in summer 2017 induced a rise of the contribution of sulphate reduction to the degradation of organic matter and a shallower reduction of metal oxides in the sediments, affecting the benthic mineralization of organic matter. During the summer, oxic mineralization became less important with an increased contribution of reduced species to oxygen consumption and anaerobic mineralization turned into the dominant pathway during this poorly oxygenated event.

ACKNOWLEDGEMENTS

This research was funded by the Fond de la Recherche Scientifique (FRS-FNRS) in the framework of the BENTHOX project (Convention no. PDR T.1009.15). AP received a PhD grant from the BENTHOX project. The authors would like to thank the EMBLAS project for providing berths during their sampling cruises in the Black Sea in May 2016 and in August-September 2017. The officers and crewmembers of the *R/V. Mare Nigrum* are acknowledged for their logistic and technical assistance.

References

Aller, R. C., & Rude, P. D. (1987). Complete oxidation of solid phase sulfides by manganese and bacteria in anoxic marine sediments. *Geochim. et Cosmo. Ac., 52*, 751-765.

Almazov, N. M. (1961). Stok ratverennykh soley I biogennykh veschetv kotorye vynoseatsya rekami USSR v Chernoe More. *Naukovi Zapiski Odes. Biol. St. Kiev*, 99-107.

Archer, D. E., Lyle, M. W., Rodgers, K., & Froelich, P. N. (1993). What controls opal preservation in tropical deep-sea sediments. *Paleoceanography, 8*, 7–21.

Archer, D., & Devol, A. (1992). Benthic oxygen fluxes on the Washington shelf and slope: a comparison of in-situ micro electrode and flux chamber measurements. *Limnol. Oceanogr., 37*, 614–629.

Berner, R. (1980). *Early Diagenesis: A theoritical approach.* Princeton University Press.

Berner, R. A. (1982). Burial of Ogranic Carbon and Pyrite sulfur in the modern ocean: Its geochemical and envrionmental significance. *Am. J. Sci., 282*, 451-473.

Bidle, K. D., & Azam, F. (1999). Accelerated dissolution of diatom silica by marine bac- terial assemblages. *Nature, 397*, 508-512.

Bidle, K. D., & Azam, F. (2001). Bacterial control of silicon regeneration from diatom detritus: Significance of bacterial ectohydrolases and species identity. *Limnology and Oceanography, 46*, 1606–1623.

Borowski, W. S., Paull, C. K., & Ussler, W. (1999). Global and local variations of interstitial sulfate gradients in deep-water, continental margin sediments: Sensitivity to underlying methane and gas hydrates. *Marine Geology, 159*, 131-154.

Boudreau, B. P. (1996). The diffusive tortuosity of fine-grained unlithified sediments. *Geochim. Cosmochim. Acta, 60*, 3139-3142.

Brady, D. C., Testa, J. M., Di Toro, D. M., Boynton, W. R., & Kemp, W. M. (2013). Sediment flux modeling: Calibration and application for coastal systems. *Estuar. Coast. Shelf Sci., 117*, 107-124.

Burdige, D. (2006). *Geochemistry of Marine Sediments.* Princeton University Press.

Cai, W.-J., & Sayles, F. L. (1996). Oxygen penetration depths and fluxes in marine sediments. *Marine Chemistry, 52*, 123-131.

Canfield, D. E., Jorgensen, B. B., Fossing, H., Glud, R., Gundersen, J., Ramsing, N. B., . . . Hall, P. O. (1993). Pathways of organic carbon oxidation in three continental margin sediments. *Marine Geology, 113*, 27-40.

Capet, A., Beckers, J.-M., & Gregoire, M. (2013). Drivers, mechanisms and long-term variability of seasonal hypoxia on the Black Sea northwestern shelf – is there any recovery after eutrophication? *Biogeosciences, 10*, 3943–3962.

Capet, A., Meysman, F. J., Akoumianaki, I., Soetaert, K., & Grégoire, M. (2016). Integrating sediment biogeochemistry into 3D oceanic models: A study of benthic-pelagic coupling in the Black Sea. *Ocean Modelling, 101*, 83–100.

Cline, J. D. (1969). Spectrophotometric determination of hydrogen sulfide in natural waters. *Limnology and Oceanography, 14*, 454-458.

Cociasu, A., Dorogan, L., Humborg, C., & Popa, L. (1996). Long-term ecological changes in the Romanian coastal waters of the Black Sea. *Marine Pollution Bulletin, 32*, 32-38.

Conley, D. J., Carstensen, J., Ærtebjerg, G., Christensen, P. B., Dalsgaard, T., Hansen, J. L., & Josefson, A. B. (2007). Long-term changes and impacts of hypoxia in Danish coastal waters. *Ecol. Appl., 17*, 165-184.

Dauwe, B., Middelburg, J. J., & Herman, P. M. (2001). Effect of oxygen on the degradability of organic matter in subtidal and intertidal sediments of the North Sea area. *Mar. Ecol. Prog. Ser., 215*, 13–22.

Devol, A. H., & Christensen, J. P. (1993). Benthic fluxes and nitrogen cycling in sediments of the continental margin of the eastern North Pacific. *J. Mar. Res., 51*, 345–372.

Diaz, R. J., & Rosenberg, R. (2008). Spreading dead zones and consequences for marine ecosystems. *Science, 321*, 926-929.

Dijkstra, N., Kraal, P., Kuypers, M. M., Schnetger, B., & Slomp, C. P. (2014). Are iron-phosphate minerals a sink for phosphorus in anoxic Black sea sediments? *PLoSONE, 9*, e101139.

Dixit, S., Van Cappellen, P., & van Bennekom, A. J. (2001). Processes controlling solubility of biogenic silica and pore water build-up of silicic acid in marine sediments. *Mar. Chem., 73*, 333–352.

Fanning, K. A., & Pilson, M. E. (1974). The diffusion of dissolved silica out of deep-sea sediments. *J. Geophys. Res:Oceans, 79*, 1293–1297.

Friedrich, J., Dinkel, C., Friedl, G., Pimenov, N., wijsman, J., Gomoiu, M.-T., . . . Wehrli, B. (2002). Benthic nutrient cycling and diagenetic pathways in the North-western Black Sea. *Estuarine, Coastal and Shelf Science, 54*, 369-383.

Froelich, P. N., Klinkhammer, G. P., Bender, M. L., Luedtke, N. A., Heath, G. R., Cullen, D., . . . Hartman, B. (1979). Early oxidation of organic matter in pelagic sediments of the eastern equatorial Atlantic: suboxic diagenesis. *Geochim. Cosmochom., 43*, 1075-1090.

Glud, R. N. (2008). Oxygen dynamics of marine sediments. *Mar. Biol., 4*, 243-289.

Glud, R. N., Gundersen, J. K., Roy, H., & Jorgensen, B. B. (2003). Seasonal dynamics of benthic O2 utpake in a semienclosed bay: Importance of diffusion and faunal activity. *Limnol. Oceanogr., 48*, 1265-1276.

Grasshoff, K., Ehrhardt, M., & Kremling, K. (1983). *Methods of Seawater Analysis.* Weinheim: Verlag Chemie.

Gray, J. S., Wu, R. S., & Or, Y. Y. (2002). Effect of hypoxia and organic enrichment on the coastal marine environment. *Marine Ecology Progress Series, 238*, 249-279.

Grégoire, M., & Soetaert, K. (2010). Carbon, nitrogen, oxygen and sulfide budgets in the Black Sea: A biogeochemical model of the whole water column coupling the oxic and anoxic parts. *Ecological Modelling, 221*, 2287–2301.

Hedges, J. I., & Keil, R. G. (1995). Sedimentary organic matter preservation: an assessment and speculative synthesis. Authors' closing comments. *Mar. Chem., 49*, 137-139.

Holmes, R. M., Aminot, A., Kérouel, R., Hooker, B. A., & Peterson, B. J. (1999). A simple and precise method for measuring ammonium in marine and freshwater ecosystems. *Can. J. fish. Aqua. Sci., 56*, 1801-1808.

Jorgensen, B. B. (1977). The sulfur cycle of a coastal marine sediment (Limfjorden). *Limnol. Oceanogr., 22*, 814-832.

Jorgensen, B. B. (1982). Mineralization of organic matter in the sea bed – the role of sulphate reduction. *Nature, 296*, 643–645.

Jorgensen, B. B., & Revsbech, N. P. (1985). Diffusive boundary layers and the oxygen uptake of sediments and detritus. *Limnology and Oceanography, 30*, 111-122.

Jorgensen, B. B., & Sorensen, J. (1985). Seasonal cycles of O2, NO3- and SO42- reduction in estuarine sediments: the significance of an . *Marine Ecology Progress Series, 24*, 65-74.

Jorgensen, B. B., Weber, A., & Zopfi, J. (2001). Sulfate reduction and anaerobic methane oxidation in Black Sea sediments. *Deep Sea REsearch Part I: Oceanographic Research Papers, 48*, 2097-2120.

Kemp, W. M., Boynton, W. R., Adolf, J. E., Boesch, D. F., Boicourt, W. C., Brush, G., . . . St. (2005). Eutrophication of Chesapeake Bay: historical trends and ecological interactions. *Marine Ecology Progress Series, 303*, 1-29.

Kemp, W. M., Sampou, P., Caffrey, J., Mayer, M., Henriksen, K., & Boynton, W. R. (1990). Ammonium recycling versus denitrification in chesapeake bay sediments. *Limnol. Oceanogr., 35*, 1545– 1563.

Kemp, W. M., Testa, J. M., Conley, D. J., Gilbert, D., & Hagy, J. D. (2009). Temporal responses of coastal hypoxia to nutrient loading and physical controls. *Biogeosciences, 6*, 2985-3008.

Kristensen, E. (2000). Organic matter diagenesis at the oxic/anoxic interface in coastal marine sediments, with emphasis on the role of burrowing animals. In G. Liebezeit, S. Dittmann, & I. Kröncke (Eds.), *Life at interfaces and under extreme conditons* (Vol. 151, pp. 1-24). Springer, Dordrecht.

Lichtschlag, A., Donis, D., Janssen, F., Jessen, G. L., Holtappels, M., Wenzhöfer, F., . . . Boetius, A. (2015). Effects of fluctuating hypoxia on benthic oxygen consumption in the Black Sea (Crimean shelf). *Biogeosciences, 12*, 5075–5092.

LOICZ. (1995). *Implementation Plan 1995.* Global Change IGBP Report No. 33.

Loucaides, S., Van Cappellen, P., & Behrends, T. (2008). Dissolution of biogenic silica from land to ocean: Role of salinity and pH. *Limnology and Oceanography, 53*, 1614–1621.

Mackenzie, F. T., & Garrels, R. M. (1966). Chemical mass balance between rivers and oceans. *Am. J. Sci., 264*, 507–525.

Mackenzie, F. T., & Kump, L. R. (1995). reverse weathering, clay mineral formation, and oceanic element cycles. *Science, 270*, 586-587.

McCarthy, J. J., Yilmaz, A., Coban-Yildiz, Y., & Nevins, J. L. (2007). Nitrogen cycling in the offshore waters of the Black Sea. *Estuar. Coast. Shelf Sci., 74*, 493-514.

McCarthy, M. J., McNea, K. S., Morse, J. W., & Gardner, W. S. (2008). Bottom-water hypoxia effects on sediment-water interface nitrogen transformations in a seasonally hypoxic, shallow bay (Corpus christi bay, TX, USA). *Estuar. Coasts, 31*, 521–531.

McCave, I. N., Bryant, R. J., Cook, H. F., & Coughanowr, C. A. (1986). Evaluation of a Laser-Diffraction-Size Analyzer for Use with Natural Sediments. *J. Sediment. Res., 56*, 561-564.

McManus, J., Hammond, D. E., Berelson, W. M., Kilgore, T. E., DeMaster, D. J., & Ragueneau, O. G. (1995). Early diagenesis of biogenic opal: dissolution rates, kinetics, and paleoceanographic implications. *Deep Sea Res. II, 42*, 871–903.

Meyers, P. A. (1994). Preservation of elemental and isotopic source identification of sedimentary organic matter. *Chemical Geology, 114*, 289-302.

Michalopoulos, P., & Aller, R. C. (1995). Rapid clay mineral formation in Amazon delta sediments: reverse weathering and oceanic elemental cycles. *Science, 270*, 614-617.

Middelburg, J. J., & Levin, L. A. (2009). Coastal hypoxia and sediment biogeochemistry. *Biogeosciences, 6*, 1273-1293.

Moodley, L., Middelburg, J. J., Herman, P. M., Soetaert, K., & Lange, G. J. (2005). Oxygenation and organic-matter preservation in marine sediments: Direct experimental evidence from ancient organic carbon-rich deposits. *Geology, 33*, 889–892.

Passow, U., French, M. A., & Robert, M. (2011). Biological controls on dissolution of diatom frustules during their descent to the deep ocean: Lessons learned from controlled laboratory experiments. *Deep Sea Research Part I - Oceanographic Research Papers, 58*, 1147–1157.

Rabouille, C., Denis, L., Dedieu, K., Stora, G., Lansard, B., & Grenz, C. (2003). Oxygen demand in coastal marine sediments: comparing in situ microelectrodes and laboratory core incubations. *Journal of Experimental Marine Biology and Ecology, 285*, 49-69.

Redfield, A. C. (1958). The biological control of chemical factors in the environment. *American Scientist*, 230A, 205-221.

Reschke, K., IttekkotV., & Panin, N. (2002). The nature of organic matter in the Danube river particles and north-western Black Sea sediments. *Estuarine, Coastal and Shelf Science, 54*, 563–574.

Sørensen, J., & Jørgensen, B. B. (1987). Early diagenesis in sediments from Danish coastal waters: Microbial activity and Mn-Fe-S geochemistry. *Geochim. et Cosmo. Ac., 51*, 1583-1590.

Sarazin, G., Michard, G., & Prevot, F. (1999). A rapid and accurate spectroscopic method for alkalinity measurment in sea water samples. *Water Ressources, 33*, 290-294.

Sayles, F. L., Deuser, W. G., Goudreau, J. E., DIckinson, W. H., Jickells, T. D., & King, P. (1996). The benthic cycle of biogenic opal at the Bermuda Atlantic time series site. *Deep Sea Res. I Oceanogr. Res. Pap., 43*, 383–409.

Schulz, H. D., & Zabel, M. (2006). *Marine Geochemistry* (2nd edition ed.). Springer.

Seeberg- Elverfeldt, J., Schlüter, M., Feseker, T., & Kölling, M. (2005). Rhizon sampling of pore waters near the sediment-water interface of aquatic systems. *Limnology and oceanography : Methods, 3*, 361–371.

Slomp, C. P., Mort, H. P., Jilbert, T., Reed, D. C., Gustafsson, B. G., & Wolthers, M. (2013). coupled dynamics of iron and phosphorus in sediments of an oligotrophic coastal basin and the impact of anaerobic oxidation of methane. *PLoS ONE, 8*.

Soetaert, K., Herman, P. M., & Middelburg, J. J. (1996). A model of early diagenetic processes from the shelf to abyssal depths. *Geochim. Cosmochim. Acta., 60*, 1019-1040.

Soetaert, K., Petzoldt, T., & Meysman, F. J. (2010a). marelac: Tools for Aquatic Sciences R package version 2.1.

Sundby, B., Anderson, L. G., Hall, P. O., Iverfeld, A., Rutgers van der Loeff, M. M., & Westerlund, S. F. (1986). The effect of oxygen on release and uptake of cobalt, manganese, iron and phosphate at the sediment–water interface. *Geochim. Cosmochim. Acta, 50*, 1281–1288.

Sundby, B., Gobeil, C., Silverberg, N., & Mucci, A. (1992). The phosphorus cycle in coastal marine sediments. *Limnol. Oceanogr., 37*, 1129-1145.

Thamdrup, B. (2000). Bacterial manganese and iron reduction in aquatic sediments. *Adv. Microb. Ecol., 16*, 41–84.

Thamdrup, B., Hansen, J. W., & Jorgensen, B. B. (1998). Temperature dependence of aerobic respiration in a coastal sediment. *FEMS Microbiol. Ecol., 25*, 189-200.

Wenzhöfer, F., & Glud, R. N. (2004). Small-scale spatial and temporal variability in coastal benthic O2 dynamics: Effects of fauna activity. *Limnol. Oceanogr., 49*, 1471-1481.

Wijsman, J. W., Herman, P. M., Middelburg, J. J., & Soetaert, K. (2002). A model for early diagenetic processes in sediments of the continental shelf of the Black Sea. *Estuarine, Coastal and Shelf Science, 54*, 403-421.

Wijsman, J. W., Middelburg, J. J., Herman, P. M., Böttcher, M. E., & Heip, C. H. (2001). Sulfur and iron speciation in surface sediment along the northwestern margin of the Black Sea. *Marine Chemistry, 74*, 261-278.

Wijsman, J., Herman, P., & Gomoiu , M. T. (1999). Spatial distribution in sediment characteristics and benthic activity on the northwestern Black Sea shelf. *Mar. Ecol. Prog. Ser., 181*, 25–39.

Chapter 4

Sulphur and iron biogeochemical cycling in surface sediments on the NW Black Sea shelf during seasonal bottom water deoxygenation

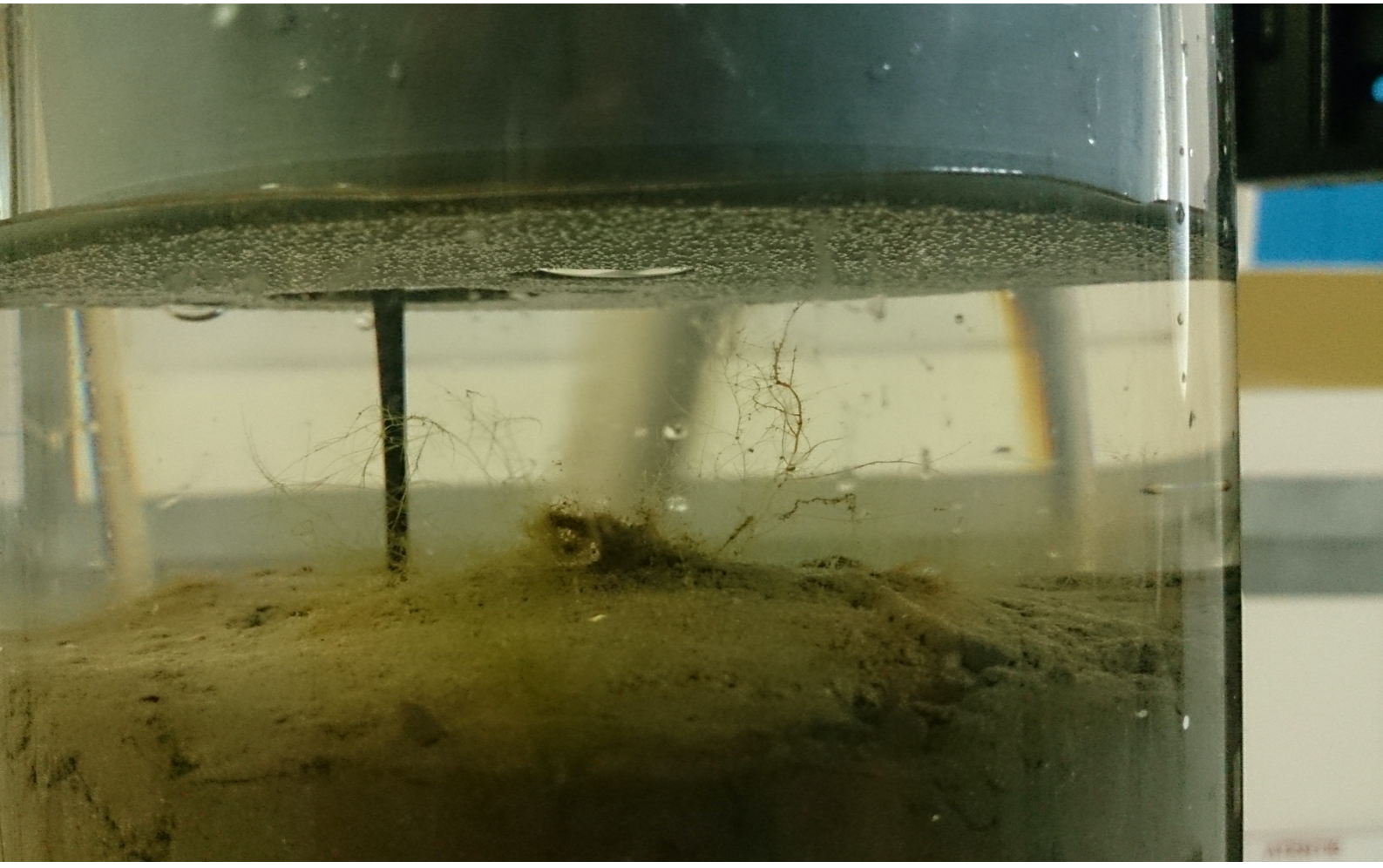

Picture of microprofiling of H_2S through a core sampled on the NW shelf in 2016.

Sulphur and iron biogeochemical cycling in surface sediments on the NW Black Sea shelf during seasonal bottom water deoxygenation

Audrey Plante, Arthur Capet, Nathalie Roevros, Marilaure Grégoire, Nathalie Fagel and Lei Chou (in preparation)

ABSTRACT

Over the last decades, the north-western (NW) shelf of the Black Sea has been prone to seasonal bottom water deoxygenation. The impact of this phenomenon on early diagenesis and, in particular the Fe-S sedimentary cycle, still needs to be better understood. Sediments, porewaters and bottom waters were sampled on the Ukrainian shelf of the Black Sea (August-September 2017). Geochemical analyses of the solid phase and porewater have been carried out to determine the speciation of sedimentary sulphur (AVS, CRS, ΣH_2S and dissolved sulphate) and iron (dithionite extractable Fe, total Fe, HCl extractable Fe and dissolved Fe). The shelf sediments were enriched in total iron but depleted in highly reactive iron as has already been observed previously. The absence of free sulphides and the observation of pyrite give information about the state of their transformation. The presence of pyrite at the sediment-water interface was attributed to their formation in the water column and/or by their upward transport by benthic feeders. The shelf sediments exhibited low degree of sulphidization and of pyritization which could be explained by the hydrodynamics conditions, the dredging and the high sedimentation rate. Despite spatial variations, the Fe and S cycles were closely linked and were influenced by various parameters such as the organic matter input, the presence of Fe-compounds, and the oxygen level in the bottom waters.

4.1 Introduction

Dissolved oxygen is a fundamental component for marine life involved in the biogeochemical cycling of elements (Glud, 2008). Since the middle of the 20th century, the occurrence of hypoxic and anoxic events seems to have expanded in the coastal zones impacted by anthropogenic activities whereas these deoxygenation phenomena have existed through the geological time (Breitburg, et al., 2018). River deltas and continental shelves are important locations for the iron and sulphur cycles because both the formation and the burial of authigenic iron sulphide take place in these zones (Wijsman et al., 2001a). The north-western (NW) shelf of the Black Sea has been affected by seasonal hypoxia over the last decades (Capet et al., 2013). The shelf has undergone excess loadings of nutrient, organic matter and reactive iron from the discharge of rivers, mainly the Danube. Oxygen depletion alters the biogeochemical cycles in the water column as well as the sediments, with an impact on the degradation of organic matter in the sediments through anaerobic diagenetic reactions. Sulphate reduction, representing between 10 % and 90 % of the organic matter degradation in coastal environments and becomes a dominant process for the oxidation of organic carbon under hypoxic conditions (Jorgensen, 1977; Canfield, et al., 1993; Kostka & Luther III, 1994; Thamdrup & Canfield, 1996). The reduction of sulphate with organic matter produces hydrogen sulphide which quickly reacts with sedimentary reactive iron and forms iron monosulphides (FeS) which then react with dissolved sulphide, elemental sulphur or polysulphide to form pyrite (FeS_2) at longer timescale which will be buried. The processes of transport and turnover rates of sulphate reduction may be impacted by the formation of pyrite and thus the sulphur and iron cycles. Once reactive iron is depleted, hydrogen sulphide would diffuse upward through the sediments reaching the water column where it may be re-oxidized to sulphur intermediate or to sulphate (Jorgensen & Kasten, 2006; Zhang & Millero, 1993), or may react with organic matter (Sinninghe Damsté & De Leeuw, 1990). However, the S-Fe cycle is influenced by the macrofauna activity as bioturbation and bio-irrigation would enhance the recycling of iron and sulphide within the sediments (Wijsman et al., 2001b).

Oxygen deficiency in the bottom waters induces major changes in biogeochemical processes, giving rise to reactions of anaerobic mineralisation of organic matter (Middelburg & Levin, 2009). Oxygen content has a direct effect on the re-oxidation of dissolved sulphide and iron and an indirect effect on macrofaunal communities.

Previous studies in the Black Sea have focused on the anoxic water column (1991), the shelf edge (Shaffer, 1986; Lyons et al., 1993) or the deep-sea sediments (Canfield et al., 1996; Lyons, 1997). More recently, Friedrich et al. (2002) investigated benthic nutrient cycling in the NW Black Sea during two campaigns conducted in 1995 and 1997. In the present investigation, the early diagenesis in the shelf sediments has been examined with a special emphasis on the iron and sulphur cycling during hypoxia in summer 2017 in the NW Black Sea.

4.2 Material and Methods

4.2.1 Location

Sampling was carried out, in collaboration with the EMBLAS-II project, aboard the *R/V Mare Nigrum* on the Ukrainian shelf of the Black Sea (Figure 4.1). Station 1A' was located near the mouth of the Danube river and Station 1 was situated on the shelf under the influence of the Dnieper river (Table 4.1).

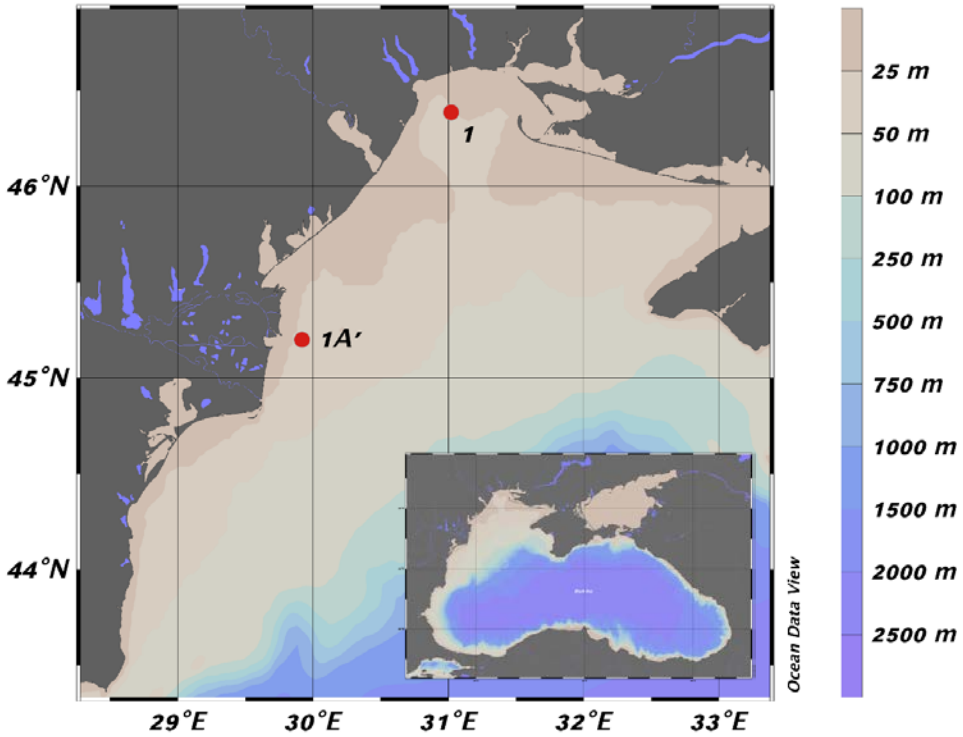

Figure 4.1. Map of the sampled stations (red dots) on the NW shelf of the Black Sea.

Table 4.1. Characteristics of the sampling stations in the NW shelf of the Black Sea.

Station	Position	Area	Depth (m)	O_2 (μM)
1A’	45° 12.0’N, 29° 48.6’E	Danube area	19.9	7.4
1	46° 26.0’N, 31° 01.0’E	Dniester area	22.0	58.2

4.2.2 Sampling and sample treatment

Water column sampling was performed at all stations using a CTD rosette equipped with Niskin bottles and profiles of temperature, salinity and oxygen were also recorded. At each station, a set of 4 cores (10 cm inner diameter; 60 cm long) were collected with a multicorer. One core was for microprofiling of geochemical gradients using microsensors, a second core was for the extraction of porewaters, a third core was for the collection of sediment samples and one last core was kept aside for additional analyses if necessary. For porewater sampling, the sediment core tubes were predrilled at 2-cm intervals to allow the insertion of rhizons into the sediment. Subsequently, syringes were attached to the rhizons to create a vacuum. The extraction of porewaters was conducted under N_2 atmosphere in a glove bag. Once the porewaters were extracted, the samples were dispatched into individual vials for the various analyses. For the sediment sampling, the first cm of the sediments was sampled and then the sediment cores were sliced at 2 cm intervals for solid phase analyses. Sediment layers were stored in plastic recipients. Another core, used for the study of iron and sulphur cycling, was directly sliced at 2 cm intervals and put in plastic bags which were placed under N_2 atmosphere before sealing and stored frozen.

4.2.3 Microprofiling of geochemical gradients

Shortly after the cores were taken, microprofiling of geochemical gradients was performed, using commercially available microsensors of O_2 (100 μm tip), H_2S (100 μm tip) and an automated profiling system (UNISENSE A.S., Denmark). O_2 was calibrated with a 2-point calibration using air-saturated seawater (100 % O_2 saturation) and a solution of sodium ascorbate 0.1 M (0 % of O_2 saturation). H_2S was calibrated with a 3-points curve using Na_2S solutions prepared daily. Microprofilings were conducted on cores under a N_2 flux over the headspace of the core.

4.2.4 Porewater analysis

Samples for dissolved metal (Fe, Mn) analyses were acidified and stored at 4 °C until analysis; they were diluted 10 times with acidified milli-Q water and analysed by Inductively Coupled Plasma-Optical Emission Spectroscopy (ICP-OES, Varian Liberty serie II). Samples for SO_4^{2-} analyses were stored at 4 °C and analysed by ion chromatography with a Dionex-ICS5000 (ThermoScientific) after a dilution of 250 times. Samples for free sulphide analysis were fixed with ZnAc (5 %) and measured spectrophotometrically following the method of Cline (1969).

4.2.5 Porosity

Based on weight-volume determinations, each slice of sediment was dried at 45 °C until a constant weight in order to calculate the porosity from the water content and a reference density value of 2.6 g cm^{-3}, a typical value for siliciclastic sediments (Wijsman et al., 2002).

4.2.6 Solid phase analysis

Freeze-dried sediment samples were ground to a fine powder and analysed for various parameters.

Sedimentation rate, POC, PN

In order to establish the chronology of the cores, ^{210}Pb and ^{14}C were analysed on fine sediments (<63 μm) and bivalve shells sampled in 2016. The sedimentation rate was calculated with the software CLAM version 2.2 using the depth 0 cm for the year of core collection (2016 AD) (see Appendix A of this thesis).

Organic carbon and nitrogen (POC, PN, % dry weight) as well as $\delta^{13}C$ and $\delta^{15}N$ were measured on decarbonated samples with a Vario Microcube CNS elemental analyser coupled with an IRMS isoprime 100 isotope ration mass spectrometer.

Particulate Al, Fe and Mn contents

Powdered sediment (50 mg) was loaded into a Teflon bomb and digested in acid solutions ($HCl/HNO_3/HF$) in a microwave oven. The digests were diluted and analysed for Al, Fe and Mn by ICP-OES. Analysis of an international soil and sediment standard (BRC320 and BCR277) showed that this method extracted for BCR320: 102 % of Al, 98 % of Fe and 69 %

of Mn, and for BCR277: 117 % of Al, 108 % of Fe and 95 % of Mn. The Fe content was considered as the total Fe (Fe_{tot}).

Iron and sulphur speciation

A subsample of 375 mg was used for the sequential extraction of reactive iron as described in Claff et al. (2010) which was modified later by Kraal et al. (2013). This extraction procedure determines 4 operational iron phases: (i) HCl extractable iron (Fe_H), (ii) iron bound to organic matter (Fe_{org}), (iii) iron in crystalline minerals (Fe_{ox}) and (iv) iron in pyrite (Fe_{pyr}). The solutions used to extract the iron phases and the extraction times are summarized in Table 4.2. For each extraction, 15 mL of extractant was added, and the sample was left under constant agitation. After the extraction, the sample was centrifuged (3000 rpm for 10 min) and the supernatant was filtered (0.45 μm cellulose acetate) and stored at 4 °C for later analysis by spectrophotometry. The subsequent extraction started immediately after the previous one. Concentrations of iron were measured colorimetrically using the 1,10-phenantholine method. Total Fe extracted was determined as Fe(II) in all extracts after reducing Fe(III) by a 0.4 M hydroxylamine hydrochloride solution. The sum of Fe in all extracts after each of the four extracting steps represents the highly reactive iron (Fe_{HR}) which corresponds to the sum of iron associated with the four iron phases ($Fe_H + Fe_{org} + Fe_{ox} + Fe_{pyr}$). The difference between the total iron (Fe_{tot}) and Fe_{HR} represents the poorly reactive and unreactive iron (Fe_U).

Table 4.2. Sequential extraction of Fe and S species.

Step	Extractant	Duration	Target phase
Fe fractionation (Claff et al., 2010)			
1	1 M HCl	4 h	FeH: Fe(II) + Fe(III)
2	0.1 M Na-pyrophosphate, pH 10.4	16 h	Fe_{org}
3	0.35 M acetic acid/ 0.2 M Na_3-citrate with 50 g L^{-1} sodium dithionite, pH 4.8	4 h	Fe_{ox}
4	Concentrated HNO_3	2 h	Fe_{pyr}
S fractionation (Burton et al., 2008)			
1	6 M HCl/ 0.1 M ascorbic acid	24 h	AVS
2	500 g L^{-1} chromous chloride in 32% HCl	48 h	CRS

A subsample (500 mg) was analysed for acid-volatile sulphide (AVS) and chromium reducible sulphide (CRS) following the sequence of Kraal et al. (2013) and using the material described in Burton et al. (2008) and. The dry sediment and a trap solution (5 % ZnAc) were placed in a septum cap glass bottle (*Schott*) which was purged with N_2 gas. Ascorbic acid and HCl were added to the sediment through the septum with a needle and a syringe. After AVS extraction, the trap solution was changed for the CRS extraction and Cr(II) solution was added. The solutions used to extract the sulphur phases and the extraction times are summarized in Table 4.2. Samples were placed under agitation for each step of extraction. Sulphur concentrations were measured colorimetrically following the method of Cline (1969). The sum of AVS and CRS is named S_{inorg}.

AVS is considered to represent the FeS phase while the Fe_H fraction includes the FeS as well as other mineral phases associated with Fe(II). AVS can thus be used to determine the Fe content in FeS (Fe_{AVS}). The difference between Fe_H and Fe_{AVS} corresponds then to the labile Fe(II) not linked to FeS. The sum of Fe_{AVS} and that Fe_{pyr} (Fe in pyrite) constitutes the total sulphidized iron. The degree of sulphidization of total highly reactive Fe (DOS_{HR}) can then be calculated according to Boesen and Postma (1988):

$$DOS_{HR} = \frac{(Fe_{AVS}+Fe_{pyr})}{Fe_{HR}} \qquad \text{(Eq. 4.1)}$$

To understand the iron limitation in the sediments for pyrite formation and to estimate the content of Fe_{HR} in the form of pyrite, the degree of pyritization (DOP) can be calculated (Raiswell & Berner, 1985):

$$DOP = \frac{Fe_{pyr}}{Fe_{HR}} \qquad \text{(Eq. 4.2)}$$

4.3 Results

4.3.1 Bottom water conditions

During summer 2017, the measurements of salinity and temperature showed a stratification of the water column (Figure 4.2). One week before the cruise, the water column stratification was disrupted by an intensive wind, resulting in a weaker stratification during sampling. CTD profiles showed that the dissolved oxygen concentrations decreased with depth at both stations. Station 1A' presented a smaller oxygen concentration in bottom waters than that at Station 1, with 95 μM and 144 μM respectively. These concentrations are characteristic of an oxic system 1 m above the seabed during the sampling period.

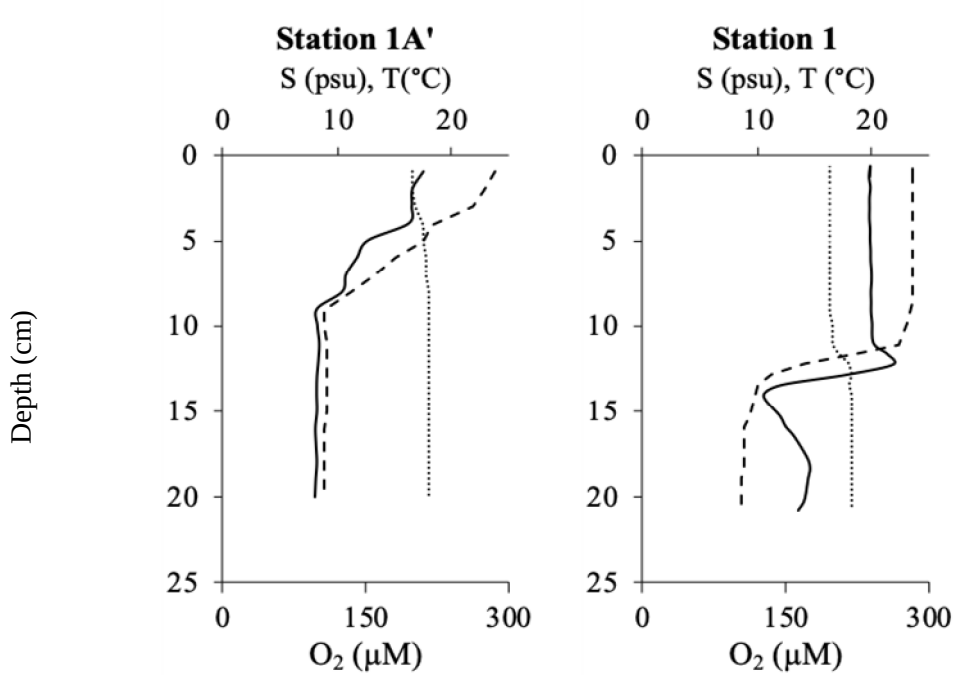

Figure 4.2. CTD profiles obtained during the 2017 summer cruise. Dashed line is temperature (°C), dotted line denotes salinity and black line refers to oxygen concentration (μM).

However, the dissolved oxygen concentrations measured with the O_2 microsensor showed that the bottom water was rather hypoxic (Figure 4.3), suggesting a sharp gradient of dissolved oxygen concentration above the sediment-water interface.

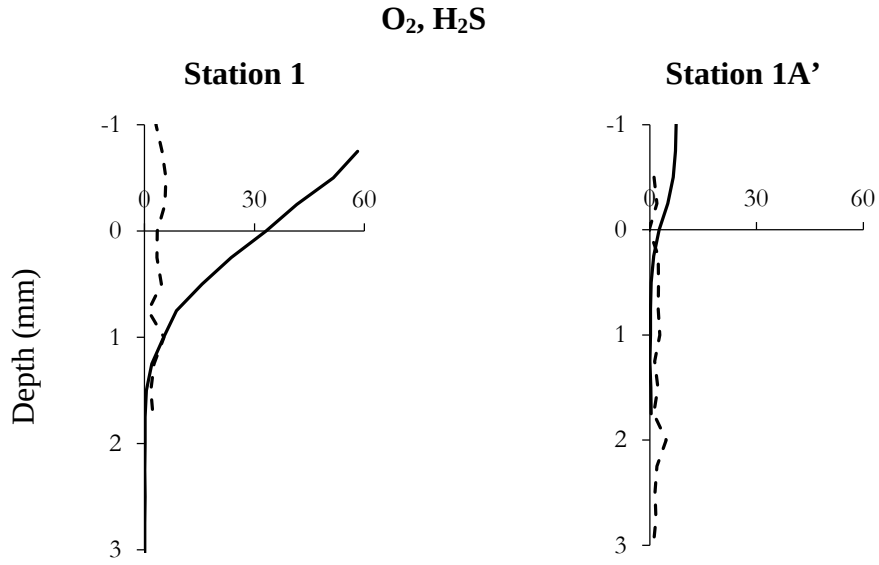

Figure 4.3. Microprofiles of oxygen (black line, μM) and hydrogen sulphide (dashed line, μM).

4.3.2 Porosity and sediment accumulation rates

Sediment porosity decreased with depth at both stations (Figure 4.4). Near the sediment-water interface, the porosity was higher than at Station 1A', with values of 0.95 and 0.87 respectively. In the deeper part of the core, the porosity remained relatively constant at a value close to 0.77 at both stations. The difference in porosity in the surface sediment showed a spatial variation, which might be due to the presence of a fluffy layer and a higher content of sand at Station 1. The variation of sedimentation rate on the shelf could also explain the difference in the measured porosity. The sediment accumulation rate at Station 1A' (0.4 cm y^{-1}) was lower than at Station 1 (0.6 cm y^{-1}). The sediment flux, J_{sed} (g cm^{-2} y^{-1}) considered to be constant for the sediment core taken, can be calculated following (van de Velde, et al., 2018):

$$J_{sed} = v_0 (1 - \phi_{av}) \rho_{solid,av} \qquad \text{(Eq. 4.3)}$$

where v_0 is the depth averaged sedimentation rate (cm y^{-1}), ϕ_{av} is the depth averaged porosity and $\rho_{solid,av}$ is the solid phase density (2.6 g cm^{-3}, Wijsman et al., 2002). The calculated J_{sed}

was slightly lower at Station 1A' (0.24 g cm^{-2} y^{-1}) compared to Station 1 (0.40 g cm^{-2} y^{-1}) and was consistent with those observed in the shallow environments ranging from 0.03 to 1 g cm^{-2} y^{-1} (Aller , 2014).

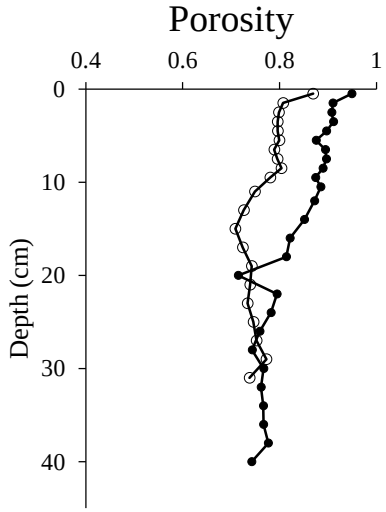

Figure 4.4. Profiles of porosity of the sediments sampled at both stations. Open circles represent Station 1A' and the solid circles Station 1.

4.3.3 Solid phase geochemistry

The bulk organic C and N contents (weight %) of the Danube delta sediments ranged from 0.95 % to 1.81 % for POC and from 0.13 % to 0.22 % for PN respectively whereas those of the shelf sediments ranged from 2.01 to 6.77 % for POC and 0.24 % to 0.87 % for PN, respectively. Contrary to Station 1A', the profile of Station 1 showed a decrease in organic C and N contents with depth (Figure 4.5). The C/N ratios, ranging from 7.1 to 8.5, showed a slight increase with depth at both stations indicating a preferential nitrogen mineralization.

Profiles of Fe/Al showed an enrichment of Fe at mid-depth of the core at Station 1 compared to Station 1A' (Figure 4.5) and the Fe/Al ratios were above the value of 0.44 observed for the average upper crust (McLennan, 2001). Profiles of Mn/Al indicated an alternance between depletion and enrichment in Mn with depth at both stations, suggesting the switching between reducing and oxidizing conditions over time. The variations in Fe/Al and Mn/Al observed at Station 1 seemed to be the opposite of those at Station 1A', revealing contrasting behaviour. Since both stations were situated close to the river mouths, the two sites would receive important detrital inputs.

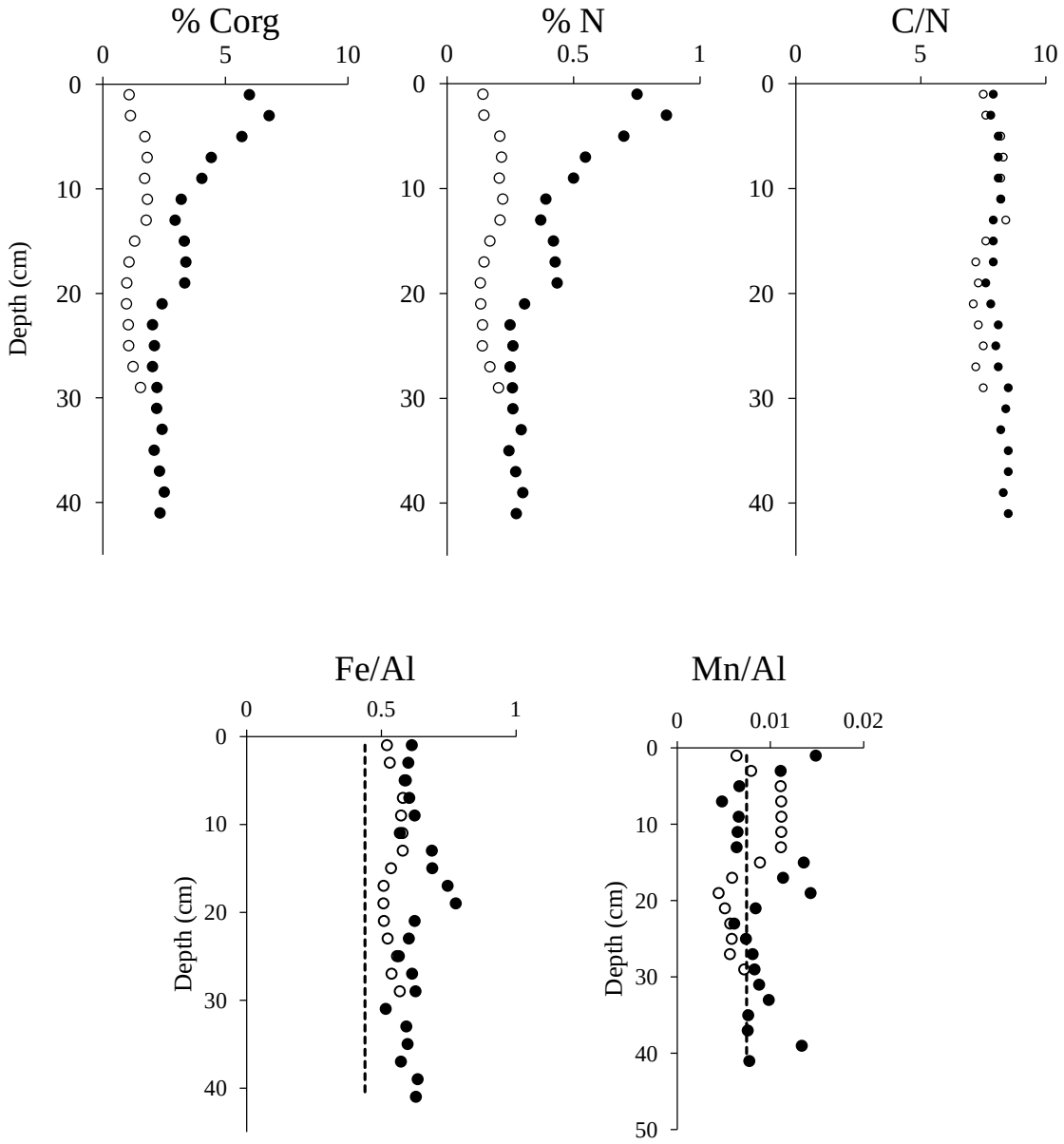

Figure 4.5. Profiles of particulate organic C and N contents and C/N ratios (upper panel) and of Fe/Al and Mn/Al ratios (lower panel) in the sediments at both stations. Open circles represent Station 1A' and the solid circles Station 1. The dashed lines indicate the values for average upper crust, 0.44 for Fe/Al and 0.0075 for Mn/Al.

4.3.4 Iron and sulphur speciation

Results of the determination of iron and sulphur speciation are summarized in Figure 4.6. Most of the Fe was unreactive at both stations and the highly reactive Fe represented on average 9 % and 25 % of total Fe at Stations 1 and 1A', respectively. The depth-averaged Fe_{HR} was 5 times higher at Station 1A' than at Station 1, with values of 0.26% Fe and 1.34 %

Fe respectively. The highly reactive iron contents are higher near the sediment-water interface with a maximum at 3 cm at Station 1 and at 5 cm at Station 1A'.

Both stations showed that Fe_H was the dominant fraction over the sediment column, representing on average 84 % and 89 % of Fe_{HR} for Station 1 and Station 1A' respectively, and that the contents of this phase decreased with depth (Table 4.3, Figure 4.6). At Station 1, a higher amount of Fe^{3+} than Fe^{2+} was extracted from the Fe_H fraction at the sediment-water interface, suggesting the presence of labile ferric iron as oxyhydroxide minerals, and below 7 cm ferrous and ferric irons showed similar abundances in Fe_H. In contrast, Station 1A' displayed in general a higher content of ferrous iron that ferric iron associated to the Fe_H phase, reflecting the presence of labile ferrous iron as FeS or $FeCO_3$. The Fe_{org} contents were low at both station with Station 1A' showing higher values compared to Station 1, which increased slightly from surface down to 5 cm depth and remained constant further downcore. The Fe_{ox} contents were low at both stations, representing less than 2 % of Fe_{HR}, but they were higher at Station 1A' compared to Station 1 and showed higher values in the top 17 cm of sediments implying the presence of iron in crystalline oxide minerals. Iron in pyrite, Fe_{pyr}, constituted the second dominant phase and represented 5 % and 14 % of Fe_{HR} at Station 1A' and Station 1 respectively. Compared to Station 1, the Fe_{pyr} contents were higher at Station 1A'. At Station 1 Fe_{pyr} increased with depth down to 5 cm depth, which then remained constant, while at Station 1A' pyrite iron exhibited a subsurface maximum at the depth of about 7 cm. Fe_{pyr} contents ranged from 0.02 to 0.04 % Fe at Station 1 and from 0.05 to 0.09 % Fe at Station 1A'.

Vertical distributions of S_{inorg}, sum of AVS and CRS, showed in general an increase downcore with a higher content at Station 1 than at Station 1A'. For both stations, CRS represented the major constituent of S_{inorg}. At Station 1, CRS contents increased with depth reaching a maximum of 1.87 % S at 17 cm depth while at Station 1A', the CRS profile showed a subsurface maximum of 0.62 % S at a depth of 5 cm. There was almost no AVS found at Station 1 while at Station 1A', the AVS contents increased slowly with depth with two maximal values of 0.29 % S at 5 cm and 0.30 % S at 21 cm.

Table 4.4: Depth distribution (cm) of various iron and sulphur phases and the degree of sulphidization in the NW shelf sediments of the Black Sea. Fe_{tot}, Fe^{2+}, Fe^{3+}, Fe_{org}, Fe_{ox}, Fe_{pyr} and Fe_{HR} are given in wt % Fe. Note that $Fe_H = Fe^{2+} + Fe^{3+}$. AVS and CRS are given in wt % S.

Station	Depth	Fe_{tot}	Fe^{2+}	Fe^{3+}	Fe_{org}	Fe_{ox}	Fe_{pyr}	Fe_{HR}	AVS	CRS	DOS_{HR}
1	1	2.73	0.07	0.29	<0.01	<0.01	0.02	0.38	<0.01	0.30	0.06
	3	3.03	0.16	0.32	<0.01	<0.01	0.03	0.53	<0.01	0.70	0.08
	5	2.91	0.26	0.18	<0.01	<0.01	0.04	0.48	<0.01	0.44	0.10
	7	3.40	0.11	0.10	<0.01	<0.01	0.04	0.25	<0.01	0.52	0.16
	11	2.49	0.09	0.05	<0.01	<0.01	0.04	0.19	<0.01	1.01	0.21
	13	3.09	0.09	0.05	<0.01	<0.01	0.04	0.18	<0.01	0.41	0.21
	17	3.75	0.13	0.05	<0.01	<0.01	0.04	0.22	<0.01	1.87	0.18
	19	3.17	0.10	0.08	<0.01	<0.01	0.04	0.22	<0.01	0.62	0.17
	21	2.23	0.07	0.04	<0.01	<0.01	0.04	0.14	<0.01	0.76	0.26
	25	1.92	0.06	0.03	<0.01	<0.01	0.04	0.13	<0.01	0.54	0.28
	39	2.55	0.11	0.07	<0.01	<0.01	0.04	0.22	<0.01	1.65	0.17
	41	2.35	0.05	0.03	<0.01	<0.01	0.04	0.13	<0.01	0.40	0.30
1A’	1	5.05	0.60	0.32	0.05	0.02	0.05	1.04	0.20	0.23	0.25
	3	5.12	0.62	0.36	0.06	0.03	0.06	1.12	0.20	0.29	0.23
	5	5.48	1.00	0.58	0.06	0.02	0.07	1.73	0.29	0.62	0.20
	7	5.54	0.83	0.57	0.06	0.02	0.09	1.57	0.15	0.35	0.25
	17	4.63	0.46	0.50	0.06	0.02	0.08	1.12	0.20	0.28	0.25
	21	5.22	0.92	0.32	0.06	0.01	0.06	1.38	0.30	0.32	0.26
	25	5.87	0.73	0.42	0.06	0.01	0.05	1.27	0.27	0.27	0.25
	29	5.09	0.56	0.73	0.06	0.06	0.06	2.46	0.10	0.45	0.11

Station 1

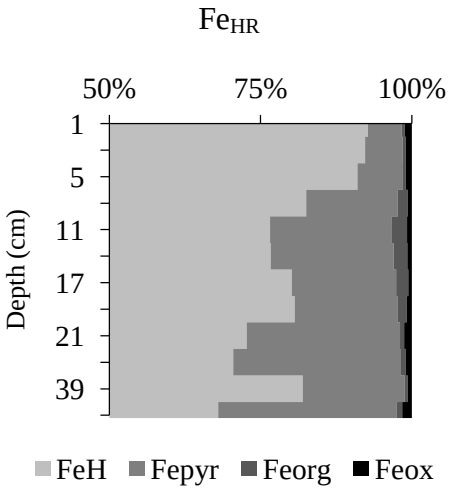

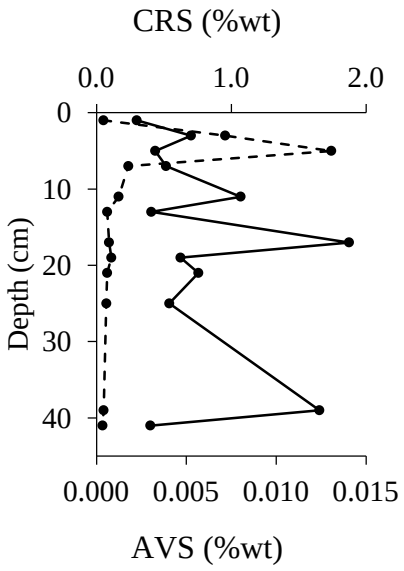

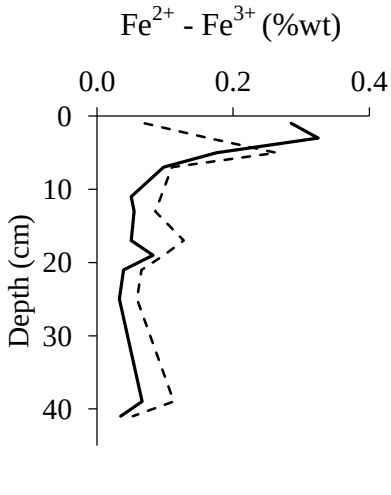

Station 1A'

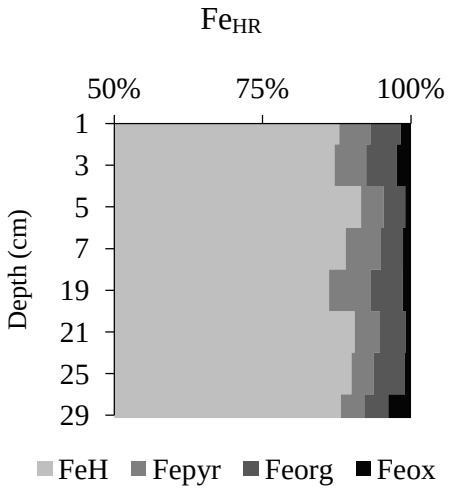

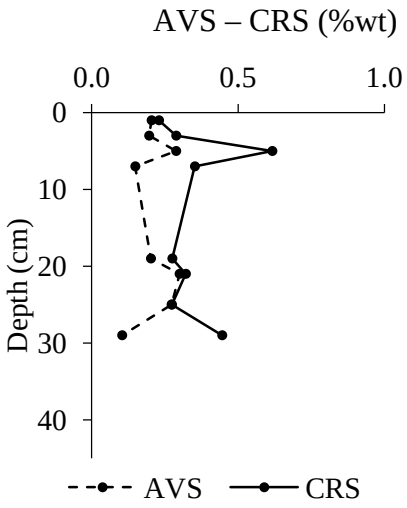

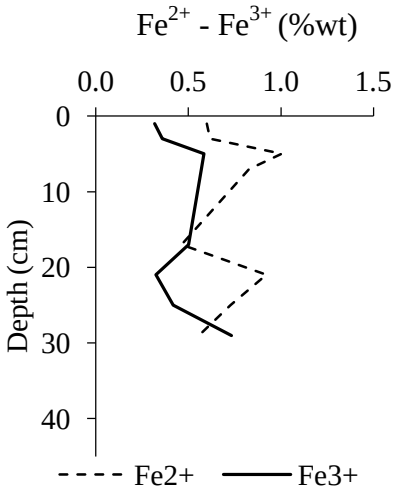

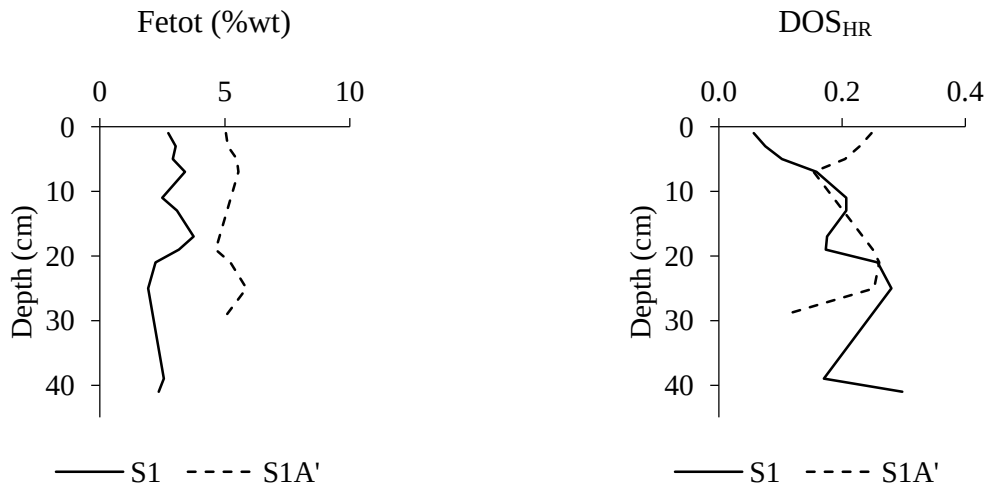

Figure 4.6. Depth profile (cm) of various iron and sulphur phases and the degree of sulphidization in the NW shelf sediments of the Black Sea. Fe_{tot}, Fe^{2+}, Fe^{3+}, Fe_{org}, Fe_{ox}, Fe_{pyr} and Fe_{HR} are given in wt % Fe. Note that $Fe_H = Fe^{2+} + Fe^{3+}$. AVS and CRS are given in wt % S.

4.3.5 Porewater geochemistry

At both stations, the oxygen concentrations in the bottom waters were below 63 μM, the hypoxic threshold, as shown in Figure 4.3 (Diaz & Rosenberg, 2008; Breitburg et al., 2016). The hypoxia was more intense at Station 1A' (7.39 μM O_2) while at Station 1, the dissolved oxygen concentration was 58.2 μM at the sediment-water interface. The oxygen penetration depths (OPDs) were also impacted by this lack of oxygen in the benthic compartment, leading to very shallow OPDs, 0.50 mm at Station 1A' and 1.75 mm at Station 1.

Profiling with microsensors showed that hydrogen sulphide concentrations at both stations were low at the sediment-water interface (Figure 4.3).

During summer 2017, sulphate concentrations decreased considerably with depth at Station 1A', close to the Danube delta, which exhibited a higher sulphate reduction activity compared to Station 1 (Figure 4.7). Moreover, the two stations displayed different sulphate profiles.

At Station 1A', the shape was linear, which reflected the diffusive drawdown of sulphate and might be induced by the decrease of porosities with depth (Jorgensen et al., 2001). The profile at Station 1 exhibited a concave-down curvature with constant sulphate concentrations from 8 cm down, usually attributed to the degradation of the organic matter over depth (Borowski et al., 1999). At both stations, the total sulphide concentrations were low, at the μM level, over

depth (Figure 4.7). Station 1A' showed a relatively constant concentration with depth, with an averaged concentration of 1.68 ± 0.10 μM. For Station 1, the concentration increased from 0.7 μM at 5 cm to 6 μM at 29 cm, which then decreased further downcore.

The two stations displayed different profiles of dissolved Fe (Figure 4.7). At Station 1, the Fe concentrations raised from 127 μM to 243 μM at 3 cm. Below 3 cm, the concentrations sharply decreased to reach 5.99 μM at 9 cm depth. Deeper, the concentrations were stable. At Station 1A', Fe concentrations were 181 μM at the sediment-water interface and decreased to 74 μM at 3 cm. Deeper, the profile showed an increase of concentrations reaching 244 μM at 29 cm. between 3 and 9 cm, then, a weak increase with depth to 244.24 μM.

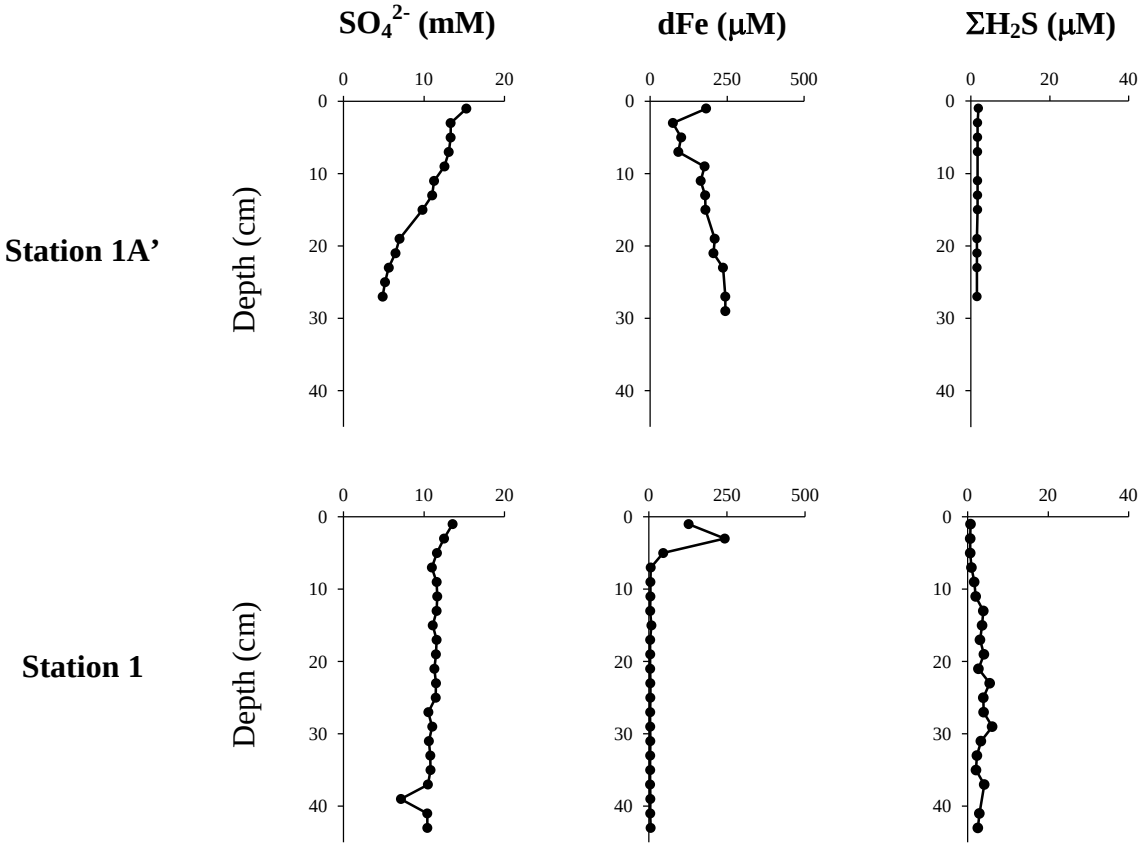

Figure 4.7. Profiles of SO_4^{2-}, dFe and ΣH_2S in porewaters at Stations 1A' and 1.

4.4 Discussion

4.4.1 Origin of the sediments

Our results revealed contrasting geochemistry of the sediments for the two sampled sites. The deviation of Fe/Al and Mn/Al ratios from the averaged upper crust signal showed enrichment in Fe and depletion in Mn compared to the upper crust material, which could be due to diagenetic reactions taking place in the sediments. The difference in organic matter supply, with higher rates at Station 1 as witnessed by the higher organic carbon content, would play a role in the early diagenesis and thus modify the sediment geochemistry. Moreover, the sediments at Station 1A' contained more iron and less sulphur compared to Station 1, which could be attributed to the dissimilar inputs of organic matter. The terrestrial inputs to the shelf as riverine loading were relatively high in Fe compared to the averaged upper crust signal. However, C/N ratios indicated similar marine origin (Meyers, 1994) and the sediment accumulation rates were comparable. Figure 4.8 showed that the organic matter in the sediments from both sites exhibited C/N ratios higher than the Redfield ratio for the marine plankton (Redfield, 1958), varying from 7.1 to 8.5.

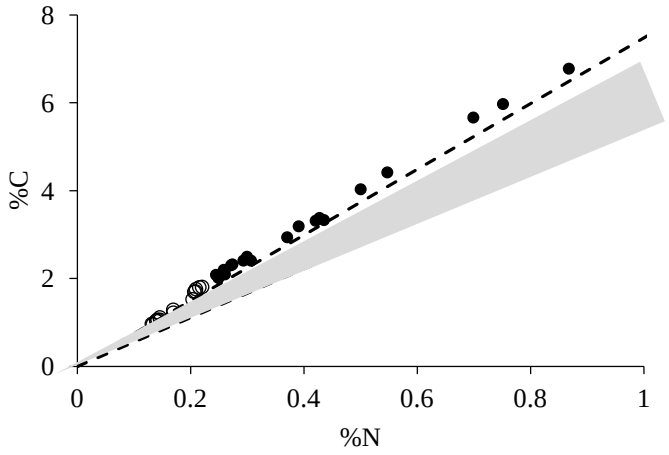

Figure 4.8. Particulate organic carbon content (%) as a function of particulate nitrogen content (%) in the shelf sediments at the two stations in comparison with marine phytoplankton defined by Redfield ratio shown as the grey area. Open circles are data from Station 1A' and solid circles are those from Station 1.

The values observed could be explained by a selective degradation of organic matter in the water column and/or by variations in organic matter input (Rullkötter, 2006). Values of % C_{org} and % N at Station 1A' were lower than at Station 1 indicating spatial variation on the

shelf of riverine inputs and/or productivity. Station 1A' was subject to smaller riverine inputs than Station 1 inducing a probable lower productivity at Station 1A'.

4.4.2 Downcore distribution of iron and sulphur species

The decrease in sulphate concentration with depth in porewaters observed at both stations revealed sulphate consumption by microbial activity through sulphate reduction. Rivers discharge an important amount of nutrient and suspended solids, inducing a gradient of sedimentation rate and of organic matter and iron loading into the sediments on the shelf. The absence of free sulphide in porewaters and the low measured concentrations of AVS might suggest that hydrogen sulphide produced during sulphate reduction were converted quickly into other species due to the possible presence of elemental sulphur and polysulphides (Jorgensen, 1977). The presence of pyrites (Figure 4.9), less vulnerable to oxidation than AVS, observed at the sediment-water interface at both stations might be explained by its formation in the water column (Bond & Wignall, 2010) and/or their upward transport by macrobenthos (Wijsman et al., 1999). A decrease of pyrite concentrations was observed at 5 cm and 17 cm at Stations 1 and 1A', respectively (Figure 4.6). The possible oxidation of pyrite would be low at these depths testifying a non-steady state deposition. Wijsman et al. (2001b) also observed this phenomenon on the north-western shelf and justified it by fluctuations in bottom water salinities or oxygen contents, or in the delivery of organic carbon and suspended solids. Moreover, dissolved Fe in porewaters and Fe_{ox} contents in sediment showed the presence of reactive Fe oxides. Wijsman et al. (2002) have developed a model for early diagenetic processes in the shelf sediments of the Black Sea and showed that two different systems could take place according to the benthic mineralization rate of organic carbon: (1) the Fe-dominated system and (2) the S-dominated system. Comparing with their results, in 2017 the NW shelf sediments were dominated by Fe due to the absence of free sulphide in porewaters, the presence of iron oxides and the high concentration of Fe^{2+}. Furthermore, the benthic mineralization rates were lower than 0.25 mmol C cm^{-2} y^{-1} on the shelf (Plante et al., 2020a) reinforcing the hypothesis of a Fe-dominated system as suggested by these authors.

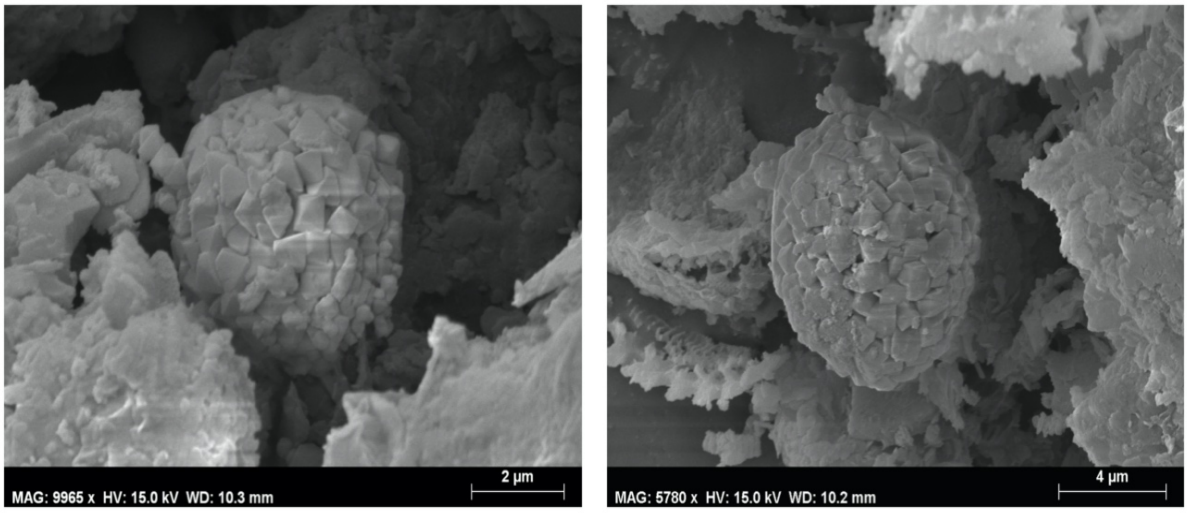

Figure 4.9. SEM images of framboidal pyrite at Station 1 at 39 cm depth (Photo credit: Sarah Robinet).

4.4.3 Reactive iron

The major part of iron in the sediments was composed of unreactive and poorly reactive iron like normal marine sediment of the continental margins as reported by Poulton and Raiswell (2002) with $Fe_{HR}/Fe_{tot} = 0.28 \pm 0.009$ and by Wijsman et al. (2001a) with $Fe_{HR}/Fe_{tot} = 0.19 \pm 0.024$. The ratios of Fe_{HR}/Fe_{tot} were 0.09 ± 0.04 and 0.27 ± 0.04 at Stations 1 and 1A', respectively. The lowest value obtained at Station 1 might be due to a significant detrital Fe component contained in the particulate riverine Fe. A low organic matter input under oxidizing conditions (Kostka et al., 1999; Anderson & Raiswell, 2004) and a low runoff (Poulton & Raiswell, 2002) could explain this low value. The processes of sportion and precipitation might remove the Fe_{HR} from the particulates transported by rivers leading to a low content of reactive iron. Wijsman et al. (2001a) proposed a re-allocation of Fe_{HR}, especially the dissolved iron, from the shelf to the deep-water euxinic sediments as evidenced by the elevated concentration of dissolved iron observed in the upper part of the anoxic water column in the Black Sea (Lewis & Landing, 1991; Muramoto, et al., 1991).

The decreasing Fe_{HR} content downcore could be explained by intensive sediment reworking that promoted iron recycling. A subsurface maximum of Fe_{HR} contents below the sediment-water interface characterizes the shelf sediments, indicating a Fe-enriched phase composed of Fe-oxides, as suggested by the speciation determination, resulting from sedimentation of organic matter or re-oxidation of reduced iron in the upper part of the sediments (2001a).

The relationships of Fe_{HR} *vs.* Fe_{tot} and Fe_U *vs.* Fe_{tot} are compared with the results of the Danube Delta area obtained by Wijsman et al. (2001a) (Figure 4.10). The highest concentrations of highly reactive iron were measured at stations located close to the Danube river mouth. In contrast, stations close to the Dniester delta displayed the lowest Fe_{HR} concentrations. Finally, the unreactive iron contents were found to be positively correlated with the total iron contents: $Fe_U = 0.73Fe_{tot} – 0.034$, similar to the relationship suggested by Wijsman et al. (2001a). In this study, the iron pool was found to be composed entirely of reactive iron when total iron content was lower than 0.05 wt%.

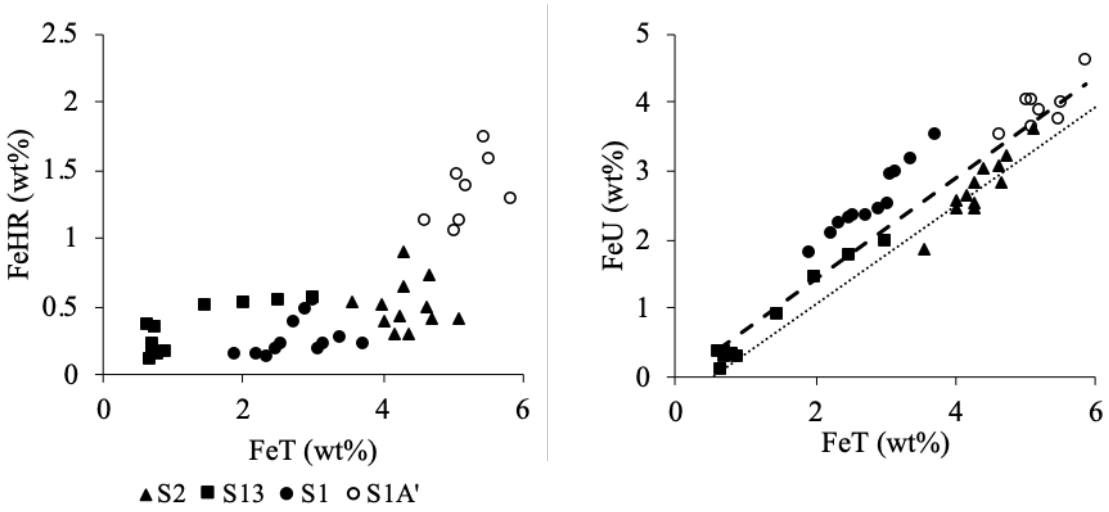

Figure 4.10. Highly reactive iron content (left) and unreactive iron content (right) as a function of the total iron content in the shelf sediments of the Black Sea. The data for Station 2 (S2) and Station 13 (S13) are taken from the study of Wijsman et al. (2001a). Dotted line represents the regression based on the data obtained by Wijsman et al. (2001a) and dashed line denotes the regression based on the data of this study.

4.4.4 Degree of sulphidization and pyritization

The degree of sulphidization (DOS_{HR}) represents the measure of the fraction of the reactive iron that is sulphidized (Levanthal & Taylor, 1990). DOS_{HR} was similar at both stations (Figure 4.6), with an averaged value of 0.18 at Station 1 and of 0.21 at Station 1A', falling in the lower range obtained by Wijsman et al. (from 0.03 to 0.75; Wijsman et al., 2001a). Contrary to Kraal et al. (2013), the values obtained in this study reflected a slow and slight reduction of iron oxides and sulphidization of iron in the surface sediments. Station 1A'

displayed no significant variation of the DOS_{HR} between the top and the bottom part of the sediments. The low DOS_{HR} could also suggest the presence of Fe-(oxyhydr)oxides due to low organic matter contents.

The degree of pyritization (DOP) has been defined as the extent to which the reactive iron has been converted to pyrite, corresponding to the ratio of Fe_{pyr}/Fe_{HR} (Berner, 1970; Raiswell et al., 1988). According to Raiswell et al. (1988), the DOP value is less than 0.46 for sediments deposited under oxic conditions, 0.46 to 0.8 for dysoxic depositional settings and 0.55 to 0.93 for euxinic environments. At Station 1, DOS_{HR} values are similar to those of DOP (Figure 4.11).

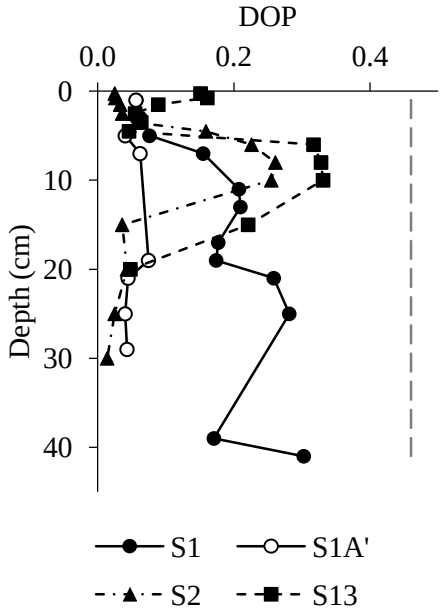

Figure 4.11. Depth profiles of DOP in the shelf sediments of the Black Sea. Data for S2 and S13 are from Wijsman et al. (2001a). The vertical dashed line indicates a DOP value of 0.46, corresponding to a situation where the sediments are deposited under oxic conditions.

At Station 1A', richer in AVS, DOP was lower than DOS_{HR}, similar to the observation made by Wijsman et al. (2001a) for their Station 2. The average DOP values of the sediment cores were 0.18 and 0.07 at Station 1 and Station 1A', respectively. These low DOP values might be explained by hydrodynamic conditions, as well as by the dredging for the maintenance of harbours. For shallow water environments, the sedimentation rates can be high leading to young surficial sediment and the processes of organic matter degradation and pyrite formation may not be completed. A part of the Fe_{HR} might still be in the process of being converted to pyrite during burial. As reported by Roychoudhury et al. (2003), the DOP could indicate sediment chemistry and porewaters redox conditions rather than the degree of bottom water

oxygenation. At Station 1, DOP increased first with depth and then decreased at around 19 cm depth as shown for Station 13 from Wijsman et al. (2001a) suggesting a non-steady state deposition.

4.5 Conclusions

Despite a marine origin of the NW shelf sediments, the results obtained in this study revealed an enrichment in total iron and an alternance between enrichment and depletion in manganese at different depth levels depending on their location. River loadings, productivity intensity and diagenetic reactions are linked to these variations. The vertical distribution of the various Fe and S species in the sediments allowed a better understanding of the Fe and S cycling on the shelf under low oxygen conditions. Sulphate reduction constituted a major diagenetic reaction in shelf sediments releasing reactive free sulphides. The presence of pyrite at the sediment-water interface highlighted the possibility of their formation directly in the water column and/ or by their upward transport by benthic feeders. It has been suggested by Wijsman et al. (2001) that the sediments from the oxic continental shelf of the Black sea were depleted in highly reactive iron. Twenty years later, new data from the shelf sediments confirms the deficiency of this highly reactive iron. Moreover, the sediments of the shelf are subject to fluctuations in salinity, dissolved oxygen content as well as fluxes of organic matter leading to a non-steady state sedimentary deposition, with consequences on the biogeochemical cycles. However, our results indicated an enrichment of highly reactive iron in the subsurface of the sediments which could be explained by the sedimentation of organic matter and the re-oxidation of the reduced iron. The Danube river mouth exhibited higher highly reactive iron contents in the sediments than the station near the Dniestr river. This spatial variation of the Fe-S cycle could be attributed to the different fluvial inputs, sorption and/or precipitation processes or yet to a distinct re-allocation of the reactive iron of the shelf deposits towards the sediments in deep and euxinic waters.

A low sulphidization of iron and the presence of iron oxides led to a low degree of sulphidization, especially confirmed by the low concentrations of AVS. A low degree of pyritization, as reflected by the low contents of pyrite, was found on the shelf probably induced by the hydrodynamic conditions, the dredging and the high sedimentation rate.

References

Aller, R. (2014). Sedimentary diagenesis, depositional environments, and benthic fluxes. In Treatise on geochemistry, 2nd edn (Vol. 8). Amsterdam: Elsevier Ltd.

Aller, R. C., & Rude, P. D. (1988). Complete oxidation of solid-phase sulphides by manganese and bacteria in anoxic marine sediments. Geochim. Cosmochim. Acta., 52, 751–765.

Anderson, T. F., & Raiswell, R. (2004). Sources and mechanisms for the enrichment of highly reactive iron in euxinic Black Sea sediments. American Journal of Science, 304, 203-233.

Berner, R. A. (1970). Sedimentary pyrite formation. Am. J. Sci., 268, 1-23.

Boesen, C., & Postma, D. (1988). Pyrite formation in anoxic environments of the Baltic. Am. J. Sci, 288, 575–603.

Bond, D. P., & Wignall, P. B. (2010). Pyrite framboid study of marine Permian–Triassic boundary sections: A complex anoxic event and its relationship to contemporaneous mass extinction. GSA Bulletin, 122, 1265–1279.

Borowski, W. S., Paull, C. K., & Ussler, W. (1999). Global and local variations of interstitial sulfate gradients in deep-water, continental margin sediments: Sensitivity to underlying methane and gas hydrates. Marine Geology, 159, 131-154.

Breitburg, D., Grégoire, M., & Isensee, K. (2016). The ocean is losing its breath: Declining oxygen in the world's ocean and coastal waters. IOC-UNESCO, IOC Technical Series. Global Ocean Oxygen Network 2018.

Breitburg, D., Levin, L. A., Oschlies, A., Grégoire, M., Chavez, F. P., Conley, D. J., . . . Rose, K. (2018). Declining oxygen in the global ocean and coastal waters. Science, 359(46).

Burton, E. D., Sullivan, L. A., Bush, R. T., Johnston, S. G., & Keene, A. F. (2008). A simple and inexpensive chromium-reducible sulfur method for acid-sulfate soils. Applied Geochemistry, 23, 2759–2766.

Canfield, D. E., Jorgensen, B. B., Fossing, H., Glud, R., Gundersen, J., Ramsing, N. B., . . . Hall, P. O. (1993). Pathways of organic carbon oxidation in three continental margin sediments. Marine Geology, 113, 27-40.

Canfield, D. E., Lyons, T. W., & Raiswell, R. (1996). A model for iron deposition to euxinic Black Sea sediments. Am. J. Sci., 296, 818-834.

Capet, A., Beckers, J.-M., & Gregoire, M. (2013). Drivers, mechanisms and long-term variability of seasonal hypoxia on the Black Sea northwestern shelf – is there any recovery after eutrophication? Biogeosciences, 10, 3943–3962.

Chen, X., Andersen, T. J., Morono, Y., Inagaki, F., Jørgensen, B. B., & Lever, M. A. (2017). Bioturbation as a key driver behind the dominance of Bacteria over Archaea in near-surface sediment. Sci Rep, 7, 2400.

Claff, S. R., Sullivan, L. A., Burton, E. D., & Bush, R. T. (2010). A sequential extraction procedure for acid sulfate soils: Partitioning of iron. Geoderma, 155, 224–230.

Cline, J. D. (1969). Spectrophotometric determination of hydrogen sulfide in natural waters. Limnol. Oceanogr., 14, 454-458.

Diaz, R. J., & Rosenberg, R. (2008). Spreading dead zone and consequences for marine ecosystems. Science, 321, 926-929.

Friedrich, J., Dinkel, C., Friedl, G., Pimenov, N., wijsman, J., Gomoiu, M.-T., . . . Wehrli, B. (2002). Benthic nutrient cycling and diagenetic pathways in the North-western Black Sea. Estuarine, Coastal and Shelf Science, 54, 369-383.

Glud, R. N. (2008). Oxygen dynamics of marine sediments. Mar. Biol., 4, 243-289.

Jorgensen, B. B. (1977). The sulfur cycle of a coastal marine sediment (Limfjorden). Limnol. Oceanogr., 22, 814-832.

Jorgensen, B. B., & Kasten, S. (2006). Sulfur Cycling and Methane Oxidation. In H. D. Schulz, & M. Zabel (Eds.), Marine Geochemistry. Berlin: Springer.

Jorgensen, B. B., Weber, A., & Zopfi, J. (2001). Sulfate reduction and anaerobic methane oxidation in Black Sea sediments. Deep Sea REsearch Part I: Oceanographic Research Papers, 48, 2097-2120.

Kirstensen, E., Penha-Lopes, G., Delefosse, M., Valdemarsen, T., Quintana, C. O., & Banta, G. T. (2012). What is bioturbation? The need for a precise definition for fauna in aquatic sciences. Mar. Ecol. Prog. Ser., 446, 285-302.

Kostka, J. E., & Luther III, G. W. (1994). Partitioning and speciation of solid phase iron in saltmarsh sediments. Geochim. Cosmochim. Acta, 58, 1701–1710.

Kostka, J. E., Thamdrup, B., Glud, R. N., & Canfield, D. E. (1999). Rates and pathways of carbon oxidation in permanently cold Arctic sediments. Marine Ecology Progress Series, 180, 7–21.

Kraal, P., Burton, E. D., & Bush, R. T. (2013). Iron monosulfide accumulation and pyrite formation in eutrophic estuarine sediments. Geochim. et Cosmochim. Acta, 122, 75–88.

Levanthal, J., & Taylor, C. (1990). Comparison of methods to determine degree of pyritization. Geochim. et Cosmochim. Acta, 54, 2621-2625.

Lewis, B. L., & Landing, W. M. (1991). The biogeochemistry of manganese and iron in the Black Sea. Deep Sea Res. Part A, 38, S773-S803.

Lewis, B. L., & Landing, W. M. (1991). The biogeochemistry of manganese and iron in the Black Sea. Deep Sea Research Part A. Oceanographic Research Papers, 38, S773-S803.

LOICZ. (1995). Implementation Plan 1995. Global Change IGBP Report No. 33.

Lyons, T. W. (1997). Sulfur isotopic trends and pathways of iron sulfide formation in upper Holocene sediments of the anoxic Black Sea. Geochim. et Cosmochim. Acta, 61, 3367-3382.

Lyons, T. W., Berner, R. A., & Anderson, R. F. (1993). Evidence for large pre-industrial perturbations of the Black Sea chemocline. Nature, 538–540.

Lyons, T. W., Reinhard, C. T., & Planavsky, N. J. (2014). The rise of oxygen in Earth's early ocean and atmosphere. Nature, 506, 307–315.

Lyons, T. W., Werne, J. P., Hallander, D. J., & Murray, R. W. (2003). Contrasting sulfur geochemistry and Fe/Al and Mo/Al ratios accross the last oxic-to-anoxic trasnition in the Cariaco Basin, Venezuela. Chem. Geol., 195, 131-157.

McLennan, S. M. (2001.). Relationships between the trace element composition of sedimentary rocks and upper continental crust. Geochem. Geophys. Geosyst., 2.

Meyers, P. A. (1994). Preservation of elemental and isotopic source identification of sedimentary organic matter. Chem. Geol., 114, 289-302.

Middelburg, J. J., & Levin, L. A. (2009). Coastal hypoxia and sediment biogeochemistry. Biogeosciences, 6, 1273-1293.

Muramoto, J. A., Honjo, S., Fry, B., Hay, B. J., Howarth, R. W., & Cisne, J. L. (1991). Sulfur, iron and organic carbon fluxes in the Black Sea: sulfur isotopic evidence for origin of sulfur fluxes. Deep Sea Research Part A. Oceanographic Research Papers, 38, S1151-S118.

Poulton, S. W., & Raiswell, R. (2002). The low-temperature geochemical cycle of iron: From continental fluxes to marine sediment deposition. American Journal of Science, 302, 774-805.

Raiswell, R., & Berner, R. A. (1985). Pyrite formation in euxinic and semi-euxinic sediments. Am. J. of Sci., 285, 710-724.

Raiswell, R., Buckley, F., Berner, R. A., & Anderson, T. F. (1988). Degree of pyritisation of iron as a paleoenvironmental indicator of bottom-water oxygenation. Journal of Sedimentary Research, 58, 812-819.

Redfield, A. C. (1958). The biological control of chemical factors in the environment. American Scientist, 230A, 205-221.

Roychoudhury, A. N., Kostka, J. E., & Van Cappellen, P. (2003). Pyritization: a palaeoenvironmental and redox proxy reevaluated. Estuar. Coast. Shelf Sci, 57, 1183-1193.

Rullkötter, J. (2006). Organic Matter: The Driving Force for Early Diagenesis. In H. D. Schulz, & M. Zabel, Marine Geochemistry (pp. 125-168). Berlin: Springer.

Seitaj, D., Schauer, R., Sulu-Gambari, F., Hidalgo-Martinez, S., Malkin, S. Y., Burdorf, L. D., . . . Meysman, F. J. (2015). Cable bacteria generate a firewall against euxinia in seasonally hypoxic basins. PNAS, 112, 13278-13283.

Shaffer, G. (1986). Phosphate pumps and shuttles in the Black Sea. Nature, 321, 515–517.

Sinninghe Damsté, J. S., & De Leeuw, J. W. (1990). Analysis, structure and geochemical significance of organically-bound sulphur in the geosphere: State of the art and future research. Organic Geochemistry, 16, 1077-1101.

Thamdrup, B., & Canfield, D. E. (1996). Pathways of carbon oxidation in continental margin sediments off central Chile. Limnol. Oceanogr., 41, 1629-1650.

van de Velde, S., Callebaut, I., Hidalgo-Martinez, S., Antler, G., Leermakers, M., & Meysman, F. J. (2018). Early diagenesis of carbon, iron and sulphur in salt marsh sediments: the importance of burrowing fauna. In S. van de Velde, Electron shuttling and elemental cycling in the seafloor. Brussels: VUBPRESS.

Wijsman, J. W., Herman, P. M., Middelburg, J. J., & Stoetaert, K. (2002). A model for early diagenetic processes in sediments of the continental shelf of the Black Sea. Estuarine, Coastal and Shelf Science, 54, 403-421.

Wijsman, J. W., Middelburg, J. J., & Heip, C. H. (2001a). Reactive iron in Black Sea Sediments: implications for iron cycling. Marine Geology, 172, 167–180.

Wijsman, J. W., Middelburg, J. J., Herman, P. M., Böttcher, M. E., & Heip, C. H. (2001b). Sulfur and iron speciation in surface sediment along the northwestern margin of the Black Sea. Marine Chemistry, 74, 261-278.

Wijsman, J., Herman, P., & Gomoiu, M. T. (1999). Spatial distribution in sediment characteristics and benthic activity on the northwestern Black Sea shelf. Mar. Ecol. Prog. Ser., 181, 25–39.

Zhang, J. Z., & Millero, F. J. (1993). The products from the oxidation of H2S in seawater. Geochim. et Cosmochim. Acta, 57, 1705-1718.

Chapter 5

Biogeochemistry of trace metals in the sediments of the NW shelf of the Black Sea

Photo credit: Manana Qveliashvili

Biogeochemistry of trace metals in the sediments of the NW shelf of the Black Sea

Audrey Plante, Arthur Capet, Nathalie Roevros, Marilaure Grégoire, Nathalie Fagel and Lei Chou (in preparation).

ABSTRACT

The North-western (NW) shelf of the Black Sea receives high inputs of organic matter from rivers and is subject to seasonal oxygen depletion impacting the early diagenesis and the exchanges at the sediment-water interface. The shelf constitutes a good environment to study the biogeochemistry of major elements (SO_4^{2-}, Fe and Mn minerals), nutrients (PO_4^{3-} and NH_4^+) and trace elements (Ni, Zn, Cu, Co and Cd) in well-oxygenated water column as well as under low oxygen conditions. Based on concentration profiles of major elements and nutrients in porewaters and trace element contents in the solid phase, the various diagenetic reactions controlling the mobility of trace elements in the sediments were examined. Under oxic conditions, primary redox reactions were identified which followed the traditional diagenetic sequence for the stations located near the Danube delta and in the Odessa Bay region. Under poor-oxygenated conditions, the main reactions were disrupted with a limitation of aerobic respiration and denitrification leading to the mineralization of organic matter by anaerobic pathways. Adsorption and co-precipitations with Fe oxides and Mn oxides could be established as the main processes controlling Ni and Zn.

Trace metals are known to increase the level of pollution of both the water column and the sediments influencing the life of marine organisms. The modern sediments of the NW shelf were studied to assess the enrichment of trace metals in the surface sediments. Data revealed an enrichment of Ni, Cu and Zn close to the Danube river mouth and an enhancement of Co and Cd in the Odessa Bay region. Data were compared with those reported in the late 20^{th} century to evaluate their variability over times. An increase in metallic pollutants was observed especially in areas close to the Danube mouth while the pollution level in the Odessa Bay region remained relatively stable for Cu, Cd, Ni and Zn.

5.1 Introduction

In modern aquatic systems, sedimentary trace metals have been used as proxies for productivity and redox conditions (Morford & Emerson, 1999; Brumsack, 2006; Tribovillard et al., 2006). Heavy metals are the most widespread contaminants and are remobilized in the sediments depending on the physicochemical conditions both in the water column and in the sediments. Trace metal concentrations are often low under well-oxygenated conditions in the water column (McLennan, 2001) while under low oxygen, heavy metals will be released to the water column due to interactions of several processes (Tribovillard et al., 2006).

Trace metals are linked to organic matter in the water column and sediments (Tribovillard et al., 2006**;** Canfield, 1994). The efficient remineralization of organic matter in the water column under oxygenated conditions allows a small fraction of the organic-bound trace metals in the water column to reach the sediment-water interface, which contributes to an increase of flux of Cu, for example, from the water column to sediments (Riedel et al., 1997). An increased input of organic-bound trace metals to sediments and a flux of Fe, Mn, As, Co and Hg from the sediments to the water column (Sundby et al., 1986; Emili et al., 2011) may take place under low oxygen conditions due to the low remineralization rate of organic matter. The oxygenation status of the water column affects also the fluxes of dissolved phosphate, nitrate+nitrite, ammonium and total sulphides, which are important for environmental quality of marine waters. Fluxes of phosphate, ammonium and total sulphides to the water column and that of nitrate to the sediments were observed during a hypoxic and anoxic events whereas these exchanges tended to cease or reverse in a well-oxygenated water column (Middelburg & Levin, 2009; Sundby et al., 1986; Emili et al., 2011)**.**

An enrichment of trace metal in sediments could also be due to their adsorption on Mn- and Fe-(oxyhydr)oxides. Variable redox conditions would facilitate the high mobility of these particles, leading to a reiteration of dissolution and re-precipitation cycles of these metals (Froelich et al., 1979; Shaw et al., 1990; Tribovillard et al., 2006). Although trace metals may be preserved in Mn- and Fe-oxides on the seafloor under well-oxygenated conditions, the release of trace metals during the dissolution of oxides in surface sediments and their subsequent sequestration by organic matter, sulphide minerals or other reduced phases is more frequent than one would think (Morford & Emerson, 1999; Tribovillard et al., 2006).

The diffusive transport from the water column into the sediments influences the trace metal enrichment in the sediments as well as the ensuing sequestration in the organic matter or

authigenic minerals. The sedimentary enhancement depends on the metal and the stage of bottom water oxygen depletion going from hypoxic, anoxic to euxinic conditions (Crusius et al., 1996; Olson, 2017). During the last century, most coastal zones have been largely impacted by the development of anthropogenic activities. Trace metals were used for many applications in agriculture and industries (e.g., fertilizers, pesticides, pigments and lubricants). Their use has led to an increase of inputs of contaminants and/or nutrients by fluvial and eolian pathways where they are adsorbed onto clay particles and oxides or complexed by organic compounds (Nriagu et al., 1988; Windom et al., 1989; Liaghati et al., 2004). These releases have been significantly reduced during the last decades because of new regulations but contaminants have been accumulated in the sediments over time. Nowadays, sediments represent a potential source of contaminants for the water column which may alter the water quality and threat aquatic organisms. The assessment of anthropogenic pollution in modern sediments may be achieved by determining trace metal enrichment factors (Caccia et al., 2003; Ip et al., 2007).

The influence of oxygen concentration in the water column on sedimentary processes and on fluxes at the sediment-water interface is still poorly understood, especially when oxygen concentration oscillates seasonally (Morse & Eldridge, 2007). The Black Sea is an ideal location because it is known as one of the largest anoxic basins in the world. It is a landlocked sea with a restricted access to the open ocean characterized by excessive loading of nutrients delivered by the rivers, especially the Danube river (Popa, 1993; Panin & Jipa, 2002). The NW shelf is a particularly interesting area, due to its seasonal oxygen depletion in the bottom water, to assess the trace metal enrichment in the sediments and to understand the link between trace metals and changes in bottom water oxygenation as well as anthropogenic pollution. In recent decades, the increasing number of coastal areas influenced by seasonal or permanent hypoxic events raised and strengthened the interest to discern the diagenetic pathways and to evaluate the fluxes across the sediment-water interface under hypoxic conditions (Diaz & Rosenberg, 2008).

In this paper, the diagenetic reactions taking place will first be identified with a focus on the mobility of trace metals in the sediments. The distribution in shelf sediments of trace elements and the enrichment factor as well as the geo-accumulation index will be then described and discussed.

5.2 Material and methods

5.2.1 Sampling and samples treatment

The study zone concerned the Ukrainian continental shelf, which received freshwater inputs from several rivers such as the Danube and the Dnieper (Figure 5.1). Four stations were examined under oxic conditions in May 2016 with bottom water oxygen concentrations of 109 µM at Station 6, 145 µM at Station 7, 182 µM at Station 12 and 265 µM at Station 15. Two stations were visited in August 2017 during an oxygen depletion occurring in bottom waters and the measured oxygen concentrations were 7.4 µM at Station 1A' and 58.2 µM at Station 1. Stations 7 and 1A' were situated at the same location but sampled during two different campaigns. Stations 6, 7 and 1A' were located in the Danube delta front, Stations 1 and 12 were in the Dnieper region and Station 15 was in the Odessa Bay (Table 5.1).

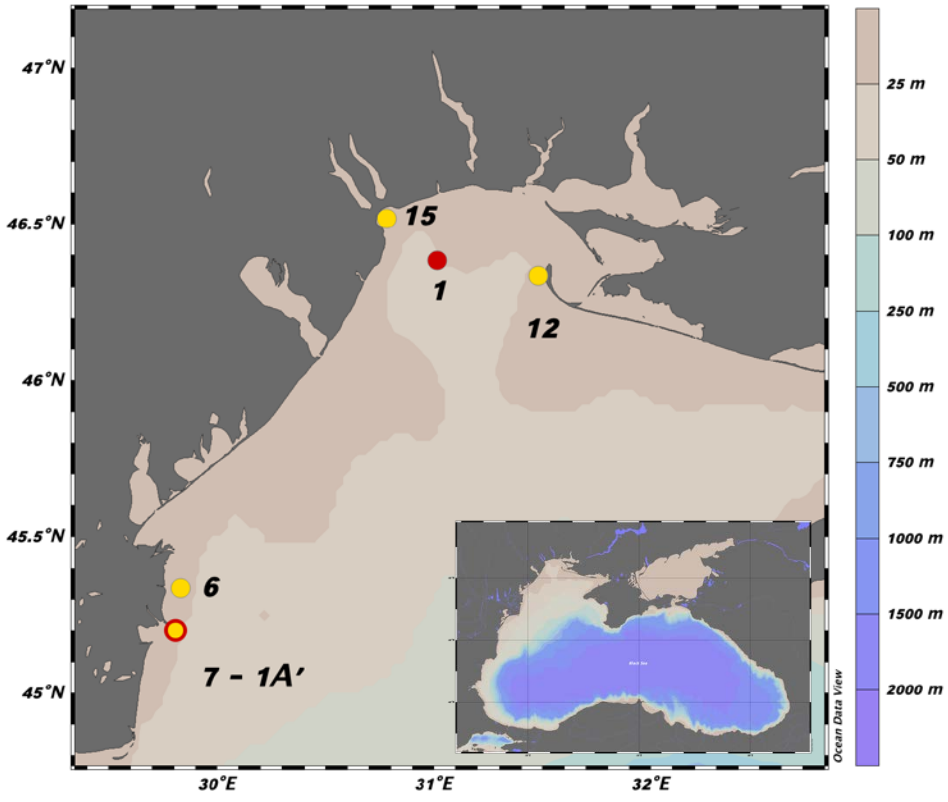

Figure 5.1. Map of the sampling stations on the Ukrainian shelf and map of the Black Sea (bottom right corner). Yellow points represent stations sampled during the 2016 cruise, red points refer to those visited during the 2017 cruise and yellow point with red circle denotes the station sampled during both cruises.

Table 5.1. Positions and water depths of the sampling stations on the Ukrainian shelf, together with hydrographic data of bottom waters. Temperature, salinity and pH are from the CTD data and O_2 concentrations (μM) are obtained from the O_2 microsensor measurements. Stations 6, 7, 12 and 15 were sampled in spring 2016 and Stations 1A' and 1 were visited in summer 2017. N.A.: Not available.

Station	Position	Water depth (m)	Temperature (°C)	Salinity (psu)	pH	O_2 (μM)
6	45°20.0'N, 29°50.6'E	21.0	7.48	17.94	8.23	109
7	45° 12.0'N, 29°48.6'E	18.6	7.55	18.00	8.22	145
12	46° 20.0'N, 31°29.0'E	14.4	8.91	17.85	8.33	182
15	46° 31.6'N, 30°47.5'E	17.1	8.46	7.87	8.38	265
1A'	45° 12.0'N, 29°48.6'E	19.9	8.91	18.27	N.A.	7.4
1	46° 26.0'N, 31°01.0'E	22.0	8.60	18.02	N.A.	58.2

Sediment cores (inner diameter 10 cm) were collected with plexiglass tubes using a multicorer. After inspection, only undisturbed cores were used for measurements. Within two hours after collection, microprofiling of geochemical gradients was performed under N_2 atmosphere in the headspace. Porewater extractions were performed using the Rhizon technique (pore size 0.15 μm) in a glove bag under N_2 atmosphere at every 2 cm interval. The Rhizons were inserted in the predrilled holes on the tube which were covered with an electric tape during sampling. The extraction of porewaters took several hours to complete. Subsamples were taken for the analyses of alkalinity, nutrients (nitrate/nitrite, ammonium, phosphate, silicate), dissolved Fe^{2+}, Mn^{2+}, Cl^-, SO_4^{2-} and ΣH_2S. All nutrient samples were stored frozen except for silicate which was stored at 4°C together with water samples for other analyses. One sediment core was sliced at 1-4 cm for the solid phase analyses.

5.2.2 Solid phase analyses

The grain size distribution of the sediments was determined by laser diffraction using a Malvern Mastersizer 3000. Organic carbon (% dry weight) was measured on decarbonated sample with a Vario Microcube CNS elemental analyser coupled with an IRMS isoprime 100 isotope ratio mass spectrometer. $\%CaCO_3$ was determined using the Loss Of Ignition (LOI)

method (Dean, 1974) which consisted of sequential heating of samples, first at 550 °C during 4h and then at 950 °C during 2h.

An aliquot of dried sediments from each slice was placed in a Teflon bomb and digested entirely in a mixture of ultrapure HCl, HNO_3 and HF in a microwave oven. Blanks were taken with every series to determine the reproducibility (RSD < 9 %).The digests were analysed for metal concentrations (Al, Fe, Mn, Cu, Zn, Ni, Co, Mo, Si); samples for Stations 12, 15, 1 and 1A' were diluted 40 times prior to measurement by ICP-OES (Precision was < 2 % for major elements and < 5 % for minor elements) and those for Stations 6 and 7 were diluted 200 times or more prior to analysis by ICP-MS (Precision < 2 %). The precision and the accuracy were assessed by analysing the Certified Reference Materials (CRM) BCR-277 (Table 5.2). External calibrations were made at the beginning and the middle of the run to detect an eventual drift. All the results were corrected by a correction factor determined with the recovery of BCR-277 measurements. For example, the measured concentrations of Al on samples with ICP-AES were corrected by a factor of 1.02. For more details, see §2.2.9 in Chapter 2.

Table 5.2. Certified or indicative values, measured concentration (mg kg^{-1}) and recovery (%) of the BCR-277 analyzed by ICP-MS and ICP-AES.

BCR - 277	Certified/indicative value (mg/kg)	Measured value (mg/kg)		Recovery (%)	
		ICP-MS	ICP-AES	ICP-MS	ICP-AES
Al	49000 ± 1000	45668 ± 312	50218 ± 1742	93	102
Mn	1580 ± 10	1520 ± 19	1335 ± 76	96	85
Co	17.9 ± 0.5	17.4 ± 0.2	16.0 ± 2.1	99	90
Ni	43.4 ± 1.6	76.7± 1.0	58.0	177	134
Cu	101.7 ± 1.6	103.2 ± 1.0	103.3 ± 5.7	101	102
Zn	547 ± 12	539 ± 4	475 ± 16	99	87
Cd	11.9 ± 0.4	11.62± 0.4	15.1	98	126
Fe	46100 ± 1500	43623 ± 595	50034 ± 2614	95	106

Total Hg was measured by Direct Mercury Analyzer (DMA 80, Milestone Inc., Pittsburgh, PA) in which samples were combusted at 750 °C and vapors of mercury were retained on a gold trap for analysis by cold vapor atomic absorption spectrometry. Certified reference

materials (Tort-2 and Dorm-2, Institute for Environmental Chemistry, National Research Council of Canada, Ottawa, Canada; SO-2: sediment, Canadian Centre for Mineral and Energy Technology, Canada) were used to standardize the instrument. Tort-2 recovery averaged 284.3 ± 14.4 ng g^{-1} (n = 2) corresponding to 105 ± 5 % of the certified value. SO-2 recovery averaged 85.5 ± 1.3 ng g^{-1} (n = 8) corresponding to 104 ± 2 % of the certified value.

The reactive fraction of the solid phase was determined on freeze-dried sediments using the method of Kraal et al. (2013) for the iron extractions and for the sulphide extractions.

5.2.3 Oxygen measurement by microelectrode

Oxygen microsensor profiling was performed using commercial microelectrodes (Clark-type O_2 microelectrode: OX100 standard, UNISENSE, A.S., Denmark) equipped with an internal reference and a guard cathode. The sensor tip diameter was 100 µm, the stirring sensitivity was 1.5 % and the 90 % response time was < 8 s. The sensor was connected to a high quality picoampere-meter (PA2000, UNISENSE) and mounted on a motor-controlled micromanipulator. Oxygen microprofilings were performed at 250 µm resolution, with a 2-point calibration made in air-saturated seawater (100 % O_2 saturation) and in an ascorbate solution (0 % O_2 saturation). The position of the sediment-water interface was determined based on the break in the O_2 concentration gradient.

5.2.4 Porewater analyses

Alkalinity was measured by a spectrophotometric method following the procedure of Sarazin (1999). Ammonium was analysed fluometrically at 460 nm following excitation at 360 nm according to the method of Holmes (1999); the samples were reacted with ophthalaldehyde (OPA) in the presence of sodium sulphite and borate buffer to form a fluorescent species in a proportional quantity to ammonium concentration. PO_4^{3-} were determined by colorimetric methods (Grasshoff et al., 1983). Dissolved Fe and Mn concentrations were determined by Inductively Coupled Plasma – Optical Emission Spectroscopy (ICP-OES, Varian Liberty serie II) on acidified samples after a 10x dilution. Chlorides and sulphates were measured after a dilution of 250 times by ion chromatography on Dionex-ICS5000. Total sulphides ($\Sigma H_2S = [HS^-] + [S^{2-}] + [H_2S]$) were measured colorimetrically following the method of Cline et al. (1969)

5.3 Results

5.3.1 Water column conditions

During spring 2016, the water column was stratified for temperature and salinity but did not show any clear stratification for dissolved oxygen displaying oxic bottom waters. Conversely, during summer 2017 the water column was stratified for temperature, salinity and oxygen. Concentrations of oxygen at Stations 1 and 1A' decreased to 161 μM to 95 μM respectively, 1 m above the seabed, indicating oxic waters. Nonetheless, dissolved oxygen concentrations determined by the O_2 microsensor revealed a poor-oxygenated system in the overlying water right above the sediment-water interface, suggesting a strong gradient in the last meter of the bottom water. Values of pH were relatively constant on the shelf in spring 2016 varying from 8.22 to 8.38 and the salinities of the bottom waters were heterogeneous for the two cruises ranging from 7.87 psu to 18.27 psu (Table 5.1).

5.3.2 Sediment characteristics and geochemistry

Sediments of the shelf consisted of fine mud with a median grain size of 24.3 μm on average and a mean of silt content of 85.5 ± 9.2 %. The sediments at Station 12 had a granulometry sandier than that at other stations due to its location close to the Tendra Spit.

Shelf sediments had a mean organic carbon content of 2.28 % near the sediment-water interface. Sediments from stations close to the river mouths and from those sampled during summer contained more organic matter. Profiles of $\%C_{org}$ showed different contents of organic carbon with depth and with the location (Figure 5.2). Stations 6, 7, 12 and 1A' exhibited the lowest content of organic carbon in the sediments on the shelf whereas Stations 15 and 1 revealed higher values. The carbonate contents were higher at the Stations 12 and 1. The depth profiles at all stations, except for Stations 12 and 1A', did not show much variation with depth.

Contents of major and minor elements in the sediments did not show clear distribution patterns with depth but dissimilarities between the stations were observed (Figure 5.2 and Figure 5.3). Station 12 exhibited the lowest contents of Al (average of 2.4 ± 0.5 wt%), Fe (average of 1.0 ± 0.3 wt%) and Mn (average of 0.2 ± 0.09 wt%).

Trace element profiles in the sediments displayed variations with depth without a clear trend (Figure 5.4 and Figure 5.5). The shapes of trace element profile exhibited similar variations to those for major elements at each station. Shelf sediments had higher contents at different levels in Zn, Cu and Ni compared to Co and Cd. The Cd contents were especially high at Station 12. At station 7, all metals exhibited a higher value at a depth between 10 cm and 12 cm. At Station 6, metal contents were lower at 12 cm and 25 cm depths where lower contents of organic carbon were also observed. Hg profiles revealed that there was a subsurface minimum at 12 cm depth at Station 6 and a subsurface maximum at a depth close to 10 cm (Figure 5.6).

Wijsman et al. (2001) and Plante et al. (2020a, *submitted*) showed that shelf sediments were depleted in reactive iron which represented 9 % and 25 % of the total iron at the Station 1 and Station 1A' respectively during summer 2017, suggesting the presence of (oxyhydr)oxide minerals. Although a low concentration of acid-volatile sulphide was observed, the presence of pyrite was detected by scanning electron microscopy at stations sampled in 2017 and the abundance of this sulphide mineral increased with depth (Chapter 4).

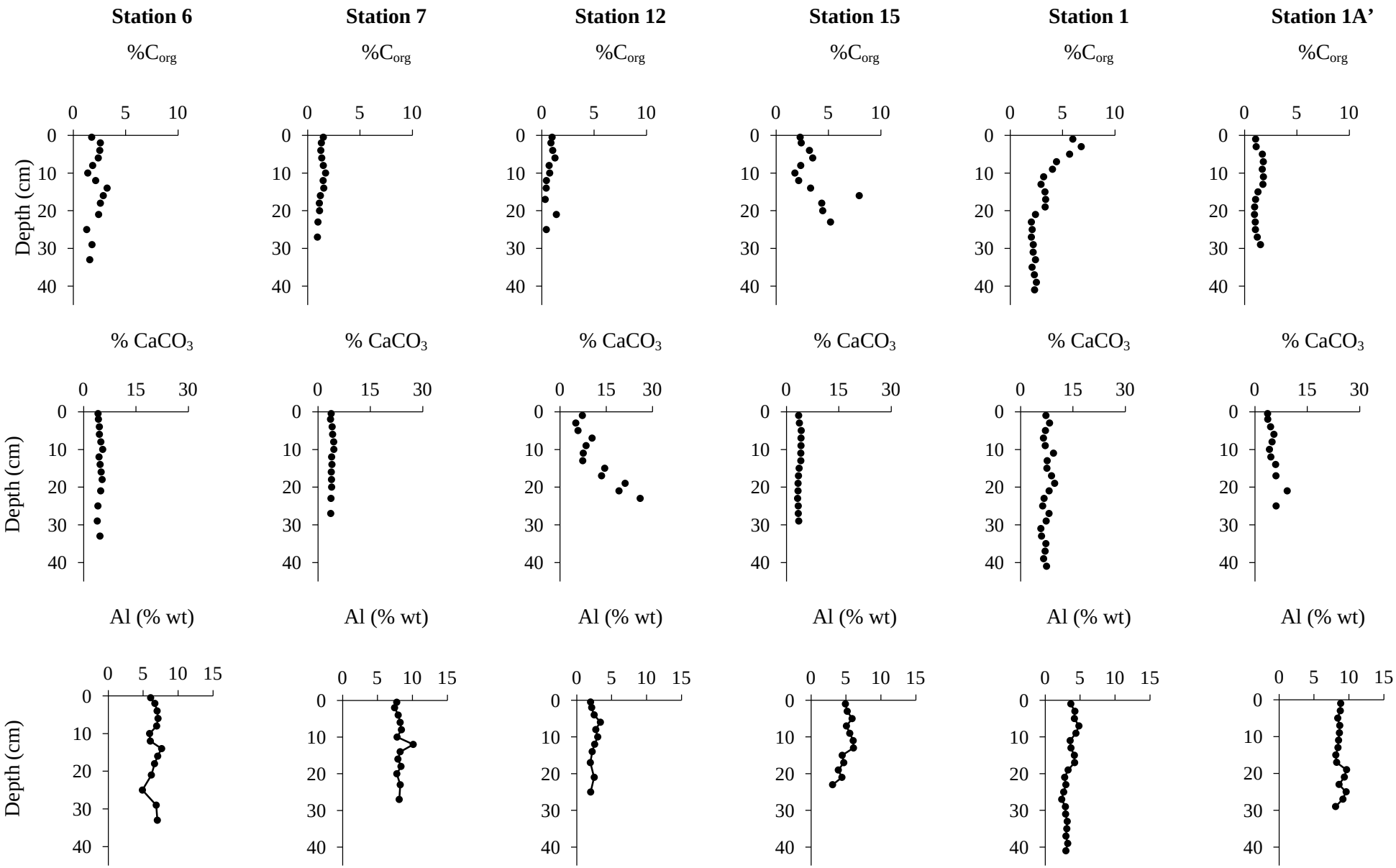

Figure 5.2. Depth profiles of $\%C_{org}$, $\%CaCO_3$ and %Al at all stations.

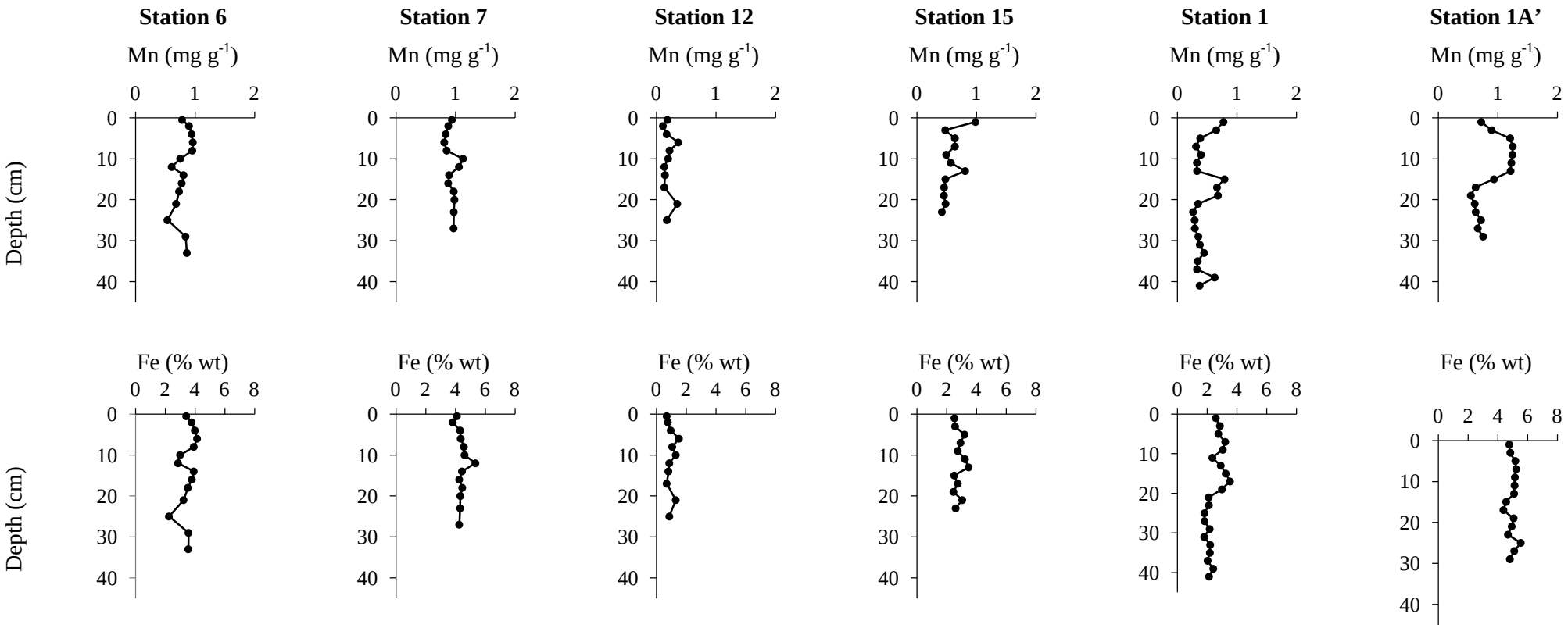

Figure 5.3. Depth profiles of Mn and Fe at all stations.

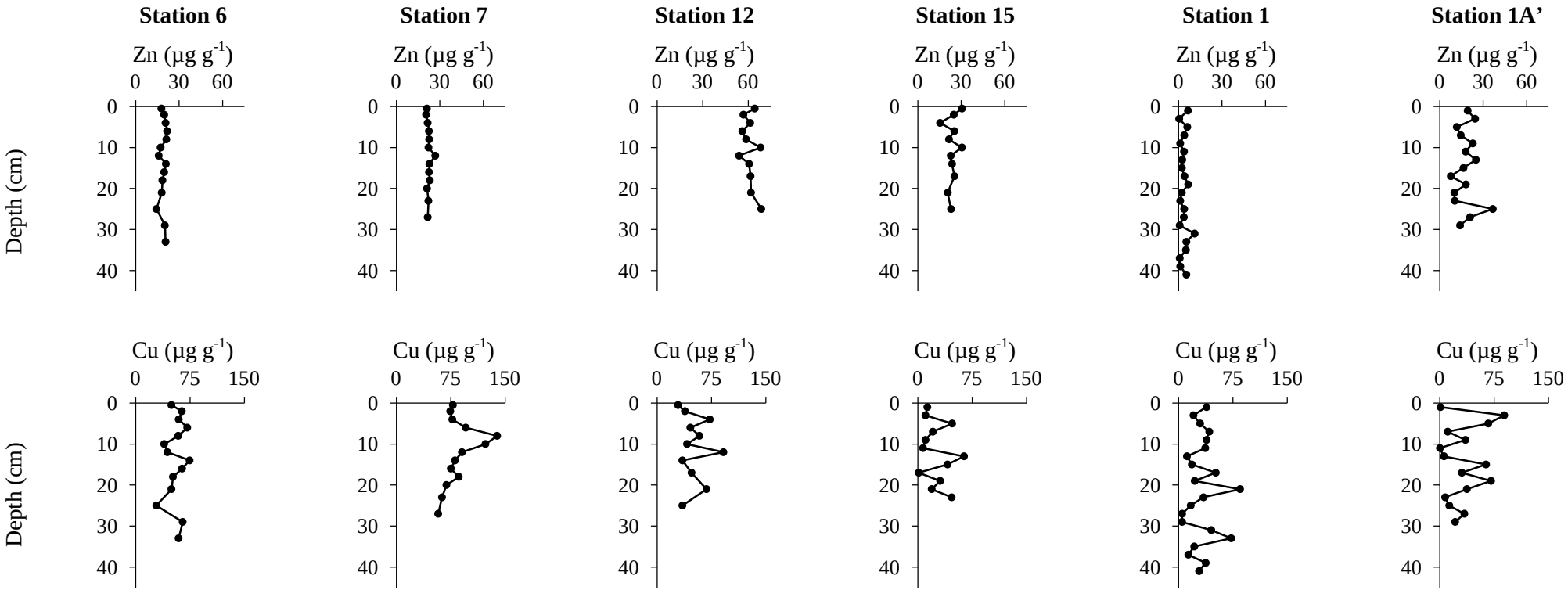

Figure 5.4. Depth profiles of Zn an Cu at all stations.

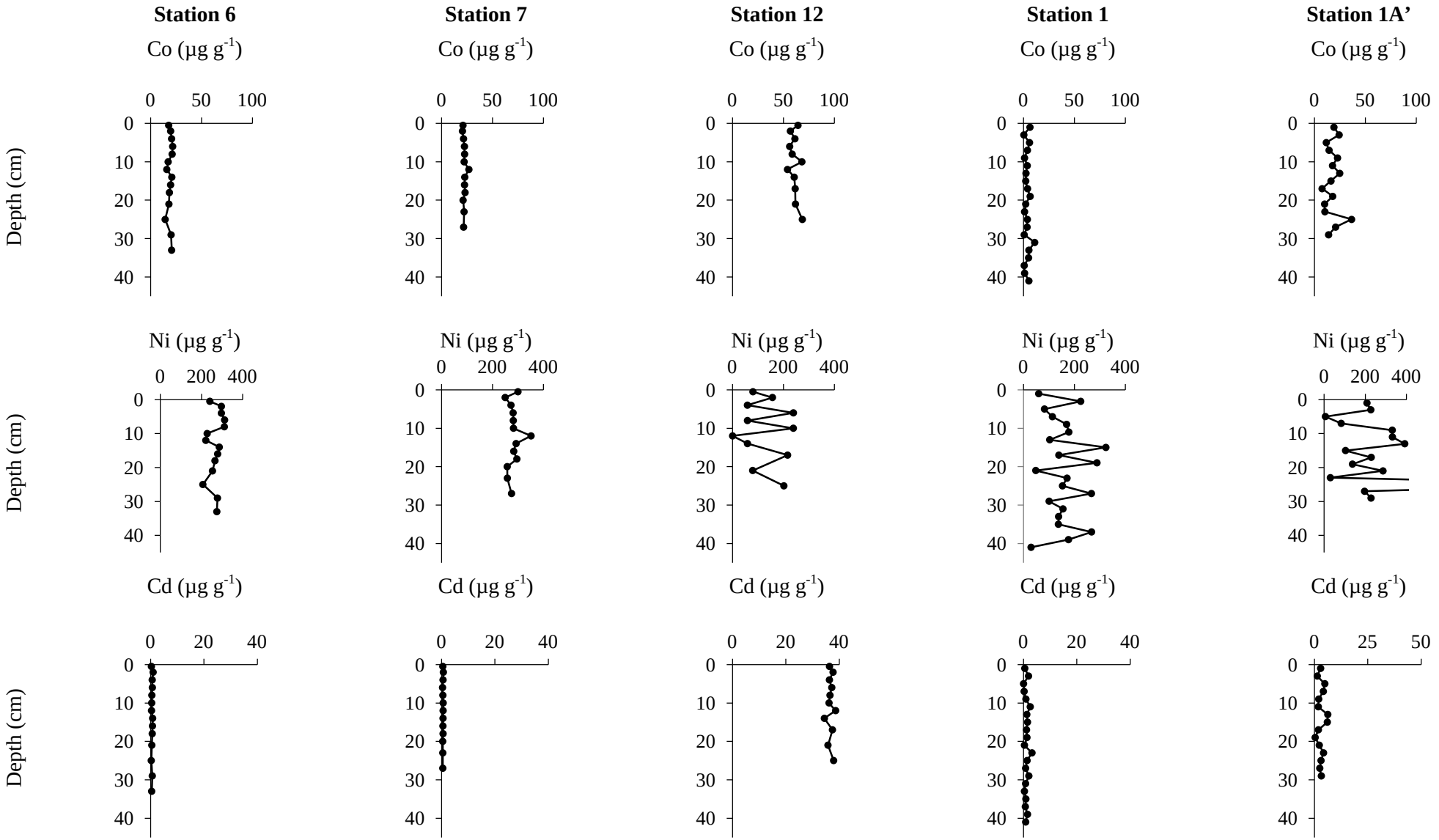

Figure 5.5. Depth profiles of Co, Ni and Cd at all stations except for Station 15 where these elements were below the detection limit. Station 1A’ presents an off-scale value of 1402 µg g^{-1}.

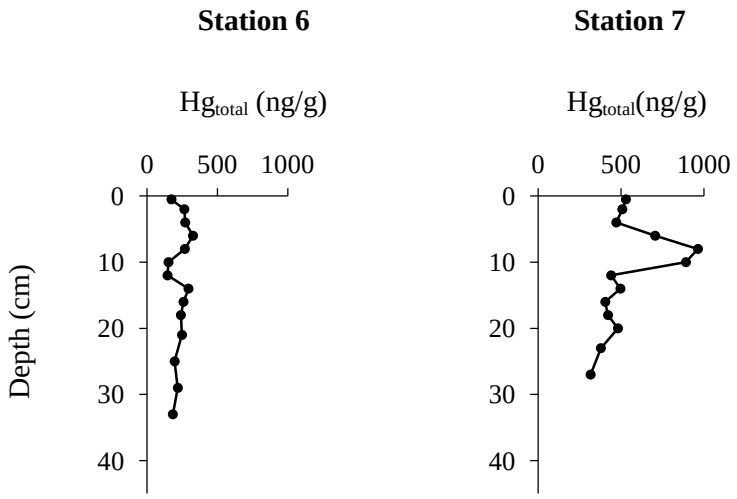

Figure 5.6. Hg profiles at Stations 6 and 7.

5.3.3 Porewaters

Physicochemical characteristics

The salinity in the water column was measured with the CTD sensor and that in the porewater was determined based on the measurement of chloride concentration (Table 5.1, Figure 5.7). Chloride profiles showed a slight decrease of salinity with depth except for Station 6 which revealed a slight increase below the sediment-water interface.

Dissolved species

All profiles of dissolved species were described in Plante et al. (2020a, 2020b, *submitted*) and reported in Figure 5.7 and Figure 5.8. The concentrations of nitrate and nitrite were very low and are not shown.

Oxygen microprofilings (Figure 5.9) showed a rapid decrease of oxygen concentration in the first few cm of the sediments at all stations. During poor-oxygenated event, the oxygen penetration depth (OPD) was shallower than that under well-oxygenated conditions; the OPDs ranged from 0.5 mm at Station 1A' to 4 mm at Station 12.

Alkalinity profiles (Figure 5.7) displayed an increase with depth at all stations except for Station 12. Station 6 exhibited a high alkalinity starting at the sediment-water interface which increased strongly with depth downcore. The gradient at Stations 15 and 1 is high from the

sediment-water interface down to 7 cm and 5 cm depth respectively. At Station 1A' the gradient increased from 13 cm to 23 cm depth and in this depth range the porewaters sampled during the low oxygen period contained more alkalinity than during the oxic period. In general, the sediments were a source of alkalinity for the water column.

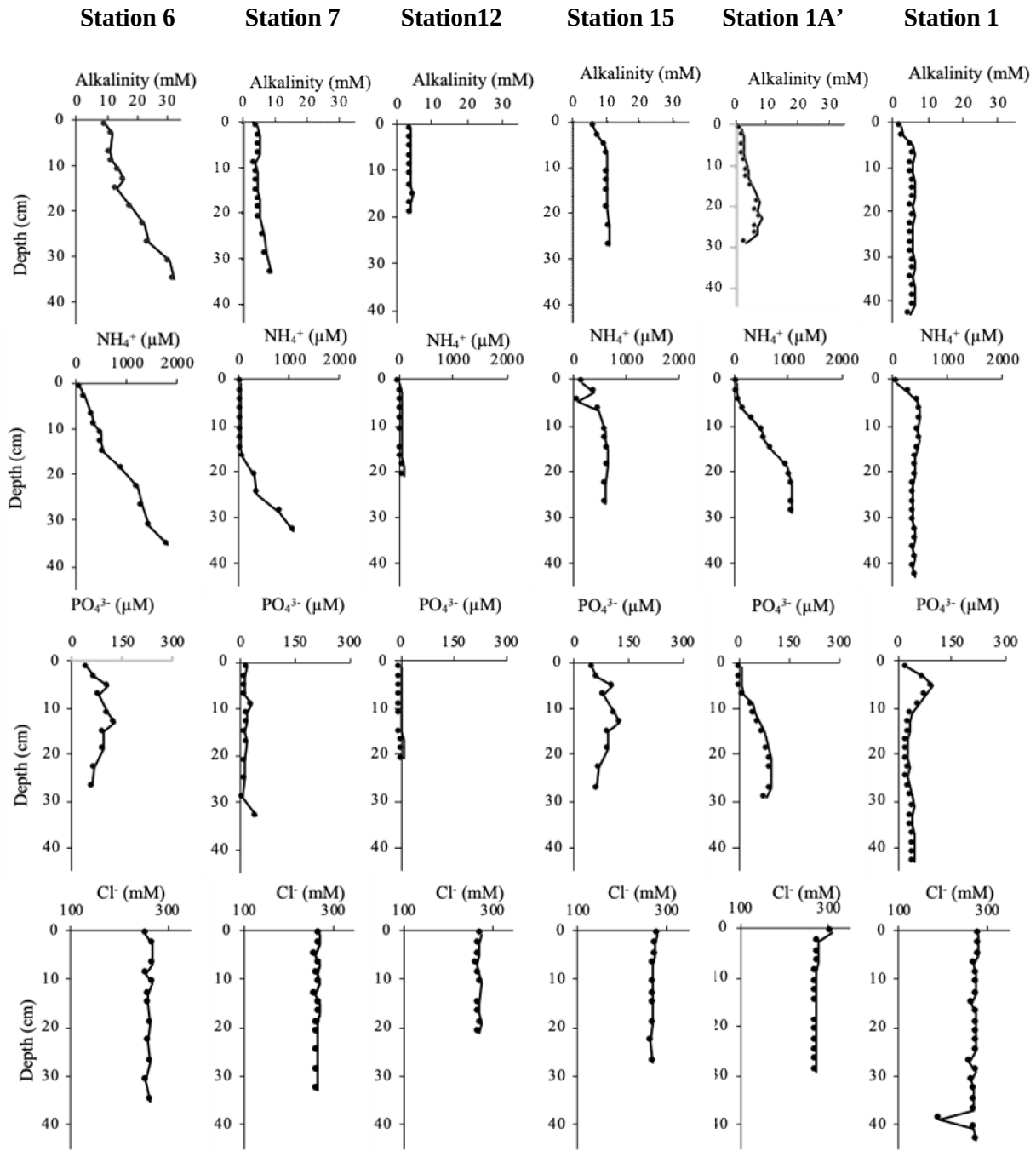

Figure 5.7. Porewater profiles of alkalinity, NH_4^+, PO_4^{3-} and Cl^- for stations sampled in spring 2016 and summer 2017.

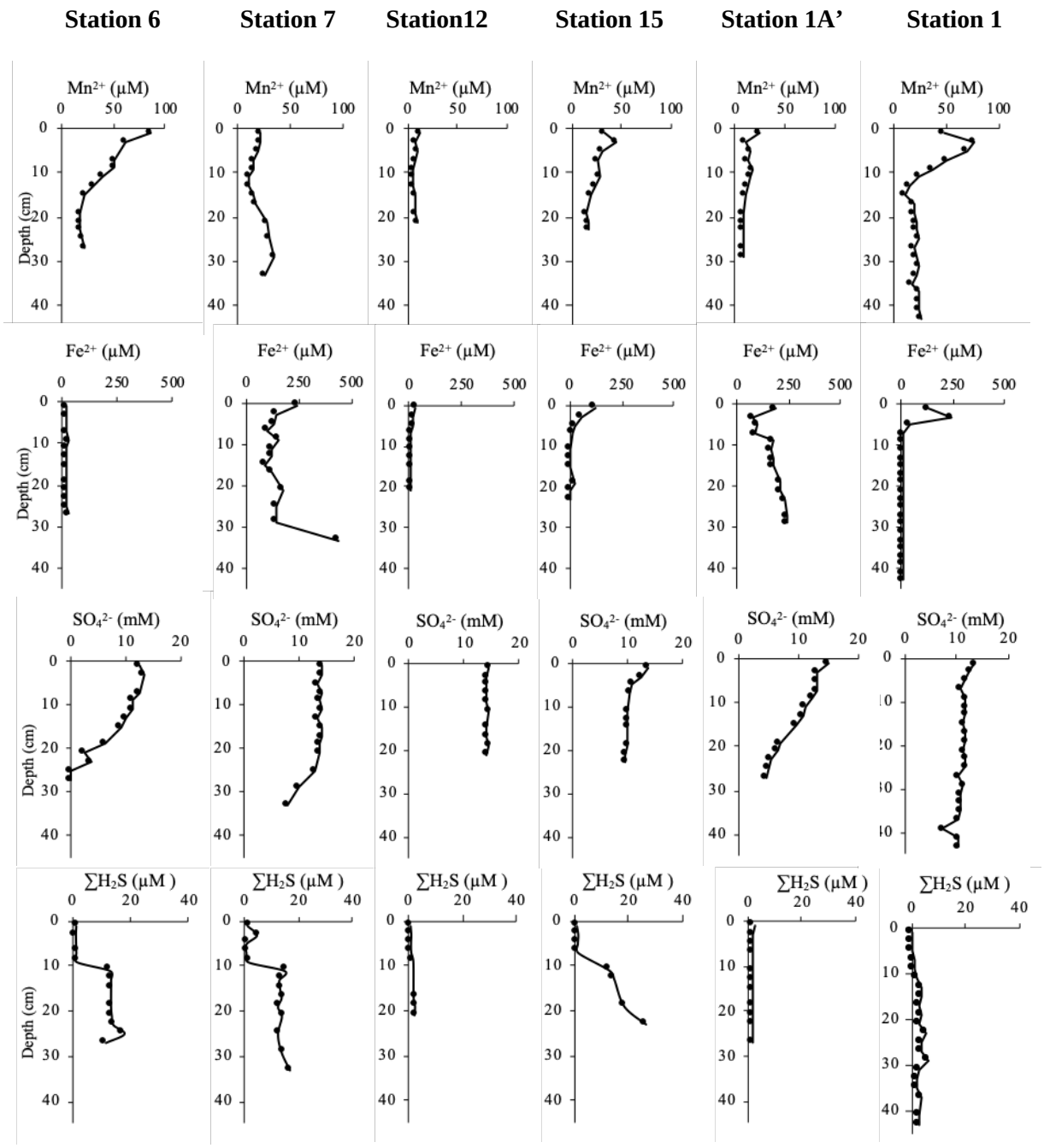

Figure 5.8. Porewater profiles of Mn^{2+}, Fe^{2+}, SO_4^{2-} and total sulphides for stations sampled in spring 2016 and summer 2017.

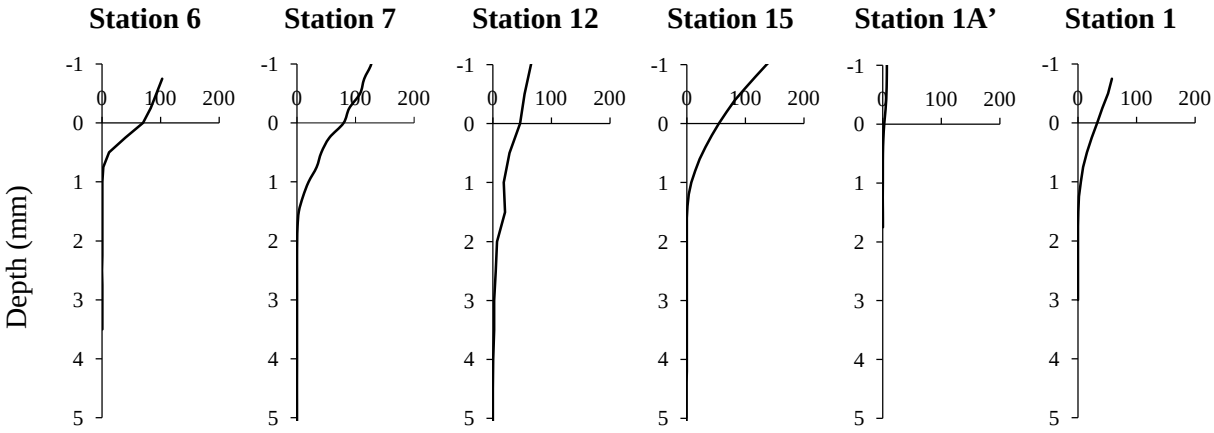

Figure 5.9. Microprofiles of oxygen (μM) at the stations sampled in 2016 and 2017.

The concentrations of PO_4^{3-} and NH_4^+ increased sharply from the sediment-water interface to depth (Figure 5.7), indicating that the sediments constituted a source of these two nutrients for the water column. Higher concentrations were observed at Stations 6, 15, 1A' and 1. Porewaters in surface sediments were depleted in ammonium and phosphates at the Stations 7 and 1A' probably affected by bioturbation and Fe-oxide precipitation.

Dissolved manganese profiles (Figure 5.8) illustrated in general a decreasing trend with depth at all stations. Stations with sediments rich in organic carbon exhibited higher dissolved manganese concentrations. Higher values of dissolved manganese were noted at Station 6 where bottom water was oxygenated.

Dissolved iron profiles showed a decrease with depth at all stations except for Station 1A'. Stations 7 and 15 close to the river mouths exhibited a higher concentration of dissolved iron. Compared to Station 7, porewaters in the surface sediments of Station 1A' sampled during summer displayed higher dissolved Fe concentrations suggesting a higher reduction of iron oxides.

Finally, sulphate profiles revealed a decrease with depth at all stations except for station 12 indicating the occurrence of sulphate reduction (Berner, 1980) with a spatial variation of the sulphate consumption with depth on the shelf. Under low oxygen conditions, the intensity of sulphate reduction appeared to be stronger compared to the oxic period displaying a seasonal effect.

The profiles of ΣH_2S showed an increase with depth at Stations 6, 7 and 15, which corresponds to the decline of sulphate concentrations with depth. But the concentrations of the total sulphides were much less than those of sulphates consumed by sulphate reduction induced by microbial activity.

5.4 Discussion

5.4.1 Identification of diagenetic reactions

Main diagenetic reactions

The main diagenetic reactions, summarised in Table 5.3, refer to the following: (i) primary redox reactions which play a role in the mineralization of the organic matter; (ii) secondary redox reactions involving the products from the primary redox reactions and the remaining oxidants; (iii) non-redox precipitation reactions and (iv) reactions involving trace element mobility in the sediments. The identification of the reactions will be achieved if two species of the considered reaction are present in measurable concentrations at the same depth as suggested by Rigaud et al. (2013).

The organic matter is mineralized following the primary reactions (R1 – R6) described also in Plante et al. (2020a, *submitted*). Stations 6 and 15 followed the classical diagenetic sequence illustrated by Froelich et al. (1979) with dissolved oxygen consumption (within the first 0.1 and 0.2 cm respectively), nitrates reduction (< detection limit, supposed 0 to 1 cm), Mn-oxide reduction (0 to 7 cm and 1 to 5 cm respectively), Fe-oxide reduction (7 to 11 cm and 0 to 5 cm respectively) and sulphates reduction (3 to 13 cm and 7 to 13 cm respectively). Alkalinity can be produced or consumed during diagenesis. The alkalinity profile of Station 6 confirmed the intense diagenesis of organic matter with a strong gradient over the entire depth (Figure 5.7). Moreover, the high concentrations at the sediment-water interface could be attributed to the oxic respiration of organic carbon producing CO_2 which led to the dissolution of $CaCO_3$ present in the sediments. Regarding Station 15, the high intensity of sulphate reduction in the subsurface (upper 7 cm) and it stabilization with depth (Plante et al., 2020a, submitted) could be evidenced by the mirror image of the alkalinity profile. Station profiles determined under oxic conditions, revealed that Mn produced in porewaters diffused downward and might be related to Mn-oxide production, Mn-carbonate precipitation (R23) and/or co-precipitation of carbonates (R31). Mn^{2+} also diffused upward and would be re-oxidized by oxygen (R9)

and/or NO_3^- (R13). The consumption of Fe^{2+}, detected based on the profiles, was rather linked to the precipitation of Fe-oxides in subsurface sediments. Otherwise, Fe^{2+} released by the reduction of Fe-oxides, diffused upward (R4, R19 and R20) which would be re-oxidized to Fe-oxides by Mn-oxides (R17). In deeper sediments, this consumption was rather linked to the formation of Fe sulphides (R25) and could be recognized based on the occurrence of FeS and pyrite (R25, R26), identified at Station 7 by scanning electron microscopy (Robinet, 2019) and detected at Station 6 by XRD (Pyrite: 0.9 % of abundance (Roman Romin, 2017)), and the depletion of sulphate concentration leading to the loss of S in the porewaters.

The sediments of Station 12 were coarser. At this site, the diagenetic reactions could not be illustrated, and only oxygen consumption was evident from the microprofiling (Figure 5.9).

Under low oxygen levels, the oxidant availability for the diagenetic cascade from Froechlich (1979) was contrasting, as highlighted by Stations 1 and 1A'. Since dissolved oxygen and nitrates were limited, the anaerobic processes of this sequence became prevailing. The mineralization of organic matter took place mainly through the reduction of Mn-oxides, Fe-oxides and sulphate leading to the production of Mn^{2+} (R3, R16 and R18) and Fe^{2+} (R4, R19 and R20) and to the consumption of sulphates (R5). The anoxic sediments might be subject to a shallow and rapid consumption of Fe^{2+} contributing to the production of FeS (R25). The precipitation of FeS in the surface sediments could be related to the reduction of Fe-oxides and the precipitation of FeS at the same depth and the reduction kinetics of Fe-oxides is secondary with regard to the kinetics of FeS. This could explain the inversion of the Fe and Mn peaks in the porewater profiles. Surprisingly, Station 7 with oxic bottom waters showed the characteristics reported previously for stations with low oxygen level. The presence of H_2S in surface sediments suggested the precipitation of FeS (R25) at the same depth where Fe was reduced.

Table 5.3. Main diagenetic reactions and reactions involving trace elements (Me2+, FeOOH and MnO2) modified from Rigaud, et al., 2013. (1) Wang and Van Cappellen, 1996; (2) Canavan et al., 2006; (3) Anschutz et al., 2000; (4) Hulth et al., 1999; (5) Boudreau, 1997; (6) Rigaud, et al., 2013.

No	Description	References
Primary redox reactions		
R1	Aerobic respiration: $CH_2O + O_2 \rightarrow CO_2 + H2O$	1,2
R2	Denitrification: $CH_2O + \frac{4}{5}NO_3^- + \frac{4}{5}H^+ \rightarrow CO_2 + \frac{2}{5}N_2 + \frac{7}{5}H_2O$	1,2
R3	MnO_2 reduction: $CH_2O + 2MnO_2 + 4H^+ \rightarrow CO_2 + 2Mn^{2+} + 3H_2O$	1,2
R4	FeOOH reduction: $CH_2O + 4\,FeOOH + 8H^+ \rightarrow CO_2 + 4Fe^{2+} + 7H_2O$	1,2
R5	Sulphates reduction: $CH_2O + \frac{1}{2}SO_4^{2-} + \frac{1}{2}H^+ \rightarrow CO_2 + \frac{1}{2}HS^- + H_2O$	1,2
R6	Methanogenesis: $CH_2O \rightarrow \frac{1}{2}CO_2 + \frac{1}{2}CH_4$	1,2
Secondary redox reactions		
R7	NH_4^+ oxidation by O_2: $NH_4^+ + 2O_2 + 2HCO_3^- \rightarrow NO_3^- + 2CO_2 + 3H_2O$	1,2,3,4
R8	H_2S oxidation by O_2: $H_2S + 2O_2 + 2HCO_3^- \rightarrow SO_4^{2-} + 2CO_2 + 3H_2O$	1,2
R9	Mn^{2+} oxidation by O_2: $Mn^{2+} + \frac{1}{2}O_2 + 2HCO_3^- \rightarrow MnO_2 + 2CO_2 + 2H_2O$	1,2,3
R10	Fe^{2+} oxidation by O_2: $Fe^{2+} + \frac{1}{4}O_2 + 2HCO_3^- + \frac{1}{2}H_2O \rightarrow Fe(OH)_3 + 2CO_2$	1,2
R11	CH_4 oxidation by O_2: $CH_4 + 2O_2 \rightarrow CO_2 + 2H_2O$	1,2
R12	FeS oxidation by O_2: $FeS + 2O_2 \rightarrow Fe^{2+} + SO_4^{2-}$	1,2
R13	Mn^{2+} oxidation by NO_3^-: $5Mn^{2+} + 2NO_3^- + 4H_2O \rightarrow 5MnO_2 + N_2 + 8H^+$	4
R14	Fe^{2+} oxidation by NO_3^-: $5Fe^{2+} + NO_3^- + 12H_2O \rightarrow 5Fe(OH)_3 + \frac{1}{2}N_2 + 9H^+$	4

R15	FeS oxidation by NO_3^-: $5FeS + 8NO_3^- + 8H^+ \rightarrow 5Fe^{2+} + 5SO_4^{2-} + 4N_2 + 4H_2O$	4
R16	NH_4^+ oxidation by MnO_2: $NH_4^+ + 4MnO_2 + 6H^+ \rightarrow 4Mn^{2+} + NO_3^- + 5H_2O$	3,4
R17	Fe^{2+} oxidation by MnO_2: $2Fe^{2+} + MnO_2 + 2HCO_3^- + 2H_2O \rightarrow 2Fe(OH)_3 + Mn^{2+} + 2CO_2$	1,2
R18	H_2S oxidation by MnO_2: $H_2S + 4MnO_2 + 6CO_2 + 2H_2O \rightarrow 4Mn^{2+} + 6HCO_3^- + SO_4^{2-}$	2
R19	NH_4^+ oxidation by $Fe(OH)_3$: $NH_4^+ + 8Fe(OH)_3 + 14H^+ \rightarrow 8Fe^{2+} + NO_3^- + 21H_2O$	3
R20	H_2S oxidation by $Fe(OH)_3$: $H_2S + 8Fe(OH)_3 + 14CO_2 \rightarrow 8Fe^{2+} + 14HCO_3^- + SO_4^{2-} + 6H_2O$	2
R21	CH_4 oxidation by SO_4^{2-}: $CH_4 + CO_2 + SO_4^{2-} \rightarrow 2HCO_3^- + H_2S$	1,2
Precipitation reactions		
R22	$CaCO_3$ precipitation: $Ca^{2+} + 2HCO_3^- \rightarrow CaCO_3 + CO_2 + H_2O$	5
R23	$MnCO_3$ precipitation: $Mn^{2+} + 2HCO_3^- \rightarrow MnCO_3 + CO_2 + H_2O$	1
R24	$FeCO_3$ precipitation: $Fe^{2+} + 2HCO_3^- \rightarrow FeCO_3 + CO_2 + H_2O$	1
R25	FeS precipitation: $Fe^{2+} + 2HCO_3^- + H_2S \rightarrow FeS + 2CO_2 + 2H_2O$	1,2
R26	Pyrite precipitation: $FeS + H_2S \rightarrow FeS_2 + H_2$	2
Reaction involving trace elements		
R27	Trace metal sulphide precipitation: $Me^{2+} + H_2S \rightarrow MeS + 2H^+$	6
R28	Adsorption/coprecipitation on FeS/FeS_2: $Me^{2+} + FeS \rightarrow Me - FeS \; or \; Me^{2+} + FeS_2 \rightarrow Me - FeS_2$	6
R29	Adsorption/coprecipitation $Fe(OH)_3$: $Me^{2+} + Fe(OH)_3 \rightarrow Me{-}Fe(OH)_3$	6
R30	Adsorption/coprecipitation on MnO_2: $Me^{2+} + MnO_2 \rightarrow Me - MnO_2$	6
R31	Adsorption/coprecipitation CO_3^{2-}: $Me^{2+} + CO_3^{2-} \rightarrow Me - CO_3$	6
R32	Adsorption on OM: $Me^{2+} + CH_2O \rightarrow Me - CH_2O$	6

Trace metals reactivity

Zn and Ni concentrations were correlated to the concentrations of Fe in the sediments with R = 0.75 and R = 0.70 suggesting their association with the iron phase. It is possible that these correlations reflect their link to the Fe-oxides (R29) by adsorption and coprecipitation. The behaviour of Ni was in accordance with those observed by Santos-Echeandia et al. (2009) in sediments. Profiles of Ni and Zn displayed similarities to the depth profile of Fe. The remobilization of Zn might occur at the same depth of total Fe which could reinforce their link. Moreover, Cu concentrations presented a slight correlation to Fe with R = 0.54.

Trace elements can be bound to Mn-oxides and participate in the Mn-cycle in the sediments (R30). On the shelf of the Black Sea, Zn and Ni seemed to be integrated in the sedimentary Mn-cycle. Ni was correlated to Mn with R = 0.72 and Zn to Mn with R = 0.77 which might indicate their association by adsorption and co-precipitation to Mn-oxides. The relationship at various depths between Mn in sediments and remobilization of trace elements such as Zn and Ni could support their hypothetic association. Cu concentrations presented a slight correlation to Mn with R = 0.52. Similarities of the profiles were also noted at Stations 6, 7, 12, 15 and 1 for Zn and Mn. Stations 6, 7, 12 (regarding only deeper sediments), 15 and 1 were presumably subject to processes of adsorption and/or co-precipitation with Mn-oxides due to the analogy in their respective depth intervals.

Trace elements often diffuse downward after their remobilization in sediments and are consumed in deeper layers where dissolved sulphides are present. In sulfidic environments, the mobility of these elements is reduced notably due to the formation of insoluble sulphides (Huerta-Diaz et al., 1998; Morse & Luther III, 1999). Thus, their reactions with sulphides are dependant of the oxygen levels in the marine environment. The precipitation of metal sulphides and the adsorption of trace metals onto iron sulphides are the main processes for the formation of metal sulphides. In the sediments of the NW shelf, the decrease of Cu in the solid phase with depth seemed to correspond to an increase of dissolved sulphides in porewaters with depth reflecting possibly the precipitation of solid metal sulphides especially at Station 6. Regarding the other trace elements, no clear correlation was found with sulphides.

5.4.2 Distribution on the shelf

Surface sediments

The continental shelf receives large river inputs impacting the distribution of elements. Two areas were emerging from this study: the Danube river mouth and the northern shelf. The sediments of Stations 6 and 7 exhibited larger contents of Fe, Mn, Ni, Cu and Zn because of the inputs of the Danube river, known as one of the largest rivers in Europe. The main application of Mn is the metallurgy although Mn is also used in agriculture as manganese sulphate. Cu and Zn were often used by industries and architecture, and as alloys. Station 12 received less inputs of these metals compared to Station 15 located close the Dniester mouth. Sediments of Stations 12 and 15 contained more Co and Cd compared to other stations. Cd could be derived from industrial discharges, as some companies used Cd for electroplating, pigment in painting, glass or inks. Although Station 1 received the highest input of organic carbon (Plante, et al., 2020a), it followed the same trend as Stations 12 and 15 for Ni, Cu, Zn, Cd and Fe, and presented the lowest concentration of Co.

Comparing with data obtained in 2016 by Denga et al. (2017), our results were in the same range for Zn and Cu for 2016 and 2017. The concentrations of Cd were higher in 2017 than those obtained by these authors. Nonetheless, our results of Ni were much higher than the concentrations of Denga et al. (2017) varying from 2 to 4.5 times more.

Metal enrichment in sediments

Trace metals are often responsible for the pollution of both the water column and the sediments impacting the living organisms and the biogeochemical cycles. In this study, the single metal enrichment factor (EF) and the geo-accumulation index (Igeo) were used to assess this pollution (Table 5.4 and Table 5.5).

Table 5.4. Enrichment factor (EF) and geo-accumulation index (Igeo) classes of soil quality (Zahra et al., 2014).

EF		**Igeo**	
Classes	**Soil quality**	**Classes**	**Soil quality**
<1	No enrichment	0-1	Unpolluted
1 - <3	Minor enrichment	1-2	Unpolluted to moderately polluted
3 - <5	Moderate enrichment	2-3	Moderately polluted
5 - <10	Moderate severe enrichment	3-4	Moderately to highly polluted
10 - < 25	Severe enrichment	4-5	Highly polluted
25 - <50	Very severe enrichment	5-6	Highly to very highly polluted
>50	Extremely enrichment	>6	Very highly polluted

Enrichment factor (EF)

EF is used to discriminate between natural and anthropogenic sources and reflects the status of environmental contamination. It is based on the use of a normalization element in order to alleviate the variations caused by the heterogeneity of the sediments (Zahra et al., 2014). The reference material for normalization is the average shale (Calvert & Pedersen, 1993). Little et al. (2015) recommended the use of proximal oxic sediments as a correct normalizing lithogenic background because the average shale was not fully representative of the local background deposits. In this study, the normalization was made with respect to the upper continental crust (Rudnick & Gao, 2003) to evaluate the enrichment factors of trace metals in the shelf sediments which were subject to seasonal hypoxia following Eq. 5.1.

$$EF = ([Element]/[Al]\,)_s/([Element]/[Al]\,)_{ref} \qquad \text{(Eq. 5.1)}$$

where $(Element]/[Al])_s$ is the ratio of metal to Al contents in the measured sample and $([Element]/[Al])_{ref}$ is that in the upper continental crust.

According to the classification of Taylor (1964, Table 5.4), the EF values for each metal in the sediments of the various stations investigated were interpreted and reported inTable 5.5. The results revealed that some metals such as Fe (except for Stations 1), Mn at Station 12, Co (except for Stations 6, 12 and 15), Cu at Stations 15 and 1A' and Zn at Station 15 were ≤ 1, indicating that the surface sediments of the shelf were not enriched in these metals.

Table 5.5. Values and classes of enrichment factor and Igeo of the metals in the sediments of the various stations investigated. N.A.: not available.

Station	**6**	**7**	**12**	**15**	**1**	**1A'**
			EF			
Mn	1.3	1.1	0.8	1.1	1.1	1.2
Co	1.0	0.9	8.1	1.6	0.3	0.7
Ni	5.7	4.7	7.1	N.A.	4.5	3.1
Cu	2.0	2.9	4.3	0.8	2.0	0.9
Zn	2.5	2.2	2.3	1.0	1.3	1.5
Cd	5.2	4.0	827.6	N.A.	14.7	19.6
Fe	0.9	0.9	0.7	0.9	1.1	1.0
			Igeo			
Mn	0	0	-2.1	-0.5	-0.9	0.3
Co	-0.4	-0.2	1.3	-0.1	-2.8	-0.5
Ni	2.1	2.1	1.1	N.A.	1.1	1.6
Cu	0.6	1.4	0.3	-1.0	-0.1	-0.2
Zn	0.9	1.0	-0.5	-0.7	-0.8	0.6
Cd	2.0	1.8	7.9	N.A.	2.8	4.3
Fe	-0.5	-0.3	-2.3	-0.9	-0.9	-0.1

For Cd, the EF values at all stations, except for Station 12, were comprised between 4.0 and 19.6 indicating that the sediments were moderately to severely enriched in this metal. In general, sediments from stations receiving the Danube inputs were subject to lower pollution and those from the northern shelf would be more impacted by Cd enrichment. Station 12 exhibited the highest level of Cd enrichment, considerably higher than 50, indicating an extreme enrichment pointing towards a strong pollution by anthropogenic activities. The results also showed that the sediments of Stations sampled in summer 2017 were more enriched in Cd, suggesting the formation of Cd-sulphides under low oxygen conditions.

The EF values for Fe and Co ranged from 0 to 1 at all Stations except for Station 1 and Stations 12 and 15 which indicate no enrichment in the sediments. The EF values for Mn, Zn, Cu (except for Station 15) in most of stations were in the range of 1 - 3 revealing a minor enrichment in the sediments. For Ni, the range was from 3 to 5 at all Stations except for Station 12 implying a moderate enrichment of the sediments. Station 12 exhibited the highest EF values for Co, Ni, Cu and Cd and showed the lowest numbers for Mn and Fe.

Secrieru and Secrieru (2002) revealed that Zn, Cu and Cd represented the main pollutants in 1995 for the stations close to the Danube Delta and Co and Cd for the stations close to the Dniester river, in agreement with the results of this study for which the sampling was carried out in 2016-2017. The authors estimated using another equation, an enrichment of 7 % for Ni, 108 % for Co, 51 % for Cu, 76 % for Zn and 213 % for Cd. Since 1996, the sediments of NW shelf of the Black Sea seemed to be strongly enriched in cadmium.

Geo-accumulation index (Igeo)

Another assessment criterion of metallic contamination is the geo-accumulation index as defined by Müller (1969) for the Rhine River. The factor compares a given concentration for a specific metal to a lithogenic reference value of this metal. A coefficient of 1.5 (correction factor) is applied to take into account any variations which could occur in the background level due to the lithologic effects. Igeo is calculated following Eq. 5.2:

$$Igeo = log_2\left(\frac{C_x}{1.5 \times Bg_n}\right) \qquad \text{(Eq. 5.2)}$$

where C_x is the measured concentration of the element x and Bg is the geochemical background of this element.

Müller (1981) defined a scale of six classes of Igeo reported in Table 5.4 and the results of this study were interpreted according to these classes. The Igeo values reported in Table 5.5indicated that Mn, Co (except for Station 12), Cu (except for Station 7), Zn (except for Station 7) and Fe fell in the category of ‘no pollution’ with values lower than 1. Igeo results for Stations 6 and 7 in the case of Ni, Zn (only Station 7) and Cu (only Station 7) were comprised between 1 and 3 revealing a moderate pollution. Station 1A’ was moderately polluted in Ni. Station 12 was part of the moderately polluted class for Co and Ni. For Cd, a spatial variation was observed on the shelf fluctuating between moderately polluted and very

high polluted; Stations 6 and 7 belonged to the class moderately polluted, Station 1 moderate to strongly polluted, Station 1A' highly polluted and Station 12 very highly polluted category. These results evidenced that the sediments on the northern shelf were highly contaminated by cadmium whereas those near the Danube river mouth were rather polluted by Zn, Cu and Ni, as suggested by Secrieru & Secrieru (2002).

Temporal evolution

Over times, modernisation and industrialisation have improved and river discharges have fluctuated transporting heavy metals in various concentrations to the sea. Data reported in previous studies allow the follow-up of pollution assessment of these metals in the surface sediments at several locations of the shelf. Berlinskyi et al. (2016) focused on sediments from the Danube delta whereas Dyatlov (2015) put emphasis of his work on the Odessa region. Secrieru & Secrieru (2002) presented average values with statistics of their measurements of the sediments over the entire shelf. Combining the data obtained near the Danube delta area from previous studies with the results of this study revealed a strong increase in the metallic pollutant contents in the shelf sediments from the 2000s (Figure 5.10). After 1997, the pollution status of sediments improved for the concentrations of Cu, Cd, Ni and Zn. The contents of Cu, Ni and Zn were the highest in 2016; a slight improvement could be noted for the surface sediments sampled in 2017 although the pollutant concentrations were still high. Secrieru & Secrieru (2002) estimated normal background values for the shelf sediments of the Black sea for several metals (22.40 µg g^{-1} for Cu, 48.85 µg g^{-1} for Ni, 9.82 µg g^{-1} for Co, 69.93 µg g^{-1} for Zn and 0.26 µg g^{-1} for Cd) which serve as threshold for heavy metal enrichment. Comparing with these threshold values, the surface sediments sampled in 2016 and 2017 were enriched in Cu, Cd, Ni, Zn and Co, consistent with the results of EF, except for Co.

Dyatlov (2015) demonstrated a temporal variation of heavy metal pollution in the sediments of the Odessa region, particularly for Ni and Cu closely linked to the grape agriculture. In 2017, the level of Cu increased strongly exceeding the threshold value defined by Secrieru & Secrieru (2002) which could be attributed to the bad weather leading to increasing runoff the week before sampling (Figure 5.11). Ni levels have remained stable since 2010 but a strong increase could be noted in 2017. The data available showed that the Odessa region was not affected by pollution of Zn whose contents were more or less stable below the threshold value.

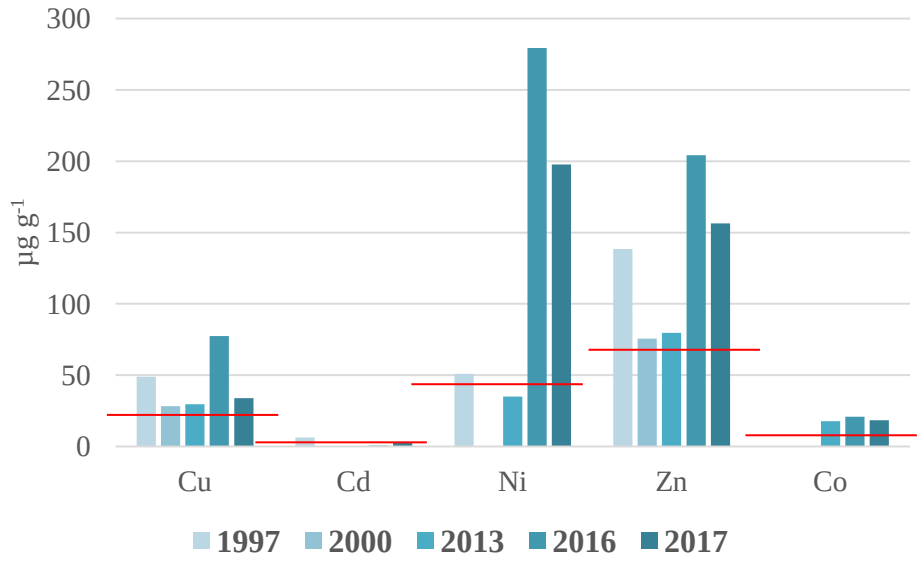

Figure 5.10. Temporal evolution of heavy metal pollution (Cu, Cd, Ni, Zn and Co) in the sediments near the Danube river mouth. Data for the years 1997, 2000 and 2013 were from Berlinskyi et al. (2016). Data from this study were used for the year 2016 (Stations 6 and 7) and for the year 2017 (Station 1A') The red lines represent the threshold values estimated by Secrieru & Secrieru (2002).

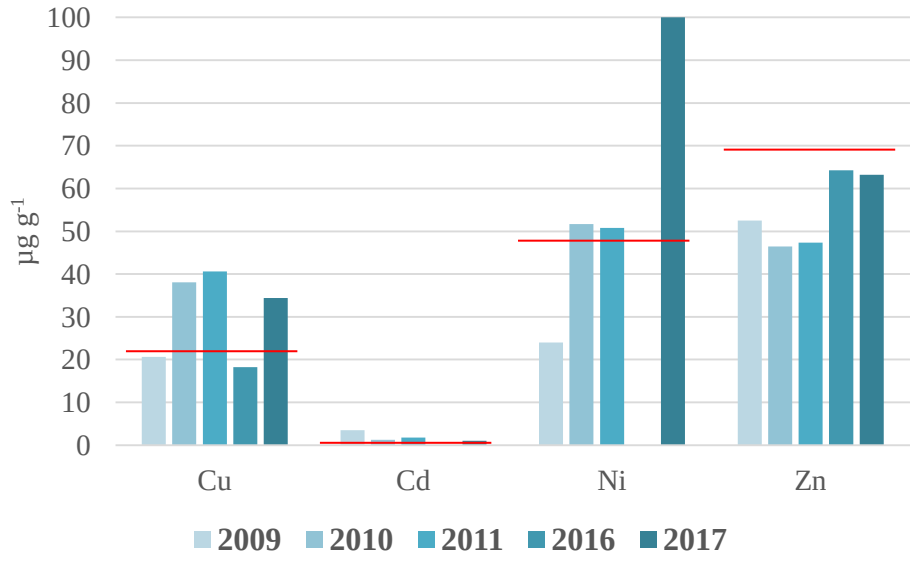

Figure 5.11. Temporal evolution of heavy metal pollution (Cu, Cd, Ni and Zn) in the sediments in the Odessa region. Data for the years 2009, 2010 and 2011 were from Dyatlov (2015). The results of this study were used for the year 2016 (Station 15) and for the year 2017 (Station 1). Data of Dyatlov (2015) were used for the years 2009, 2010 and 2011. The red lines represent the threshold values estimated by Secrieru & Secrieru (2002).

5.5 Conclusions

The combined results obtained with microsensors, porewater analysis and solid phase analysis allowed the assessment and identification of some diagenetic reactions regulating the mobility of metals (Mn, Fe, Ni, Zn, Cu, Cd, Co and Hg) under oxic and low oxygen conditions. Ni and Zn could be involved in adsorption onto and co-precipitation with Fe oxides and Mn oxides. Reactions with sulphides were suggested for Cu but no clear correlation was found. When Fe and Mn oxyhydroxides are reduced, the remobilization of trace elements occurs but the presence of sulphides may prevent this remobilization, which depends on the kinetics of the reactions. At low oxygen levels, Fe and Mn oxides are reduced directly below the sediment-water interface releasing metals in the dissolved phase which could be diffused from the sediments to the water column or could likely react with sulphides due to the competition between remobilization and trapping.

The distribution of trace metals in the shelf sediments exhibited spatial variations. The Danube delta sediments were enriched in Ni, Cu and Zn whereas the Odessa region in Co and Cd. This heterogeneity could be explained by the various land uses, in particular agriculture and industries. The Igeo index allowed the assessment of the quality sediments which were contaminated at different scales ranging from unpolluted to very highly polluted. Results of EF and Igeo were consistent with previous studies. Comparison of our data with those reported since the late 20^{th} century allowed the evaluation of the variability over times showing an increase of metallic pollutant contents in shelf sediments especially close to the Danube river mouth. The results of Odessa region were stable for Cu and Cd.

References

Archer, D., & Devol, A. (1992). Benthic oxygen fluxes on the Washington shelf and slope: a comparison of in-situ micro electrode and flux chamber measurements. Limnol. Oceanogr., 37, 614–629.

Berlinskyi, N., & Safranov, T. (2016). Spatial and temporal variability of in the bottom sediments in the Northwest part of the Black Sea. Environmental Problems, 1, 73-76.

Berner, R. A. (1980). Early Diagenesis: A theoritical approach. Princeton University Press.

Berner, R. A. (1982). Burial of Ogranic Carbon and Pyrite sulfur in the modern ocean: Its geochemical and envrionmental significance. Am. J. Sci., 282, 451-473.

Borowski, W. S., Paull, C. K., & Ussler, W. (1999). Global and local variations of interstitial sulfate gradients in deep-water, continental margin sediments: Sensitivity to underlying methane and gas hydrates. Marine Geology, 159, 131-154.

Boudreau, B. P. (1996). The diffusive tortuosity of fine-grained unlithified sediments. Geochim. Cosmochim. Acta, 60, 3139-3142.

Brady, D. C., Testa, J. M., Di Toro, D. M., Boynton, W. R., & Kemp, W. M. (2013). Sediment flux modeling: Calibration and application for coastal systems. Estuar. Coast. Shelf Sci., 117, 107-124.

Brumsack, H. J. (2006). The trace metal content of recent organic carbon-rich sediments: implications for Cretaceous black shale formation. Palaeogeogr. Palaeoclimatol. Palaeoecol., 232, 344–361.

Burdige, D. (2006). Geochemistry of Marine Sediments. Princeton University Press.

Burton, E. D., Sullivan, L. A., Bush, R. T., Johnston, S. G., & Keene, A. F. (2008). A simple and inexpensive chromium-reducible sulfur method for acid-sulfate soils. Applied Geochemistry, 23, 2759–2766.

Caccia, V. G., Millero, F. J., & Palanques, A. (2003). The distribution of trace metals in Florida Bay sediments. Mar. Pollut. Bull., 1420–1433.

Cai, W.-J., & Sayles, F. L. (1996). Oxygen penetration depths and fluxes in marine sediments. Marine Chemistry, 52, 123-131.

Calvert, S. E., & Pedersen, T. F. (1993). Geochemistry of Recent oxic and anoxic marine sediments: Implications for the geological record. Mar. Geol., 113, 67-88.

Canfield, D. E. (1994). Factors influencing organic carbon preservation in marine sediments. Chem. Geol., 114, 315–329.

Canfield, D. E., Jorgensen, B. B., Fossing, H., Glud, R., Gundersen, J., Ramsing, N. B., . . . Hall, P. O. (1993). Pathways of organic carbon oxidation in three continental margin sediments. Marine Geology, 113, 27-40.

Capet, A., Beckers, J.-M., & Gregoire, M. (2013). Drivers, mechanisms and long-term variability of seasonal hypoxia on the Black Sea northwestern shelf – is there any recovery after eutrophication? Biogeosciences, 10, 3943–3962.

Cline, J. D. (1969). Spectrophotometric determination of hydrogen sulfide in natural waters. Limnology and Oceanography, 14, 454-458.

Cociasu, A., Dorogan, L., Humborg, C., & Popa, L. (1996). Long-term ecological changes in the Romanian coastal waters of the Black Sea. Marine Pollution Bulletin, 32, 32-38.

Conley, D. J., Carstensen, J., Ærtebjerg, G., Christensen, P. B., Dalsgaard, T., Hansen, J. L., & Josefson, A. B. (2007). Long-term changes and impacts of hypoxia in Danish coastal waters. Ecol. Appl., 17, 165-184.

Crusius, J., Calvert, S., Pedersen, T., & Sage, D. (1996). Rhenium and molybdenum enrichments in sediments as indicators of oxic, suboxic and sulfidic conditions of deposition. Earth Planet. Sci. Lett., 145, 65–78.

Dauwe, B., Middelburg, J. J., & Herman, P. M. (2001). Effect of oxygen on the degradability of organic matter in subtidal and intertidal sediments of the North Sea area. Mar. Ecol. Prog. Ser., 215, 13–22.

Dean, W. E. (1974). Determination of carbonate and organic matter in calcareous sediments and sedimentary rocks by loss of ignition: comparison with other methods. J. of Sedimentary Petrology, 44, 242-248.

Denga, Y., Orlova, I., Komorin, V., Oleynik, Y., Korshenko, A., Hushchyna, K., . . . Zhugailo. (2017). National Pilot Monitoring Studies & Joint Open Sea Surveys in Georgia, Russian Federation and Ukraine, 2016.

Devol, A. H., & Christensen, J. P. (1993). Benthic fluxes and nitrogen cycling in sediments of the continental margin of the eastern North Pacific. J. Mar. Res., 51, 345–372.

Diaz, R. J., & Rosenberg, R. (2008). Spreading dead zones and consequences for marine ecosystems. Science, 321, 926-929.

Dyatlov, S. Y. (2015). Heavy metals in water and bottom sediments of Odessa region of the Black sea. Journal of shipping and ocean engineering, 5, 51-58.

Emili, A., Koron, N., Covelli, S., Faganeli, J. A., Acquavita, A., Predonzani, S., & Vittor, C. D. (2011). Does anoxia affect mercury cycling at the sediment–water interface in the Gulf of Trieste (northern Adriatic Sea)? Incubation experiments using benthic flux chambers. Appl. Geochem., 26, 194–204.

Friedrich, J., Dinkel, C., Friedl, G., Pimenov, N., wijsman, J., Gomoiu, M.-T., . . . Wehrli, B. (2002). Benthic nutrient cycling and diagenetic pathways in the North-western Black Sea. Estuarine, Coastal and Shelf Science, 54, 369-383.

Froelich, P. N., Klinkhammer, G. P., Bender, M. L., Luedtke, N. A., Heath, G. R., Cullen, D., . . . Hartman, B. (1979). Early oxidation of organic matter in pelagic sediments of the eastern equatorial Atlantic: suboxic diagenesis. Geochim. Cosmochom., 43, 1075-1090.

Glud, R. N. (2008). Oxygen dynamics of marine sediments. Mar. Biol., 4, 243-289.

Almazov, N. M. (1961). Stok ratverennykh soley I biogennykh veschetv kotorye vynoseatsya rekami USSR v Chernoe More. Naukovi Zapiski Odes. Biol. St. Kiev, 99-107.

Glud, R. N., Gundersen, J. K., Roy, H., & Jorgensen, B. B. (2003). Seasonal dynamics of benthic O2 utpake in a semienclosed bay: Importance of diffusion and faunal activity. Limnol. Oceanogr., 48, 1265-1276.

Grasshoff, K., Ehrhardt, M., & Kremling, K. (1983). Methods of Seawater Analysis. Weinheim: Verlag Chemie.

Gray, J. S., Wu, R. S., & Or, Y. Y. (2002). Effect of hypoxia and organic enrichment on the coastal marine environment. Marine Ecology Progress Series, 238, 249-279.

Grégoire, M., & Soetaert, K. (2010). Carbon, nitrogen, oxygen and sulfide budgets in the Black Sea: A biogeochemical model of the whole water column coupling the oxic and anoxic parts. Ecological Modelling, 221, 2287–2301.

Hedges, J. I., & Keil, R. G. (1995). Sedimentary organic matter preservation: an assessment and speculative synthesis. Authors' closing comments. Mar. Chem., 49, 137-139.

Hollweg, T. A., Gilmour, C. C., & Mason, R. P. (2009). Methylmercury production in sediments of Chesapeake Bay and the mid-Atlantic continental margin. Mar. Chem., 114, 86–101.

Holmes, R. M., Aminot, A., Kérouel, R., Hooker, B. A., & Peterson, B. J. (1999). A simple and precise method for measuring ammonium in marine and freshwater ecosystems. Can. J. fish. Aqua. Sci., 56, 1801-1808.

Huerta-Diaz, M. A., Tessier, A., & Carignan, R. (1998). Geochemistry of trace metals associated with reduced sulfur in freshwater sediments. Appl. Geochem., 114, 213–233.

Ip, C. C., Li, X. D., & Zhang, G. (2007). Trace metal distribution in sediments of the Pearl River Estuary and the surrounding coastal area, South China. Environ. Pollut., 147, 311–323.

Jacobs, L., & Emerson, S. (1982). Trace metal solubility in an anoxic fjord. Earth and Planetary Sci. Lett., 60, 237-252.

Jorgensen, B. B. (1977). The sulfur cycle of a coastal marine sediment (Limfjorden). Limnol. Oceanogr., 22, 814-832.

Jorgensen, B. B. (1982). Mineralization of organic matter in the sea bed – the role of sulphate reduction. Nature, 296, 643–645.

Jorgensen, B. B., & Revsbech, N. P. (1985). Diffusive boundary layers and the oxygen uptake of sediments and detritus. Limnology and Oceanography, 30, 111-122.

Jorgensen, B. B., & Sorensen, J. (1985). Seasonal cycles of O2, NO3- and SO42- reduction in estuarine sediments: the significance of an . Marine Ecology Progress Series, 24, 65-74.

Jorgensen, B. B., Weber, A., & Zopfi, J. (2001). Sulfate reduction and anaerobic methane oxidation in Black Sea sediments. Deep Sea REsearch Part I: Oceanographic Research Papers, 48, 2097-2120.

Kemp, W. M., Boynton, W. R., Adolf, J. E., Boesch, D. F., Boicourt, W. C., Brush, G., . . . St. (2005). Eutrophication of Chesapeake Bay: historical trends and ecological interactions. Marine Ecology Progress Series, 303, 1-29.

Kemp, W. M., Sampou, P., Caffrey, J., Mayer, M., Henriksen, K., & Boynton, W. R. (1990). Ammonium recycling versus denitrification in chesapeake bay sediments. Limnol. Oceanogr., 35, 1545– 1563.

Kemp, W. M., Testa, J. M., Conley, D. J., Gilbert, D., & Hagy, J. D. (2009). Temporal responses of coastal hypoxia to nutrient loading and physical controls. Biogeosciences, 6, 2985-3008.

Kraal, P., Burton, E. D., & Bush, R. T. (2013). Iron monosulfide accumulation and pyrite formation in eutrophic estuarine sediments. Geochim. et Cosmochim. Acta, 122, 75–88.

Kristensen, E. (2000). Organic matter diagenesis at the oxic/anoxic interface in coastal marine sediments, with emphasis on the role of burrowing animals. In G. Liebezeit, S. Dittmann, & I. Kröncke (Eds.), Life at interfaces and under extreme conditons (Vol. 151, pp. 1-24). Springer, Dordrecht.

Liaghati, T., Preda, M., & Cox, M. (2004). Heavy metal distribution and controlling factors within coastal plain sediments, Bells Creek catchment, southeast Queensland, Australia. Environ. Int., 29, 935–948.

Lichtschlag, A., Donis, D., Janssen, F., Jessen, G. L., Holtappels, M., Wenzhöfer, F., . . . Boetius, A. (2015). Effects of fluctuating hypoxia on benthic oxygen consumption in the Black Sea (Crimean shelf). Biogeosciences, 12, 5075–5092.

Little, S. H., Vance, D., Lyons, T. W., & McManus, J. (2015). Controls on trace metal authigenic enrichment in reducing sediments: Insights from modern oxygen-deficient settings. Am. J. Sci., 315, 77-119.

LOICZ. (1995). Implementation Plan 1995. Global Change IGBP Report No. 33.

McCarthy, J. J., Yilmaz, A., Coban-Yildiz, Y., & Nevins, J. L. (2007). Nitrogen cycling in the offshore waters of the Black Sea. Estuar. Coast. Shelf Sci., 74, 493-514.

McCarthy, M. J., McNea, K. S., Morse, J. W., & Gardner, W. S. (2008). Bottom-water hypoxia effects on sediment-water interface nitrogen transformations in a seasonally hypoxic, shallow bay (Corpus christi bay, TX, USA). Estuar. Coasts, 31, 521–531.

McLennan, S. M. (2001.). Relationships between the trace element composition of sedimentary rocks and upper continental crust. Geochem. Geophys. Geosyst., 2.

Meyers, P. A. (1994). Preservation of elemental and isotopic source identification of sedimentary organic matter. Chemical Geology, 114, 289-302.

Middelburg, J. J., & Levin, L. A. (2009). Coastal hypoxia and sediment biogeochemistry. Biogeosciences, 6, 1273-1293.

Moodley, L., Middelburg, J. J., Herman, P. M., Soetaert, K., & Lange, G. J. (2005). Oxygenation and organic-matter preservation in marine sediments: Direct experimental evidence from ancient organic carbon-rich deposits. Geology, 33, 889–892.

Morford, J. L., & Emerson, S. (1999). The geochemistry of redox sensitive trace metals in sediments. Geochim. Cosmochim. Acta, 63, 1735–1750.

Morse, J. W., & Eldridge, P. M. (2007). A non-steady state diagenetic model for changes in sediment biogeochemistry in response to seasonally hypoxic/anoxic conditions in the ‘‘dead zone’’ of the Louisiana shelf. Mar. Chem., 106, 239–255.

Morse, J. W., & Luther III, G. W. (1999). Chemical influences on trace metal–sulfide interactions in anoxic sediments. Geochim. Cosmochim. Acta, 63, 3373–3378.

Müller, G. (1969). Index of geoaccumulation in sediments of the Rhine River. Geology Journal, 109-118.

Müller, G. (1981). The heavy metal pollution of the sediments of Neckars and its tributary: a stock taking. Chemical Zeitung, 105, 157-164.

Nriagu, J. P. (1988). Quantitative assessment of worldwide contamination of air, water and soils by trace metals. Nature, 134–139.

Olson, L. Q. (2017). Trace metal diagenesis in sulfidic sediments: insights from Chesapeake Bay. Chem. Geol., 452, 47–59.

Panin, N., & Jipa, D. (2002). Danube river sediment input and its interaction with the Northwestern Black Sea. Estuar. Coast. Shelf Sci., 54, 551–562.

Plante, A., Capet, A., Roevros, N., Grégoire, M., Fagel, N., & Chou, L. (2020a). Impact of bottom hypoxia on the diagenetic processes and benthic fluxes on the North-western shelf of the Black Sea.

Plante, A., Capet, A., Roevros, N., Grégoire, M., Fagel, N., & Chou, L. (2020b). Sulphur and iron biogeochemical cycling in the surface sediments during a seasonal hypoxia.

Popa, A. (1993). Liquid and Sediment Inputs of the Danube River into the North-Western Black Sea. Transport of carbon and nutrients in lakes and estuaries, (Part 6). pp. 137–149.

Rabouille, C., Denis, L., Dedieu, K., Stora, G., Lansard, B., & Grenz, C. (2003). Oxygen demand in coastal marine sediments: comparing in situ microelectrodes and laboratory core incubations. Journal of Experimental Marine Biology and Ecology, 285, 49-69.

Riedel, G. F., Sanders, J. G., & Osman, R. W. (1997). Biogeochemical control on the flux of trace elements from estuarine sediments: water column oxygen concentrations and benthic infauna. Estuar. Coast Shelf Sci. 44, . 23–38.

Rigaud, S., Radakovitch, O., Couture, R.-M., Deflandre, D., Cossa, D., Garnier, C., & Garnier, J.-M. (2013). Mobility and fluxes of trace elements and nutrients at the sediment–water interface of a lagoon under contrasting water column oxygenation conditions. Applied Geochemistry, 31, 35–51.

Robinet, S. (2019). Hypoxie au cours de l'Holocène sur la plateforme NW de la mer Noire - traceurs géochimiques. Université de Liège, Liège, Belgique: Unpublished master's thesis.

Roman Romin, O. (2017). Sedimentological, geochemical and biological proxies as indicators for hypoxia in the northwestern-shelf of the Black Sea (BENTHOX project). Université de Liège, Liège, Belgique: Unpublished master's thesis.

Rudnick, R. L., & Gao, S. (2003). Composition of the continental crust (Vol. 3). Amsterdam: Elsevier.

Salomons, W., & Forstner, U. (1984). Metals in the Hydro Cycle. Berlin: Springer Verlag.

Salomons, W., Rooij, N. M., Kerdijk, H., & Bril, J. (1987). Sediments as a source for contaminants? Hydrobi01ogi, 149, 13- 30.

Santos-Echeandia , J., Prego, R., Cobelo-GarcÌa, A., & Millward, G. E. (2009). Porewater geochemistry in a Galician Ria (NW Iberian Peninsula): implications for benthic fluxes of dissolved trace elements (Co, Cu, Ni, Pb, V, Zn). Mar. Chem., 117, 77–87.

Sarazin, G., Michard, G., & Prevot, F. (1999). A rapid and accurate spectroscopic method for alkalinity measurment in sea water samples. Water Ressources, 33, 290-294.

Schulz, H. D., & Zabel, M. (2006). Marine Geochemistry (2nd edition ed.). Springer.

Secrieru, D., & Secrieru, A. (2002). Heavy metal enrichment of man-made origin of superficial sediment on the continental shelf of the North-western Black Sea. Estuarine, Coastal and Shelf Science, 54, 513–526.

Shaw, T. J., Gieskes, J. M., & Jahnke, R. A. (1990). Early diagenesis in differing depositional environments: the response of transition metals in pore water. Geochim. Cosmochim., 54, 1233–1246.

Soetaert, K., Herman, P. M., & Middelburg, J. J. (1996). A model of early diagenetic processes from the shelf to abyssal depths. Geochim. Cosmochim. Acta., 60, 1019-1040.

Sooetaert, K., Petzoldt, T., & Meysman, F. J. (2010a). marelac: Tools for Aquatic Sciences R package version 2.1.

Sundby, B., Anderson, L. G., Hall, P. O., Iverfeld, A., Rutgers van der Loeff, M. M., & Westerlund, S. F. (1986). The effect of oxygen on release and uptake of cobalt, manganese, iron and phosphate at the sediment–water interface. Geochim. Cosmochim. Acta, 50, 1281–1288.

Taylor, S. R. (1964). Abundance of chemical elements in the continental crust: a new table. Geochimica et Cosmochimica Acta, 28, 1273-1285.

Thamdrup, B. (2000). Bacterial manganese and iron reduction in aquatic sediments. Adv. Microb. Ecol., 16, 41–84.

Thamdrup, B., Hansen, J. W., & Jorgensen, B. B. (1998). Temperature dependence of aerobic respiration in a coastal sediment. FEMS Microbiol. Ecol., 25, 189-200.

Tribovillard, N., Algeo, T. J., Lyons, T., & Riboulleau, A. (2006). Trace metals as paleoredox and paleoproductivity proxies: an update. Chem. Geol., 12–32.

Wenzhöfer, F., & Glud, R. N. (2004). Small-scale spatial and temporal variability in coastal benthic O2 dynamics: Effects of fauna activity. Limnol. Oceanogr., 49, 1471-1481.

Wijsman, J. W., Herman, P. M., Middelburg, J. J., & Soetaert, K. (2002). A model for early diagenetic processes in sediments of the continental shelf of the Black Sea. Estuarine, Coastal and Shelf Science, 54, 403-421.

Wijsman, J. W., Middelburg, J. J., Herman, P. M., Böttcher, M. E., & Heip, C. H. (2001). Sulfur and iron speciation in surface sediment along the northwestern margin of the Black Sea. Marine Chemistry, 74, 261-278.

Wijsman, J., Herman, P., & Gomoiu , M. T. (1999). Spatial distribution in sediment characteristics and benthic activity on the northwestern Black Sea shelf. Mar. Ecol. Prog. Ser., 181, 25–39.

Windom, H. S. (1989). Natural trace metal concentrations in estuarine and coastal marine sediments of the southeastern United States. Environ. Sci. Technol., 23, 314–320.

Zahra, A., Hashmi, M. Z., Malik, R. N., & Ahmed, Z. (2014). Enrichment and geo-accumulation of heavy metals and risk assessment of sediments of the Kurang Nallah—Feeding tributary of the Rawal Lake Reservoir, Pakistan. Science of The Total Environment, 470-471, 925-933.

Chapter 6

General conclusions and perspectives

Picture of the Black Sea in 2016.

6.1 Oxygen depletion: early diagenesis, benthic fluxes and trace metals

Coastal hypoxia occurs when rivers discharge a high quantity of nutrients of anthropogenic origin leading to intensive algal blooms and thus eutrophication (Figure 6.1). After the decline of the bloom, the algae sink to the seabed which provides a rich food source for benthic bacteria consuming dissolved oxygen from the bottom waters. Thus, the mineralization of organic matter by bacteria brings about a decline of dissolved oxygen in the benthic compartment. Furthermore, during summer the water column stratifies and prevents the mixing of surface water with bottom water hindering the benthic compartment to become oxygenated (Diaz & Rosenberg, 2008).

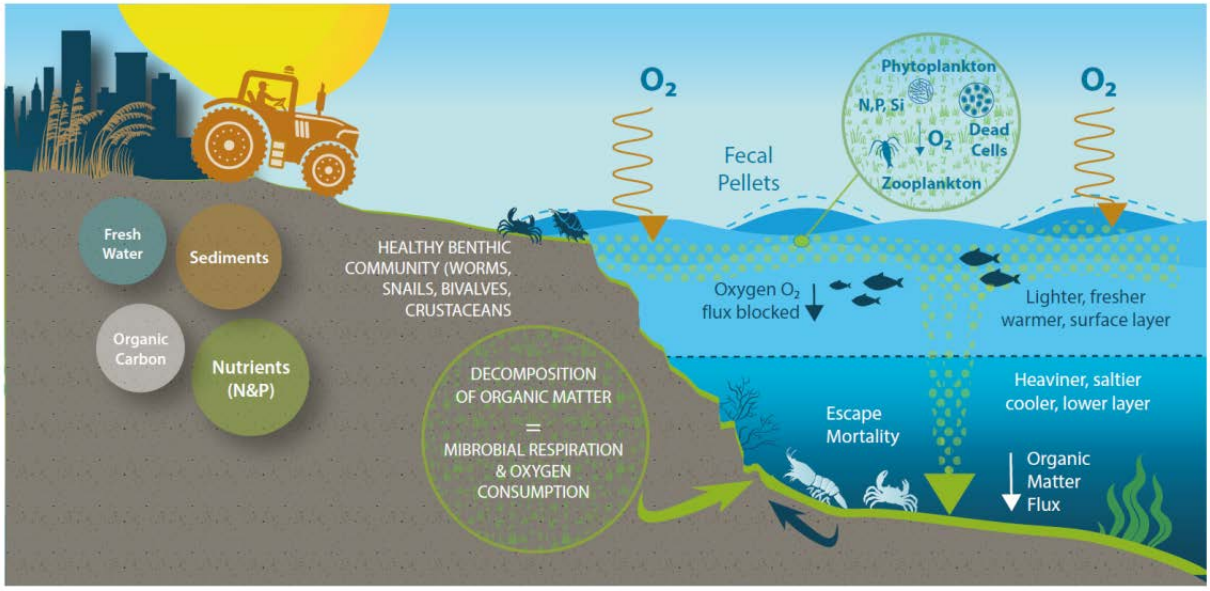

Figure 6.1. Schematic diagram showing the impact of eutrophication on ocean oxygen content (from Isensee, 2015).

Today, oxygen depletion in the bottom waters of the coastal zone is known to be an annual, periodic and/or isolated event and has become more and more a worldwide phenomenon. Different environments are affected by hypoxia: fjords, semi-enclosed seas, ocean (called oxygen minimum zones) and coastal systems. The increasing occurrence of hypoxic systems is an emerging environmental issue that needs to be addressed regarding its development process and impacts. Furthermore, hypoxia can lead to an accumulation of free sulphides rendering the systems euxinic which is harmful for marine life. Moreover, under hypoxic conditions, the fishing activity would intensify in the surface waters richer in nutrients and

algae, impacting the marine ecosystems. As a consequence, understanding the causes and consequences of coastal hypoxia is of economical relevance.

Sediments play a role in the oxic and anoxic mineralization of organic matter and regulate the biogeochemistry of the water column. Under certain conditions, the water column affects the sediments especially when the oxygen concentrations fluctuate. Without oxygen, the most favorable electron donor, the diagenetic reactions are disturbed (Middelburg & Levin, 2009; Figure 6.2).

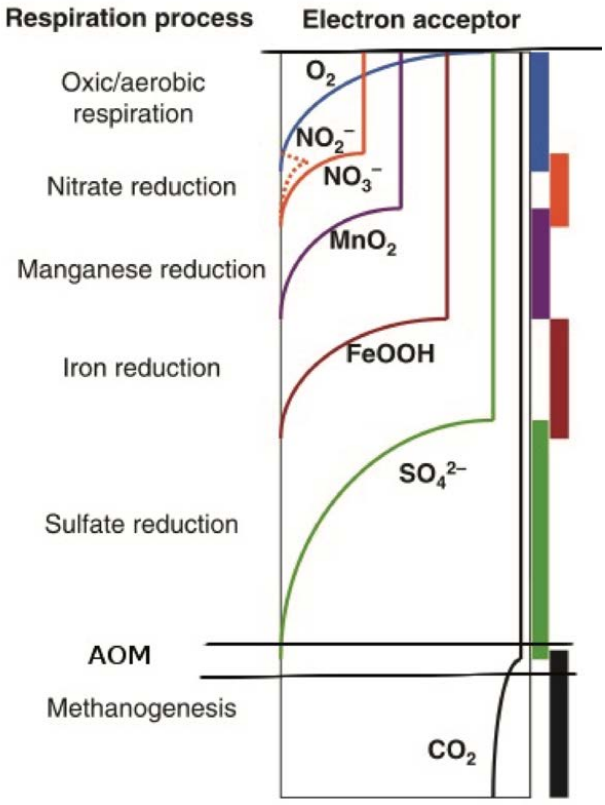

Figure 6.2. Depth distribution of common electron acceptors in the sediments and the associated respiration processes (from Canfield & Thamdrup, 2009).

The Black Sea is a semi-enclosed sea with limited renewal and long residence times of bottom waters. It is a particular system because it exhibits two types of oxygen depletion. The deep basin, well studied, is known to be one of the largest anoxic and euxinic basin of the world. Despite the fact that the deep basin is famous for its anoxia, the NW shelf is prone to seasonal hypoxia. Before 1960, the shelf of the Black Sea was highly productive and was covered by a carpet of *Phyllaphora* algae and bivalves such as mussels, living in symbiosis. Between 1960 and 1980, the agricultural and industrial sectors were modernized and the use of chemical products such as fertilizers and pesticides was intensified, resulting in increased riverine fluxes of nutrients and metallic pollutants to the sea. Since 1980, countries bordering

the Black Sea could not afford the fertilizers and the less intensive agricultural activities led to a decline in the nutrient loadings in rivers and to some recovery of the ecosystem in the late 1990s (Mee, 2006).

Twenty years later, the NW shelf of the Black Sea is still subject to oxygen limitation and has been chosen as the study site during two oceanographic campaigns (spring 2016 and summer 2017) to better understand the causes and impacts of coastal hypoxia using a multidisciplinary approach. The impact of the low oxygen levels in the bottom waters on the sediment-water exchanges and the reactions of early diagenesis (Figure 6.2) can be summarized as follows:

- Oxic respiration is less intense and shallower with shallower oxygen penetration depths and lower DOUs. The reduced species contribute to an important part of the oxygen consumption. Thus, the oxic mineralization rate of organic matter becomes less intense.
- Nitrification and denitrification occur merely in the first centimetres of the sediments and are not quantifiable.
- Reduction of Mn- and Fe-oxides is shallower in the sediments inducing higher contents of dissolved species in the porewaters diffusing to the oxic layer where they may be re-oxidized or escape to the water column. Moreover, the Mn- and Fe-cycles are linked to phosphate, so called ‘Mn-Fe-P shuttle’ forming precipitates of Fe-P and Mn-P during the reductive dissolution of iron and manganese oxides.
- Sulphate reduction is dominant although it occurs at a shallower depth with a stronger gradient accentuating the production of hydrogen sulphide in the porewaters. The anoxic mineralization of organic matter is taking place through sulphate reduction and thus influenced by the flux of sulphate in the sediments and showed a higher contribution during the summer comprising between 79 % and 86 %. Usually, under low oxygen conditions, the production of hydrogen sulphide in the sediments becomes higher but the NW shelf sediments were depleted in hydrogen sulphide in the porewaters due to their fast conversion to sulphide minerals. Despite the depletion of reactive iron in the shelf sediments, the presence of iron oxides would lead to the low AVS in the sediments. The low content of pyrite could be attributed to (1) the insufficient time for the pyrite to be formed and (2) the transport of FeS_2 from the shelf to deep basin caused by the hydrodynamic conditions and/or the dredging of sediments. The present study, with sampling campaigns carried out in 2016 and 2017,

indicates that the NW shelf sediment of the Black Sea is a Fe-dominated system as suggested by Wijsman et al. (2002).

- Trace metals could play a role in the diagenetic reactions which needs to be taken into consideration. Indeed, the metals can be associated to Fe and Mn oxides by adsorption and/or co-precipitation and in deeper layers they can precipitate with or adsorb onto sulphides to form metal sulphides such as ZnS or CuS (Rigaud et al., 2013; Mee, 2006). In this study, no clear correlations were found about these hypotheses. In a system with an alternative regime of oxygen dynamics, it would be interesting to better examine their relationship with these oxides and sulphides because heavy metals could be released to the water column affecting the ecosystems.

The present study allowed the evaluation of the spatial variability of early diagenesis and sediment-water exchanges on the NW shelf and two main zones could be highlighted: (1) areas close to the river mouths and (2) the central shelf. Near the river mouths, the stations exhibit a higher oxic mineralization rate of organic matter due to the river discharges which bring various levels and types of organic matter to the sea and to the high primary productivity. Sediment characteristics can play a role in the efficiency of organic matter degradation they by affecting the diffusion of dissolved species in the sediments as well as the bioturbation. Trace metals are known for several applications as proxies for productivity, redox conditions and contaminants which are harmful for ecosystems (Morford & Emerson, 1999; Brumsack, 2006; Tribovillard et al. , 2006). As pollutants, trace metals are remobilized in the sediments depending on the physicochemical conditions both in the water column and in the sediments. A spatial heterogeneity is highlighted on the shelf and two zones can be identified: (1) the Danube delta area and (2) the Odessa region. Sediments near the Danube river mouth were enriched in Ni, Zn and Cu while in the Dnieper area they were enriched in Co. Particulate Cd contents were relatively high everywhere on the shelf especially in area close to the Tendra spit. Assessment of the enrichment factors confirmed several levels of pollution in the surface sediments of the shelf varying from being unpolluted to being extremely polluted. Despite new environmental regulations and a progressive recovery since 1995, the sediments were still impacted by trace metal contaminations. It is urgent to advance our knowledge in the biogeochemical cycles of trace metals in the sediments in order to accelerate the recovery.

6.2 Advantages and limits of the methodology used

In the framework of the Benthox project, a large dataset was collected and allowed a new state of the art of the NW shelf to be established. However, some aspects were missing to obtain a complete view of the NW shelf system.

Thanks to the EMBLAS program, two unique opportunities were given to sample sediments and bottom waters throughout the NW shelf of the Black Sea. As guests on the cruise, it was impossible to choose our sampling points and the better moment of the year to sample.

During our first field campaign in 2016, the information about the types of sediments and fauna living on the seabed were incorrect which limited our sampling and an adaptation of the cruise schedule had to be adopted. Initially, more stations had to be sampled. So, not enough data were collected to assess a seasonal event such as hypoxia, and to study the complete spatial variations on the shelf.

Few methods, such as NOx and ammonium determination, were old methods but they are validated due to their sensitivity and accuracy.

The extraction of porewaters by the *Rhizon* technique in a glove bag flushed continuously with nitrogen gas is easy to handle and a non-destructive technique. It allows one to preserve the anoxic environment of the porewaters which is important for the study of oxidizable species. Moreover, thanks to this technique the scientist can optimize the time and proceeds to other analysis once the *Rhizons* are installed.

The colorimetric method for alkalinity analyses and the methylene blue method (also by colorimetry) for sulphides measurements are easy to apply and are practical due to the possibility to measure a large set of samples in a short period of time. Furthermore, these two methods are accurate. The method used for the sulphide determination presents other non-negligible advantages: (1) the use of a single reagent, (2) the intensity and the stability of the color developed at low sulphide concentrations and (3) a sensitive method.

Other parameters have not been measured and could have been of interest in this study, for example:

- DIC (dissolved inorganic carbon) which is involved in the mineralization of organic matter.

- the speciation of metallic compounds to have more details about their interactions with the early diagenesis and the identification/quantification of intermediate species in the Fe cycles.

On-board core incubations should be performed to obtain an accurate estimate of the rate of benthic oxygen uptake which can be used as a proxy for the overall intensity of mineralization. Unfortunately, the incubation experiments carried out were not successful due to technical problems on the ship and the impact of the benthos on oxygen consumption could not be not studied.

The use of a microprofiler was of crucial importance. This material has made it possible to obtain high-resolution geochemical gradients, in particular oxygen and hydrogen sulphide, at the sediment-water interface.

In our study, the fluxes were calculated manually based on the Fick's first law. The use of the modelling approach would help to understand and validate the processes occurring on the NW shelf. Moreover, this approach will help to predict the spreading or the reduction of the hypoxic zones.

6.3 Perspectives

6.3.1 Temporal and spatial variability

Previous studies and this thesis have demonstrated temporal and seasonal variabilities of diagenetic processes on the NW shelf of the Black Sea. It would be interesting to set up a regular monitoring and sampling program to identify and quantify in detail the prominence of the different diagenetic reactions, especially when the system is subject to seasonal hypoxia. The use of a benthic lander will make it possible to obtain high resolution 1D geochemical gradients without the risk of oxidizing and/or disturbing the sediments. Additional data on isotope dating and/or pollen types would help to understand the origin of marine sediments and identify hypoxic periods.

6.3.2 Iron and sulphides

Fe-S cyling is dependant of the oxygen levels in the bottom waters. The dissolved reduced species diffusing to the oxic layer of the sediments are expected to be re-oxidized. However, if the sediments are completely anoxic, these species will interact more intensely and produce higher amounts of FeS and FeS_2. The transformation of ferrous oxides to stable iron sulphides

is composed of different steps (Figure 6.3) and it would be useful to study each step in order to fully understand the sulphide cycle in the shelf sediments of the Black Sea. The quantification of the greigite and pyrrhotite, metastable intermediate in the reaction pathway to pyrite, would help to understand reactions involving the free sulphide. On the shelf, the production of FeS was not visible during our sampling and thus the monitoring will help and improve the detection of these species.

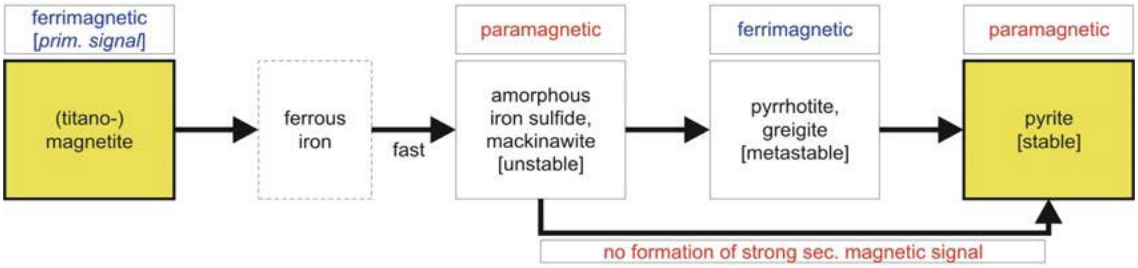

Figure 6.3. Schematic diagram showing the major pathways of the transformation of iron oxides to iron sulphides associated to their magnetic signal (from Jorgensen and Kasten, 2006).

Furthermore, it would be useful to measure the hydrogen sulphide in the porewaters directly aboard the ship to improve the quality of results and avoid their oxidation between the sampling and the analyses.

Finally, iron can be involved in other biogeochemical cycles such as phosphorus. Thus, it would be interesting to study, in the shelf sediments, the seasonal dynamics between iron and phosphorus by the speciation of these two elements in the sediments. The phosphorus speciation can be determined using the SEDEX method (Ruttenberg, 1992). This study could be extended to cover different seasons especially in the seasonally hypoxic regions where the high mobilization of P occurs due to the reductive dissolution of Fe oxides under oxygen depleted conditions. Moreover, the Fe-Mn-P shuttle theory in the sediments can also be explored.

6.3.3 Anthropogenic pressures

This study of heavy metals in the surface sediments of the shelf revealed an enrichment and pollution of the sediments by the metallic contaminants. These enrichments probably played a role in the diagenetic sequence due to their adsorption/co-precipitation with sulphides, iron and manganese oxides, organic matter and carbonates. It should be significant to study their

speciation in the sediments and the water column to understand the full processes. The spatial variability was attributed to their different uses on land especially by agricultures and industries. The shelf sediments are prone to an increase of metallic pollutant contents in the Danube delta area as revealed by an evaluation of heavy metal contents since the late 20th century. However, the Odessa region displayed stable contents of Cu, Cd, Ni and Zn over the same period. Thus, a sampling along the dilution gradients of the water column and sediments (e.g., along each branch of the Danube Delta and along the Dnieper mouth) would improve the knowledge about the anthropogenic impact on the sediment quality.

In order to assess this pollution and its impacts, the monitoring is rather a good option which could help the policy makers to regulate the uses of heavy metals.

References

Brumsack, H. J. (2006). The trace metal content of recent organic carbon-rich sediments: implications for Cretaceous black shale formation. Paleogeogr. Paleoecol., 232, 344-361.

Canfield, D. E., & Thamdrup, B. (2009). Towards a consistent classification scheme for geochemical environments, or, why we wish the term 'suboxic' would go away. Geobiology, 7, 385–392.

Diaz, R. J., & Rosenberg, R. (2008). Spreading dead zone and consequences for marine ecosystems. Science, 321, 926-929.

Isensee, K. (2015). The Ocean is Losing its Breath. In Ocean and Climate Scientific Notes, ed. 2 (pp. 20-32).

Mee, L. (2006). Reviving dead zones. Sci. Am., 295, 78–85.

Middelburg, J. J., & Levin, L. A. (2009). Costal hypoxia and sediment biogeochemistry. Biogeosciences, 6, 1272-1293.

Morford, J. L., & Emerson, S. (1999). The geochemistry of redox sensitive trace metals in sediments. Geochim. Cosmochim. Acta, 63, 1735-1750.

Rigaud, S., Radakovitch, O., Couture, R. M., Deflandre, D., Cossa, D., Garnier, C., & Garnier, J.-M. (2013). Mobility and fluxes of trace elements and nutrients at the sediment-water interface of a lagoon under contrasting water column oxygenation conditions. Applied Geochemistry, 31, 35-51.

Ruttenberg KC. 1992. Development of a Sequential Extraction Method for Different Forms of Phosphorus in Marine Sediments. Limnology and Oceanography 37: 1460-82.

Tribovillard, N., Algeo, T. J., Lyons, T., & Riboulleau, A. (2006). Trace metals as paleoredox and paleoproductivity proxies: an update. Chem. Geol., 12-32.

Wijsman, J. W., Herman, P. M., Middelburg, J. J., & Soetaert, K. (2002). A model for early diagenetic processes in sediments of the continental shelf of the Black Sea. *Estuarine, Coastal and Shelf Science, 54*, 403-421.

List of references

Aksu, A. E., Hiscott, R. N., Mudie, P. J., Rochon, A., Kaminski, M., Abrajano, T., & Yasar, D. (2002). Persistent Holocene outflow from the Black Sea to the Eastern Mediterranean contradicts Noah's Flood hypothesis. *GSA Today, 12*, 4-10.

Aller, R. (2014). Sedimentary diagenesis, depositional environments, and benthic fluxes. In *Treatise on geochemistry, 2nd edn* (Vol. 8). Amsterdam: Elsevier Ltd.

Aller, R. C., & Rude, P. D. (1988). Complete oxidation of solid-phase sulphides by manganese and bacteria in anoxic marine sediments. *Geochim. Cosmochim. Acta., 52*, 751–765.

Almazov, N. M. (1961). Stok ratverennykh soley I biogennykh veschetv kotorye vynoseatsya rekami USSR v Chernoe More. *Naukovi Zapiski Odes. Biol. St. Kiev*, 99-107.

Altabet, M. A., & Francois, R. (1994). Sedimentary isotopic ratio as a recorder for surface ocean nitrate utilization. *Global Biogeochem. Cy., 8*, 103–116.

Alve, E. (1990). Variations in estuarine foraminiferal biofacies with diminishing oxygen conditions in Drammensfjord, SE Norway. In C. Hemleben, M. A. Kaminski, W. Kuhnt, & D. B. Scott (Eds.), *Paleoecology, Biostratigraphy, Paleoceanography and Taxonomy of Agglutinated Foraminifera* (Vol. 327). Dordrecht: Springer.

Alve, E. (2003). A common opportunistic foraminiferal species as an indicator of rapidly changing conditions in a range of environments. *Estuarine coastal and shelf science, 57*, 501-514.

Anderson, T. F., & Raiswell, R. (2004). Sources and mechanisms for the enrichment of highly reactive iron in euxinic Black Sea sediments. *American Journal of Science, 304*, 203-233.

Andrén, E. (1999). : Changes in the composition of the marine diatom flora ´ during the past century indicate increased eutrophication of the Oder estuary, southwestern Baltic Sea. *Estuarine, Coastal and Shelf Science, 48*, 665-676.

APHA. (2005). Standard Methods for the Examination of Water and Wastewater, 21st ed. American Public Health Association – American Water Works Association – Water Environment Federation.

Archer, D. E., Lyle, M. W., Rodgers, K., & Froelich, P. N. (1993). What controls opal preservation in tropical deep-sea sediments. *Paleoceanography, 8*, 7–21.

Archer, D., & Devol, A. (1992). Benthic oxygen fluxes on the Washington shelf and slope: a comparison of in-situ micro electrode and flux chamber measurements. *Limnol. Oceanogr., 37*, 614–629.

Armstrong, H. A., & Brasier, M. D. (2013). Foraminifera. In *Microfossils* (p. 142-187). John Wiley & Sons, Ltd. https://doi.org/10.1002/9781118685440.ch15

Arnold, A. J., & Parker, W. C. (1999). Biogeography of Planktonic Foraminifera. In *Modern Foraminifera* (pp. 103-122). Dordrecht: Springer.

Berlinskyi, N., & Safranov, T. (2016). Spatial and temporal variability of in the bottom sediments in the Northwest part of the Black Sea. *Environmental Problems, 1*, 73-76.

Berner, R. (1980). *Early Diagenesis: A theoritical approach.* Princeton University Press.

Berner, R. A. (1970). Sedimentary pyrite formation. *Am. J. Sci., 268*, 1-23.

Berner, R. A. (1980). *Early Diagenesis: A theoritical approach.* Princeton University Press.

Berner, R. A. (1981). A new geochemical classification of sedimentary environments. *J. Sediment. Petrol, 51*, 359-365.

Berner, R. A. (1982). Burial of Ogranic Carbon and Pyrite sulfur in the modern ocean: Its geochemical and envrionmental significance. *Am. J. Sci., 282*, 451-473.

Berner, R. A. (1984). Sedimentary pyrite formation: An update. *Geochim. Cosmochim. Acta, 48*, 605-615.

Berner, R. A. (1989). Biogeochemical cycles of carbon and sulfur and their effect on atmospheric oxygen over phanerozoic time. *Paleogeography, Paleoclimatology, Paleoecol., 75*, 97-122.

Bidle, K. D., & Azam, F. (1999). Accelerated dissolution of diatom silica by marine bac- terial assemblages. *Nature, 397*, 508-512.

Bidle, K. D., & Azam, F. (2001). Bacterial control of silicon regeneration from diatom detritus: Significance of bacterial ectohydrolases and species identity. *Limnology and Oceanography, 46*, 1606–1623.

Boesen, C., & Postma, D. (1988). Pyrite formation in anoxic environments of the Baltic. *Am. J. Sci, 288*, 575–603.

Bond, D. P., & Wignall, P. B. (2010). Pyrite framboid study of marine Permian–Triassic boundary sections: A complex anoxic event and its relationship to contemporaneous mass extinction. *GSA Bulletin, 122*, 1265–1279.

Borowski, W. S., Paull, C. K., & Ussler, W. (1999). Global and local variations of interstitial sulfate gradients in deep-water, continental margin sediments: Sensitivity to underlying methane and gas hydrates. *Marine Geology, 159*, 131-154.

Bottrell, S. H., & Newton, R. J. (2006). Reconstruction of changes in global sulfur cycling from marine sulfate isotopes. *Earth Sci. Rev., 75*, 59-83.

Boudreau, B. P. (1996). The diffusive tortuosity of fine-grained unlithified sediments. *Geochim. Cosmochim. Acta, 60*, 3139-3142.

Brady, D. C., Testa, J. M., Di Toro, D. M., Boynton, W. R., & Kemp, W. M. (2013). Sediment flux modeling: Calibration and application for coastal systems. *Estuar. Coast. Shelf Sci., 117*, 107-124.

Brandes, J. A., & Devol, A. H. (2002). A global marine-fixed nitrogen isotopic budget: Implications for Holocene nitrogen cycling. *Global Biogeochem. Cy., 14*, 1120.

Brandes, J. A., Devol, A. H., Yoshinari, T., Jayakumar, A., & Naqvi, S. W. (1998). Isotopic composition of nitrate in the central Arabian Sea and eastern tropical North Pacific: A tracer for mixing and nitrogen cycles. *Limnol. Oceanogr., 43*, 1680–1689.

Bratton, J. R., Colman, S. M., & Seal, R. R. (2003). Eutrophication and carbon sources in Chesapeake Bay over the last 2700 yr: human impacts in context. *Geochim. Cosmochim. Ac., 67*, 3385–3402.

Breitburg, D., Grégoire, M., & Isensee, K. (2016). *The ocean is losing its breath: Declining oxygen in the world's ocean and coastal waters.* IOC-UNESCO, IOC Technical Series. Global Ocean Oxygen Network 2018.

Brocks, J. J., Logan, G. A., Buick, R., & Summons, R. E. (1999). Archean molecular fossils and the early rise of eukaryotes. *Science, 285*, 1033-1036.

Brumsack, H. J. (2006). The trace metal content of recent organic carbon-rich sediments: implications for Cretaceous black shale formation. *Paleogeogr. Paleoecol., 232*, 344-361.

Brunner, C. A., Beall, J. M., Bentley, S. J., & Furukawa, Y. (2006). Hypoxia hotspots in the

Mississippi Bight. *J. Foramin. Res., 36*, 95–107.

Burdige, D. (2006). *Geochemistry of Marine Sediments.* Princeton University Press.

Burdige, D. J. (2007). Preservation of organic matter in marine sediments: controls, mechanisms, and an imbalance in sediment organic carbon budgets? *Chem. Rev., 107*, 467-485.

Burdige, D. J. (2011). Estuarine and coastal sediments - Coupled biogeochemical cycling. In D. J. Burdige, *Treatrise on estuarine and coastal science* (Vol. 5, pp. 279-308). Academic Press.

Burton, E. D., Sullivan, L. A., Bush, R. T., Johnston, S. G., & Keene, A. F. (2008). A simple and inexpensive chromium-reducible sulfur method for acid-sulfate soils. *Applied Geochemistry, 23*, 2759–2766.

Caccia, V. G., Millero, F. J., & Palanques, A. (2003). The distribution of trace metals in Florida Bay sediments. *Mar. Pollut. Bull.*, 1420–1433.

Cai, W.-J. (2011). Estuarine and coastal ocean carbon paradox: CO2 sinks or sites of terrestrial carbon incineration ? *Annual Review of Marine Science, 3*, 123-145.

Cai, W.-J., & Sayles, F. L. (1996). Oxygen penetration depths and fluxes in marine sediments. *Marine Chemistry, 52*, 123-131.

Calvert, S. E., & Pedersen, T. F. (1993). Geochemistry of Recent oxic and anoxic marine sediments: Implications for the geological record. *Mar. Geol., 113*, 67-88.

Calvert, S. E., & Pedersen, T. F. (2007). Elemental proxies for palaeoclimatic and palaeoceanographic variability in marine sediments: interpretation and application. In C. Hillaire-Marcel, & A. De Vernal (Eds.), *Proxies in Late Cenozoic Paleoceanography* (pp. 567-644). Amsterdam, Boston, Heidelberg, London, New York, Oxford, Paris, San Diego, San Francisco, Singapore, Sydney, Tokyo: Elsevier.

Canfield, D. E. (1994). Factors influencing organic carbon preservation in marine sediments. *Chem. Geol., 114*, 315–329.

Canfield, D. E., & Thamdrup, B. (2009). Towards a consistent classification scheme for geochemical environments, or, why we wish the term ‘suboxic’ would go away. *Geobiology, 7*, 385–392.

Canfield, D. E., Jorgensen, B. B., Fossing, H., Glud, R., Gundersen, J., Ramsing, N. B., . . . Hall, P. O. (1993a). Pathways of organic carbon oxidation in three continental margin sediments. *Marine Geology, 113*, 27-40.

Canfield, D. E., Thamdrup, B., & Hansen, J. W. (1993b). The anaerobic degradation of organic matter in Danish coastal sediments: Iron reduction, manganese reduction, and sulfate reduction. *Geochimica et Cosmochimica Acta, 57*, 3867-3883.

Canfield, D. E., Lyons, T. W., & Raiswell, R. (1996). A model for iron deposition to euxinic Black Sea sediments. *Am. J. Sci., 296*, 818-834.

Capet, A., Beckers, J.-M., & Gregoire, M. (2013). Drivers, mechanisms and long-term variability of seasonal hypoxia on the Black Sea northwestern shelf – is there any recovery after eutrophication? *Biogeosciences, 10*, 3943–3962.

Capet, A., Meysman, F. J., Akoumianaki, I., Soetaert, K., & Grégoire, M. (2016a). Integrating sediment biogeochemistry into 3D oceanic models: A study of benthic-pelagic coupling in the Black Sea. *Ocean Modelling, 101*, 83–100.

Capet, A., Stanev, E. V., Beckers, J.-M., Murray, J. W., & Grégoire, M. (2016b). Decline of the Black Sea oxygen inventory. *Biogeosciences, 13*, 1287-1297.

Chen, C.-T. A., & Borgès, A. V. (2009). Reconciling opposing views on carbon cycling in the coastal ocean: Continental shelves as sinks and near-shore ecosystems as sources of atmospheric CO2. *Deep Sea Research Part II: Tropical studies in oceanography, 8*, 578-590.

Chen, X., Andersen, T. J., Morono, Y., Inagaki, F., Jørgensen, B. B., & Lever, M. A. (2017). Bioturbation as a key driver behind the dominance of Bacteria over Archaea in near-surface sediment. *Sci Rep, 7*, 2400.

Claff, S. R., Sullivan, L. A., Burton, E. D., & Bush, R. T. (2010). A sequential extraction procedure for acid sulfate soils: Partitioning of iron. *Geoderma, 155*, 224–230.

Cline, J. D. (1969). Spectrophotometric determination of hydrogen sulfide in natural waters. *Limnol. Oceanogr., 14*, 454-458.

Cociasu, A., Dorogan, L., Humborg, C., & Popa, L. (1996). Long-term ecological changes in the Romanian coastal waters of the Black Sea. *Marine Pollution Bulletin, 32*, 32-38.

Commission, n. L. (1958). *Convention on the Continental Shelf.* United Nations. Geneva: Treaty Series.

Conley, D. J., Bjorck, S., Bonsdorff, E., Carstensen, J., Destouni, G., Gustafsson, B. G., . . . Rosenberg, R. (2009). Hypoxia-related processes in the Baltic Sea. *Environ. Sci. Technol, 43*, 3412–3420.

Conley, D. J., Carstensen, J., Ærtebjerg, G., Christensen, P. B., Dalsgaard, T., Hansen, J. L., & Josefson, A. B. (2007). Long-term changes and impacts of hypoxia in Danish coastal waters. *Ecol. Appl., 17*, 165-184.

Cooper, S. R., & Brush, G. S. (1991). Long-Term History of Chesapeake Bay Anoxia. *Science, 254*, 992-996.

Crusius, J., Calvert, S., Pedersen, T., & Sage, D. (1996). Rhenium and molybdenum enrichments in sediments as indicators of oxic, suboxic and sulfidic conditions of deposition. *Earth Planet. Sci. Lett., 145*, 65–78.

Dauwe, B., Middelburg, J. J., & Herman, P. M. (2001). Effect of oxygen on the degradability of organic matter in subtidal and intertidal sediments of the North Sea area. *Mar. Ecol. Prog. Ser., 215*, 13–22.

Dean, W. E. (1974). Determination of carbonate and organic matter in calcareous sediments and sedimentary rocks by loss of ignition: comparison with other methods. J. of Sedimentary Petrology, 44, 242-248.

Denga, Y., Orlova, I., Komorin, V., Oleynik, Y., Korshenko, A., Hushchyna, K., . . . Zhugailo. (2017). *National Pilot Monitoring Studies & Joint Open Sea Surveys in Georgia, Russian Federation and Ukraine, 2016.*

Deuser, W. G. (1974). Evolution of anoxic conditions in Black Sea during Holocene. In E. T. Degens, & D. A. Ross, *The Black Sea-Geology, chemistry and biology* (pp. 133-136). Tulsa: AAPG Memoir 20.

Devol, A. H., & Christensen, J. P. (1993). Benthic fluxes and nitrogen cycling in sediments of the continental margin of the eastern North Pacific. *J. Mar. Res., 51*, 345–372.

Dewey, J. F., Pittman, W. C., Ryan, W. B., & Bonnin, J. (1973). Plate tectonics and the evolution of the Alpine System. *Geol. Soc. Am. Bull., 84*, 3137-3180.

Diaz, R. J., & Rosenberg, R. (1995). MArine benthic hypoxia: a review of its ecological effects and the behavioural responses of benthic macrofauna. *Oceanogr. and Mar. Biol., 33*, 245-303.

Diaz, R. J., & Rosenberg, R. (2008). Spreading dead zones and consequences for marine ecosystems.

Science, 321, 926-929.

Dickson, A. G. (1981). An exact definition of total alkalinity and a procedure for the esti- mation of alkalinity and total inorganic carbon from titration data. Deep Sea Research, 28, 609–623.

Dijkstra, N., Kraal, P., Kuypers, M. M., Schnetger, B., & Slomp, C. P. (2014). Are iron-phosphate minerals a sink for phosphorus in anoxic Black sea sediments? *PLoSONE, 9*, e101139.

Dijkstra, N., Slomp, C. P., & Behrends, T. (2016). Vivianite is a key sink for phosphorus in sediments of the Landsort Deep, an intermittently anoxic deep basin in the Baltic Sea. *Chemical Geology*, *438*, 58-72. https://doi.org/10.1016/j.chemgeo.2016.05.025

Dixit, S., Van Cappellen, P., & van Bennekom, A. J. (2001). Processes controlling solubility of biogenic silica and pore water build-up of silicic acid in marine sediments. *Mar. Chem., 73*, 333–352.

Dyatlov, S. Y. (2015). Heavy metals in water and bottom sediments of Odessa region of the Black sea. *Journal of shipping and ocean engineering, 5*, 51-58.

Ehlers, J., Gibbard, P. L., & Hughes, P. D. (2011). *Quaternary glaciations : extent and chronology : a closer look.* Amsterdam: Elsevier.

Emili, A., Koron, N., Covelli, S., Faganeli, J. A., Acquavita, A., Predonzani, S., & Vittor, C. D. (2011). Does anoxia affect mercury cycling at the sediment–water interface in the Gulf of Trieste (northern Adriatic Sea)? Incubation experiments using benthic flux chambers. *Appl. Geochem., 26*, 194–204.

Erwin, D. H. (2006). *Extinction: How Life on Earth Nearly Ended 250 Million Years Ago.* Princeton: Princeton Univ. Press.

Falkowski, P. G., Algeo, T., Codispoti, L., Deutsch, C., Emerson, S., Hales, B., . . . Pilcher, C. B. (2011). Past, Present, and Future. *Eos, 92*, 409-410.

Fanning, K. A., & Pilson, M. E. (1974). The diffusion of dissolved silica out of deep-sea sediments. *J. Geophys. Res:Oceans, 79*, 1293–1297.

Fernandes Martins, M. J., Namiotko, T., Cabral, M. C., Fatela, F., & Boavida, M. J. (2010). Contribution to the knowledge of the freshwater Ostracoda fauna in continental Portugal, with an updated cheklist of Recent and Quaternary species. *J. Limnol., 69*, 160-173.

Friedrich, J., Dinkel, C., Friedl, G., Pimenov, N., wijsman, J., Gomoiu, M.-T., . . . Wehrli, B. (2002). Benthic nutrient cycling and diagenetic pathways in the North-western Black Sea. *Estuarine, Coastal and Shelf Science, 54*, 369-383.

Froelich, P. N., Klinkhammer, G. P., Bender, M. L., Luedtke, N. A., Heath, G. R., Cullen, D., . . . Hartman, B. (1979). Early oxidation of organic matter in pelagic sediments of the eastern equatorial Atlantic: suboxic diagenesis. *Geochim. Cosmochom., 43*, 1075-1090.

Galbraith, E. D., Kienast, M., Pedersen, T. F., & Calvert, S. E. (2004). Glacial-interglacial modulation of the marine nitrogen cycle by high-latitude O2 supply to the global thermocline. *Paleoceanography, 19*, PA4007.

Glud, R. N. (2008). Oxygen dynamics of marine sediments. *Mar. Biol., 4*, 243-289.

Glud, R. N., Gundersen, J. K., Roy, H., & Jorgensen, B. B. (2003). Seasonal dynamics of benthic O2 utpake in a semienclosed bay: Importance of diffusion and faunal activity. *Limnol. Oceanogr., 48*, 1265-1276.

Gorur, N. (1988). Timing of opening of the Black Sea. *Tectonophys., 147*, 247-262.

Grasshoff, K., Ehrhardt, M., & Kremling, K. (1983). *Methods of Seawater Analysis.* Weinheim: Verlag Chemie.

Gray, J. S., Wu, R. S., & Or, Y. Y. (2002). Effect of hypoxia and organic enrichment on the coastal marine environment. *Marine Ecology Progress Series, 238*, 249-279.

Grégoire, M., & Soetaert, K. (2010). Carbon, nitrogen, oxygen and sulfide budgets in the Black Sea: A biogeochemical model of the whole water column coupling the oxic and anoxic parts. *Ecological Modelling, 221*, 2287–2301.

Hedges, J. I., & Keil, R. G. (1995). Sedimentary organic matter preservation: an assessment and speculative synthesis. Authors' closing comments. *Mar. Chem., 49*, 137-139.

Helly, J., & Levin, L. (2004). Global distribution of naturally occurring marine hypoxia on continental margins. *Deep See Res.I, 51*, 1159-1168.

Holland, H. D. (2002). Volcanic gases, black smokers, and the great oxidation event. *Geochim. Cosmochim. Acta., 66*, 3811-3826.

Hollweg, T. A., Gilmour, C. C., & Mason, R. P. (2009). Methylmercury production in sediments of Chesapeake Bay and the mid-Atlantic continental margin. *Mar. Chem., 114*, 86–101.

Holmes, R. M., Aminot, A., Kérouel, R., Hooker, B. A., & Peterson, B. J. (1999). A simple and precise method for measuring ammonium in marine and freshwater ecosystems. *Can. J. fish. Aqua. Sci., 56*, 1801-1808.

Hsü, K. J., Nacev, I. K., & Vuchev, V. T. (1977). Geologic evolution of Bulgaria in the light of plate tectonics. *Tectonophys., 40*, 245-256.

Huerta-Diaz, M. A., Tessier, A., & Carignan, R. (1998). Geochemistry of trace metals associated with reduced sulfur in freshwater sediments. *Appl. Geochem., 114*, 213–233.

Ip, C. C., Li, X. D., & Zhang, G. (2007). Trace metal distribution in sediments of the Pearl River Estuary and the surrounding coastal area, South China. *Environ. Pollut., 147*, 311–323.

Isensee, K. (2016). The Ocean is Losing its Breath. In *Ocean and Climate Scientific Notes, ed. 2* (pp. 20-32).

Ivanov, V. A., & Belokopytov, V. N. (2013). *Oceanogrpahy of the Black Sea.* Sevastopol: National Academy of Science of Ukraine, Marine Hydrophysical Institute.

Jackson, J. B., Kirby, M. X., Berger, W. H., Bjorndal, K. A., Botsford, L. W., Bourque, B. J., . . . Steneck. (2001). Historical Overfishing and the Recent Collapse of Coastal Ecosystems. *Science, 293*, 629– 637.

Jacobs, L., & Emerson, S. (1982). Trace metal solubility in an anoxic fjord. *Earth and Planetary Sci. Lett., 60*, 237-252.

Jeroschewski, P., Steuckart, C., & Kühl, M. (1996). An Amperometric Microsensor for the Determination of H2S in Aquatic Environments. Anal. Chem., 68, 4351–4357.

Jilbert, T., Slomp, C. P., Gustafsson, B. G., & Boer, W. (2011). Beyond the Fe-P-redox connection: preferential regeneration of phosphorus from organic matter as a key control on Baltic Sea nutrient cycles. *Biogeosciences, 8*, 1699 - 1722.

Jones, G. A., & Gagnon, A. R. (1994). Radiocarbon chronology of Black Sea sediments. *Deep-Sea Research l, 41*, 531-557.

Jorgensen, B. B. (1977). The sulfur cycle of a coastal marine sediment (Limfjorden). *Limnol. Oceanogr., 22*, 814-832.

Jorgensen, B. B. (1982). Mineralization of organic matter in the sea bed – the role of sulphate reduction. *Nature, 296*, 643–645.

Jorgensen, B. B., & Kasten, S. (2006). Sulfur Cycling and Methane Oxidation. In H. D. Schulz, & M. Zabel (Eds.), *Marine Geochemistry.* Berlin: Springer.

Jorgensen, B. B., & Nelson, D. C. (2004). Sulfide oxidation in marine sediments: geochemistry meets microbiology. In J. P. Amend, K. J. Edwards, & T. W. Lyons (Eds.), *Sulfur biogeochemistry-past and present* (pp. 283-284). The Geochemical Society of America.

Jorgensen, B. B., & Revsbech, N. P. (1985). Diffusive boundary layers and the oxygen uptake of sediments and detritus. *Limnology and Oceanography, 30*, 111-122.

Jorgensen, B. B., & Sorensen, J. (1985). Seasonal cycles of O2, NO3- and SO42- reduction in estuarine sediments: the significance of an . *Marine Ecology Progress Series, 24*, 65-74.

Jorgensen, B. B., Weber, A., & Zopfi, J. (2001). Sulfate reduction and anaerobic methane oxidation in Black Sea sediments. *Deep Sea REsearch Part I: Oceanographic Research Papers, 48*, 2097-2120.

Jorgensen, B. B., Weber, A., & Zopfi, J. (2001). Sulfate reduction and anaerobic methane oxidation in Black Sea sediments. *Deep Sea REsearch Part I: Oceanographic Research Papers, 48*, 2097-2120.

Jourabchi, P., Van Cappellen, P., & Regnier, P. (2005). Quantitative interpretation of pH distributions in aquatic sediments: A reaction-transport modeling approach. Am. J. Sci., 305, 919–956.

Karlsen, A. W., Cronin, T. M., & Ishman, S. E. (2000). Historical trends in Chesapeake Bay dissolved oxygen based on benthic foraminifera from sediment cores. *Estuaries, 23*, 488–508.

Kemp, W. M., Boynton, W. R., Adolf, J. E., Boesch, D. F., Boicourt, W. C., Brush, G., . . . St. (2005). Eutrophication of Chesapeake Bay: historical trends and ecological interactions. *Marine Ecology Progress Series, 303*, 1-29.

Kemp, W. M., Sampou, P., Caffrey, J., Mayer, M., Henriksen, K., & Boynton, W. R. (1990). Ammonium recycling versus denitrification in chesapeake bay sediments. *Limnol. Oceanogr., 35*, 1545– 1563.

Kemp, W. M., Testa, J. M., Conley, D. J., Gilbert, D., & Hagy, J. D. (2009). Temporal responses of coastal hypoxia to nutrient loading and physical controls. *Biogeosciences, 6*, 2985-3008.

Kerey, I. E., Meric, E., Tunoglu, C., Kelling, G., Brenner, R. L., & Dogan, A. U. (2004). Black Sea-Marmara Sea Quaternary connections: new data from the Bosphorus, Istanbul, Turkey. *Paleogeography, paleolim., paleoecol., 204*, 277-295.

Kirstensen, E., Penha-Lopes, G., Delefosse, M., Valdemarsen, T., Quintana, C. O., & Banta, G. T. (2012). What is bioturbation? The need for a precise definition for fauna in aquatic sciences. *Mar. Ecol. Prog. Ser., 446*, 285-302.

Konovalov, S. K., Luther, G. W., & Yucel, M. (2007). Porewater redox species and processes in the Black Sea sediments. *Chem. Geol., 245*, 254–274.

Kosarev, A. N., & Kostianoy, A. G. (2007). Introduction. In A. N. Kosarev, *The Black Sea Environment* (Vol. 5, pp. 1-10). Berlin: Springer Berlin Heidelberg.

Kostka, J. E., & Luther III, G. W. (1994). Partitioning and speciation of solid phase iron in saltmarsh sediments. *Geochim. Cosmochim. Acta, 58*, 1701–1710.

Kostka, J. E., Thamdrup, B., Glud, R. N., & Canfield, D. E. (1999). Rates and pathways of carbon oxidation in permanently cold Arctic sediments. *Marine Ecology Progress Series, 180*, 7–21.

Kraal, P., Burton, E. D., & Bush, R. T. (2013). Iron monosulfide accumulation and pyrite formation in eutrophic estuarine sediments. *Geochim. et Cosmochim. Acta, 122*, 75–88.

Kristensen, E. (2000). Organic matter diagenesis at the oxic/anoxic interface in coastal marine sediments, with emphasis on the role of burrowing animals. In G. Liebezeit, S. Dittmann, & I. Kröncke (Eds.), *Life at interfaces and under extreme conditons* (Vol. 151, pp. 1-24). Springer, Dordrecht.

Langmead, O., McQuatters-Gollop, A., Mee, L. D., Friedrich, J., Gilbert, A. J., Gomoiu, M.-T., . . . Todorova, V. (2009). Recovery or decline of the northwestern Black Sea: A societal choice revealed by socio-ecological modelling. *Ecological Modelling, 220*, 2927-2939.

Letouzey, J., Biju-Duval, B., Dorkel, A., Gonnard, R., Kristchev, K., Montadert, L., & Sungurlu, O. (1977). The Black Sea-a marginal basin. In *Structural history of the Mediterranean basins* (pp. 363-376). Paris: Editions Technip.

Levanthal, J., & Taylor, C. (1990). Comparison of methods to determine degree of pyritization. *Geochim. et Cosmochim. Acta, 54*, 2621-2625.

Levin, L. A., Ekau, W., Gooday, A. J., Jorissen, F., Middelburg, J. J., Naqvi, W., . . . Zhang, J. (2009). Effects of natural and human-induced hypoxia on coastal benthos. *Biogeosciences, 6*, 3563–3654.

Lewis, B. L., & Landing, W. M. (1991). The biogeochemistry of manganese and iron in the Black Sea. *Deep Sea Research Part A. Oceanographic Research Papers, 38*, S773-S803.

Liaghati, T., Preda, M., & Cox, M. (2004). Heavy metal distribution and controlling factors within coastal plain sediments, Bells Creek catchment, southeast Queensland, Australia. *Environ. Int., 29*, 935–948.

Lichtschlag, A., Donis, D., Janssen, F., Jessen, G. L., Holtappels, M., Wenzhöfer, F., . . . Boetius, A. (2015). Effects of fluctuating hypoxia on benthic oxygen consumption in the Black Sea (Crimean shelf). *Biogeosciences, 12*, 5075–5092.

Lin, Q., Wang, J., Algeo, T. J., Sun, F., & Lin, R. (2016). Enhanced framboidal pyrite formation related to anaerobic oxidation of methane in the sulfate-methane transition zone of the northern South China Sea. *Marine Geology, 379*, 100-108. https://doi.org/10.1016/j.margeo.2016.05.016

Little, S. H., Vance, D., Lyons, T. W., & McManus, J. (2015). Controls on trace metal authigenic enrichment in reducing sediments: Insights from modern oxygen-deficient settings. *Am. J. Sci., 315*, 77-119.

LOICZ. (1995). *Implementation Plan 1995.* Global Change IGBP Report No. 33.

Loucaides, S., Van Cappellen, P., & Behrends, T. (2008). Dissolution of biogenic silica from land to ocean: Role of salinity and pH. *Limnology and Oceanography, 53*, 1614–1621.

Luther III, G. W., Findlay, A. J., MacDonald, D. J., Owings, S. M., Hanson, T. E., Beinart, R. A., & Girguis, P. R. (2011). Thermodynamics and kinetics of sulfide oxidation by oxygen: a look at inorganically controlled reactions and biologically mediated processes in the environment. *Front. Microbiol., 2*, 1-9.

Lyons, T. W. (1997). Sulfur isotopic trends and pathways of iron sulfide formation in upper Holocene sediments of the anoxic Black Sea. *Geochim. et Cosmochim. Acta, 61*, 3367-3382.

Lyons, T. W., Berner, R. A., & Anderson, R. F. (1993). Evidence for large pre-industrial perturbations of the Black Sea chemocline. *Nature*, 538–540.

Lyons, T. W., Reinhard, C. T., & Planavsky, N. J. (2014). The rise of oxygen in Earth's early ocean and atmosphere. *Nature, 506*, 307–315.

Lyons, T. W., Werne, J. P., Hallander, D. J., & Murray, R. W. (2003). Contrasting sulfur geochemistry and Fe/Al and Mo/Al ratios accross the last oxic-to-anoxic trasnition in the Cariaco Basin, Venezuela. *Chem. Geol., 195*, 131-157.

Mackenzie, F. T., & Garrels, R. M. (1966). Chemical mass balance between rivers and oceans. *Am. J. Sci., 264*, 507–525.

Mackenzie, F. T., & Kump, L. R. (1995). reverse weathering, clay mineral formation, and oceanic element cycles. *Science, 270*, 586-587.

McCarthy, J. J., Yilmaz, A., Coban-Yildiz, Y., & Nevins, J. L. (2007). Nitrogen cycling in the offshore waters of the Black Sea. *Estuar. Coast. Shelf Sci., 74*, 493-514.

McCarthy, M. J., McNea, K. S., Morse, J. W., & Gardner, W. S. (2008). Bottom-water hypoxia effects on sediment-water interface nitrogen transformations in a seasonally hypoxic, shallow bay (Corpus christi bay, TX, USA). *Estuar. Coasts, 31*, 521–531.

McCave, I. N., Bryant, R. J., Cook, H. F., & Coughanowr, C. A. (1986). Evaluation of a Laser-Diffraction-Size Analyzer for Use with Natural Sediments. *J. Sediment. Res., 56*, 561-564.

McClelland, J. W., & Valiela, I. (1998). Linking nitrogen in estuarine producers to land-derived sources. *Limnol. Oceanogr., 43*, 577– 585.

McLennan, S. M. (2001.). Relationships between the trace element composition of sedimentary rocks and upper continental crust. *Geochem. Geophys. Geosyst., 2*.

McManus, J., Hammond, D. E., Berelson, W. M., Kilgore, T. E., DeMaster, D. J., & Ragueneau, O. G. (1995). Early diagenesis of biogenic opal: dissolution rates, kinetics, and paleoceanographic implications. *Deep Sea Res. II, 42*, 871–903.

Mee, L. (2006). Reviving dead zones. *Sci. Am., 295*, 78–85.

Meyers, P. A. (1994). Preservation of elemental and isotopic source identification of sedimentary organic matter. *Chem. Geol., 114*, 289-302.

Meyers, P. A. (1994). Preservation of elemental and isotopic source identification of sedimentary organic matter. *Chemical Geology, 114*, 289-302.

Michalopoulos, P., & Aller, R. C. (1995). Rapid clay mineral formation in Amazon delta sediments: reverse weathering and oceanic elemental cycles. *Science, 270*, 614-617.

Middelburg, J. J., & Levin, L. A. (2009). Coastal hypoxia and sediment biogeochemistry. *Biogeosciences, 6*, 1273-1293.

Middelburg, J. J., & Meysman, F. J. (2007). Burial at sea. *Science, 316*, 1294-1295.

Middleburg, J. J., & Levin, L. A. (2009). Costal hypoxia and sediment biogeochemistry. *Biogeosciences, 6*, 1272-1293.

Millero, F. J., Hubinger, S., Fernandez, M., & Garnett, S. (1987). Oxidation of H2S in seawater as a function of temperature, pH, and ionic strength. *Envir. Sci. Technol., 21*, 439-443.

Moodley, L., Middelburg, J. J., Herman, P. M., Soetaert, K., & Lange, G. J. (2005). Oxygenation and organic-matter preservation in marine sediments: Direct experimental evidence from ancient organic carbon-rich deposits. *Geology, 33*, 889–892.

Morford, J. L., & Emerson, S. (1999). The geochemistry of redox sensitive trace metals in sediments. *Geochim. Cosmochim. Acta, 63*, 1735-1750.

Morse, J. W., & Eldridge, P. M. (2007). A non-steady state diagenetic model for changes in sediment biogeochemistry in response to seasonally hypoxic/anoxic conditions in the ‘‘dead zone’’ of the Louisiana shelf. *Mar. Chem., 106*, 239–255.

Morse, J. W., & Luther III, G. W. (1999). Chemical influences on trace metal–sulfide interactions in anoxic sediments. *Geochim. Cosmochim. Acta, 63*, 3373–3378.

Müller, G. (1969). Index of geoaccumulation in sediments of the Rhine River. *Geology Journal*, 109-118.

Müller, G. (1981). The heavy metal pollution of the sediments of Neckars and its tributary: a stock taking. *Chemical Zeitung, 105*, 157-164.

Muramoto, J. A., Honjo, S., Fry, B., Hay, B. J., Howarth, R. W., & Cisne, J. L. (1991). Sulfur, iron and organic carbon fluxes in the Black Sea: sulfur isotopic evidence for origin of sulfur fluxes. *Deep Sea Research Part A. Oceanographic Research Papers, 38*, S1151-S118.

Murray, J. W. (2001). The niche of benthic foraminifera, critical threshold and proxies. *Marine Micropaleontology*, 1-7.

Murray, J. W., Top, Z., & Ozsoy, E. (1991). Hydrographic properties and ventilation of the Black Sea. *Deep-Sea Res., 38*, S663-S689.

Nriagu, J. P. (1988). Quantitative assessment of worldwide contamination of air, water and soils by trace metals. *Nature*, 134–139.

Olson, L. Q. (2017). Trace metal diagenesis in sulfidic sediments: insights from Chesapeake Bay. *Chem. Geol., 452*, 47–59.

Ozsoy, E., & Unluata, U. (1997). Oceanography of the Black Sea: a review of some recent results. *Earth-Science Reviews, 42*, 231-272.

Özsoy, E., Latif, M. A., Tugrul, S., & Ünlüata, Ü. (1995). Exchanges with the Mediterranean, fluxes, and boundary mixing processes in the Black Sea. *Bulletin de l'Institut océanographique, 15*, 1-25.

Panin, N., & Jipa, D. (2002). Danube river sediment input and its interaction with the Northwestern Black Sea. *Estuar. Coast. Shelf Sci., 54*, 551–562.

Passow, U., French, M. A., & Robert, M. (2011). Biological controls on dissolution of diatom frustules during their descent to the deep ocean: Lessons learned from controlled laboratory experiments. *Deep Sea Research Part I - Oceanographic Research Papers, 58*, 1147–1157.

Pinturier-Geiss, L., Méjanelle, L., Dale, B., & Karlsen, D. A. (2002). Lipids as indicators of eutrophication in marine coastal sediments. *J. Microbiol. Meth., 48*, 239-257.

Plante, A., Capet, A., Roevros, N., Grégoire, M., Fagel, N., & Chou, L. (2020a). Impact of bottom hypoxia on the diagenetic processes and benthic fluxes on the North-western shelf of the Black Sea.

Plante, A., Capet, A., Roevros, N., Grégoire, M., Fagel, N., & Chou, L. (2020b). Sulphur and iron biogeochemical cycling in the surface sediments during a seasonal hypoxia.

Popa, A. (1993). Liquid and Sediment Inputs of the Danube River into the North-Western Black Sea. Transport of carbon and nutrients in lakes and estuaries, (Part 6). pp. 137–149.

Poulton, S. W., & Raiswell, R. (2002). The low-temperature geochemical cycle of iron: From continental fluxes to marine sediment deposition. *American Journal of Science, 302*, 774-805.

Rabalais, N. N., Turner, E. R., & Wiseman, Jr., W. J. (2002). Gulf of Mexico hypoxia, aka ''The dead zone.''. *Ann. Rev. Ecol. Syst., 33*, 235-263.

Rabouille, C., Denis, L., Dedieu, K., Stora, G., Lansard, B., & Grenz, C. (2003). Oxygen demand in coastal marine sediments: comparing in situ microelectrodes and laboratory core incubations. *Journal of Experimental Marine Biology and Ecology, 285*, 49-69.

Raiswell, R., & Berner, R. A. (1985). Pyrite formation in euxinic and semi-euxinic sediments. *Am. J. of Sci., 285*, 710-724.

Raiswell, R., Buckley, F., Berner, R. A., & Anderson, T. F. (1988). Degree of pyritisation of iron as a paleoenvironmental indicator of bottom-water oxygenation. *Journal of Sedimentary Research, 58*, 812-819.

Redfield, A. C. (1958). The biological control of chemical factors in the environment. *American Scientist*, 230A, 205-221.

Reschke, K., IttekkotV., & Panin, N. (2002). The nature of organic matter in the Danube river particles and north-western Black Sea sediments. *Estuarine, Coastal and Shelf Science, 54*, 563–574.

Rickard, D. (2006). The solubility of FeS. *Geochim. Cosmochim. Acta., 70*, 5779-5789.

Rickard, D., & Luther, G. W. (2007). Chemistry of iron sulphide. *Chem. Rev., 107*, 514-562.

Riedel, G. F., Sanders, J. G., & Osman, R. W. (1997). Biogeochemical control on the flux of trace elements from estuarine sediments: water column oxygen concentrations and benthic infauna. Estuar. Coast Shelf Sci. 44, . 23–38.

Rigaud, S., Radakovitch, O., Couture, R. M., Deflandre, D., Cossa, D., Garnier, C., & Garnier, J.-M. (2013). Mobility and fluxes of trace elements and nutrients at the sediment-water interface of a lagoon under contrasting water column oxygenation conditions. *Applied Geochemistry, 31*, 35-51.

Robinet, S. (2019). *Hypoxie au cours de l'Holocène sur la plateforme NW de la mer Noire - traceurs géochimiques.* Université de Liège, Liège, Belgique: Unpublished master's thesis.

Robinson, A., Spadini, G., Cloetingh, S., & Rudat, J. (1995). Stratigraphic evolution of the Black Sea: interferences from basin modelling. *Marine and Petroleum Geology, 12*, 821-835.

Roman Romin, O. (2017). *Sedimentological, geochemical and biological proxies as indicators for hypoxia in the northwestern-shelf of the Black Sea (BENTHOX project).* Université de Liège, Liège, Belgique: Unpublished master's thesis.

Ross, D. A., Degens, E. T., & MacIlvaine, J. (1970). Black sea: recent sedimentary history. *Science, 170*, 163-165.

Ross, D. A., Uchupi, E., Prada, K. E., & MacIlvaine, J. C. (1974). Bathymetry and microtopography of Black Sea. In *The Black Seageology, chemistry and biology* (pp. 1-10). Tulsa: AAPG Memoir 20.

Roychoudhury, A. N., Kostka, J. E., & Van Cappellen, P. (2003). Pyritization: a palaeoenvironmental and redox proxy reevaluated. *Estuar. Coast. Shelf Sci, 57*, 1183-1193.

Rudnick, R. L., & Gao, S. (2003). *Composition of the continental crust* (Vol. 3). Amsterdam: Elsevier.

Rullkötter, J. (2006). Organic Matter: The Driving Force for Early Diagenesis. In H. D. Schulz, & M. Zabel, *Marine Geochemistry* (pp. 125-168). Berlin: Springer.

Ruttenberg KC. 1992. Development of a Sequential Extraction Method for Different Forms of Phosphorus in Marine Sediments. Limnology and Oceanography 37: 1460-82.

Ryan, W. B., Pitman, W. C., Major, C. O., Shimkus, K., Moskalenko, V., Jones, G. A., . . . Yuce, H. (1997). An abrupt drowning of the Black Sea shelf. *Marine Geology, 138*, 119-126.

Salomons, W., & Forstner, U. (1984). *Metals in the Hydro Cycle.* Berlin: Springer Verlag.

Salomons, W., Rooij, N. M., Kerdijk, H., & Bril, J. (1987). Sediments as a source for contaminants? *Hydrobi01ogi, 149*, 13- 30.

Santos-Echeandia , J., Prego, R., Cobelo-GarcÌa, A., & Millward, G. E. (2009). Porewater geochemistry in a Galician Ria (NW Iberian Peninsula): implications for benthic fluxes of dissolved trace elements (Co, Cu, Ni, Pb, V, Zn). *Mar. Chem., 117*, 77–87.

Sarazin, G., Michard, G., & Prevot, F. (1999). A rapid and accurate spectroscopic method for alkalinity measurment in sea water samples. Water Ressources, 33, 290-294.

Sayles, F. L., Deuser, W. G., Goudreau, J. E., DIckinson, W. H., Jickells, T. D., & King, P. (1996). The benthic cycle of biogenic opal at the Bermuda Atlantic time series site. *Deep Sea Res. I Oceanogr. Res. Pap., 43*, 383–409.

Schmiedl, G., Mitschele, A., Beck, S., Emeis, K.-C., Hemleben, C., Schulz, H., . . . Weldeab, S. (2003). Benthic foraminiferal record of ecosystem variability inthe eastern Mediterranean Sea during times of sapropel S5and S6 deposition. *Palaeogeography, Palaeoclimatology, Palaeoecology, 190*, 139-164.

Scholz, F., Severmann, S., McManus, J., Noffke, A., Lomnitz, U., & Hensen, C. (2014). On the isotope composition of reactive iron in marine sediments: Redox shuttle versus early diagenesis. *Chemical Geology, 389*, 48-59.

Schulz, H. D., & Zabel, M. (2006). Marine Geochemistry (2nd edition ed.). Springer.

Schulz, H. N., & Jorgensen, B. B. (2001). Big Bacteria. *Annu. Rev. Microbiol., 55*, 105-137.

Schulz, H. N., & Schulz, H. D. (2005). Large sulfur bacteria and the formation of phosphorite. *Science, 307*, 416-418.

Secrieru, D., & Secrieru, A. (2002). Heavy metal enrichment of man-made origin of superficial sediment on the continental shelf of the North-western Black Sea. *Estuarine, Coastal and Shelf Science, 54*, 513–526.

Seeberg- Elverfeldt, J., Schlüter, M., Feseker, T., & Kölling, M. (2005). Rhizon sampling of pore waters near the sediment-water interface of aquatic systems. *Limnology and oceanography : Methods, 3*, 361–371.

Seitaj, D., Schauer, R., Sulu-Gambari, F., Hidalgo-Martinez, S., Malkin, S. Y., Burdorf, L. D., . . . Meysman, F. J. (2015). Cable bacteria generate a firewall against euxinia in seasonally hypoxic basins. *PNAS, 112*, 13278-13283.

Sen Gupta, B. K. (Ed.). (1999). *Modern Foraminifera.* Dordrecht: Kluwer.

Shaffer, G. (1986). Phosphate pumps and shuttles in the Black Sea. *Nature, 321*, 515–517.

Shaw, T. J., Gieskes, J. M., & Jahnke, R. A. (1990). Early diagenesis in differing depositional environments: the response of transition metals in pore water. *Geochim. Cosmochim., 54*, 1233–1246.

Sinninghe Damsté, J. S., & De Leeuw, J. W. (1990). Analysis, structure and geochemical significance of organically-bound sulphur in the geosphere: State of the art and future research. *Organic Geochemistry, 16*, 1077-1101.

Slomp, C. P., Epping, E. H., Helder, W., & Van Raaphorst, W. (1996). A key role for iron-bound phosphorus in authigenic apatite formation in North Atlantic continental platform sediments. *J. Mar. Res., 54*, 1179–1205.

Slomp, C. P., Mort, H. P., Jilbert, T., Reed, D. C., Gustafsson, B. G., & Wolthers, M. (2013). coupled dynamics of iron and phosphorus in sediments of an oligotrophic coastal basin and the impact of anaerobic oxidation of methane. *PLoS ONE, 8*.

Soetaert, K., Herman, P. M., & Middelburg, J. J. (1996a). A model of early diagenetic processes from the shelf to abyssal depths. *Geochim. Cosmochim. Acta., 60*, 1019-1040.

Soetaert, K., Herman, P. M., & Middelburg, J. J. (1996b). Dynamic response of deep-sea sediments to seasonal variations: A model. *Limnology and Oceanography, 41*, 1651-1668.

Soetaert, K., Petzoldt, T., & Meysman, F. J. (2010a). marelac: Tools for Aquatic Sciences R package

version 2.1.

Sørensen, J., & Jørgensen, B. B. (1987). Early diagenesis in sediments from Danish coastal waters: Microbial activity and Mn-Fe-S geochemistry. *Geochim. et Cosmo. Ac., 51*, 1583-1590.

Soulet, G., Ménot, G., Lericolais, G., & Bard, E. (2011). A revised calendar age for the last reconnection of the Black Sea to the global ocean. *Quaternary Sci. Rev., 30*, 1019-1026.

Staneva, J., & Stanev, E. (2002). Water mass formation in the Black Sea during 1991–1995. *J. Marine Syst., 32*, 199-218.

Steckbauer, A., Duarte, C. M., Carstensen, J., Vaquer-Sunyer, R., & Conley, D. J. (2011). Ecosystem impacts of hypoxia: Thresholds of hypoxia and pathways to recovery. *Environ. Res. Lett., 6*, 025003.

Stramma, L., Johnson, G. C., Sprintall, J., & Mohrholz , V. (2008). Expanding oxygen-minimum zones in the tropical oceans. *Science, 320*, 655-658.

Strous, M., & Jetten, M. S. (2004). Anaerobic oxidation of methane and ammonium. *Annu. Rev. Microbiol., 58*, 99-117.

Struck, U., Emeis, K.-C., Voss, M., Christiansen, C., & Kunzendorf, H. (2000). Records of southern and central Baltic Sea eutrophication in δ 15N of sedimentary organic matter. *Mar. Geol., 164*, 157-171.

Suess, E. (1979). Mineral phases formed in anoxic sediments by microbial decomposition of organic matter. *Geochim. Cosmochim. Acta, 43*, 339–352.

Sundby, B., Anderson, L. G., Hall, P. O., Iverfeld, A., Rutgers van der Loeff, M. M., & Westerlund, S. F. (1986). The effect of oxygen on release and uptake of cobalt, manganese, iron and phosphate at the sediment–water interface. *Geochim. Cosmochim. Acta, 50*, 1281–1288.

Sundby, B., Gobeil, C., Silverberg, N., & Mucci, A. (1992). The phosphorus cycle in coastal marine sediments. *Limnol. Oceanogr., 37*, 1129-1145.

Taylor, S. R. (1964). Abundance of chemical elements in the continental crust: a new table. *Geochimica et Cosmochimica Acta, 28*, 1273-1285.

Testa, J. M., & Kemp, W. M. (2011). Oxygen—dynamics and biogeochemical consequences. In J. M. Testa, W. M. Kemp, E. Wolansky, & D. S. McLusky (Eds.), *Treatise on Estuarine and Coastal Science* (Vol. 5, pp. 163-199). Waltham: Academic Press.

Thamdrup, B. (2000). Bacterial manganese and iron reduction in aquatic sediments. *Adv. Microb. Ecol., 16*, 41–84.

Thamdrup, B., & Canfield, D. E. (1996). Pathways of carbon oxidation in continental margin sediments off central Chile. *Limnol. Oceanogr., 41*, 1629-1650.

Thamdrup, B., Canfield, D. E., Ferdelman, T. G., Glud, R. N., & Gundersen, J. K. (1996). A biogeochemical survey of the anoxic basin Golfo Dulce, Costa Rica. *Rev. Biol. Trop., 3*, 19–33.

Thamdrup, B., Fossing, H., & Jorgensen, B. B. (1994). Manganese, iron, and sulfur cycling in a coastal marine sediment, Aarhus Bay, Denmark. *Geochim. Cosmochim. Acta, 58*, 5115-5129.

Thamdrup, B., Hansen, J. W., & Jorgensen, B. B. (1998). Temperature dependence of aerobic respiration in a coastal sediment. *FEMS Microbiol. Ecol., 25*, 189-200.

Thomas, E., Gapotchenko, T., Varekamp, J. C., Mecray, E. L., & Buchholtz ten Brink, M. R. (2000). Benthic Foraminifera and Environmental Changes in Long Island Sound. *Journal of Coastal Research, 16*, 641-655.

Tribovillard, N., Algeo, T. J., Lyons, T., & Riboulleau, A. (2006). Trace metals as paleoredox and

paleoproductivity proxies: an update. *Chem. Geol.*, 12-32.

Ukrainskii V.V. & Popov Y.I. 2009. Climatic and hydrophysical conditions of the development of hypoxia in waters of the northwest shelf of the Black Sea. *Physical Oceanography* 19 (3), 140–150. http://dx.doi.org/10.1007/s11110-009-9046-6

Ukrayinskyy, V., Komorin, V., Kovalyshyna, S., Hushchyna, K., Korshenko, A., Mikaelyan, A., . . . Zhugailo, S. (2017). *National Pilot Monitoring Studies & Joints Open Sea Surveys in Georgia, Russian Federation and Ukraine, 2016.*

Ünlüata, Ü., Oğuz, T., Latif, M. A., & Özsoy, E. (1990). *On the physical oceanography of the Turkish straits* (NATO /ASI Series Kluwer ed.). Dordrecht: Pratt, L.J.

van de Velde, S., Callebaut, I., Hidalgo-Martinez, S., Antler, G., Leermakers, M., & Meysman, F. J. (2018). Early diagenesis of carbon, iron and sulphur in salt marsh sediments: the importance of burrowing fauna. In S. van de Velde, *Electron shuttling and elemental cycling in the seafloor*. Brussels: VUBPRESS.

van Helmond, N. A. G. M., Jilbert, T., & Slomp, C. P. (2018). Hypoxia in the Holocene Baltic Sea : Comparing modern versus past intervals using sedimentary trace metals. *Chemical Geology*, *493*, 478-490. https://doi.org/10.1016/j.chemgeo.2018.06.028

Voss, M., Larsen, B., Leivuori, M., & Vallius, H. (2000). Stable isotope signals of eutrophication in Baltic Sea sediments. *J. Marine Syst., 25*, 287-298.

Wenzhöfer, F., & Glud, R. N. (2004). Small-scale spatial and temporal variability in coastal benthic O2 dynamics: Effects of fauna activity. *Limnol. Oceanogr., 49*, 1471-1481.

Wijsman, J. W., Herman, P. M., Middelburg, J. J., & Stoetaert, K. (2002). A model for early diagenetic processes in sediments of the continental shelf of the Black Sea. *Estuarine, Coastal and Shelf Science, 54*, 403-421.

Wijsman, J. W., Middelburg, J. J., & Heip, C. H. (2001a). Reactive iron in Black Sea Sediments: implications for iron cycling. *Marine Geology, 172*, 167–180.

Wijsman, J. W., Middelburg, J. J., Herman, P. M., Böttcher, M. E., & Heip, C. H. (2001b). Sulfur and iron speciation in surface sediment along the northwestern margin of the Black Sea. *Marine Chemistry, 74*, 261-278.

Wijsman, J., Herman, P., & Gomoiu , M. T. (1999). Spatial distribution in sediment characteristics and benthic activity on the northwestern Black Sea shelf. *Mar. Ecol. Prog. Ser., 181*, 25–39.

Wilkin, R. T., Barnes, H. L., & Brantley, S. L. (1996). The size distribution of framboidal pyrite in modern sediments: An indicator of redox conditions. *Geochim. Cosmochim. Ac., 60*, 3897–3912.

Windom, H. S. (1989). Natural trace metal concentrations in estuarine and coastal marine sediments of the southeastern United States. *Environ. Sci. Technol., 23*, 314–320.

Wollast, R. (1998). Evaluation and comparison of the global carbon cycleinthe coastal zone and in the open ocean. In R. Wollast, K. H. Brink, & A. R. Robinson (Eds.), *The Sea: Ideas and Observations on Progress in the Study of the Seas.* (Vol. 10, pp. 213-252). Hoboken: John Wiley & sons.

Wüchter, C., Abbas, B., Coolen, M. J., Herfort, L., van Bleijswijk, J., Timmers, P., . . . Damsté, J. S. (2006). Archeal nitrification in the oceans. *P. Natl. Acad. Sci. USA, 103*, 12317-12322.

Yanko-Hombach, V., Mudie, P. J., Kadurin, S., & Larchenkov, E. (2014). Holocene marine transgression in the Black Sea: New evidence from the northwestern Black Sea shelf. *Quaternary International, 345*, 100–118.

Zahra, A., Hashmi, M. Z., Malik, R. N., & Ahmed, Z. (2014). Enrichment and geo-accumulation of heavy metals and risk assessment of sediments of the Kurang Nallah—Feeding tributary of the Rawal Lake Reservoir, Pakistan. *Science of The Total Environment, 470-471*, 925-933.

Zaïbi, C., Carbonel, P., Kamoun, F., Fontugne, M., Azri, C., Jedoui, Y., & Montacer, M. (2012). Evolution of the sebkha Dreîaa (South-Eastern Tunisia, Gulf of Gabes) during the Late Holocene: response of ostracod assemblages. *Revue de Micropaléontologie, 55*, 83-97.

Zhang, J. Z., & Millero, F. J. (1993). The products from the oxidation of H2S in seawater. *Geochim. et Cosmochim. Acta, 57*, 1705-1718.

Zhang, R., Follows, M. J., Grotzinger, J. P., & Marshall, J. (2001). Could the Late Permian deep ocean have been anoxic? *Paleoceanography, 16*, 317-329.

Zillén, L., Conley, D. J., Andrén, T., Andrén, E., & Björck, S. (2008). Past occurrences of hypoxia in the Baltic Sea and the role of climate variability,environmental change and human impact. *81Earth-Science Reviews, 91*, 77–92.

Zimmerman, A. R., & Canuel, E. A. (2000). A geochemical record of eutrophication and anoxia in Chesapeake Bay sediments: anthropogenir influence on organic matter composition. *Marine Chemistry, 69*, 117-137.

Zimmerman, A. R., & Canuel, E. A. (2002). Sediment geochemical records of eutrophication in the mesohaline Chesapeake Bay. *Limnol. Oceanogr., 47*, 1084-1093.

Appendix A

Reconstruction of hypoxia on the NW shelf of the Black Sea during Holocene via a multiproxy approach

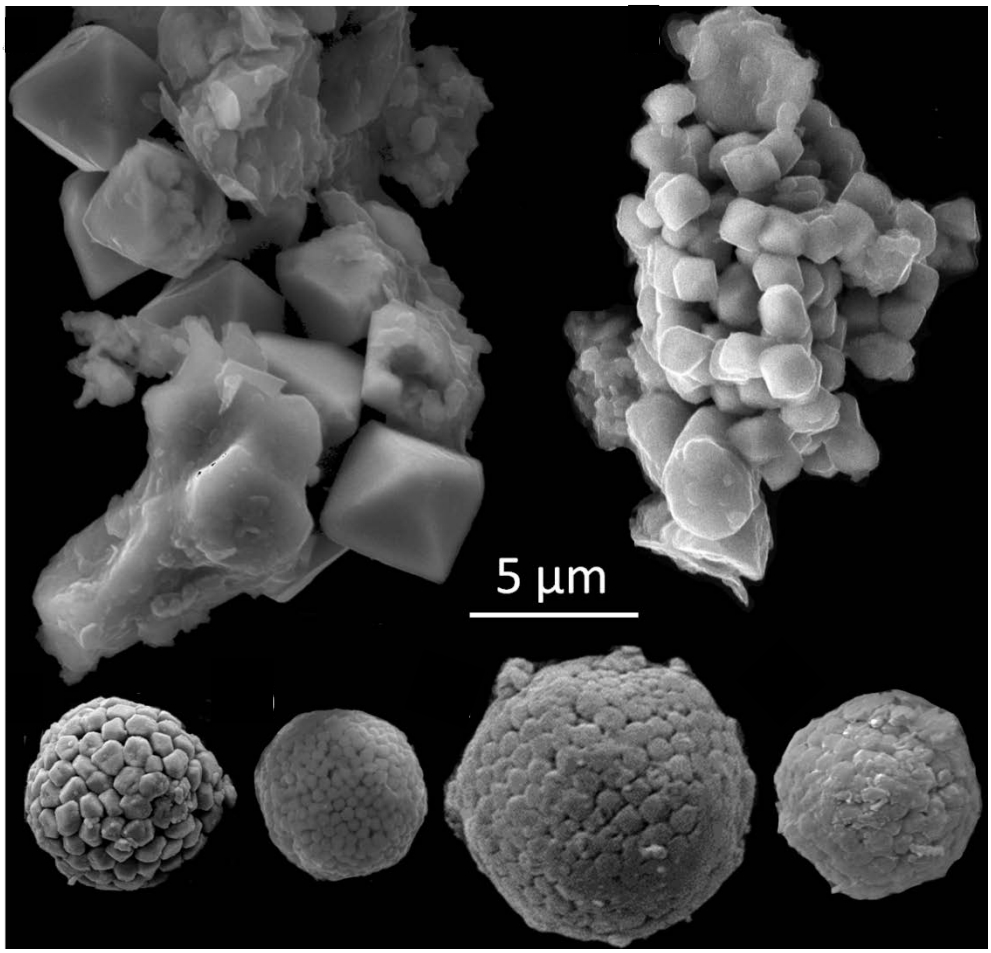

Picture of the different morphologies of framboidal pyrites from Odessa Bay

SEM images by Sarah Robinet

Reconstruction of hypoxia on the NW shelf of the Black Sea during Holocene via a multiproxy approach

Audrey Plante, Sarah Robinet, Alice Matossian, Marilaure Grégoire, Arthur Capet, Nathalie Fagel, Lei Chou.

This appendix is about a multiproxy study on the shelf of the Black Sea realized by Robinet et al. Following this work, a draft article* was written. This appendix constitutes a summary of this draft.

*Sarah Robinet, Alice O. Matossian, Arthur Capet, Lei Chou, François Fontaine, Marilaure Grégoire, Gilles Lepoint, Natalia Piotrowsk, Audrey Plante, Olaya Román Romín and Nathalie Fagel (in preparation) A multi-proxy approach to reconstruct hypoxia on the NW Black Sea shelf over the Holocene.

A.1 Introduction

Dissolved oxygen is an essential element to maintain the life in ecosystems and participate in various biogeochemical cycles. Oxygen depletion causes important perturbations of marine ecosystems and impairs fisheries. The degree of oxygen content has different levels: oxic, hypoxic and anoxic. Some authors consider that the hypoxic threshold is reached when the oxygen concentration is below 63 μM (2 mg L^{-1}) (Diaz & Rosenberg, 2008). Over time, more and more areas are affected by hypoxia and the frequency and duration of its occurrence are variable (Capet et al., 2013). The Black Sea is known to be one of the largest anoxic basins of the world and its north-western (NW) shelf has been subject to seasonal hypoxia since the 1970s (Friedrich et al., 2002). The shelf receives significant riverine inputs from the Danube, Dniestr, Bug and Dniepr which influence the productivity of the region. During the summer, the water column of the shelf is stratified allowing the separation of the oxic layer from the hypoxic bottom waters.

In order to better understand better how the hypoxia develops, it is necessary to study its history. A few investigations were carried out on the oxygenation levels in the coastal sediments of the Black Sea but not with a multiproxy approach.

The aim of this chapter is to reconstruct the age models of the shelf sediments and to identify deoxygenation levels during the Holocene on the NW shelf using different proxies:

- Biological: foraminifera
- Geochemical: organic matter contents and redox-sensitive elements
- Mineralogical: framboidal pyrite

A.2 Material and methods

Two sediment cores were retrieved with a gravity corer on the Ukrainian shelf. The first was collected close to the Danube Delta (GC7) and the second in the Odessa Bay (GC15).

The cores were cut into half-cylinders. Plastic sleeves were inserted into one half-cylinder and the second half was sliced at 1-cm intervals. Each slice was used for sedimentological (X-Ray diffraction and granulometry) and geochemical (ICP-MS and ICP-OES, reactive iron extraction) analyses as well as for foraminifera and framboidal pyrite observations.

A.3 Results

Core chronology

The chronology of the cores was estimated using ^{210}Pb analysis and AMS^{14}C dating. From these results, the age-depth models were determined with the software CLAM v2.2.

The bottom of the GC7 core was estimated to be at 250 AD and the bottom of the GC15 was 5400 BC. Table A.1 summarizes the details of the chronology with sedimentation rates using the local reservoir ages: 126 ± 40 years for GC7 and from 13 ± 60 years to 135 ± 60 years for GC15.

Table A.1. Chronology and sedimentation rates of the cores.

	Depth (cm)	**Estimated age**	**Sedimentation rate**
	cm	BC/AD	cm/year
GC7	0 → 117.5	2016 → 1700-1900AD	0.5
	117.5 → 150.5	1700-1900AD → 910-1070AD	0.04
	150.5 → 211	910-1070AD → 110BC-540AD	0.08
GC15	0 →25	2016 → 1967-1987AD	0.65
	25 → 166.5	1967-1987AD → 4803-4609BC	0.02
	166.5 → 220.5	4803-4609BC → 5028-4810BC	0.28
	220.5 → 281.5	5028-4810BC → 5502-5126BC	0.15

Benthic foraminifera

Foraminifera are organisms sensitive to oxygen concentration and can be used to follow the evolution of oxygen levels. *Ammonia* and *Elphidium* species were observed in previous studies in the Black Sea and on the shelf. *Ammonia* is known to be more resistant to oxygen

depletion than *Elphidium*. Thus, the A-E index can be used to identify hypoxic events in shallow environments. In both cores, *Ammonia* and *Elphidium* were detected and their numbers varied depending on their location on the shelf and the depth. Few individuals were found in GC7 in all the granulometric fractions while several hundred to thousands of individuals were observed in GC15. *Ammonia* genius represented more than 93 % of the individuals identified and *Elphidium* 0.5 % for GC7 and 1.8 % for GC15. The calculated A-E index ranged from 92 to 100 % for GC7 and from 94 to 100% for GC15. As suggested by Sen Gupta et al. (1996), an index close to 100 % affirms an hypoxic environment.

Organic carbon content

Organic carbon contents were estimated by IRMS and the results revealed similar contents for both cores (GC7: 1.1 wt%; GC15: 1.9 wt%). For both cores, the organic carbon content and the C/N ratio decreased with depth. In the upper 97 cm of GC7 and 60 cm of GC15 contained 1.1 wt% and 2.1 wt% of organic carbon respectively with C/N ratios of 10.1 and 13.3 respectively. In the bottom part(from 201 to 209 and from 223 to 297 cm), the sediments of GC7 and GC15 had 0.7 wt% and 0.8 wt % of organic carbon respectively with C/N ratios of 8.5 and 7.6 respectively.

Trace metals enrichment

Vanadium was correlated to Al with R^2 = 0.94 for GC7 and R^2 = 0.86 for GC15. The sediments showed a slight enrichment in uranium for GC15 with EF (Enrichment Factor) value of 1.5.

The link between Fe and detrital elements was determined using Principal Component Analysis (PCA). The statistics showed no correlation for GC7 and for the bottom part of GC15. Iron appeared to be related to sulphide. However, in the upper part of GC15 (<60 cm) iron is associated with detrital elements showing a modification of the behaviour of iron.

The speciation of iron was determined with a sequential extraction method (Kraal et al., 2013). Reactive iron represented 36 ± 4 % of the total iron for GC7 and 38 ± 6 % of total iron for GC15. Reactive iron was homogeneously distributed over the whole core of GC7 while the GC15 exhibited variations with depth ranging from 32 to 55 % of the total iron. Fe_H fraction (FeS, siderite, ferrihydrite, akageneite and lepidocrocite) was dominant for GC7 with 87 ± 4 % of the reactive iron and pyrite iron represented 6 ± 2 %. For GC15, iron linked to pyrite increased with depth going from 20 to 80 %, iron oxides decreased with depth from 20 to 3 % and Fe_H fraction decreased from 50 to 11 % revealing the reduction of iron.

Framboidal pyrite

No framboidal pyrites were found for GC7 by XRD and SEM but traces of them were identified for GC15 (Figure A.1). Two groups of diameters were established: (1) 3-6 μm and (2) 6-10μm. For both cores, no pyrite framboids were detected at the sediment-water interface.

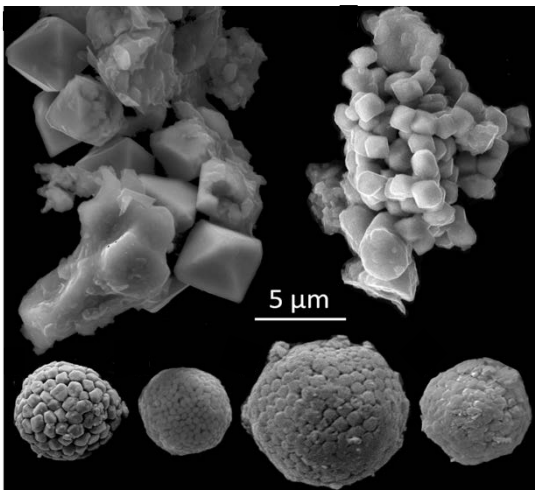

Figure A.1. SEM image of the sediments of Odessa Bay showing different morphologies of framboidal pyrites (From Robinet et al., 2020, in preparation).

A.4 Discussion

Age correlation with hypoxic periods of the Baltic Sea

Hypoxic periods in the Baltic Sea have been highlighted recently (Zillén et al., 2008; Jilbert & Slomp, 2013).

- Holocene Thermal Maximum (HTM- 8000-4000 cal. yr BP)
- Medieval Climate Anomaly (MCA, 1400-700 cal. yr BP)
- Modern hypoxic period (from 1800 AD to present)

Using the same drivers, the identification of these periods was performed on the NW shelf of the Black Sea. The HTM was identified between 50 cm and 281.5 cm, the MCA between 36 cm and 49 cm, and the Modern hypoxic period in the first 28 cm. Small and large framboidal pyrites were observed in the HTM, only small ones were found in the MCA but other framboids were also detected out of the hypoxic zones. So, the drivers used for the Baltic Sea do not work for the Black Sea.

Moreover, for GC7, the HTM was not identified and the MCA was between 137 cm and 180 cm. The results of XRD and SEM revealed a small presence of pyrite. The Modern hypoxic period corresponded to the first 106 cm of the core GC7 and no framboids were found during this period suggesting oxic conditions during these periods contrary to the results of the Baltic Sea.

Framboidal pyrites as proxy

Usually, the diameters of small framboids with a small standard deviation are characteristic of anoxic-euxinic basins (Wilkin et al., 1996). In the Odessa Bay, nine samples were considered to be in the field of anoxic-euxinic conditions. Quantification of Mo is useful to distinguish euxinic from anoxic conditions (Tribovillard et al., 2006) because this element is enriched under sulphidic conditions. The sample between 163 cm and 164 cm was selected to represent the small framboids which were analyzed for Mo. The results revealed the absence of Mo enrichment leading to the qualification of the environment as anoxic. According to Wilkin et al. (1996), modern hypoxic and oxic basins are prone to forming framboids with larger diameters and a wide standard deviation and they cannot be distinguished based only on the framboid study. For GC15, four samples belonged to the hypoxic-oxic field revealing that the Odessa Bay was subject to an alternance of regimes between anoxic and hypoxic-oxic conditions during the Holocene (Figure A.2).

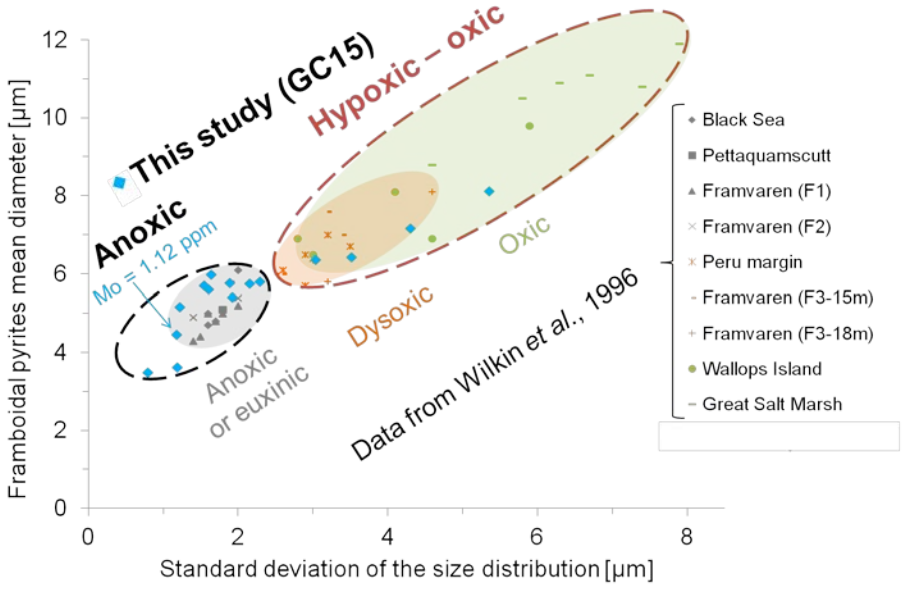

Figure A.2. Mean diameter of framboids *vs*. standard deviation of the size distribution distinguishing between anoxic and hypoxic-oxic environments according to Wilkin et al. (1996). Figure from Robinet et al. (2020, in preparation).

For GC7, no framboidal pyrites were detected inferring an oxic regime as suggested by the classification of Bond and Wignall (2010). In other modern basins, framboidal pyrites were found indicating that the oxygen levels were not the only driver controlling the formation of pyrites.

Other unusable elements as proxy

- Foraminifera were not a usable driver in this study due to the lack of results and for one major reason. The salinity plays an important role and needs to be constant to study the diversity of these organisms which are influenced by this parameter. According to Yanko-Homback (2007), a decrease in salinity would lead to a depletion of the assemblage. In this investigation, the abundance of *Ammonia* could be attributed to the decrease in salinity rather than oxygen depletion in the water column.

  Moreover, other parameters may interfere with the benthic foraminifera such as the substrate, temperature, light and nutrient availability (Armstrong & Brasier, 2013).

- Fluctuations in organic carbon contents were not significant to interpret and to identify hypoxic and anoxic conditions in the shelf sediments as made for the Baltic Sea (Jilbert & Slomp, 2013; Dijkstra et al., 2016; van Helmond et al., 2018).
- Trace metal quantification in both cores revealed no enrichment in V and Mo. A slight enrichment in U was found for GC15 suggesting reducing conditions in agreement with the observation of framboids. This enrichment was not found for GC7. V was correlated to Al suggesting the detrital origin of V which could not be used as proxy for hypoxia. Mo concentrations showed that euxinic conditions were unlikely to occur on the shelf.
- Total iron concentrations did not allow the identification of the hypoxic periods. Iron distribution for GC15 showed changes in behaviour with depth, consistent with the results of iron speciation which revealed the iron reduction due to the degradation of organic matter. No information could be highlighted about water column oxygenation.

A.5 Conclusions and perspectives

The NW shelf of the Black Sea has been prone to seasonal hypoxia since the 1970s and the study of hypoxic-anoxic events during the Holocene is complex. Sedimentological and chronological studies allowed the estimation of an age-depth model and showed that the sediments deposited on the shelf were different in the Danube delta area and in the Odessa

Bay. The bottom of the core was dated 8000 years ago for the Odessa Bay revealing the passage from lacustrine or semi-marine environment to a marine environment. Contrarily, the Danube delta sediments were dated as 250AD and did not record this change of environment. This study highlighted that the use of typical proxies applied to other basins could not be adapted to the shelf of the Black Sea. Framboidal pyrites were the most feasible proxy to study the hypoxic events on the shelf but further research are required to study: (1) the formation of small framboidal pyrites in the water column during seasonal hypoxia, (2) the formation of large framboids in the sediments at low oxygen levels, (3) the kinetics of framboid formation and (4) the conservation of pyrite in the sediments under oxic conditions. The study of sediments at the seawater-sediment interface and of particulate phase in the water column could improve the comprehension of mechanisms of framboid formation during hypoxic events. In addition, it would be interesting to consider the abundance (Bond and Wignall, 2010) and the morphology of framboidal pyrites which could provide indications on the environment in which they were formed (Lin et al., 2016).

References

Armstrong, H. A., & Brasier, M. D. (2013). Foraminifera. In Microfossils (p. 142-187). John Wiley & Sons, Ltd. https://doi.org/10.1002/9781118685440.ch15

Bond, D. P., & Wignall, P. B. (2010). Pyrite framboid study of marine Permian–Triassic boundary sections: A complex anoxic event and its relationship to contemporaneous mass extinction. GSA Bulletin, 122, 1265–1279.

Capet, A., Beckers, J.-M., & Gregoire, M. (2013). Drivers, mechanisms and long-term variability of seasonal hypoxia on the Black Sea northwestern shelf – is there any recovery after eutrophication? Biogeosciences, 10, 3943–3962.

Diaz, R. J., & Rosenberg, R. (2008). Spreading dead zone and consequences for marine ecosystems. Science, 321, 926-929.

Dijkstra, N., Slomp, C. P., & Behrends, T. (2016). Vivianite is a key sink for phosphorus in sediments of the Landsort Deep, an intermittently anoxic deep basin in the Baltic Sea. Chemical Geology, 438, 58-72. https://doi.org/10.1016/j.chemgeo.2016.05.025

Friedrich, J., Dinkel, C., Friedl, G., Pimenov, N., wijsman, J., Gomoiu, M.-T., . . . Wehrli, B. (2002). Benthic nutrient cycling and diagenetic pathways in the North-western Black Sea. Estuarine, Coastal and Shelf Science, 54, 369-383.

Jilbert, T., Slomp, C. P., Gustafsson, B. G., & Boer, W. (2011). Beyond the Fe-P-redox connection: preferential regeneration of phosphorus from organic matter as a key control on Baltic Sea nutrient cycles. Biogeosciences, 8, 1699 - 1722.

Lin, Q., Wang, J., Algeo, T. J., Sun, F., & Lin, R. (2016). Enhanced framboidal pyrite formation related to anaerobic oxidation of methane in the sulfate-methane transition zone of the northern South China Sea. Marine Geology, 379, 100-108. https://doi.org/10.1016/j.margeo.2016.05.016

van Helmond, N. A. G. M., Jilbert, T., & Slomp, C. P. (2018). Hypoxia in the Holocene Baltic Sea : Comparing modern versus past intervals using sedimentary trace metals. Chemical Geology, 493, 478-490. https://doi.org/10.1016/j.chemgeo.2018.06.028

Wilkin, R. T., Barnes, H. L., & Brantley, S. L. (1996). The size distribution of framboidal pyrite in modern sediments: An indicator of redox conditions. Geochim. Cosmochim. Ac., 60, 3897–3912.

Yanko-Hombach, V., Mudie, P. J., Kadurin, S., & Larchenkov, E. (2014). Holocene marine transgression in the Black Sea: New evidence from the northwestern Black Sea shelf. Quaternary International, 345, 100–118.

Appendix B

B.1 EGU general assembly, Vienna, Austria, 2017

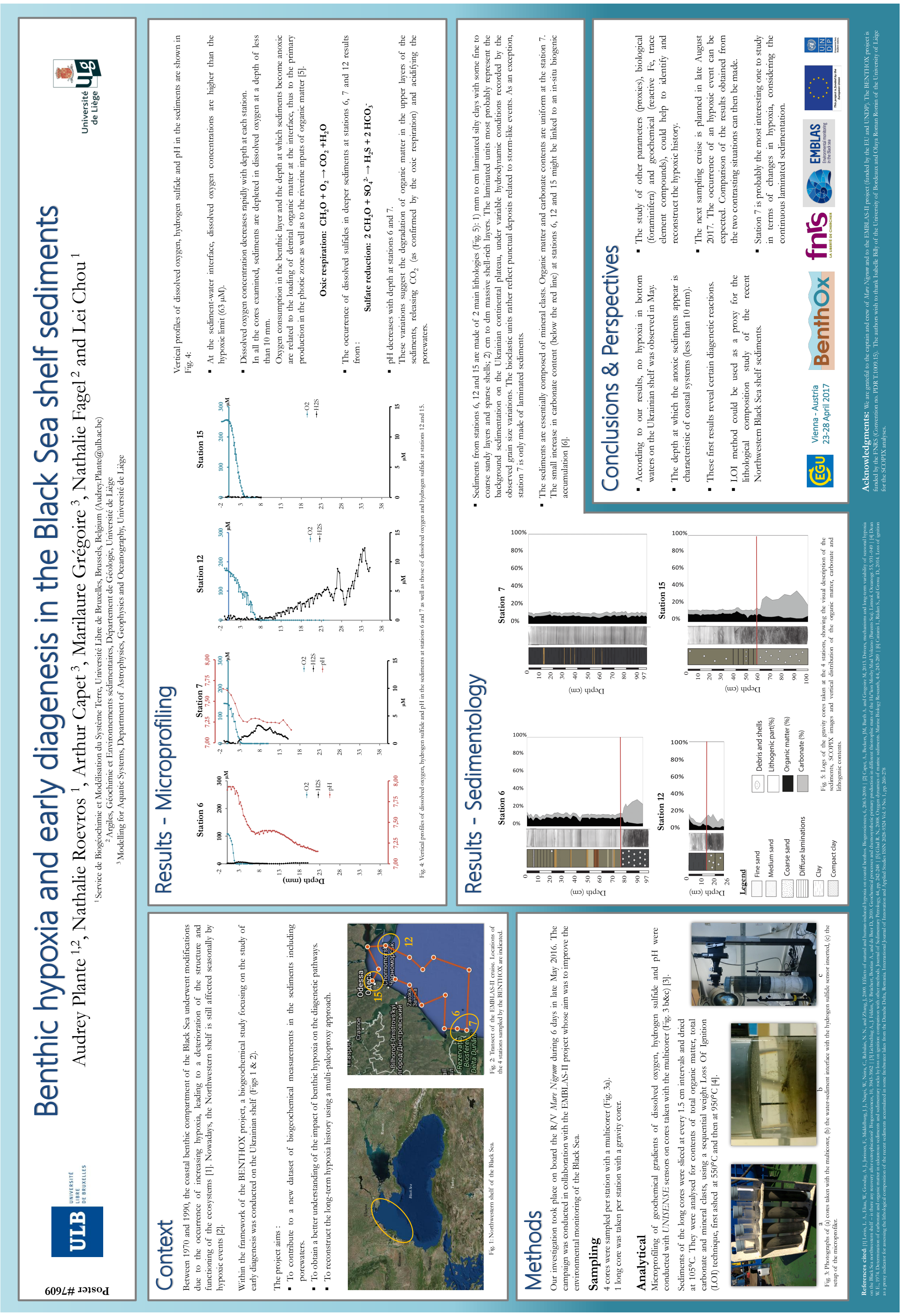

Hypoxia evolution on the Ukrainian Shelf of the Black Sea

Audrey Plante[1,2], Nathalie Roevros[1], Olaya Roman Romin[2], Arthur Capet[3], Marilaure Grégoire[3], Nathalie Fagel[2], Lei Chou[1]

[1] Service de Biogéochimie et Modélisation du Système Terre, Université Libre de Bruxelles, Brussels, Belgium (Audrey.Plante@ulb.ac.be),
[2] Argiles, Géochimie et Environnements sédimentaires, Département de Géologie, Université de Liège,
[3] Modelling for Aquatic Systems, Department of Astrophysics, Geophysics and Oceanography, Université de Liège

Poster #3052

Context & Study area

On the Northwestern shelf of the Black Sea, the occurrence of seasonally hypoxia has increased at the end of the 20th century. Deoxygenation influences the benthic compartment and causes a deterioration of the ecosystem functioning [1]. River deltas and continental shelf areas are major contributors to biogeochemical cycles of carbon and associated elements (N, P, Si and S) [2].

Fig. 1: Map of the Northwestern shelf of the Black Sea and the transect of the EMBLAS-II cruise. Locations of the 4 stations sampled by the BENTHOX are indicated.

Within the framework of the BENTHOX project, a biogeochemical investigation focusing on the study of early diagenesis was conducted on the Ukrainian shelf.

The project aims :

- To contribute to a new dataset of biogeochemical measurements in the sediments including porewaters.
- To obtain a better understanding of the impact of benthic hypoxia on the diagenetic pathways.
- To reconstruct the long-term hypoxia history using a multi-paleoproxy approach.

Methods

In collaboration with the EMBLAS project whose aim was to improve the environmental monitoring of the Black Sea, we participated in a campaign on board the *R/V Mare Nigrum* during 6 days in May 2016 (Fig. 1).

Sampling

Four cores per station were taken with a multicorer (Fig. 2a). Porewaters were extracted using the Rhizon technique under N_2 atmosphere.
One long core was taken with a gravity corer.

Analytical

Short cores
Microprofiling of geochemical gradients of dissolved oxygen and pH were conducted with *UNISENSE* sensors on cores taken with the multicorer (Fig. 2b) [3].
Sulfate and chloride concentrations were measured by ionic chromatography and sulfide concentrations were determined by colorimetry.
Sediments were sliced at every 2 cm intervals and dried at 105 °C. They were analyzed for contents of total organic matter, total carbonate and mineral clasts, using a sequential weight Loss Of Ignition (LOI) technique, first ashed at 550 °C and then at 950 °C [4].

Long cores
Archived sediments were analyzed continuously every mm by SCOPIX and core scanner X-Ray Fluorescence at the University of Bordeaux. Magnetic susceptibility data were acquired at 1 cm intervals using Bartington MS2 susceptibility system.
Sediments were sliced at every 1.5 cm intervals and dried at 105 °C, then analyzed using the same LOI method.

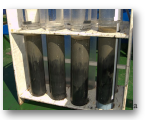

Fig. 2: Photographs of (a) cores taken with the multicorer, (b) the water-sediment interface with the hydrogen sulfide sensor inserted.

Results

Microprofiling

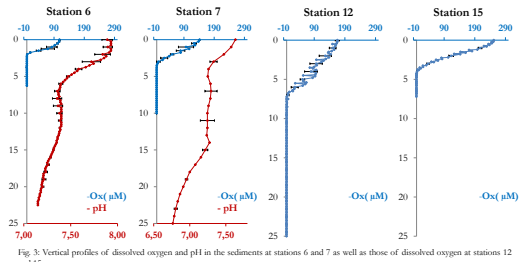

Fig. 3: Vertical profiles of dissolved oxygen and pH in the sediments at stations 6 and 7 as well as those of dissolved oxygen at stations 12 and 15.

Dissolved oxygen and pH profiles are shown in Fig. 3:

- The dissolved oxygen concentration exceeds the hypoxic limit (63 µM) at the sediment-water interface.
- All cores studied show that the sediments are depleted in dissolved oxygen at less than 10 mm-depth.
  Oxygen consumption in the benthic layer and the depth at which sediments become anoxic are related to the loading of detrital organic matter at the interface, thus to the primary production in the photic zone as well as to the riverine inputs of organic matter [5].

Oxic respiration: $CH_2O + O_2 \rightarrow CO_2 + H_2O$

- pH decreases with depth at stations 6 and 7.
  These variations suggest the degradation of organic matter in the upper layers of the sediments, releasing CO_2 (as confirmed by the oxic respiration) and acidification of the porewaters.

Focus on stations 6 & 7 – Sediment & Porewaters

Vertical profiles of organic matter content, porosity, total sulfide and sulfate concentrations are shown for stations 6 & 7 in Fig. 4:

- Small decrease in organic matter content with depth. Station 6 has a higher organic matter content than station 7, probably due to the riverine inputs. The variations are more important at station 6 and fluctuate between 15 % and 5 %.
- Porosities are higher at station 6 than at station 7 due to a sandier sediment texture at station 6.
- Sulfate concentrations decrease with depth. The decrease is greater at depths greater than 10 cm for station 6 and greater than 23 cm for station 7, which suggests a high rate of sulfate reduction. The depth at which sulfate reduction appears is likely related to the porosities and salinities [2].

Sulfate reduction: $2\,CH_2O + SO_4^{2-} \rightarrow H_2S + 2\,HCO_3^-$

- In spite of the sulfate reduction, no free sulfide were observed in porewaters.

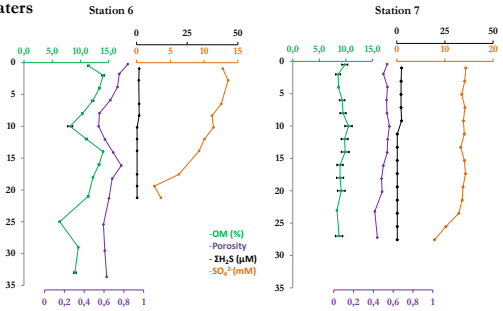

Fig. 4: Vertical profiles of organic matter content (OM) and porosities in the sediments as well as those of dissolved hydrogen sulfide ($\Sigma H_2S = H_2S + HS^- + S^{2-}$) and sulfate concentrations (SO_4^{2-}) at stations 6 and 7.

Sedimentology

Focus on station 7

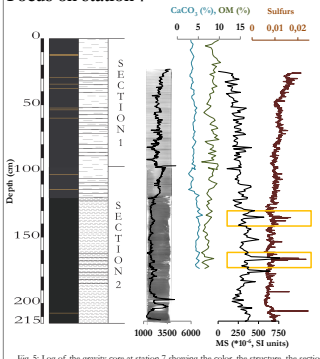

Fig. 5: Log of the gravity core at station 7 showing the color, the structure, the sections of the sediment, the SCOPIX image, the grey-scale, the carbonate (blue line) and organic matter (green line) contents, the magnetic susceptibility and the sulfur area analyzed by XRF.

Sediments from station 7 are made of one main lithology which is mm to cm laminated silty clays. Some parts are more homogeneous with diffusive laminated layers and oxidized orange layers.

The sediments are essentially composed of mineral clasts. Organic matter and carbonate contents are uniform to depth at the station 7.

The magnetic susceptibility increases slowly with depth due to the small difference in grain size with depth. Some peaks can be related to S-peaks especially at 137 cm and at 167 cm (yellow rectangles), meaning the presence of magnetic behavior and then probably the iron presence [6].

Using the PCA, we observe 3 main groups of elements likely correlated between them (Fig. 6):

- Organic matter content, Fe, S and Br.
- Al, K and Ti form a second category more terrigeneous.
- Carbonate content and Ca.

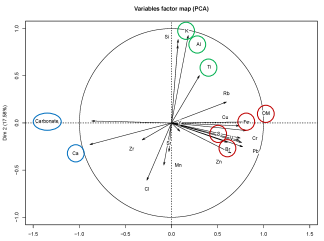

Fig. 6: Principal component analysis on each element analyzed by XRF, organic matter content (OM) and carbonate content using the "FactoMineR" package on R program.

Conclusions & Perspectives

- According to our results, no hypoxia in bottom waters on the Ukrainian shelf was observed in May.
- The depth at which the anoxic sediments appear is characteristic of coastal systems, less than10 mm.
- The depth at which the sulfate reduction appears is related to the porosity and the salinity of the environment.
- No free sulfide was observed in porewaters, probably due to the presence of AVS or to pyrite precipitation.
- These first results reveal certain diagenetic reactions in particular the oxic respiration and the sulfate reduction.
- The PCA analysis showed that different elements can be linked and could be used as proxy in further analysis.
- The study of other parameters (proxies), biological (foraminifera), and geochemical (reactive Fe, trace element compound), could help to identify and reconstruct the hypoxic history.
- The next sampling cruise is planned in late August 2017. The occurrence of an hypoxic event is expected. Comparison of the results obtained from the two contrasting situations can then be made.
- Station 7 is probably the most interesting one to study in terms of changes in hypoxia, considering the continuous laminated sedimentation.

References: [1] Levin, L. A., Ekau, W., Gooday, A. J., Jorissen, F., Middelburg, J. J., Naqvi, W., Neira, C., Rabalais, N. N., and Zhang, J. 2009. Effects of natural and human-induced hypoxia on coastal benthos. Biogeosciences, 6, 2063-2098 | [2] Wijsman, W. M. J., Middelburg, J. J., Herman M. J. P., Böttcher, E. M., and Heip, H. R. C., 2001. Sulfur and iron speciation in surface sediments along the northwestern margin of the Black Sea. Mar. Chem., 74, 261-278 | [3] Lichtschlag A., J. Felden, V. Brüchert, Boetius A., and de Beer D, 2010. Geochemical processes and chemosynthetic primary production in different thiotrophic mats of the Ha°kon Mosby Mud Volcano (Barents Sea). Limnol. Oceanogr. 55, 931–949 | [4] Dean W. E., 1974. Determination of carbonate and organic matter in calcareous sediments and sedimentary rocks by loss on ignition: comparison with other methods. Journal of Sedimentary Petrology, 44, pp. 242-248 | [5] Glud R. N., 2008. Oxygen dynamics of marine sediments. Marine Biology Research, 4:4, 243-289 | [6] Neretin, N. Lev, Böttcher, E. M, Jorgensen, B. Bo, Volkov, I., I, Lüschen, H. and Hilgenfeldt, K., 2004. Pyritization processes and greigite formation in the advancing sulfidization front in the Upper Pleistocene sediments of the Black Sea. Geochimica et Cosmochimica Acta, Vol 68, No 9, pp. 2081-2093

Acknowledgments: We are grateful to the captain and crew of *Mare Nigrum* and to the EMBLAS-II project (funded by the EU and UNDP). The BENTHOX project is funded by the FNRS (Convention no. PDR T.1009.15). The authors wish to thank Isabelle Billy of the University of Bordeaux and Olaya Roman Romin of the University of Liège for the SCOPIX analyses.

Black Sea north-western shelf hypoxia: a study based on diagenetic processes and sedimentary proxies

Audrey Plante[1,2], Nathalie Roevros[1], Arthur Capet[3], Marilaure Grégoire[3], Nathalie Fagel[2], Lei Chou[1]

[1] Service de Biogéochimie et Modélisation du Système Terre, Université Libre de Bruxelles, Brussels, Belgium (Audrey.Plante@ulb.ac.be), [2] Argiles, Géochimie et Environnements sédimentaires, Département de Géologie, Université de Liège, [3] Modelling for Aquatic Systems, Department of Astrophysics, Geophysics and Oceanography, Université de Liège

Poster #11782

Context & Study area

The Black Sea, in particular the north-western shelf, has been submitted to an oxygen depletion in the bottom waters since a few decades. Hypoxia phenomena become longer in their duration, more frequent in their occurrence and wider in their coverage, thus implying a deterioration of the coastal systems. The biogeochemical cycles in the benthic compartment are severely impacted by hypoxia especially when sulfides emanate from sediments and accumulate in the bottom waters.

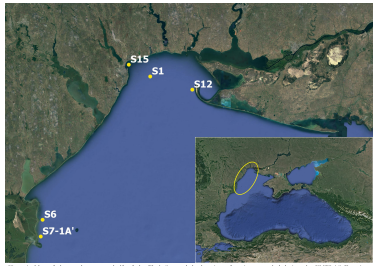

Figure1: Map of the north-western shelf of the Black Sea and the location of stations sampled during the EMBLAS-II cruises (May 2016: S6, S7, S12 and S15; August 2017: S1 and S1A')

The BENTHOX project concerns a biogeochemical study on the Ukrainian shelf aiming to:

- Supply a new dataset of biogeochemical measurements in the sediments including porewaters
- Investigate the impact of the benthic hypoxia on the diagenetic pathways
- Identify proxies for the reconstruction of long-term hypoxia history

Methods

In collaboration with the EMBLAS project whose aim was to improve the environmental monitoring of the Black Sea, we participated in two cruises aboard the *R/V Mare Nigrum* in May 2016 & August 2017 (Fig. 1).

Sampling

Four cores per station were taken with a multicorer (Fig. 2a).
Porewaters were extracted using the Rhizon technique under N_2 atmosphere.
One long core was taken with a gravity corer at station 6.

Analytical

Short cores
Microprofilings of geochemical gradients of dissolved oxygen and hydrogen sulfides were conducted using *UNISENSE* sensors on the cores taken with the multicorer (Fig. 2b).
For porewaters, sulfate concentrations were measured by ionic chromatography. Ammonium and phosphate concentrations were determined by fluorimetry [1] and colorimetry [2] respectively. Sulfide concentrations were analyzed by colorimetry [3].

Long cores
Archived sediments were analyzed continuously every mm by SCOPIX and core scanner, as well as by X-Ray fluorescence at the University of Bordeaux.
Sediments were sliced at every 1.5 cm intervals and dried at 105 °C. TOC and $\delta^{13}C$ were measured on decarbonated samples with a Vario Microcube CNS elemental analyzer coupled with an IRMS Isoprime 100 isotope ratio mass spectrometer.

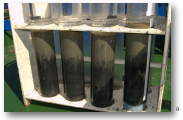

Figure 2: Photographs of (a) cores taken with a multicorer, and (b) the water-sediment interface with a hydrogen sulfide sensor inserted.

Results

2016 - cruise: nutrient concentrations in porewaters

During the spring 2016 cruise, no hypoxia was detected in the bottom waters on the north-western shelf and the oxygen penetration depths were less than 6 mm.

Porewater profiles of ammonium and phosphate are shown in Fig. 3 for the 4 stations sampled in 2016:

- Ammonium and phosphate concentrations increase with depth in the anoxic sediments except at station 12.
- The increase of ammonium concentrations suggests the organic carbon degradation [4] by ammonification in surface sediments, probably followed by the coupled nitrification/denitrification, and by dissimilative nitrate reduction to ammonium [5]. This evolution coincides with the increase in sulfate reduction activity at depth.
- The highest ammonium concentrations are located at the stations influenced by the Danube. At station 7, from the top to 15 cm, the profile shows a constant concentration probably caused by the bioturbation.
- Phosphate profiles reveal a phosphorus release from sediments. This is usually regulated by the reductive dissolution of Fe-oxides liberating the phosphate adsorbed which is induced by the organic matter inputs and the level of oxygen in the bottom waters [6].

Sediments are a source for ammonium and phosphates.

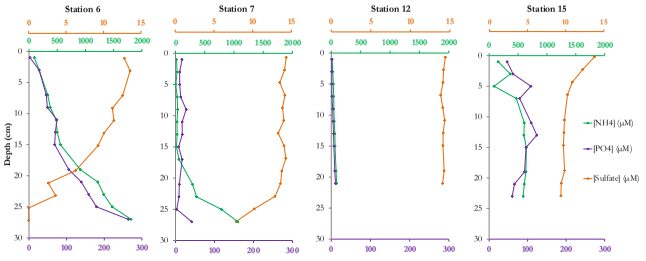

Figure 3: Vertical profiles of ammonium, phosphate and sulfate concentrations in the porewaters at the 4 stations sampled in May 2016.

2017 – cruise: microprofiling & dissolved sulfate/sulfide in porewaters

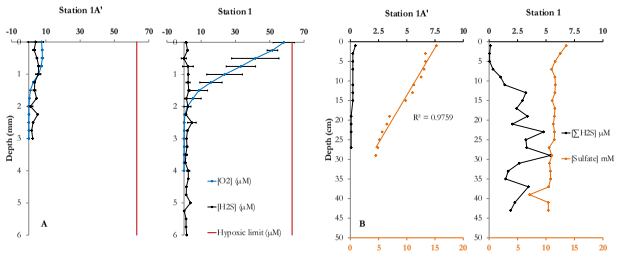

Figure 4: (A) Oxygen and hydrogen sulfide microprofiles and (B) sulfate and total dissolved sulfide concentrations in porewaters at stations 1A' & 1.

Microprofiles of dissolved oxygen and hydrogen sulfide close to the sediment-water interface and vertical profiles of sulfate and total sulfide concentrations in porewaters are shown in Fig. 4 for stations 1A' and 1:

- At the water-sediment interface for both stations, the dissolved oxygen concentration is below the hypoxic threshold (63 µM) [7].
- Below 2.5 mm-depth, the sediment is depleted in dissolved oxygen and becomes anoxic. Organic matter inputs, from photosynthetic activity and thus from riverine loads, may induce the oxygen consumption in the benthic compartment due to the respiration reaction [4].

Oxic respiration: $CH_2O + O_2 \rightarrow CO_2 + H_2O$

- No significant free sulfides at the sediment-water interface were detected at both stations. Station 1 exhibits a weak increase in sulfide concentrations from 5 cm-depth downwards but the concentrations are of the order of µM.
- The sulfate concentration shows a decrease with depth indicating sulfate consumption by microbial activity through sulfate reduction. The sulfate reduction activity is higher at Station 1A' situated in the Danube delta compared to Station 1, possibly due to a higher organic loading.

Sulfate reduction: $2\,CH_2O + SO_4^{2-} \rightarrow H_2S + 2\,HCO_3^-$

The decrease in sulfate concentration with depth at station 1A' appears to be linear whereas the profile at station 1 exhibits a concave-up curvature. For the delta station, the linear shape reflects the diffusive draw-down of sulfate; the profile linearity may be induced by the decrease of porosities with depth [8]. For station 1, the concave-down profile is usually attributed to a continuous reduction of sulfate by the degradation of the organic matter over depth [9].

Sedimentology

Focused on station 6

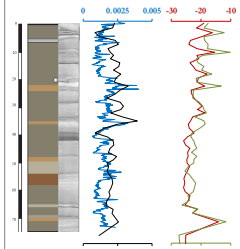

Figure 5: Log of the gravity core at station 6 showing the color and the structure of the sediments, the SCOPIX image (white = high levels of OM, black = low levels of OM), the total organic carbon (TOC: black line) contents, the $\delta^{13}C$ (red line), the C/N ratio (green line) and the Bromide area (blue line) analyzed by XRF.

- Laminated sediments are shown by SCOPIX image and TOC contents in Fig. 5. The variations in color seem to correspond to TOC contents.
- Poor preservation or degradation of the organic matter (OM) during the diagenesis is revealed by the low TOC enrichment [10].
- OM inputs of an algal type mainly marine are identified in Fig. 6 because the increases in TOC & C/N correspond to a high $\delta^{13}C$. This interpretation should be addressed with caution because the C/N ratio must be affected by the anaerobic degradation of OM [10, 11].
- Bromide (Br) profile correlates with TOC measurements which suggests a more intense OM inputs when TOC contents are high, and thus an increase in primary production. Indeed, Br is often linked to marine organic matter and has been used as OM deposition proxy [12].
- The first simulation of the reconstruction of the age-model is represented in Fig. 7. The most intense OM inputs seems to be around 2011, 1971, 1909 and 5 kyr BP.

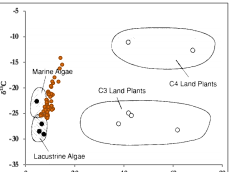

Figure 6: $\delta^{13}C$ as a function of C/N ratios for natural marine and terrestrial compounds as given by Meyers (1994) [13]. Orange dots represent our results.

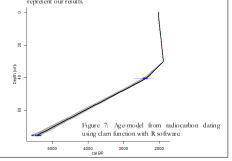

Figure 7: Age-model from radiocarbon dating using clam function with R software.

Conclusions & Perspectives

- Our results show that an hypoxic event was observed in August 2017 in the Ukrainian bottom waters, while none was detected in spring 2016.
- The sediments of the north-western shelf constitute a source for ammonium and phosphorus.
- Oxygen profiles of summer 2017 reveal the consumption of oxygen and thus the **oxic respiration**.
- **Sulfate reduction** activity is detected in 2016 & 2017. The delta stations are more impacted by this process related to the organic matter inputs.
- No free sulfide (<1µM: detection limit) is observed in the porewater profile at station 1A', probably due to the presence of AVS or to pyrite precipitation.
- Our results reveal certain diagenetic reactions in particular the oxic respiration and the sulfate reduction.
- The use of TOC contents, C/N ratio and $\delta^{13}C$ allows one to identify the origins of OM inputs.
- Bromide (Br) may be considered as a proxy for the TOC content and thus the primary production on the northwestern shelf.
  This element could also be used as a proxy for eutrophication and thus for hypoxic events. But further studies of other parameters are necessary to conclude.
- The next step of our investigation is to determine dissolved Fe & Mn concentrations in order to understand the complete redox cascade of the early diagenesis in the sediments. Regarding the solid phase, a study on the speciation of sedimentary sulfur and iron is ongoing.
- The analysis of geochemical and/or biological parameters is planned in order to reconstruct the hypoxic history.

References [1] Holmes M.R. et al., 1999. Accurate and precise method for measuring ammonium in marine and freshwater ecosystems. Canadian journal of Fish. and Aqua. Sc. 56: 1801-1808 | [2] Grasshoff K. et al., 1999. Methods of seawater analysis. Verlag Chemie, Weinheim, 3rd ed. | [3] Cline J., 1969. Spectrophotometric determination of hydrogen sulfide in natural waters. Limnol Oceanogr. 454-458 | [4] Glud R. N., 2008. Oxygen dynamics of marine sediments. Marine Biology Research, 4:4, 243-289 | [5] Kartal B. et al. 2007. Anammox bacteria disguised as denitrifiers: Nitrate reduction to dinitrogen gas via nitrite and ammonium. Environ. Microbiol. 9: 635-642 | [6] Rozan T. F. et al., 2002. Iron-sulfur-phosphorus cycling in the sediments of a shallow coastal bay: Implications for sediment nutrient release and benthic macroalgal blooms. Limnol. Oceanogr. 57: 1660-1682 | [7] Stockdower A. et al., 2011. Ecosystem impacts of hypoxia: thresholds of hypoxia and pathways to recovery. Environ. Res. Lett. 6: 25003 | [8] Jørgensen B. B., et al., 2001. Sulfate reduction and anaerobic methane oxidation at Black Sea sediments. Deep Sea Res. 48: 2097-2120 | [9] Boudreau B. P., 1997. Global and local variations of interstitial sulfate gradients in deep-water, continental margin sediments: Sensitivity to underlying methane and gas hydrates. Mar. Geo. 159: 131-154 | [10] Dinh L. et al. 2015. Paleomagnetic and geochemical record from cores from the Sea of Marmara, Turkey: Age constraints and implications of a episodic deposition on early diagenesis. Mar. Geo. 360: 40-58 | [11] Meyers P. A., 1994. Preservation of elemental and isotopic source identification of sedimentary organic matter. Chem. Geol. 114: 289-302 | [12] Ziegler M., et al. 2008. Bromine counts from XRF scanning as a estimate of the marine organic carbon content of sediment cores. Geochem. Geophys. Geosyst. 9: Q05009.

Acknowledgements We are grateful to the captain and crew of *Mare Nigrum* and the EMBLAS-II project (funded by the EU and UNEP). The BENTHOX project is funded by the FNRS (Convention n° PDR T.1010.15). The authors wish to thank Isabelle Billy and Sabine Schmidt from the University of Bordeaux and Chris Romulus Romin from the University of Liège for the SCOPIX, XRF analyses and dating.

B.3 Ocean deoxygenation conference, Kiel, Germany, 2018

Coastal hypoxia in the Black Sea: Effects on diagenetic pathways and benthic fluxes

Audrey Plante[1,2], Naman Ahmed Butt[1], Nathalie Roevros[1], Arthur Capet[3], Marilaure Grégoire[3], Nathalie Fagel[2], Lei Chou[1]

[1] Service de Biogéochimie et Modélisation du Système Terre, Université Libre de Bruxelles, Brussels, Belgium (Audrey.Plante@ulb.ac.be),
[2] Argiles, Géochimie et Environnements sédimentaires, Département de Géologie, Université de Liège,
[3] Modelling for Aquatic Systems, Department of Astrophysics, Geophysics and Oceanography, Université de Liège

ID #91

Context & Study area

Dissolved oxygen is essential for marine life and plays an important role in the global biogeochemical cycles. Human activities have contributed greatly to the widening of the hypoxic zone in coastal waters. The Northwestern shelf of the Black Sea is impacted by a seasonal hypoxia over last decades which is accentuated by the loadings of nutrients and organic matter from rivers such as the Danube. Oxygen depletion in the bottom waters influences the benthic compartment and induces changes in the biogeochemical processes.

Fig. 1: Map of the Northwestern shelf of the Black Sea and the location of stations sampled during the EMBLAS-II cruises (May 2016: S6, S7, S12 and S15 - August 2017: S1 and S1A').

Within the framework of the BENTHOX project, a biogeochemical investigation focusing on the study of early diagenesis was conducted on the Ukrainian shelf.

The project aims :

- To contribute to a new dataset of biogeochemical measurements in the sediments including porewaters.
- To obtain a better understanding of the impact of benthic hypoxia on the diagenetic pathways.
- To reconstruct the long-term hypoxia history using a multi-paleoproxy approach.

Methods

In collaboration with the EMBLAS project whose aim was to improve the environmental monitoring of the Black Sea, we participated in two cruises aboard the R/V *Mare Nigrum* in May 2016 & August 2017 (Fig. 1).

Sampling

Four cores per station were taken with a multicorer. Porewaters were extracted using the Rhizon technique under N_2 atmosphere.
Sediments were sliced at every 2 cm intervals and kept frozen until analysis.

Analytical

Microprofilings of geochemical gradients of dissolved oxygen and hydrogen sulfides were conducted with *UNISENSE* sensors on cores taken with the multicorer.
From porewaters, sulfate concentrations were measured by ionic chromatography and sulfide concentrations were analyzed by colorimetry [1].
Sulfur and iron speciations were determined following the extraction sequence of Kraal et al. (2013) [2] and by colorimetry.

Degrees of pyritization (DOP) and sulfidization (DOS) were calculated by following Wijsman et al., 1999 [3]:

$$DOP = Fe_{pyr}/(Fe_{pyr} + Fe_{reac})$$
$$DOS = (AVS+Fe_{pyr})/(Fe_{pyr} + FeH)$$

Where:
Fe_{reac}: reactive iron (Fe_{reac} = FeH + Fe_{org} + Fe_{ox} + Fe_{pyr}),
Fe_{pyr}: iron in pyrite (FeS_2),
Fe_{org}: iron bound to reactive organic matter,
Fe_{ox}: iron in crystalline oxide minerals (goethite, hematite),
FeH: HCl extractable iron (Fe(II): FeS, $FeCO_3$, Fe(III): ferrihydrite, akaganeite, lepidocrocite).

S_{inorg}: total inorganic sulfur (S_{inorg} = AVS + CRS),
AVS: Acid Volatile Sulfides (mainly FeS),
CRS: Chromium reducible Sulfides (mainly FeS_2).

Results

Microprofiling & porewater profiles

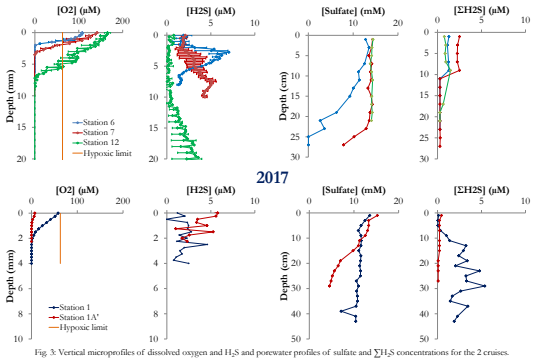

Fig. 3: Vertical microprofiles of dissolved oxygen and H_2S and porewater profiles of sulfate and $\sum H_2S$ concentrations for the 2 cruises.

Dissolved oxygen, H_2S microprofiles and sulfate, ΣH_2S concentrations are shown in Fig. 3:

- The dissolved oxygen concentration exceeds the hypoxic limit (63 µM) at the sediment-water interface in 2016 unlike 2017.
- The oxygen penetration depths are <10 mm-depth. Organic matter inputs, from photosynthetic activity and thus from riverine loads, may induce the oxygen consumption in the benthic layer due to the respiration [4].

Oxic respiration: $CH_2O + O_2 \rightarrow CO_2 + H_2O$

- No significant free sulfides are observed at the sediment-water interface at all stations.
- The sulfate concentration shows a decrease with depth indicating sulfate consumption by microbial activity through the sulfate reduction. The reaction seems to be more efficient at the stations close to the Danube, probably due to the river discharges.
- The environmental conditions (oxic/hypoxic) seem to play a role in the sulfate reduction. Under hypoxic conditions (S7 vs S1A'), this reaction is more intense and appears close to the sediment-water interface.

Sulfate reduction: $2\,CH_2O + SO_4^{2-} \rightarrow H_2S + 2\,HCO_3^-$

Focus on stations 1 & 1A'

Vertical profiles of AVS, CRS, FeH and Fe_{pyr} are shown in Fig. 4A. Sulphur and reactive iron speciations at stations 1 & 1A' are presented in Fig. 4B:

- The variations of AVS and FeH contents show a good correlation for stations 1&1A' (R=0.945 and R=0.865 respectively). AVS concentrations are low at the sediment-water interface probably due to a higher dissolved oxygen concentrations at the sediment-water interface and maybe also due to the presence of iron oxide especially at station 1A' [2].
- Labile ferrous iron, non-associated to FeS, is represented by the difference between FeH and AVS contents.
- At station 1A', vertical profiles of CRS and Fe_{pyr} concentrations exhibit a similar trend.

- Sulphur speciation reflects that the CRS is the major component of the S_{inorg}. Iron speciation results show that FeH is the dominant contributor of the reactive iron pool in the upper sediments while at depth Fepyr becomes the dominant fraction at station 1. Iron bound to the organic matter contributes significantly to the total pool.

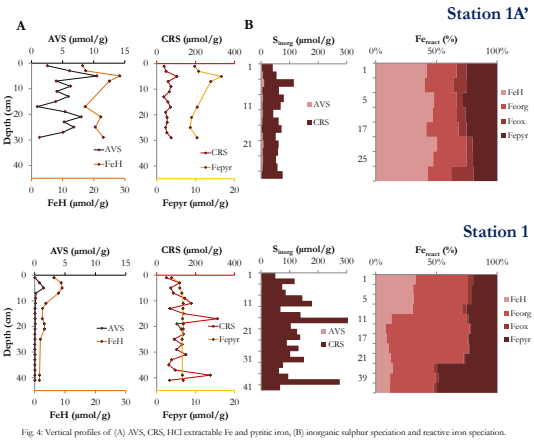

Fig. 4: Vertical profiles of (A) AVS, CRS, HCl extractable Fe and pyritic iron, (B) inorganic sulphur speciation and reactive iron speciation.

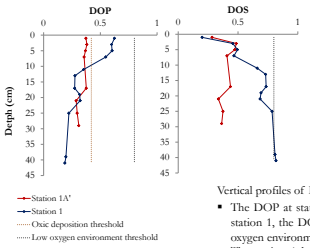

Fig. 5: Vertical depth profiles of DOP and DOS at stations 1 & 1A'.

Vertical profiles of DOP and DOS at stations 1 & 1A' are shown in Fig. 5:

- The DOP at station 1A' is more or less constant (<0.42) with depth indicating a sedimentary deposition under oxic conditions. For station 1, the DOP is higher at the sediment-water interface (between 0.42 and 0.8) which reflects a sediment deposition under low oxygen environments [5].
- The station 1 has a high DOS (average = 0.66) while at station 1A', the DOS average is only 0.39, suggesting a faster and more extensive reduction and sulfidization of iron at station 1 [2].

Benthic fluxes

Table 1: Benthic fluxes of dissolved oxygen (mmol.m^{-2}.d^{-1}) calculated with the *Unisense* software

	2016			2017	
	Station 6	Station 7	Station 12	Station 1	Station 1A'
Benthic O_2 fluxes	-7.3	-2.93	-1.98	-4.78	-1.12

Benthic fluxes of dissolved oxygen, estimated from the microprofiles of dissolved oxygen, are presented in Tab. 1:
The fluxes are more important at stations close to the Danube (6 & 7 vs. 12) during spring 2016.
At station 1A', the oxygen flux is lower than at station 7 reflecting the hypoxic conditions during the summer of 2017.

Conclusions & Perspectives

- Our results show that an hypoxic event was observed in August 2017 in the Ukrainian bottom waters, while none was detected in spring 2016.
- The oxygen penetration depths seem to be impacted by the environmental conditions.
- Oxygen profiles for summer 2017 and spring 2016 reveal a consumption of oxygen and thus an oxic respiration.
- Sulfate reduction activity is detected in 2016 & 2017. The stations in the Danube delta are more impacted by this process linked to the organic matter inputs.
- At station 1A', less free sulfides are observed in the porewaters probably due to the higher presence of AVS and pyrite than at station 1.
- The sediments of station 1A' have a small fraction of AVS except at the sediment-water interface, indicating the presence of iron oxides as confirmed by the iron speciation.
- CRS increases with depth at stations 1 & 1A', suggesting the formation of pyrite.
- DOP confirms the low oxygen sediment deposition especially at station 1A'.
- DOS indicates the occurrence of reduction and sulfidization of iron at station 1.

References: [1] Cline J., 1969. Spectrophotometric determination of hydrogen sulfide in natural waters. Limnol Oceanogr. 454-458 | [2] Kraal P., et al., 2013. Iron monosulfide accumulation and pyrite formation in eutrophic estuarine sediments. Geochimica et Cosmochimica Acta, 122, 75-88 | Dean W. E., 1974. Determination of carbonate and organic matter in calcareous sediments and sedimentary rocks by loss on ignition: comparison with other methods. Journal of Sedimentary Petrology, 44, pp. 242-248 | [4] Glud R. N., 2008. Oxygen dynamics of marine sediments. Marine Biology Research, 4:4, 243-289 | [5] Wijsman, W. M. J. et al., 2001. Sulfur and iron speciation in surface sediments along the northwestern margin of the Black Sea. Mar. Chem., 74, 261-278

Acknowledgments: We are grateful to the captain and crew of *Mare Nigrum* and to the EMBLAS-II project (funded by the EU and UNDP). The BENTHOX project is funded by the F.N.R.S (Convention no. PDR T.1009.15).